GEOSCIENCES IN THE 21st CENTURY

Symposium dedicated to the 80th anniversary of professor Emil Constantinescu

EXTENDED ABSTRACTS

EDITORS
Antoneta Seghedi, Gheorghe Ilinca, Victor Mocanu

GeoEcoMar Bucharest, 2019

Organizatori:

















Sponsorul volumului:



GEOSCIENCES IN THE 21ST CENTURY

Symposium dedicated to the 80th anniversary of Professor Emil Constantinescu

EXTENDED ABSTRACTS

EDITORS
Antoneta Seghedi, Gheorghe Ilinca, Victor Mocanu

GeoEcoMar

Bucharest 2019

NATIONAL INSTITUTE OF MARINE GEOLOGY AND GEOECOLOGY - GeoEcoMar - ROMANIA

23-25 Dimitrie Onciul St. 024053 Bucharest

Tel./Fax: +40-021-252 30 39

Contact: cristinavasiliu@geoecomar.ro

Descrierea CIP a Bibliotecii Naționale a României

Geosciences in the 21st century / editors: Antoneta Seghedi, Victor

Mocanu, Gheorghe Ilinca. - București : GeoEcoMar, 2019

Conţine bibliografie ISBN 978-606-94742-7-3

- I. Seghedi, Antoneta (ed.)
- II. Mocanu, Victor (ed.)
- III. Ilinca, Gheorghe (ed.)

55

Cover: Nicoleta Aniţăi

© GeoEcoMar 2019

CONTENTS

| Foreword |
|--|
| Nicolae Anastasiu The energy mix – the key to performance in the 21st century |
| Alexandru Andrăşanu Geoconservation as a new discipline within Geosciences1 |
| Eliza Anton, Mihaela-Carmen Melinte-Dobrinescu Biostratigraphy of the Istria Basin (Nw Black Sea Shelf) based on calcareous nannofossils14 |
| Laurenţiu Asimopolos, Natalia-Silvia Asimopolos Processing of geophysical data from potential fields for 3D geological modeling18 |
| Glicherie Caraivan Holocene landscape changes and migration of human communities in the western part of the Black Sea (Mamaia Lake area) |
| Nicolae Călin, Delia-Georgeta Dumitraș, Ștefan Marincea, Eduard Ghinescu Minerals indicated for the first time in Conțu pegmatites fields, Cindrel Mountains, Romania26 |
| Alina Coman, Elena Florinela Manea, Carmen Ortanza Cioflan, Mircea Radulian Investigations of the sedimentary structure along Transylvanian Basin2 |
| Ioan Denuţ, Alexandra Sîngeorzan, Ioan Liviu Bereş The Mineralogy Museum from Baia Mare at 30 years from the opening of the permanent Exhibition |
| George Dincă, Gheorghe C. Popescu New minerals from Săcărâmb ore deposit3! |
| Raluca Dinescu, Ioan Munteanu, Corneliu Dinu, Mihaela Popa Discrimination between shallow earthquakes and quarry blasts recorded in Deva region during 2010-2018 time interval |
| Dorin Dordea, Anca Dobrescu Capitalizing on solid mineral resources – another lost cause for Romania of the 21st century?42 |
| Mihai Ducea Missions, opportunities and challenges of the Earth Sciences in the 21st Century: Trends in Higher Education, Fundamental and Applied Research |
| Alexandra-Constanţa Dudu, Constantin-Ştefan Sava, Sorin Anghel, Corina Avram Carbon Capture and Storage activities of GeoEcoMar. An overview |
| Delia Georgeta Dumitraş, Ştefan Marincea, Aurora-Măruţa Iancu, Ciprian Constantina Brushite from several caves in Southern Romania: Crystallographic and infrared data5 |
| Dan Grigorescu Cultural Geology. Interlinking Earth Sciences, History and Philosophy5 |
| Constantin Haită Geografiaeology Applications of Sedimentology and Soil micromorphology in Archaeology 66 |

| Paulina Hîrtopanu Rare Earth minerals in Ditrău alkaline intrusive complex, Eastern Carpathians, Romania | 67 |
|--|-----|
| Viorica Iancu, Gabriel Bindea, Antoneta Seghedi Tectonic inversion and related tectono-metamorphic zonation in the pre-Alpine Getic-Supragetic and Danubian basement of the South Carpathians | 75 |
| Elena-Luisa Iatan Environmental problems associated with the mining activities in the Apuseni Mountains, Romania | 82 |
| Gheorghe Ilinca, Dan Topa Cannizzarite in Romanian occurences | 87 |
| Dumitru Ioane, Irina Stanciu Tectonic and geodynamic model for Vrancea seismic zone | 91 |
| Tatiana I. Ivankina, Sergey E. Kichanov, Octavian G. Duliu, Safa Yusuf, Mohamed M. Sherif The structure of scleractinian coral skeleton analysed by neutron tomography and neutron diffraction | 96 |
| Denisa Jianu, Cezar Iacob, Andra Mârza, Georgian Mănuc, Vlad Victor Ene, Ema Bobocioiu Connection between some of the shear zones from Romania and mantle anisotropy | 100 |
| Dan Jipa, Cornel Olariu Sedimentary history of the Albian conglomerates from the Carpathian Bend Zone | 102 |
| Marinel Kovacs, Alexandrina Fülöp, Zoltán Pécskay Miocene volcanism in Gutâi Mountains. State of the art | 104 |
| Monica Macovei, Dan Grigore, Ionuţ Barbu, Iulia Danciu Museum geoconservation – primary assessment on the condition of mineralogical samples containing pyrite/marcasite within the National Museum of Geology – Bucharest | 108 |
| Raluca Maftei, Radu Fărnoaga, Adrian Tătaru, Constantina Filipciuc, Elena Tudor The role of UAV (Unmanned Aerial Vehicle) in the study of landslides | 112 |
| Elena Florinela Manea, Erzsébet Győri, Alina Coman, Carmen Ortanza Cioflan, Mircea Radulian Non-invasive investigations along the Pannonian Basin | 115 |
| Ştefan Marincea, Delia Georgeta Dumitraş Ludwigite in magnesian skarns from Romania: A review | 118 |
| Mihaela C. Melinte-Dobrinescu, Nicolae Panin, Gheorghe Oaie, Dan Secrieru, Gabriel Ion, Dan Vasiliu, Radu-George Dimitriu Elaboration of Romanian Black Sea geological and geophysical maps: State of the art | 123 |
| Viorica Milu, Moha Ikenne, Antoneta Seghedi, Mustapha Souhassou, Nourissaid Içame, Mihaela Carmen Melinte-Dobrinescu, Alexandru Andrășanu, Iuliana Lazăr Geoheritage of the Anti-Atlas (Morocco): a natural treasure in support of sustainable development | 126 |
| Alexandra Muntean, Eduard Ilie Năstase, Victor Mocanu, Boudewijn Ambrosius Usefulness of Romanian GNSS networks for geoscience purposes | |
| Ioan Munteanu, Corneliu Dinu Contractional polarity changes, insights from analog modeling and the Black Sea case | |
| Pandele Neculae Geosciences' Support for the Oil & Gas Business Success | |

| Bogdan Mihai Niculescu, Aurelian Neguţ, Gina Andrei Applications of Modern Borehole Geophysical Logging Methods to Subsurface Characterization | 139 |
|--|-----|
| Lidia-Maria Nuţu-Dragomir, Florina Chitea Combined geological and geoelectrical methods in the study of Convolute Flysch Nappe the tectonic contact with the Macla Nappe (Fieni, Dambovita county) | 143 |
| Ionelia Panea Effects of phase variations on the signal-to-noise ratio of crooked line seismic data recorded for hydrocarbon exploration | 147 |
| Nicolae Panin The involvement of the Romanian Academy in the Sustainable Development Strategy of Romania in the following 20 years and in the National Strategy in the Field of Research and Innovation for the Romanian Danube Region | 152 |
| Adrian-Iulian Pantia, Andra-Elena Filiuță, Sarolta Lőrincz Blue Quartz in Romania – a preliminary mineralogical study | 153 |
| Constantin Pene Evaluation of the unconventional hydrocarbon resources from Romania | 158 |
| Ion Petreuş, Viorel Ionesi The cellular crystallography of Braarudosphaera bigelowii | 162 |
| Ioan Pintea Fluid and melt inclusions in minerals: applications in geosciences | 164 |
| Iulian Pojar, Friederike Stock, Christian Kochleus Microplastics in surface waters from the Northwestern Black Sea. An abundance and composition approach | 170 |
| Adrian Popa, Adrian Teacă, Mihaela Mureșan, Gabriel Ion, Begun Tatiana, Mihai Emilian Popa Habitat mapping on the Romanian shelf based on multibeam bathymetry and sidescan sonar measurements, integrated with geological and biological data | 173 |
| Mihai Emilian Popa, Gaëtan Guignard Preliminary approach for fine insights in Cycadopteris obtusifolia from Romania, using transmission electron microscopy, chemical elements and epifluorescence | 178 |
| Gheorghe C. Popescu, Antonela Neacşu The odyssey of minerals resources vs.necessities, possibilities and requirements | 181 |
| Gavril Săbău The nepheline syenitic intrusions in Southern Banat: agpaitic character, evolution trends and qualitative HFSE and REE budget | 186 |
| Gavril Săbău, Elena Negulescu Fluids strike back – alkaline autometasomatism and peralkaline melt generation at the contact of the Măgureaua Vaței pluton, South Apuseni Mountains | 189 |
| Cristina Sava, Ştefan Marincea Vesuvianite in high-temperature skarns from Romania: a review | 192 |
| Daniel Scrădeanu, Mihaela Scrădeanu Assessment and Forecasting of Pollution due to accidental leaks on Soil and Ground Water in Oil Extractive Industry | 196 |
| Antoneta Seghedi, Titus Brustur, Mihaela Carmen Melinte-Dobrinescu Studies of geological heritage in GeoEcoMar: from geodiversity to geoconservation | 201 |

| Lucian Stanciu, Eugen Mocanu Who's Who -500 Romanian Geologists - Scientific Works | 208 |
|---|-----|
| Lia Stelea Atmospheric pressure in paleoclimate. Introduction and importance | 210 |
| Robert Szabo, Gheorghe C. Popesc, Delia-Georgeta Dumitraș, Ciprian Constantina New mineral occurrences on the north side of Vâlcan Mountains | 212 |
| Mihai Tatu, Elena – Luisa Iatan New approaches on crystallization pressure of some Late Cretaceous granitoids from Romania | 217 |
| Mircea Ţicleanu, Alexandru Ţicleanu, Radu Nicolescu 39.53 model of the Solar System (based on geological phenomena cyclicity) | 223 |
| Mircea Ţicleanu, Alexandru Ţicleanu, Radu Nicolescu, Octavian Colţoi, Flori Culescu Cyclostratigraphic chart of the Meso – Neozoic (Cenozoic) time | 226 |

Foreword

The symposium **Geosciences in the 21st century** attracted presentations on various research themes investigated by the community of Romanian geoscientists living or studying here and abroad, in countries of Europe or America. The abstracts printed in this volume, authored and coauthored by Romanian and foreign geoscientists, were presented in six parallel scientific sessions and a plenary session of invited talks.

In the opening of the symposium, the missions, opportunities and challenges of the earth sciences in the 21st century were presented by Prof. Mihai Ducea from the University of Arizona, Tucson. Acad. Nicolae Anastasiu talked about the energy mix as key to performance in the 21st century and Acad. Nicolae Panin emphasized the involvement of the Romanian Academy in the Sustainable Development Strategy of Romania for the next 20 years and in the National Strategy in the Field of Research and Innovation for the Romanian Danube Region.

The scientific sessions included 53 oral and poster presentations on several major themes: Mineralogy, Crystalography and Mineral resources, Petrology, Tectonics and Volcanism, Paleontology and Stratigraphy, Geophysics and Environmental Geology and Geodiversity, Geoconservation, Geoarcheology. A special session of the Doctoral School of Geology was also organized for young researchers.

Occasioned by the 80th anniversary of Emil Constantinescu, teacher of many of us, colleague and friend for others, the symposium was a good opportunity to meditate on the role of geosiences in the society.

In the 21st century, geoscientists still study minerals, rocks, sediments, fossils, the structure of the earth's layers and tectonic processes, but apply modern technologies and are increasingly involved in interdisciplinary approach and collaborative research with national and international teams. Along with geological and sedimentological mapping, natural hazards and natural resources, geoscientist are also concerned with Carbon capture and storage, microplastics that invade our life on land and in the oceans, and are more involved in the protection of nonrenewable resources and in conservation of geological heritage.

Communicating geosciences is a challenge of our times. Although geology is relevant in many ways to modern life, and a wealth of geoscience knowledge is available today, the modern society is unable to recognize its value. Therefore, there is a constant shortage of funding for geosciences, and this derives from failing to properly communicate their importance to the society. The future depends on the ability of the geosciences community to develop products and systems that meet the needs of the 21st century.

The Editors

THE ENERGY MIX – THE KEY TO PERFORMANCE IN THE 21ST CENTURY

Nicolae ANASTASIU

The Romanian Academy
Calea Victoriei 125, Bucharest, e-mail: nicanastasiu@gmail.com

The ENERGY resources of the Earth's crust constitute an important basis of raw materials for Romania's economic development. Romania has an important volume of identified resources and calculated reserves that are operationally in different stages of exploration and/or exploitation or of a stopped activity. The unequal degree of knowledge, geoeconomically, does not currently allow for their effective recovery.

Romania has the strategic objective of owning a balanced and diversified electricity mix.

All types of primary energy sources available in Romania at competitive costs are found in it. For energy security considerations, the Strategy consents the place of traditional fuels in the mix – *crude oil, natural gas, nuclear energy* and *coal*. The energy transition aims to increase the share of electricity production without GHG emissions, often from intermittent sources such as wind and photovoltaic energy.

Crude oil and natural gas. Currently, in Romania, is being exploited 400 deposits of crude oil and natural gas, of which:

- 1. OMV Petrom operates more than 200 commercial deposits of crude oil and natural gas in Romania. In the Black Sea, OMV Petrom operates on seven fixed platforms;
 - 2. Romgaz operates as sole oil-holder, on 8 perimeters of exploration, development, exploitation.

Natural gas has a share of about 30% of domestic primary energy consumption. Their important share is explained by the relatively high availability of indigenous resources, the low environmental impact and the ability to balance electricity produced from intermittent SRE. The existing infrastructure for extraction, transport, underground storage and distribution is extended throughout the territory of the country.

Coal is the basic primary energy resource in the composition of the energy mix, being a strategic fuel in support of national and regional energy security.

The lignite resources in Romania are estimated at 690 million tons (124 mil. Toe), of which exploits in the perimeters concesed 290 million tons (52 mil. Toe).

The bituminous coal resources in Romania known are 232 million tons (85 mil. Toe) of which exploits in the perimeters concesed 83 million tons (30 mil. Toe).

Romania has a completely open cycle of nuclear fuel, developed on the basis of Canadian CANDU technology. *Uranium* dioxide (UO²), used for the manufacture of nuclear fuel required for reactors 1 and 2 from Cernavodă, is the product of processing and refining uranium extracted from indigenous production. Existing and exploatable ore reserves ensure demand for natural uranium for the operation of nuclear-electric units throughout the operating period.

Romania, by its geographic position, through the diversity of landscape, the hydrographic network, by soil quality and forestry potential, is one of the few countries European Union, which can include in its energy mix *renewable resources*: wind, solar, hydroenergy, geothermal and bioenergy.

Technical developments and new technological lines, the successful examples in these areas, have encouraged Romanian and foreign investors, as early as the '90, to use such resources and launch the necessary Law framework.

Wind energy potential at country level is (14 000 MW installed power), the solar system is raises in Dobrogea and Romanian Plain to more 1400 MJ/m². Production capacity of hydrotechnical planning reaches almost 40 000 GWh/year, geothermal potential is very little capitalized (only in Crişana and Muntenia), even if the waters in the basement areas of Carpathians and Subcarpathians reach temperatures between 40° and 120°C. Finally, the conversion of biomass (agricultural, forestry,

zootechnical, household waste) in natural gas, liquid and solid fuels could help a lot of transport, heating or production of electricity.

All SRE will know a development in Romania after the year 2020, the growth rate of each being determined by the evolution of the relative costs of technologies.

Worldwide, the development of science has outlined new concepts, and technological development has created modern processes of processing and use in the economy of new types of energy resources. They constitute an *alternative* to the accelerated consumption of renewable and non-renewable resources exploited to date.

- 1. Exploitation of natural gas from clay formations (gas shales);
- 2. Oil extraction technologies from "aged" tanks by secondary recovery of hydrocarbons that could not be exploited (*tight sands*, *tight gas*);

The key words of the performance strategy are: energy security, competitiveness, modernizing and developing the system, and the important targets we set are: discovering new reserves (which would imply considerable investments), developing deposits and concentrating our activity in exploitation perimeters with real economic potential.

References

- Anastasiu, N. et al., 2013. Resurse de gaze naturale din zăcăminte neconvenționle potențial și valorificare. Comitetul Național Român al Consiliului Mondial al Energiei, Proiect CENTGAS, 119 p.
- Constantinescu, E., Anastasiu, N., 2017. Resursele minerale ale României, Resurse energetice. vol. III, Editura Academiei Române, București, 648 p.
- Popescu, B., Anastasiu, N., 2016. *An Overview of Unconventional Resources of Romania. Pending challenges*, 35 p., Cap. In Springer book series: The Handbook of Environmental Chemistry; Book title: Shale Gas: Ecology, Politics, Economy.
- Rosca, M., Bendea, C, Cucueteanu, D., 2013. Geothermal Energy Use, Country Update for Romania, Proceedings, European GeothermalCongress 2013, Pisa, Italy.
- Stoica-Negulescu, E.R., SWER, 2015. *Romanian Oil and Gas from Geopysics to Petroleum Systems*. Editura Vergiliu, București, 97 p.
- Turcu, I., 2010. Studiu privind evaluarea potențialului energetic actual al surselor regenerabile de energie în Romania (solar, vânt, biomasă, microhidro, geotermie), identificarea celor mai bune locații pentru dezvoltarea investițiilor în producerea de energie electrică neconvențională. ICEMENERG SA, 52 p.
- Veliciu, Ş., 2011. An Overview on Geothermal Potential of Romania, DR-AHK Symposium Geothermie in Rumänien, Bucharest.
- Vlad, I.V., 2015, 2016. Strategia de dezvoltare a ROMÂNIEI în următorii 20 de ani. Proiect 2. Resursele naturale rezerve strategice, ce folosim și ce lăsăm generațiilor viitoare (coordonator: Acad. Bogdan C. Simionescu); ANASTASIU N.-coord și autor la Subdomeniul 6 Resursele subsolului și Subdomeniul 7 Deșeuri miniere. Editura Academiei Române. București. ISBN 978-973-27-2555-9.

* * * * * *

Proiectul 3. Securitatea și eficiența energetică. Alocarea resurselor energetice necesare în evoluția și dezvoltarea sistemului energetic pentru dezvoltarea economică a României în perioada 2018–2038 (coordonator: prof. univ. dr. Filip Cârlea).

Strategia Energetică a României 2016–2030, cu perspectiva anului 2050. Ministerul Energiei, 2016.

Strategia energetică a României pentru perioada 2007-2020 actualizată pentru perioada 2011-2020.

GEOCONSERVATION AS A NEW DISCIPLINE WITHIN GEOSCIENCES

Alexandru ANDRĂŞANU

University of Bucharest, Faculty of Geology and Geophysics e-mail: alexandru.andrasanu@unibuc.ro

Abstract

Specific activities dedicated to identification and protection of unique or rare geological and paleontological features have a long history. A systematic approach of geodiversity assessment and geological heritage management was strongly implemented only in the last 25 years. New concepts like geodiversity, geoheritage, geoparks, geotourism, geoeducation, and geoproducts have been developed. Geoconservation is an emerging discipline within geosciences aiming to integrate the concepts mentioned above and train new specialists able to implement them. Geoconservation goal is to identify the geodiversity values, in connection with biodiversity and cultural values, for a proper management and sustainable use for socio-economic development.

Introduction

A simple search of the word Geoconservation on web is revealing tens of thousands of results. The number of books, specific events and trained specialists increased continuously in the last twenty years proofing the need, interest and utility of this new area of activity.

Several stages in geoconservation development (Gonggrijp, 2000; Burek & Prosser, 2008; Wimbledon & Smith-Meyer, 2012; Gray, 2013; Reynard & Brilha, 2018). An early stage when enthusiast geoscientists identified and promoted geological assets as part of nature conservation and public awareness. A second stage is defined by coherent activities of ProGEO (the European Association for the Conservation of the Geological Heritage), Digne Declaration (1991), international concern for sustainable use of natural resources and the development of the geopark concept. All these created the stage for a more professional approach. The rapid development of Global Geoparks after 2004 and the establishment of the International Geoscience and Geoparks Programme by UNESCO in November 2015 generated a global recognition of geoconservation activities and the role can play in geosciences development and promotion.

Conservation activities in Romania were encouraged by different legal frameworks and geologists and natural scientists, mainly form research institute and universities, have been involved in identification and protection of geological sites. The number of geological monuments and geological reserves increased after 1990 and became part of the National Network of Protected Areas. ProGeo Romania and other institutions and associations promoted different strategies aiming to protect geological heritage (Grigorescu, 1994, 1996; Andrăşanu, 1996, 2009; Andrăşanu & Grigorescu, 2012). University of Bucharest was the first institution to develop in the late 1990s a new course dedicated to geoconservation and have developed since 2009 a dedicated master degree (GBA, 2019). It was the first to apply, since 2016, the UNESCO Global Geopark Program in Romania and to develop local and national partnerships in order to create and manage Hateg Country UNESCO Global Geopark, as a model for other geopark projects (Andrăşanu, 2017). Geoconservation activities in Romania are still in an early stage of implementation.

Concepts and terminology

Geoconservation is a relatively new area of nature conservation aiming to preserve the natural diversity of the non-living environment (geodiversity) for its values (Sharples, 2002; Gray, 2013) and developed a set of actions aiming the management of geological sites comprising inventory, assessment, conservation, legal protection, interpretation, and monitoring of sites (ProGeo, 2017). Also could be defined as the identification and care of sites which make a special contribution to our Earth heritage and which can illustrate the Earth history.

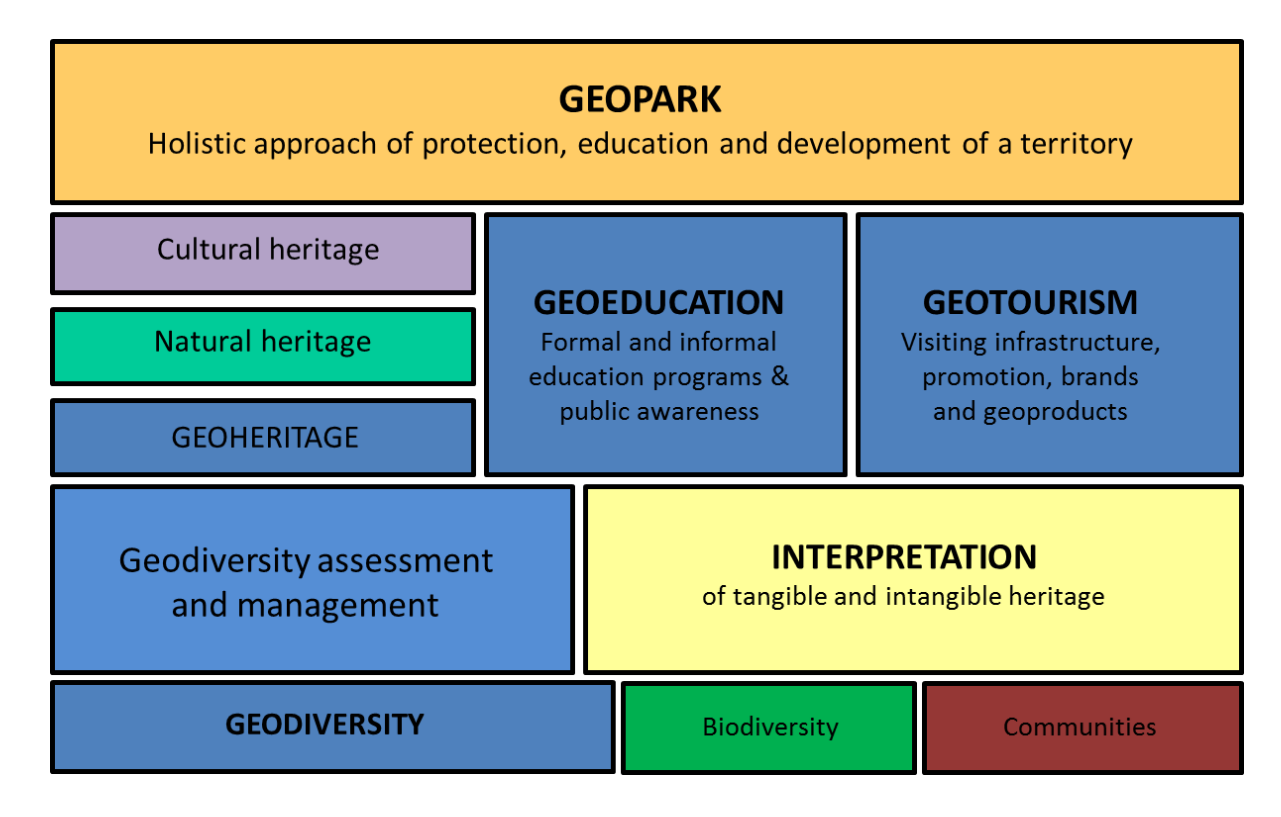


Fig. 1. Geoconservation key concepts and their relationship

Geoconservation focuses on multidisciplinary research of geodiversity components and their role in shaping natural environment and human communities. Approaching Earth evolution through a cultural lens, geoconservation makes geosciences and geological processes and phenomena accessible and interesting whenever possible.

Geoconservation concepts, methodology, their relationship (see figure 1) and related activities could be grouped in four main areas of intervention presented bellow (table 1):

- A. Identify values and benefits of geodiversity. The planet we live is offering natural services or values. Some of these are intrinsic and part of the Earth system mechanism, others are supporting services for life and knowledge and cultural services. Geoheritage is part of geodiversity we appreciate and consider for conservation;
- B. Inventory, Assessment & Mapping criteria were developed aiming to support geodiversity inventory, mapping assessment and related values. Systematic studies of an area allow an unbiased selection of sites with the lowest degree of subjectivity possible (Brilha, 2018);
- C. Development of coherent management activities based on strategies an action plans and financed activities for a sustainable use of geodiversity components, geoheritage conservation and aiming to generate social, cultural and economic benefits;
- D. Development of specific strategies and tools for geodiversity interpretation in order to help visitors to experience a personal relationship with geodiversity and to promote geosciences and geoconservation.

As a new discipline, geoconservation developed specific terminology briefly presented below.

Geodiversity – The concept appeared during the 1990s and was developed by different authors (Sharples, 1993; Prosser, 2002; Gray, 2004, 2013). Geodiversity is reflecting the Earth evolution since its creation, creating the support for life development. Geodiversity could be defined as the variety of earth materials, fossils, forms and processes shaping the Earth at the global and local level. Geodiversity components are variable in time as a result of previous processes or ongoing ones and is continuously transformed including complete removal of some components or development of totally new ones.

Geodiversity Action Plans (GAP) – The GAP concept was developed in UK aim to identify geological assets for a well-defined territory and to provide a mechanism for establishing common actions for geodiversity and associated components geoconservation.

Table 1. Geoconservation areas of intervention and methodological concepts

| Area | s of intervention | Concepts | |
|------|------------------------------|--|--|
| A. | Identify values and benefits | GEODIVERSITY SERVICES. Natural processes, life support, natural | |
| | of geodiversity for humans | resources, knowledge, cultural identity | |
| В. | Inventory, Assessment & | GEOHERITAGE – tangible geoheritage (GEOSITES, collections), intangible | |
| | Mapping of geodiversity | geoheritage (mythology, knowledge, sense of place) | |
| C. | Coherent management | GEOPARKS & GEOPRODUCTS, GEODIVERSITY ACTION PLANS, Geosite | |
| | activities | management and conservation | |
| D. | Interpretation | GEOEDUCATION & Public awareness, GEOTOURISM | |

Geoeducation — all tools, materials and indoor and outdoor activities describing educational experience dedicated to teach and learn about Earth geodiversity and its impact on life and human activities. Geoeducation provides people with the knowledge of how the human and natural worlds work at local, regional and global scales, and to use different perspectives to understand the world.

Geoheritage or Geological heritage – part of geodiversity identified as being important from the cultural, scientific, educational and touristic point of view and worthing to be preserved.

Geopark – Global Geoparks are unique geographical areas where sites and landscapes of international geological significance are managed with a holistic concept of protection, education and sustainable development on the benefit of local communities.

Geoproducts – are a locally manufactured product linked with geopark activities and are symbols of local geological and cultural heritage. As marketable goods they introduce the local products and local handicrafts as cultural objects for tourists and also contribute to increasing the public's knowledge about geology. The concept of geoproducts is a key element of the geopark's organization, often associated with the geopark's mission for socioeconomic development.

Geosite – or geological site or geotop is an area where geodiversity has special or distinguishing features expressing a specific geologic framework worthing to be preserved and managed for research, education or tourism.

Geotourism – is tourism which sustains and enhances the identity of a territory, taking into consideration its geology, environment, culture, aesthetics, heritage and the well-being of its residents. Geological tourism is one of the multiple components of geotourism.

Interpretation of geodiversity — interpretation is not transmitting dry geologic information. Interpretation aims to help visitors to develop a personal relationship with geodiversity and to promote geosciences and geoconservation. The interpretation aims to provoke a reaction, then relate this to people's experience and finally reveal new connections and make them curios about geodiversity and possible connections with other subjects and implications in everyday life.

Conclusions

Geoconservation evolved in the last decade and now its basic concepts, structure and methodology are well defined. Main areas of activity are focused around few basic concepts, some of them already known for a long time but now reorganized and integrated into a logical and coherent framework. Geoconservation is an emerging discipline within geosciences aiming to identify the geodiversity values, in connection with biodiversity and cultural values, for a proper management and sustainable use for socioeconomic development. Geoconservation development is offering a good opportunity for new research and education projects, new type of jobs and supports a better promotion of geosciences.

References

- Andrășanu, A., 2017. Geoparcul UNESCO model de dezvoltare comunitară și construcție de brand. In: Rujoiu, O., *Societate, Publicitate, Consumator.* Editura ASE, pp 185-212.
- Andrășanu, A., Grigorescu, D., 2012. Geoheritage in Romania and its conservation. In: Wimbledon, W., Smith-Meyer, S. (Eds.), *Geoheritage in Europe and its conservation*. ProGEO, pp.151 163, ISBN 978-82-426-247-5.
- Andrășanu, A, 2009. Geoconservarea. Metode, principii, aplicatii. Geoconservarea depozitelor de virsta Cretacic inferior din Bazinul Dimbovicioara, Teza de doctorat, Geomedia, Bucuresti, 450 p.
- Andrășanu, A., 1996. Geological Heritage Conservation in Romania, legislation, strategies, organizations involved. *Geologica Balcanica* LX, 156 160.
- Andrășanu, A., Grigorescu, D., 2012. Geoheritage in Romania and its conservation. In *Geoheritage in Europe and its coservation*, Wimbledon, W., Smith-Meyer, S. (edts), ProGEO, ISBN 978-82-426-247-5, pp 151 163;
- Andrășanu, A., Gamet, J., Dupuy, O., 2009. Dialogul Omului cu Pamântul, Ed. Amanda, București, 48 p.
- Burek, C.V., Prosser, C.D. (Eds.), 2008. *The history of geoconservation*. The Geological Society, London, Special Publication 300.
- Gonggrijp, G. 2000. The early years of ProGEO. ProGEO NEWS 3, 2000. Available from http://www.progeo. ngo/assets/progeo news 2018 2.pdf (accessed 08.09.2019)
- Gray, M., 2013. Geodiversity: Valuing and Conserving Abiotic Nature. Second ed. Wiley Blackwell, Chichester.
- Grigorescu, D., 1990. Earth Science Conservation in Romania. Earth Science Conservation 27, 6-8.
- Grigorescu, D., 1996. Geotopes conservation in Romania, future measures in a regional Carpato Balkan Cooperation. *Geologica Balcanica*, 26, 1, 87 90, Sofia.
- Sharples, C., 1993. A Methodology for the Identification of Significant Landforms and Geological Sites for Geoconservation Purposes. Forestry Commission. Tasmania.
- Wimbledon W.A.P., Smith-Meyer, S. (edts) 2012. Geoheritage in Europe and its Conservation. ProGEO
- Reynard, E., Brilha, J. (Eds.) 2018. Geoheritage. Assessment, Protection, and Management, Elsevier Inc.

* * * * *

Digne Declaration, 1991. International Declaration of the Rights of the Memory of the Earth. Available from: http://www.igc.usp.br/index.php?id5778. (accessed 07.09.19).

GBA, 2019. http://www.master-geobio.ro/ (Accessed 09.09.2019)

BIOSTRATIGRAPHY OF THE ISTRIA BASIN (NW BLACK SEA SHELF) BASED ON CALCAREOUS NANNOFOSSILS

Eliza-Mădălina ANTON^{1,2}, Mihaela C. MELINTE-DOBRINESCU¹

¹National Institute of Marine Geology and Geoecology (GeoEcoMar), 23-25 Dimitrie Onciul St, 024053 Bucharest, e-mail: antoneliza@geoecomar.ro; melinte@geoecomar.ro

²University of Bucharest, Faculty of Geology and Geophysics, 6 Traian Vuia St, Bucharest

The calcareous nannoplankton represents a unique group of organisms in the biological evolution of our planet. These micronic planktonic algae provide indicators of palaeotemperatures, past dissolved and atmospheric CO_2 dissolution, carbon cycle, salinity and sea-level changes. Because they are living organisms, the hypothesis on the past geological record could be tested in the present, and allow us to foretell future developments (Tappan, 1980; Aubry, 1992; Hay, 2004; Melinte, 2005).

The first record of the calcareous nannoplankton in geological time is placed in the Upper Triassic, discovered in the marine sediments of the Southern Alps, Italy (Bown, 1998). The radiation of this group of phytoplankton already took place in the Jurassic and continued throughout the Cretaceous. The maximum diversity of the calcareous nannoplankton in all its evolution was reached in the Upper Cretaceous interval (Perch-Nielsen, 1985). The chalk deposits of the Upper Cretaceous (giving the name of this period) resulted from the accumulation of coccoliths tests. The calcareous nannoplankton was strongly affected, as other marine planktonic organisms, by the Cretaceous-Tertiary boundary event. A mass extinction was recorded around 65 Ma ago, which led to the extinction of over 90% of the total nannofloral taxa (Lamolda et al., 2016). A recovery of the calcareous nannoplankton took place within the Paleocene (Perch-Nielsen, 1985; Bown, 1998). During the Eocene, an important development of this group of calcareous algae took place, but rapidly the nannofloral diversity shifted at the Eocene-Oligocene boundary, related to the overall climatic deterioration (Aubry, 1992). During the Miocene and the Pliocene, a new specific radiation took place, showing a maximum of taxa diversity in the Upper Miocene, while since the Quaternary this group of organisms continuously declines (Young, 1998), a tendency presently observed.

Based on calcareous nannofossil assemblages, a detailed biostratigraphy was achieved for the Triassic-Quaternary interval (Martini, 1971; Sissingh, 1977; Perch-Nielsen, 1985; Bown, 1998, among many others). Therefore, an accurate age based on calcareous nannoplankton may be given in any marine sediments onshore and offshore. As nannoplankton taxa are very small-sized and happen to be abundant, especially in marine rocks, which are the most common form of sedimentary rocks in the crust of the Earth, they have many applications to petroleum geology, especially deciphering biostratigraphy and depositional environment.

As above presented, there are two intervals in the calcareous nannoplankton history that globally show maximum abundance and diversity, i.e. the Upper Cretaceous and the Eocene. These are the intervals that are very well developed in the Istria Basin, which is part of the Western Black Sea basin (Dinu et al., 2005; Munteanu et al., 2011).

Since the end of the last century, many wells were drilled inside the aforementioned area. In this study, we have integrated the results from more than 20 boreholes drilled in the search for hydrocarbons, on the Romanian offshore, by interpreting all the results describing the found calcareous nannofossil assemblages from core reports. To note that the wells makes also available substantial data in terms of lithostratigraphy (especially due to the availability of mechanical cores) the interpretation of this feature represents a study in progress, aiming to realize further correlation between biostratigraphic findings herein presented based on calcareous nannoplankton interpretation and lithostratigraphy, including development of various facies.

The Istria Basin sedimentary cover is composed of Triassic to Cenozoic successions, this sedimentary feature being linked to the tectonic regime of those times. The opening of the Western Black Sea basin,

along with the smaller scale Istria Basin, initiated in the late Early Cretaceous, rifting and expansion continued within Upper Cretaceous times up until the middle Paleogene (Yilmaz *et al.*, 1997; Okay and Tüysüz, 1999; Dinu *et al.*, 2005; Munteanu *et al.*, 2011). In the middle Eocene, the entire WBS margin have been inverted, as a consequence of the collision of the Taurides and Pontides belts (Okay *et al.*, 1994). The compression shaped the basin until the middle Miocene (in the Sarmatian stage of the regional Eastern Paratethyan domain); next, the rapid drowning of the basin central part generated a large-scale shelf progradation (Ionescu et al., 2002; Dinu *et al.*, 2005). Concerning the calcareous nannofossil assemblages described in the wells from the Istria Basin, the observed assemblages are either Cretaceous, either Paleogene (mainly Eocene) in age.

The Cretaceous calcareous nannoplankton taxa may be divided into three distinct groups (taxonomic assignment and distribution after Perch-Nielsen, 1985, Bown, 1998 and Burnett, 1998):

- (1) Long-ranging Species, covering the whole Cretaceous interval, such as: *Biscutum constans, Broinsonia matalosa, Manivitella pemmatoidea, Retecapsa crenulata, Rhagodiscus angustus, Tegumentum stradneri, Zeugrhabdotus embergeri, Zeugrhabdotus diplogrammus* and *Watznaueria barnesiae*;
- (2) Species that have their FO (first occurrence) at the end of the Early Cretaceous interval, i.e., within the Aptian or Albian stages and survive up to the end of the Cretaceous or vanished in the uppermost Cretaceous (Campanian): Broinsonia enormis, Chiastozygus literrarius, Cribrosphaerella ehrenbergii, Eprolithus floralis, Eiffellithus turriseiffelii, Microrhabdulus decoratus and Tranolithus orionatus;
- (3) A small group of taxa occurs in the Upper Cretaceous *Arkhangelskiella cymbiformis* (firstly occurring at the base of the Campanian), *Ceratolithoides aculeus* (having its first occurrence in lower part of the upper Campanian, in CC20 biozone), *Corollithion exiguum* (FO the first occurrence in the Turonian and the last occurrence LO in the Maastrichtian) and *Lucianorhabdus cayeuxii* (FO in the Santonian and LO at the top of the Maastrichtian).

Taking into account these results, we hypothesize that the oldest calcareous nannofossil assemblages in the study area are Aptian-Albian in age; another interval pointed out is the Campanian, based on the occurrence of some taxa that have their FO in the Campanian (Fig. 1). We may not exclude the presence of the uppermost Cretaceous sedimentation, i.e. the Maastrichtian stage, as most of the taxa aforementioned vanished at the Cretaceous-Tertiary boundary. On the hand, no calcareous nannofossils yielding the FO in the upper part of the Campanian (above the CC20 biozone) or in the Maastrichtian (*Uniplanarius sissinghi, U. trifidus, Lithraphidites quadratus, Micula murus, Micula prinsii,* etc.) was not found in the investigated well logs.

A correlation with former studies on calcareous nannofossil biostratigraphy made on the southern Romanian shelf (Tândala Well - Melinte, 2006) indicates that there are some common features between the southern and northern Romanian shelves. Hence, in the southern Romanian shelf there are evidences based on calcareous nannofossils for the presence of NC7, NC8, NC9 and NC10 biozones of Roth (1978, 1983), spanning the Aptian-Albian interval, similar with findings from the Istria Basin. Additionally, in S Romanian shelf, the nannofossil zones characterizing the Valanginian stage (NK2 of Bralower et al., 1989), as well as NC3, NC4, NC5 and NC6 biozones of Roth (1978, 1983) that covers the upper Valanginian – Barremian interval are also present (Fig.1).

In the northern Romanian shelf, the presence of assemblages contain, besides long-ranging species, the significant biostratigraphic nannofossils such as: *Ceratolithoides aculeus, Arhangelskiella cymbiformis* and *Aspidolithus* spp., are indicative for the upper Campanian (lower part), respectively the CC20 biozone of Sissingh (1977). Similarly, in the southern Black Sea shelf, the CC20 was identified above the NC10 zone, indicating a marine deposition in Albian, followed by the presence of marine Campanian sediments. As for the Lower Cretaceous (Valanginian to Barremian interval), the Upper Cretaceous shows a more complete succession in the S Romanian Shelf, spanning the CC20 up to CC26 biozones (Fig. 1) than in the N Romanian shelf (Istria Basin).

| | | S Romanian Black Sea shelf (Tandala well, Melinte, 2006) | N Romanian Black Sea shelf (Histria Depression, this paper) |
|------------|---------------|---|---|
| | | Cc26 | |
| | Maastrichtian | CC25 | |
| ~ | | CC24 | |
| UPPER | | CC23 | |
| 5 | Campanian | CC22 | |
| | | CC21 | |
| | | CC20 | CC20 |
| | | NC10 | NC10 |
| | Albian | NC9 | NC9 |
| Snoa | | NC8 | NC8 |
| CRETACEOUS | Aptian | NC7 | NC7 |
| | Barremian | NC6 | |
| | Hauterivian | NC5 | |
| | Valanginian | NC4 NC3 NK2 | |
| | | | |

Fig. 1. Correlation between the biostratigraphy based on calcareous nannofossils from the southern Romanian shelf (Tândala well, after Melinte, 2006) and the N Romanian shelf (Istria Basin – results of this paper).

More diversified Tertiary calcareous nannofossil assemblages than for the Cretaceous are reported in the well logs from the Istria Basin. Therefore, assemblages indicating a continuous marine deposition from the uppermost Paleocene up to Oligocene are present. The aforementioned interval is covered by NP10 up to NP25 nannofossil zones of Martini (1971).

References

Aubry, M., 1992. Late Paleogene calcareous nannoplankton evolution: a tale of climatic deterioration. In: Prothero D.R. & Berggren W.A. (eds.): Eocene-Oligocene Climatic and Biotic Evolution. Princeton University Press, 272-309.

Bown, P.R., 1998. Calcareous nannofossils biostratigraphy. Kluwer Academic Press, 315 pp.

Bralower, T.J., Monechi, S., Thierstein, H.R., 1989. *Calcareous Nannofossil Zonation of the Jurassic-Cretaceous Boundary Interval and Correlation with the Geomagnetic Polarity Timescale*. Marine Micropaleontology 14, 153-235

Burnett, J.A., 1998. *Upper Cretaceous*. In: Bown, P.R. (Ed.), Calcareous Nannofossil Biostratigraphy. British Micropalaeontological Society Publication Series, p. 132-199.

Dinu, C., Wong, H.K., Țambrea, D., Mațenco, L., 2005. *Stratigraphic and structural characteristics of the Romanian Black Sea shelf*. Tectonophysics, 410, 417-435.

Hay, W.W., 2004. *Carbonate fluxes and calcareous nannoplankton*. In: Thierstein, H.R. & Young, J.R. (Eds.): Coccolithophores. From Molecular Processes to Global Impact. Springer-Verlag Berlin Heidelberg, 509-529.

- Ionescu, G., Sisman, M., Cataraiani, R. 2002. Source and reservoir rocks and trapping mechanism on the Romanian Black Sea shelf. In: Dinu, C., Mocanu, V. (Eds.) Geology and Tectonics of the Romanian Black Sea Shelf and its Hydrocarbon Potential. Bucharest Geoscience Forum (BGF), Special Volume, 2, 67–83.
- Lamolda, M., Melinte-Dobrinescu, M., Kaiho, K., 2016. *Calcareous nannoplankton assemblage changes linked to paleoenvironmental deterioration and recovery across the Cretaceous-Paleogene boundary in the Betic Cordillera (Agost, Spain)*. Palaeogeography, Palaeoclimatology, Palaeoecology, 441, 438-452.
- Martini, E., 1971. Standard tertiary and quaternary calcareous nannoplankton zonation. In: Farinacci, A. (Ed.), Proceedings of the second planktonic conference, Rome, 1970. Rome 737-785.
- Melinte, M.C., 2005. *Calcareous Nannoplankton, a Tool to Assign Environmental Changes*. Geo-Eco-Marina, 7-8, 136-143.
- Melinte, M.C., 2006. *Cretaceous-Cenozoic Palaeobiogeography of the Southern Romanian Black Sea Onshore and Offshore*. Geo-Eco-Marina, 9-10, 79-89, Bucharest.
- Munteanu, I., Maţenco, L., Dinu, C., Cloetingh, S., 2011. *Kinematics of back-arc inversion of the western Black Sea basin*. Tectonics, 30, TC5004.
- Okay, A.I., Şengör, A.M.C., Görür, N., 1994. *Kinematic history of the opening of the Black Sea and its effect on the surrounding regions*. Geology, 22, 267-270.
- Okay, A.I., Tüysüz, O., 1999. *Tethyan sutures of northern Turkey*. Geological Society, London, Special Publications, 156, 475-515.
- Perch-Nielsen, K., 1985. *Mesozoic calcareous nannofossils*. In: Bolli, H.M., Saunders, J.B. & Perch-Nielsen, K. (eds.): Plankton Stratigraphy. Cambridge University Press, Cambridge, 329-426.
- Roth, P.H., 1978. *Cretaceous nannoplankton biostratigraphy and oceanography of the northwestern Atlantic Ocean*. In: W.E. Benson, R.E. Sheridan and others, Initial Reports of the Deep-Sea Drilling Project, 44, U.S. Government Printing Office, Washington, D.C., pp. 731-759.
- Roth, P.H., 1983. Jurassic and Lower Cretaceous calcareous nannofossils in the western North Atlantic (Site 534): biostratigraphy, preservation and some observations on biogeography and paleoceanography. In: R.E. Sheridan, F.M. Gradstein and others, Initial Reports of the Deep-Sea Drilling Project, 76, U.S. Government Printing Office, Washington, D.C., pp. 587-621.
- Sissingh, W., 1977. Biostratigraphy of Cretaceous calcareous nannoplankton. Geologie en Mijnbouw 56, 37-65.
- Tappan, H., 1980. *Haptophyta, Coccolithophores and other calcareous nannoplankton*. The Paleobiology of Plant Protista. Freeman San Francisco, p. 678-803.
- Young, J.R., 1998. *Neogene*. In: Bown, P.R. (Ed.), Calcareous Nannofossil Biostratigraphy. British Micropalaeon-tological Society Publication Series, p. 225-265.

PROCESSING OF GEOPHYSICAL DATA FROM POTENTIAL FIELDS FOR 3D GEOLOGICAL MODELING

Laurentiu ASIMOPOLOS, Natalia-Silvia ASIMOPOLOS

Geological Institute of Romania, 1 Caransebes St., Bucharest e-mail: asimopolos@gmail.com

We present filtration procedures, correlation between several signals and other types of statistical and spectral analyses for which we have developed few procedures that can be used for correlation of geophysical parameters. The filters used provide us with information about the varying degree of regionality of the anomalies and the different depths of the sources, which of course cannot be quantified until all the information has been corroborated. These filters can bring both information about local and surface effects (through residual maps, through "high pass" filters), mid-depth structures (through "band pass" filters) and deep structure down"). The results of methods of analysing trends with polynomial surfaces are similar to those of mobile media methods representing filtration systems. In mobile averages, a portion equal to half of the mobile window used is lost on each side of the studied surface. Unlike mobile averages, the use of trend surfaces keeps the resulting surface size. Moreover, with the analytical expression of the trending surface we can extrapolate the tendency to a larger surface than the initial one. The variance of the correlation factor is calculated in a moving window that packs the entire matrix grid of values for two or more sets of parameters. This type of analysis is relevant for evaluating the correlation of parameters on certain segments of depth, given that each window used reflects the information with a certain degree of regionality and a certain depth range for the source of the studied anomalies. When the correlation factor is closer to the unit value, we can admit that the two sets of parameters studied are predominantly a common cause. Fourier analyses allow the data to be analysed by means of harmonics whose amplitudes and periods can be identified in two or more directions. The disadvantage of the Fourier transform is that with this transformation we lose the time-related information. Since many sequences in a signal are transient and non-stationary, being lost by the classical Fourier transform, we can use the shortterm Fourier transform that can analyse small signal sequences associated with time. This connects the both domains (time and frequency), while making the connection with current wavelet and multiresolution techniques.

Among the filtering methods of geological, geophysical, seismological data (data that is located on a 2D surface or in a 3D space), the moving average method, although very old, is particularly useful. Many authors have used this technique in various fields. The analysis of polynomial trends is another old method, based on the smallest squares method used for the smoothing of geological or geophysical data, which many authors have dealt [Asimopolos N.S. – 2017a,b; Asimopolos L. – 2017a,b; Farhang-Boroujeny B. – 2013; Karakus D-2011; Harbaugh J. 1972; Unwin D – 1978]. Combined use of these methods in iterative programs and compared to spectral filtering can bring quantitative information about the parameters analyzed. At the same time, Matlab currently facilitates data processing in a very fast time [Matlab-2015a; Poularikas D.-2006].

Tendency polynomial surfaces analysis in three-dimensional space is a mathematical function with a dependent variable and two independent variables. We can operate mathematically and with functions of four or more variables (hyperspace) that have great importance in some applications.

In the most general case of space \mathbf{R}^n , we choose $(\mathbf{n-1})$ independent variables and $\mathbf{1}$ dependent variable that can be expressed by the function $\mathbf{x}_n = \mathbf{f}(\mathbf{x}_1, \mathbf{x}_2, ..., \mathbf{x}_{n-1})$, representing the expression of a hyperspace . From \mathbf{n} dimensions of space Rn, we can choose up to $\mathbf{3}$ spatial dimensions (latitude, longitude and altitude) and the other $\mathbf{n-4}$ independent variables can be represented by parameters that have a causal connection with the dependent variable that we analyze by the hyperspace tendency method.

The criterion of the smallest squares, in its general form, can be expressed succinctly by:

 $\sum (X_{obs} - X_{tend})^2 = minimum$, where X_{obs} (respective X_{tend}) represent the set of observed values (respectively calculated by trend analysis). The broad description of the algorithms used, the equations of the trend surfaces and the programs developed for calculating the coefficients are in (Asimopolos N.S. – 2017a,b; Asimopolos L. – 2017a,b).

Following the same procedure, we have developed programs for the following types of surfaces: The equation of third-degree surfaces:

$$Z=A+BX+CY+DX^2+EXY+FY^2+GX^3+HX^2Y+IXY^2+JY^3$$

The equation of six-degree surfaces:

$$Z = A + BX + CX^2 + DX^3 + EY + FXY + GX^2Y + HX^3Y + IY^2 + JXY^2 + KX^2Y^2 + LX^3Y^2 + MY^3 + NXY^3 + OX^2Y^3 + PX^3Y^3 + PX^2Y^3 + PX^2Y^2 +$$

For space R4 we can calculate the hyper-surfaces z = f(x, y, w) representing a rectangular region having the nodes of the grid (xi, yl, wk), which has the equation:

$$z(x,y,w) = \sum_{i=0}^{m} \sum_{j=0}^{n} \sum_{k=0}^{p} a_{ijk} x^{i} y^{j} w^{k}$$

The equation of second degree of hyper-surfaces, from space R⁴ (X, Y, W, Z), where X, Y, W are the independent variables and Z is dependent variable:

$$Z=A+BW+CX+DY+EX^2+FWY+GXY+HWX+IW^2+JY^2$$

And so on, the equation of third degree of hyper-surfaces:

$$Z=A+BW+CX+DY+EX^2+FWY+GXY+HWX+IW^2+JY^2+KX^3+LW^3+MY^3+NX^2Y+OXY^2+PY^2W+QYW^2+RW^2X+SWX^2+TWXY$$

For mobile average method in surface we have developed programs based on the different square windows.

For moving average with different dimensions windows, we have developed programs based on the following algorithms:

We note with a_{ij} the values of the z parameter we are studying in the node of the network (i, j), where i and j take values in the range [1; n].

Also, we note $\overline{\mathbf{a}_{i,j}}$ the average values of the z parameter in the node of the network (i, j) where i and j take integer values within the related by the mobile window used.

$$\overline{a_{i,j}} = \sum_{i=-k}^{i=k} \sum_{j=-k}^{j=k} a_{ij}$$

Dimensions of window used is $4k^2$ where k is the side of a square cell for the grid used.

The variation of the correlation factor between two sets of parameters brings information for geological and tectonic assumptions. This correlation factor between two sets of data can be calculated, similarly as in mobile averages with windows of different sizes, passing through the entire network of points, bringing information from depths. The correlation between two sets of parameters may be some indicators that they are dependent on common causes.

The Fourier series is a linear combination of mono-frequential signals and describes the behavior of the original signal in time and frequency. It highlights the temporal evolution of the signal and its frequency content. If you apply direct Fourier transform to a signal is obtained the spectral function of the signal (spectral characteristic), which is a signal parameter. Spectral function is a complex quantity, which can be continuous or discrete, periodic or no periodic.

If the spectral function is discrete is called complex amplitude spectrum and characterization sizes in polar coordinates are called amplitude spectrum, respectively phase spectrum.

Even if the signal is periodic but the time window isn't chosen to be a multiple of the signal period (an integer number of periods), the spectral function obtained may be distorted. This may occur where signal acquisition isn't adapted to the signal periodicities or where periodicities of the signal purchased are not known. If the time window is chosen correctly then the actual virtual sequence coincides with infinite duration signal, otherwise the virtual signal is distorted compared the real signal. Using a time window for signal processing is equivalent to the filtering problem, but the goal is to mitigate potential discontinuities at the end of finite segment of the data evolution over time.

In order to achieve the best possible accuracy, the spectral window used (Fourier transform of the time window) must satisfy the following basic requirements:

- main lobe of the window should be very narrow;
- main lobe contains most of the window energy;
- the energy of the secondary lobes must be evenly distributed between them

Generally, these three requirements cannot be met by any window because the first two requirements are contradictory. From this point of view, we can say that there is no optimal window, each providing a compromise between the three requirements.

Bartlett temporal window provides a strong suppression of side lobes of the corresponding spectral window, however, increases the width of the main lobe and reduces its amplitude.

The Hamming time window provides a stronger suppression of the side lobes and minimizing the main lobe amplitude for the chosen frequency.

A large time window leads to a good resolution in frequency, but a low resolution in time domain (narrowband spectrogram) and a short time window determine a good location in time, but a poor frequency resolution (broadband spectrogram).

If the assessment of the power spectrum is based on direct application of Fourier transform followed by mediation, then we deal with the averaged periodogram. Mediation is usually done by dividing the signal into a variable number of segments, possibly overlapping, followed by Fourier transform calculation of all these segments (average for minute, hourly or daily of the geomagnetic signals).

Given the need for a high-performance signal analysis, many variations of spectral analysis of this type have been developed, generally called periodograms. Thus, one of the most popular periodogram mediated assessment procedures is attributed to Welch, who is a modification of the original segmentation scheme, developed by Bartlett. [Matlab-2015a].

Modern approaches of spectral analysis are designed to overcome some of the distortions produced by traditional methods and are very effective especially for short segments of analysis.

According to the Heisenberg uncertainty principle, is not possible accurate and simultaneous localization in both time domain and frequency domain.

Wavelet analysis preserves the information in the time domain and those in the frequency domain.

We performed a Fourier analysis to view the predominant frequencies for each point and can be distinguished range of frequencies.

The lower scale are correlates better with high frequencies. Small scale coefficients of continuous wavelet transform CWT highlight the fine features of the input signal. Increasing the scale values of scale allow highlight low frequency content of the signal. Wavelet cross-spectrum of two series of data, x and y,

$$C_{xy}(a,b) = S\left(C_x^*(a,b)C_y(a,b)\right)$$

 $C_{xy}(a,b) = S\left(C_x^*(a,b)C_y(a,b)\right)$, where $C_x(a,b)$ and $C_y(a,b)$ represent of continuous wavelet transform ... by Exponent * represent complex conjugate and S is an operator of smoothing.

For real values of the time series, cross-wavelet spectrum has real value. For complex values of time series, cross-wavelet spectrum is complex values. Wavelet coherence of two series of data, x and y, is:

$$\frac{S(C_{x}^{*}(a,b)C_{y}(a,b))}{\sqrt{S(C_{x}(a,b))^{2}}\sqrt{S(C_{y}(a,b))^{2}}}$$

Because the wavelet coefficients are complex valued, the coefficients provide phase and amplitude information of the signal being analyzed. Analytic wavelets are well suited for studying how the frequency content in real world nonstationary signals evolves as a function of time been a good choice when doing time-frequency analysis with the CWT.

The calculation of analytical expressions of the polynomial trends based on the least squares' method, highlight quantifiable pattern of the regional trend caused by the deep structures.

Calculating the residual values resulting from the difference between the initial values and the trend values from the network nodes used, we highlighted the superficial local effects. We also obtained information about the regional trend caused by geological structures at medium and large depths, by calculating the difference between magnetic parameters, obtained with different moving average windows or tendency surfaces with different degrees, interpolated in same network.

The types of filters presented in the paper, provide us with information with different degrees of regionality and from different depths, after all the geological and geophysical information has been corroborated. These filters can bring both information about local and surface effects (residual maps, through "high pass" filters), mid-depth structures (through "band pass" filters), and deep structure (tendency maps, through "low pass" filter).

Spectral analysis in modern approaches are designed to overcome some of the distortions produced by traditional methods, they been very effective. In Fourier spectral analysis in conformity with uncertainty principle, is not possible accurate and simultaneous localization in both time domain and frequency domain.

Wavelet analysis preserves the information both in the time domain and those in the frequency domain.

References

Asimopolos, N.S., 2017a. Contributions to deciphering the deep structure of the Vrancea seismogenic area and adjacent regions using gravimetric and geodetic data. Unpublished PhD Thesis, University of Bucharest, Faculty of Geology and Geophysics, 272 pp.

Asimopolos, L., Asimopolos, N.S., 2017a. Filtering Gravity Data Through Polinomial Trend Surfaces. DOI: 10.3997/2214-4609.201702625, 5pp.

Asimopolos, N.S., Asimopolos, L., 2017b. The importance of terrain corrections of gravity data in hydrological modeling SGEM2017 Vienna GREEN Conference Proceedings, Vol. 17, Issue 33, 363-370 pp; DOI: 10.5593/sgem2017H/33/S12.045, ISBN 978-619-7408-27-0 / ISSN 1314-2704

Asimopolos, L., Asimopolos, N.S., 2017b. Multi-parametric and correlative studies of the hydrogeological processes SGEM2017 Vienna GREEN Conference Proceedings, Vol. 17, Issue 33, 283-290 pp; DOI: 10.5593/sgem2017H/33/S12.035 ISBN 978-619-7408-27-0 / ISSN 1314-2704

Farhang-Boroujeny, B., 2013. Adaptive Filters: Theory and Applications. John Wiley & Sons, Ltd. West Sussex, 529 pp. Harbaugh, J., 1972. Aplicațiile calculatoarelor în geologie. Edit. Tehnică. București. 328 pp.

Ioane, D., Radu, I., 1995 Global geopotential models and gravity data for the territory of Romania. In: Sunkel, H., Marson, I. (Eds.), Gravity and Geoid. Joint IGC/ICG Symposium Graz, 1994, IAG Symposium No. 113, Springer, Heidelberg, 640-646.

Karakus, D., Safak, S., Onur, A. H., 2011. A new aproximation method for the trend hypersurface analysis for elevation of drilhole data. Archives of Mining Sciences. Institut Mechaniki Górotvoru. Krakow. 56, 1, 47-58.

Rădulescu, Fl., 1988. Seismic models of the crustal structure in Romania. Rev. Roum. Geol. Geophys. Geogr. Ser. Geophys., 32, 13–17.

Unwin, D., 1978. An introduction to trend surface analysis – Concept and Techniques in Modern Geography, CAT MOG 5, ISSN 0305-6142, 40 pp.

Poularikas, D., Ramadan, Z. M., 2006. Adaptive filtering primer with MatLab. Edit. CRC/Taylor & Francis Group. Boca Raton. 240 pp.

* * * * *

MATLAB and Statistics Toolbox Release 2015. The Mathworks Inc: Natick, MA, USA, 654 pp.

HOLOCENE LANDSCAPE CHANGES AND MIGRATION OF HUMAN COMMUNITIES IN THE WESTERN PART OF THE BLACK SEA (MAMAIA LAKE AREA)

Glicherie CARAIVAN

National Institute of Marine Geology and Geoecology – GeoEcoMar, Constanța branch 304 Mamaia Boulevard, 900581 Constanța, e-mail: glichericaraivan@yahoo.com

1. Introduction

Quaternary sediment samples taken from several drilling wells made along the Mamaia barrier beach where studied in details), from geological, textural, fauna points of view (Caraivan Gl., 2010; Caraivan Gl. et al., 2012).

A new opportunity to upgrade the knowledge concerning the evolution of this zone was offered by HERAS Project (MIS-ETC CODE: 578), financed through the Cross border Romania-Bulgaria Programme 2007 - 2013, when 33 samples where carefully selected for C^{14} dating, processed than by IFIN HH - Bucharest.

2. Materials and Methods

The textural, mineralogical, and faunal features of the samples were analysed in the GeoEcoMar laboratories (Caraivan Gl. et al., 2012). The depth and salinity have been estimated based on the sedimentary and faunal criteria, thus allowing the determination of several transgressive and regressive sequences.

In 2010 in the framework of the Programme of Romanian coast rehabilitation, managed by Dobrogea – Littoral Water Basin Administration, a new drilling well, 50 m depth, was made in the northern part of the Mamaia barrier beach. Undisturbed samples material where collected and significant mollusc shells where selected for C¹⁴ absolute age determinations. The radiocarbon dating process was performed at DAT (Accelerator Department Tandem) from IFIN-HH (HERAS Project), based on an AMS (Accelerator Mass Spectrometry) technique.

Absolute age data were also used, provided by Dr. Liviu Giosan from the Woods Hole Institution – USA, obtained on three samples from a depth of 10.72 to 10.00 m from the studied drill hole.

3. Results and discussions

The environmental affinities of mollusc, foraminifera and ostracod species are defined by Yanko-Hombach (2007 as: freshwater (<0.5%0), oligohaline (0.5-5%0), mesohaline (5-18%0), polyhaline (18-26%0) and eurihaline (1-26 %0). The data revealed the main stages in the recent geological evolution of the Mamaia area (Figure 1).

Zones A to C shows continental sedimentation.

Zone D reveals a continuously increasing water level and salinity. The transgression began with a silty sedimentary unit, containing brackish water fauna (**Zone D1**), with water depth estimated at about 10 m. A lacustrine stage followed (**Zone D2**) with freshwater fauna indicating a slight regression/ isolation. **Zone D3** reveals a slight rise of the brackish sea level. **Zone D4** shows a fairly rapid rise of sea level, with its upper part indicating an inner shelf marine environment (Figure 1). AMS age data indicate ages between 53690 and 47359 cal. y.B.P.

Deposits from **Zone E** have textural and faunal features of a typical cemented "beach rock", revealing that the sea level started to decrease after the maximum reached in Zone D4. The mollusc shells belong to Spisula subtruncata triangula, Chione gallina corrugatula, Paphia discrepans discrepans species. Zones D4 and E's lithologic and fauna features define them as marine landmarks.

AMS age data indicate ages between 548724 - 44604 cal. y.B.P., determined for Zone E deposits places them in MIS-3. Based on available data, a parallel could be drawn between the Zone E regressive sequence and the Tarhankutian Beds" (Shcherbakov et al., 1977). The previous marine sequence D4 is correlative with the "Surozhian Beds" of Popov (in Shcherbakov et al., 1977), revealing warmer climate conditions and higher sea level during MIS-3.

Based on the analysed data provided by the Mamaia barrier beach drill holes, we consider that the sequence D1-D4 is a typical "transgressive Surozhian" stage, and the E zone "beach rock" represents the beginning of a "regressive Tarkankutian" phase.

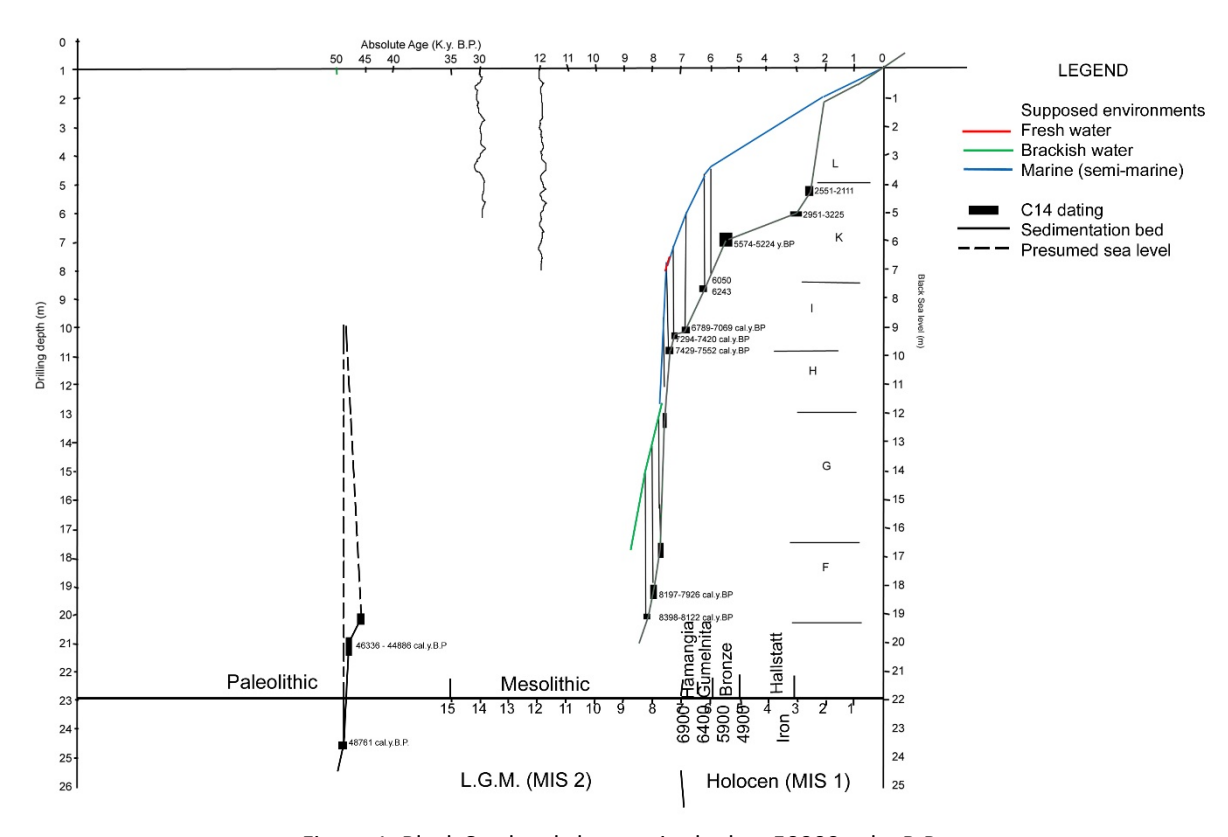


Figure 1. Black Sea level changes in the last 50000 cal.y.B.P.

Zone E, beach deposits were cemented as "beach rock" under the influence of meteoric waters, during a lasting and extended process, very common for the Last Glacial Maximum (LGM) - MIS-2 period.

After the presumed sedimentary break, subsequent to the "beach rock "genesis, a brackish water environment was established over the study area. Grey and brown clay deposits with brackish water fauna were accumulated (Zone F: 22, 57 – 20, 20 m).

At the beginning of the Holocene – MIS 1 (8408 – 8132 cal.y. B.P.), Black Sea water level grows rapidly, up to – 14 m below the present one (Figure 1). Dobrogean valleys and bays were flooded, and the shoreline became very indented. After a long lasted exposure to continental conditions, previous sediments are intensively reworked.

Zone G consists of a thick layer of fine sands accumulated in nearshore brackish water coastal conditions. The source of terrigenous material could be considered as similar to the present one (Danubian province). Sea level reaches -14 m elevation.

Zone H contains fine well-sorted and rounded sands, deposited under breaking wave conditions. According to the fauna content, basin water was of Mediterranean type, while the sediments had the same Danubian source. Sea level was about – 7 m.

Zone I (10, 72 - 8, 47 m) marks the establishment of typical inner shelf marine conditions with grey silty clay sediments, suggesting a rising sea level.

At the beginning at this sequence (10.72 to 10.00 m – **sub-Zone "J"**), Mamaia Bay is isolated from the open sea by a coastal barrier beach ("sedimentary regression"), due to a very abundant longshore sediment supply. In a swamp environment, a 40 cm thick layer of silty clay and peat was formed. The peat age is: 7429 - 7552 cal.y.B.P. at the base, and 7294 - 7420 cal.y.B.P. at its upper part. We appreciate that sea level off the sand bar was located about - 6.5 m compared to the current one.

Since 6789 - 7063 cal.y.B.P. there was a transgressive spurt ("Neolithic transgression" – Banu A.C., 1964), when the sandy bar was flooded. The sea level increased quickly by about 4.50 m in about 1000 years, locating at about -2 m to the modern one. A marine bay is formed over the Mamaia Lake area. Its western cliff followed the contour of the 2 m isobaths along Mamaia Lake western part, marked by a submerged relict terrace (Caraivan, 2010).

During this stage, the study area was probably a gulf, whose western cliffs were shaped by marine abrasion.

Zone K (8,47 – 5,00 m) is represented by a coarse lithological sequence, intensively reworked, between 5 - 1,5 Ky B.P., by the shoreward breaking waves and southward longshore currents. Sea level has risen very slowly (from - 2 m to - 0,5 m compared to the modern one. Given a weak Danubian sedimentary input, the coastal erosion intensify. The coarse sandy sediments where reworked and pushed over the "Zone I" silty-clayey sediments. The textural features of "K Zone" sediments argue a classical "sedimentary regression", of coastline retreat due to poor sedimentary budget, not to sea level rise.

Zone L (5,00 – 0,00 m) reveals the installation , during the last 1,5 K.y., of nearshore environment, similar to current conditions, but with more intensified Danubian erogenous sedimentary input.

4. Conclusions

Stratigraphic, mineralogical, textural and C 14 AMS calibrated age data have been compared with the classical Black Sea Chrono stratigraphic schemes.

The first marine sequence (Zone D 4, 40 - 60 Ky B.P.) was recorded at 38,00 - 20,20 m in the Mamaia North drill column, and may be correlated with **Surozhian beds (MIS 3)**.

The Last Glacial Maximum **(LGM)** induced the retreat of the sea level down to about 100 m below the current one (27-17 ky BP, Yanko-Hombach, 2007), followed by an advancement of the shoreline to the present position. During this period,

Zone E beach deposits, identified in the Mamaia North drill column (Tarkankutian Beds), were cemented in continental conditions.

The sea returned to Mamaia area at the beginning of the Holocene (MIS-1) stage. Consequently, the **F zone** continental deposits with scarce brackish fauna could be correlate to the Bugazian Strata. Subsequently, the Vityazevian Beds accumulated in coastal inshore conditions.

The next stage (Zone H- Lower Kalamitian Beds) marked a freshening of the coastal waters.

The accumulation of the Upper Kalamitian Strata (Zone I) is synchronous with a rapid rise of the sea level.

At the beginning at this sequence (sub-Zone "J"), Mamaia Bay is isolated from the open sea by a coastal barrier beach *("sedimentary regression")*, due to a very abundant longshore sediment supply.

Since 6789 - 7063 cal.y.B.P. there was a transgressive spurt ("Neolithic transgression" – Banu A.C., 1964), when the sandy bar was flooded. The sea level increased quickly by about 4.50 m in about 1000 years, locating at about -2 m to the modern one. A marine bay is formed over the Mamaia Lake area. Its western cliff followed the contour of the 2 m isobaths along Mamaia Lake western part, marked by a submerged relict terrace (Caraivan, 1982).

During this stage, the study area was probably a gulf, whose western cliffs were shaped by marine abrasion.

The Holocene Transgression (MIS 1) determined the sea level rise, up to the modern one. The mean rate of sea level rise was about 20 cm in 100 years, probably higher in the Atlantic Period (Climatic Optimum, 4800-7400 y.B.P.).

This process enabled the migration of the prehistoric human communities, from Asia to Europe, who established settlements on the newly created alluvial plain from the western Black Sea shelf.

Under the pressure of these environmental changes, the Neolithic settlements slowly retreated to the Dobrogean river mouths (V.Voinea, 2004-2005. That's why, traces of these prehistoric communities are found mainly along the borders of coastal lakes, and explains the scarcity of the Neolithic settlements on the adjacent shelf.

During historic times, starting with Greek colonization, the raised sea level imposed the shoreline establishment along the Dobrogean land, in configuration very similar /close to the modern one. From now on, only abrasion/sedimentation rate caused cliff shoreline retreat.

About 2200-2500 years ago, rapid coastal siltification starts. Beach sediments are intensively reworked by waves, coastal barriers being pushed landward over the previous peaty deposits.

Ancient cities closed to the Danube deltaic area remained isolated from the open sea, while those from the southern Dobrogea cliff shoreline where partially eroded and degraded and lose their economic importance.

References

- Caraivan Gl., 2010. Studiul sedimentologic al depozitelor de plaja si de selful intern, intre Portita si Tuzla. (Sedimentological study of beach and inner shelf Romanian Black Sea deposits). *EX PONTO Ed.* (In Romanian).
- Caraivan, G., Fulga, C., Opreanu P., 2012. Upper Quaternary evolution of the Mamaia Lake area (Romanian Black Sea shore), *Quaternary International 261 (2012) 14-20.*
- Peev, P.I., 2009. The Neolithisation of the Eastern Balkan Peninsula and fluctuations of the Black Sea level, *Quaternary International 197, 2009, p. 87 92.*
- Shcherbakov, F.A., Koreneva, E.V., and Zabelina, E.K., 1977. Stratigrafiia pozdnechetvertichnykh otlozhenii Chernogo moria [Stratigraphy of the Late Quaternary deposits in the Black Sea]. In *Pozdnechetvertichnaia istoriia i sedimentogenez okrainikh i vnutrennikh morei* (*Late-Quaternary History and Sedimentogenesis in Marginal and Inland Seas*), pp. 46–51. Nauka, Moscow.
- Voinea, V., 2004-2005. Cauze privind sfârşitul eneoliticului în zona litoralului vest-pontic. Aşezarea de pe Insula La Ostrov, Lacul Taşaul, Năvodari, [Causes regarding the Eneolithic End in the Western Black Sea coastal area. Lake Tasaul Ostrov Island settlement], Pontica 37 38, 2004-2005, p. 21 46.
- Yanko-Hombach, V.V., 2007. Controversy over Noach's Flood in the Black Sea: geological and foraminiferal evidence from the shelf. In: Yanko-Hombach V., Gilbert A.S., Panin N., Dolukanov P.M. (eds.), *The Black Sea Flood Question: Changes in Coastline, Climate and Human Settlement.* Springer, Dordrecht, pp. 149-203.

MINERALS INDICATED FOR THE FIRST TIME IN CONȚU PEGMATITES FIELDS, CINDREL MOUNTAINS, ROMANIA

Nicolae CĂLIN, Delia-Georgeta DUMITRAȘ, Ștefan MARINCEA, Eduard GHINESCU

Geological Institute of Romania, 012271 Bucharest, e-mail: nicolae cln@yahoo.com

The pegmatitic field is located in pegmatitic bodies, in the area between Lotru valley and Sebeş valley. The pegmatitic bodies, named Lower Conţu and Higher Conţu are located in the right and the left side of the Conţu valley. Pegmatites developed in these fields are associated with mica schists that contain kyanite and staurolite and micaceous gneisses. From mineralogical point of view, there are two types of pegmatites: (1) feldspatic pegmatites with feldspars, quartz, muscovite, biotite and accessory minerals and (2) lithium pegmatites belonging to the albite – spodumenic type in the class of rare-element pegmatites. These types are characteristic of the Conţu field (Getic pegmatites subprovince), where they can be found in lenses and lentilform bodies that are mostly in depth and to a lesser extent at the surface. The mineralogical association contains: albite, spodumene, quartz and muscovite and subordinate phosphates nests of Li, Fe, Mn, and Ca; beryl appears in the mass of quartz from Conţu pegmatites, similar to the Voislova pegmatites, Poiana Ruscă Mountain (Murariu, 2001) (Fig. 1).

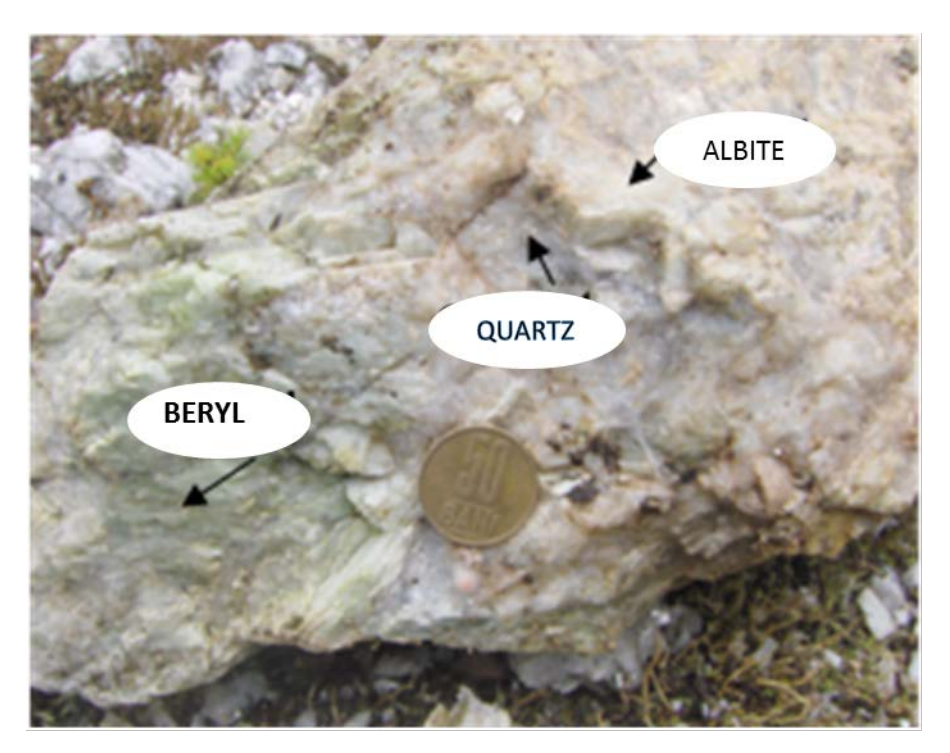


Fig. 1. Macroscopic image with green beryl in white-smoky quartz and albite, from Conţu Li-bearing pegmatites.

The analytical methods used in the study of pegmatites are electron microprobe (EMP) using a CAMECA SX50, with wavelength dispersed, BSE-EMPA, working conditioning: 15 kV and 20mA. Analyzes on EMP indicate: triphylite, ferrisicklerite, heterosite, apatite, maricite, wolfeite, ferrogatehouseite, the first mentioned mineral for the isometric series: triphylite-ferrisicklerite-heterosite and for maricite, wolfeite, the first mention in Romania from Li-bearing pegmatites from Conţu and the first mention for ferrogatehouseite in Romania and accros the globe.

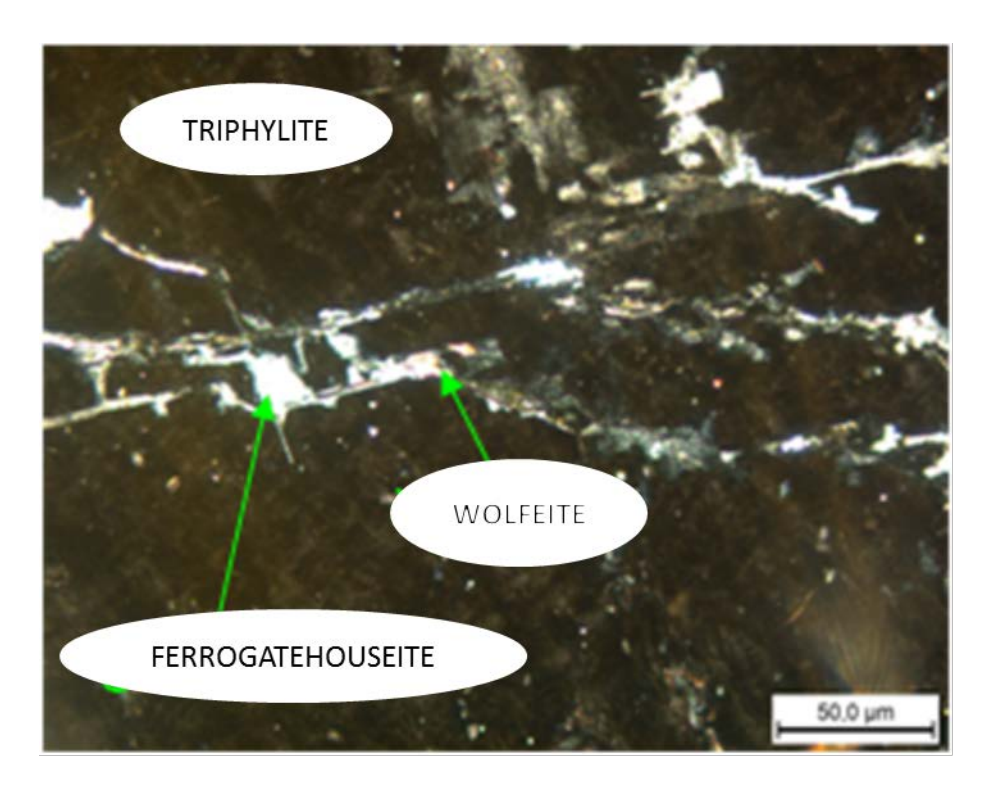


Fig. 2. Cross polarized light photo of wolfeite and ferrogatehouseite in triphylite mass, from Conţu pegmatites.

Optical microscopy was performed with Leica and Jenapol, the optical properties of the minerals were determined in plane polarized light and crossed polarized light (Fig. 2). Raman spectroscopy was conducted using a Renishaw inVia Raman microscope, with spectral values shown in sample 221-1: 113 cm⁻¹; 345 cm⁻¹; 383 cm⁻¹ corresponding to phosphates ferrisicklerite – heterosite and in sample 221-4 the spectral values corresponding to triphylite – ferrisicklerite – heterosite isometric series, the value 951 cm⁻¹, corresponding to triphylite, are here shown to be low in intensity compared to ferrisicklerite – heterosite.

References

Murariu, T., 2001. The Geochemistry of pegmatites from Romania. Editura Academiei Române, 356 pp. ISBN 973-27-0806-9.

INVESTIGATIONS OF THE SEDIMENTARY STRUCTURE ALONG TRANSYLVANIAN BASIN

Alina COMAN^{1,2}, Elena Florinela MANEA¹, Carmen Ortanza CIOFLAN¹, Mircea RADULIAN¹

¹National Institute for Earth Physics, 12 Călugăreni St., Măgurele e-mail: coman@infp.ro ²University of Bucharest, Faculty of Physics, 405 Atomiștilor St, 077125 Măgurele

The Transylvanian Basin is located inside the Carpathian Arc, in the centre of Romania, and is affected mainly by crustal seismicity manifested in surrounding seismogenic areas (e.g. Făgăraș-Campulung, Crișana-Maramureș). The current seismicity is very low in the centre of Transylvania and no large events were recorded in the last decades. In the past, 7 events Mw>5 occurred between 1223 and 1880 (ROMPLUS catalogue, Oncescu et al., 1999) with observed epicentral intensities of VII and VIII MSK. In the absence of significant Mw>6 earthquake records (from crustal and intermediate-depth events as well), we have to rely on simulation of the seismic motion induced by future/possible/expected events using realistic models of source and path propagation media. Strong amplifications are expected to occur in sedimentary cover of basins, local studies are needed to evaluate the parameters responsible for these effects.

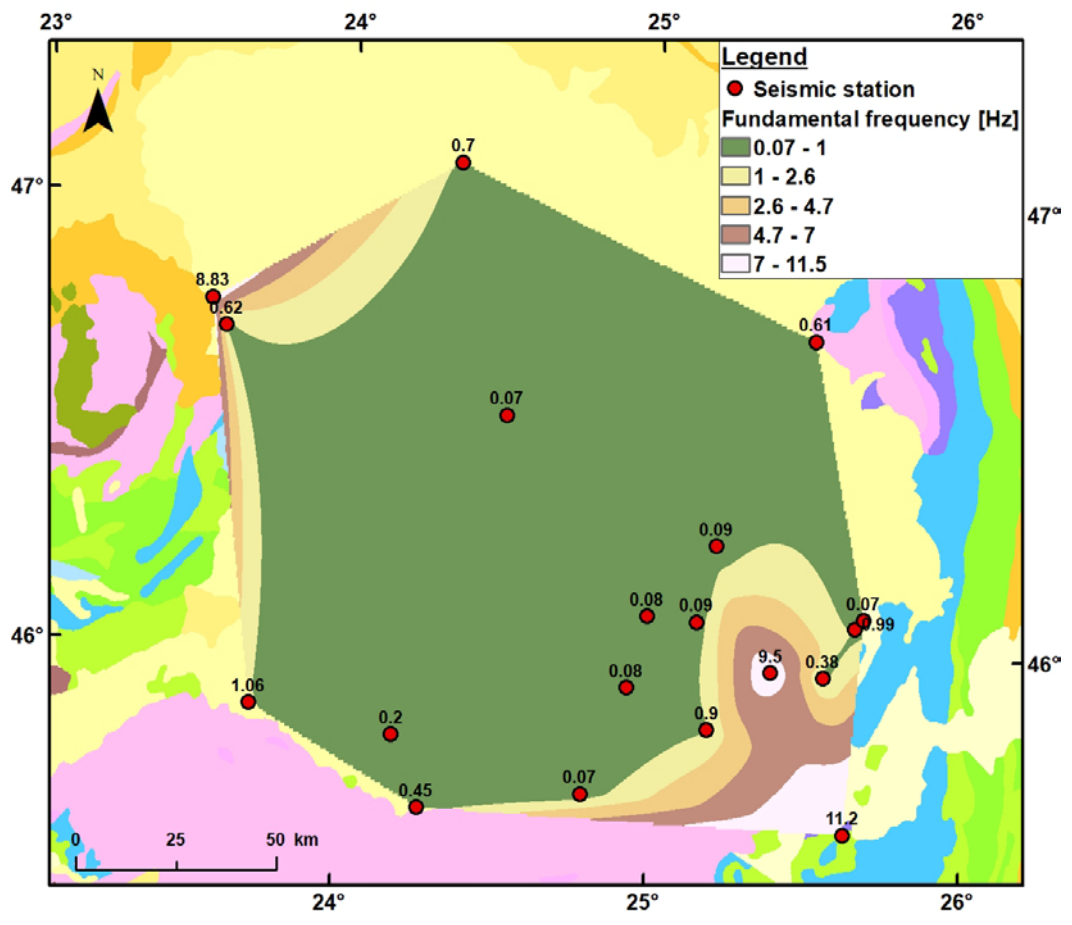


Fig. 1. Variation of fundamental frequency of resonance in the Transylvanian Basin.

The purpose of this study is to identify the sediment characteristics by mapping and interpretation of the fundamental frequency of resonance (f0) along the Transylvanian Basin using a non-invasive method applied on ambient vibration data (Fig. 1). In order to evaluate local parameters as the spatial distribution of the fundamental frequency of S-waves resonance, a non-invasive Horizontal to Vertical Spectral Ratios method (H/V, Nogoshi & Igarashi 1971; Nakamura, 1989) was performed (Fig. 2). Due to the low cost of

performing ambient vibrations measurements, this method has become increasingly used to extract essential information of the geological structure below a specific area, in order to assess the local variability. The use of this type of data is the only way to analyse essential site parameters in regions where the seismic activity is mostly absent.

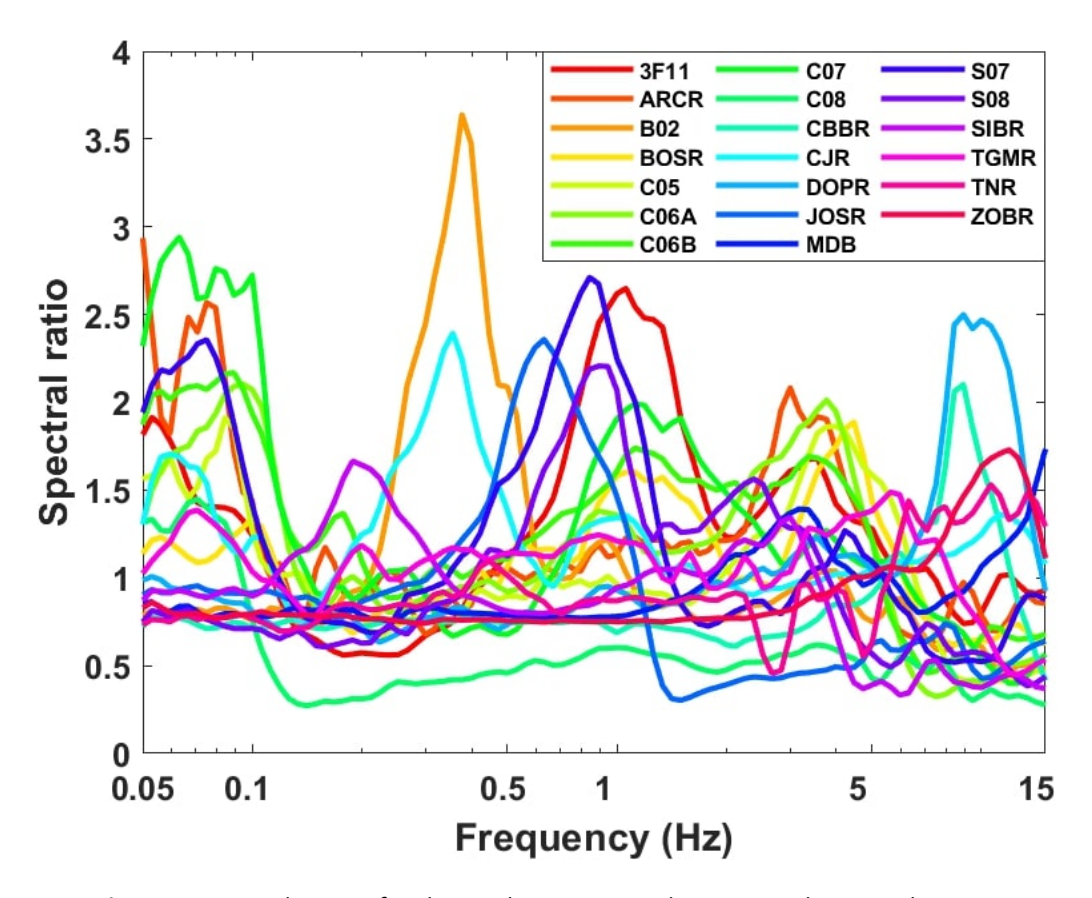


Fig. 2. HV spectral ratios of ambient vibrations at each station in the Transylvanian Basin

In this study, the H/V ratio on ambient vibrations was performed in order to retrieve the f0 along the Transylvanian Basin. This ratio was computed for 20 seismic stations deployed during two international projects, SCP - South Carpathian Project (2009 – 2011, Ren et al., 2013),) and CALIXTO - Carpathian Arc Lithosphere X-Tomography (1999, Martin et al., 2005), and the ones operated by NIEP – National Institute for Earth Physics (Neagoe C., Grecu B., Manea L. M., (2016). Earthquake monitoring at different scales in Romania, Proceedings 16th International Multidisciplinary Scientific GeoConference SGEM 2016, Albena, Bulgaria, Book 1, Vol. 3, 459 - 466).

The fundamental frequency of resonance along Transylvanian Basin varies from very low values (0.07 Hz) up to 11.2 Hz. In the light of geological layers, this peak is attributed to the geophysical bedrock and corresponds to the interface between the Badenian and Sarmatian layers. A second peak in the H/V ratios of ambient vibrations was observed, located between 0.35 and 4.9 Hz, and can be interpreted as the transition between consolidated sediments of Sarmatian age and subsequent Post-Sarmatian loose sediments. As this fundamental frequency of resonance is connected with the thickness and velocity structure of the sediments, future studies will be done on retrieving the geophysical bedrock depth based on the available geophysical/geological information.

References

Martin, M. J. R. R., Ritter, J. R. R., 2005. High-resolution teleseismic body-wave tomography beneath SE Romania—I. Implications for three-dimensional versus one-dimensional crustal correction strategies with a new crustal velocity model. Geophysical Journal International, 162, 2, 448-460.

- Nakamura, Y., 1989. A method for dynamic characteristics estimation of subsurface using microtremor on the ground surface. Rep. Railway Tech. Res. Inst., 30, 1, 25–33.
- Neagoe C., Grecu B., Manea L. M., 2016. Earthquake monitoring at different scales in Romania, Proceedings 16th International Multidisciplinary Scientific GeoConference SGEM 2016, Albena, Bulgaria, Book 1, 3, 459 466.
- Nogoshi, M., Igarashi, T., 1971. On the amplitude characteristics of microtremors, Part 2 (In Japanese with English abstract). J. Seism. Soc. Japan, 24, 26–40.
- Oncescu, M. C., Marza, V. I., Rizescu, M., Popa, M., 1999. The Romanian earthquake catalogue between 984–1997. In: Vrancea earthquakes: tectonics, hazard and risk mitigation (pp. 43-47). Springer, Dordrecht.
- Ren, Y., Grecu, B., Stuart, G., Houseman, G., Hegedüs, E., and the South Carpathians Project Working Group, 2013. Crustal structure of the Carpathian–Pannonian region from ambient noise tomography. Geophysical Journal International 195, 2, 1351-1369.

THE MINERALOGY MUSEUM FORM BAIA MARE AT 30 YEARS FROM THE OPENING OF THE PERMANENT EXHIBITION

Ioan DENUȚ^{1,2}, Alexandra SÎNGEORZAN¹, Ioan Liviu BEREȘ¹

¹County Museum of Mineralogy "Victor Gorduza" Baia Mare ²Tehnical University of Cluj-Napoca, North University Centre of Baia Mare

Introduction

The County Museum of Mineralogy "Victor Gorduza" Baia Mare (MusMin) is one of the largest museums with a geological profile from Romania and one of the most important regional museums in Europe, because the entire museum heritage comes from the mining areas of the Maramureş County.

The northwest of Romania is recognized from a geological perspective due to the products of the neogene volcanic activity and especially for those more than 20 polymetallic and gold-silver deposits, in which over 150 minerals have been described, of which 9 for the first time in the world. In addition to the significant quantities of ores extracted, geodes with unique mineral associations have been discovered through mining activities. Many of these are part of important European collections, and others, for protecting this unique heritage, constitute the collections of the MusMin today.

Brief history

The moment of setting up within the Maramureş County Museum, of the Natural Sciences Department, by Decision no. 26 of the People's Council of January 17, 1976, is a crucial moment for MusMin. To this Department, which was the basis of the creation of the Mineralogy Museum, was assigned as the main headquarters "lancu de Hunedoara" House located in the historic Old Town. The appearance of this department was demanded for the management of the existing mineral sample collection (approximately 6,000 pieces) and by the success of the first mine flower exhibition, organized in Baia Mare in 1974.

After the establishment of the Natural Sciences Department, the determination and classification of all the samples in the museum's warehouse began, the activity of purchasing mine flowers continued, and temporary exhibitions were organized in various locations in the country and abroad. In March 1982, the first mineralogical themed exhibition of a museum from Romania is organized, after the Second World War, at the Vienna House of Culture.

November 6, 1989, is very important moment in the history of MusMin, because at this date the Permanent Exhibition of the Natural Sciences Section of the Maramureş County Museum was officially opened, an exceptional cultural event appropriately evoked in the press at the time.

The building in which the Permanent Exhibition was opened and in which MusMin is still active today was designed by architect Petru Iuliu Ştefănescu and initially had as destination, on the ground floor, a shop for presentation and sale of the products from the Faimar Factory, and at the mezzanine, a gym. The agreement for the transfer of the "CORP F" building from Traian Boulevard no. 8 to the Maramureş County Museum, accomplished by issuing Decision no. 69 from 1988, of the Standing Bureau of the Executive Committee of the People's Council of Maramureş County, meant the beginning of an intense and sustained activity of elaborating the thematic of the basic exhibition, of designing the furniture and of arranging the warehouses, which culminated with the event of 6 November.

On December 10, 1992, following the decision of the Permanent Delegation of the Maramures, County Council, the Baia Mare Mineralogy Museum was officially established, with its headquarters in bd. Traian no. 8. In 2001, as a reward for the numerous exhibitions organized, the Ministry of Culture and

Religious awards to the Mineralogy Museum the "Grigore Antipa" Award, the first of its kind awarded to a museum in the field of natural sciences.

In 2014, on August 27, as post-mortem recognition of the decisive contribution that he had to the establishment of the mineralogy collection and the establishment of the Museum, the Maramureş County Council approves the attribution of the name "Victor Gorduza" to the Baia Mare Mineralogy Museum.

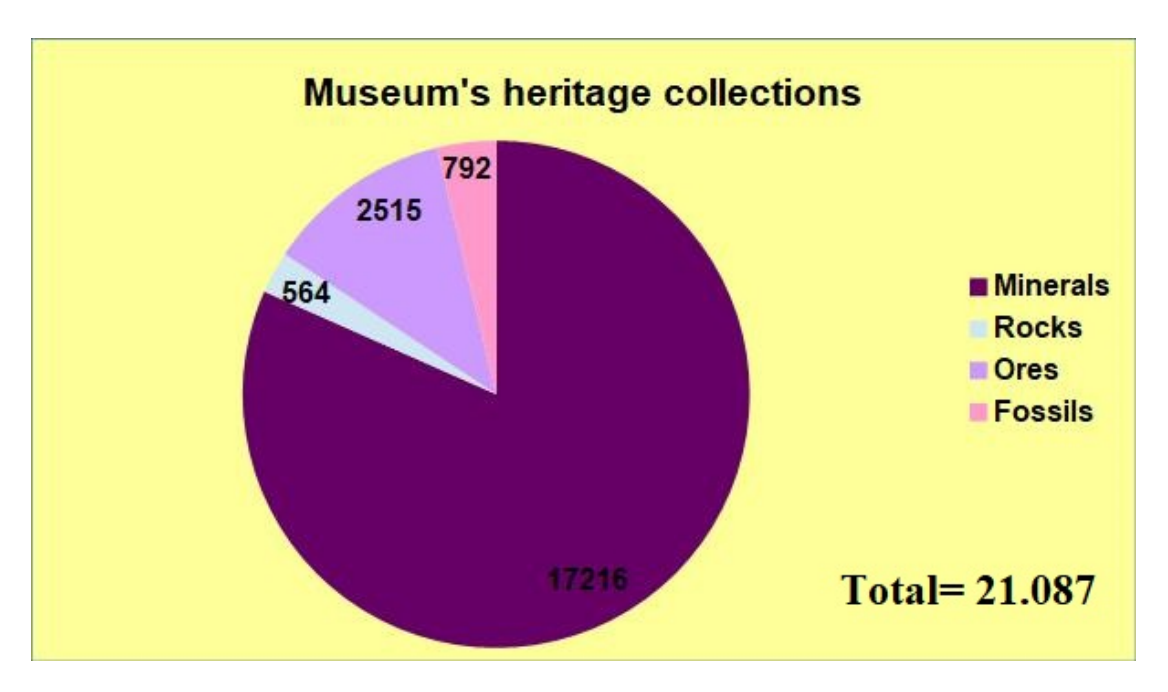


Fig. 1. The Museum's heritage collections

Museum heritage - development and capitalization

The heritage of the Mineralogy Museum was established by the purchase of mineral samples and by the receipt of donations, mainly from persons who worked in the mining operations in the Baia Mare area. The current patrimony comprises a total of 21,087 samples, grouped into four collections: minerals, fossils, rocks and ores (Fig. 1). The valorization of the museum's heritage was achieved through the permanent exhibition open at the headquarters and by organizing temporary exhibitions both in Romania and abroad.

The permanent exhibition houses over 1,000 pieces and is organized into four sections. The first three sections, located on the ground floor of the building, present the petrographic framework of the area, the properties and classification of minerals and the main characteristics of the ore deposits. The fourth section, located on the floor of the building, presents, in a unique way, in four large hexagonal windows, the most beautiful mineral samples of special aesthetic value – called mine flowers.

In the 43 years of activity, the Mineralogy Museum has reached a total of 191 temporary exhibitions, of which 45 were organized abroad, 23 at headquarters, 75 in different locations in the country, and 48 were exhibitions of other museums hosted by our museum (Fig. 2).

Evolution of visitors' number

The Mineralogy Museum is visited every year by residents of the Baia Mare area and of the Maramureş County, but also by a large number of tourists from Romania and abroad, especially from Central and Western Europe.

From the statistics regarding the annual number of visitors one can see that there is a relatively constant growth of the numbers, with two jumps, correlating with the appearance in Romania of two cultural mass events, "European Night of Museums" and the school week called "Şcoala altfel".

The current record of visitors for a year is of 32,810 visitors and was registered in 2016, and was due to the success of the temporary exhibitions organized.

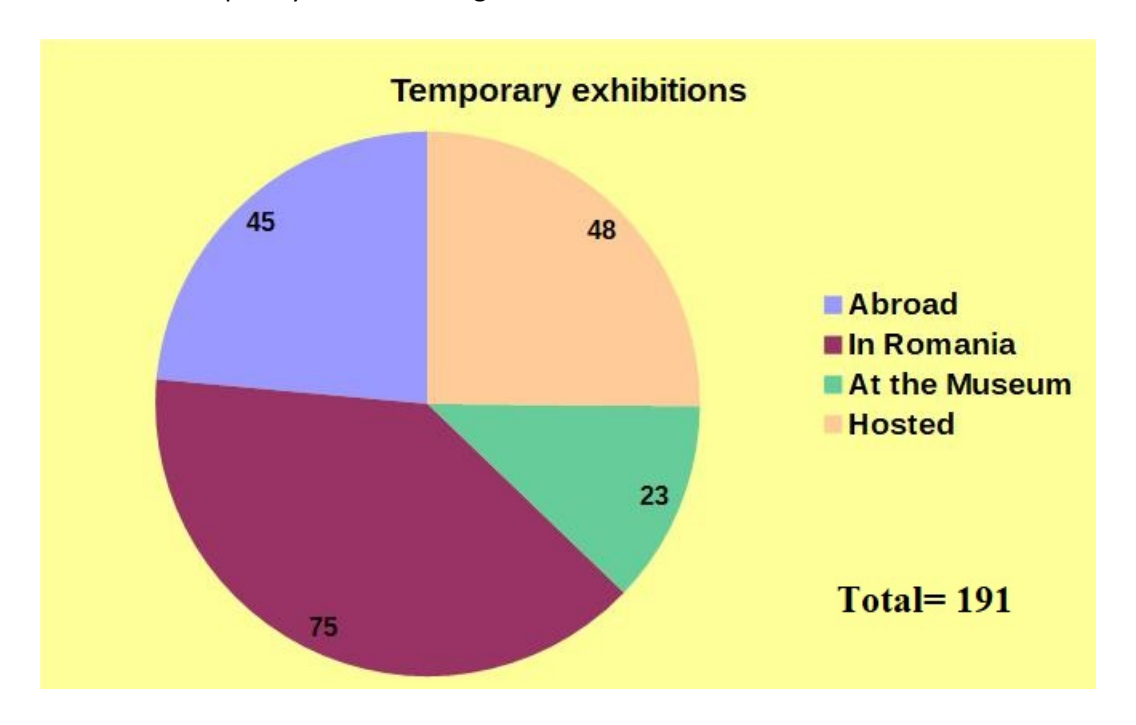


Fig. 2. Temporary exhibitions

Scientific research and museum education

The scientific research within the Mineralogy Museum aims to study the mineral and petrographic samples from its collections, in order to acquire a detailed knowledge of the physical characteristics, chemistry, genesis; this could lead to the discovery of new mineral species. The dissemination of the research results is materialized by participating in scientific manifestations in the field of earth sciences and publishing articles in specialized journals, of which we mention: Marmaţia, Drobeta, Delta Dunării, Revista Muzeelor, Studia Universitatis "Babeş-Bolyai", Scientific Bulletin of North University Center of Baia Mare, Romanian Journal of Mineral Deposits, Der Anschnitt Zeitschrift für Montangeschischtem, Mineralogy and Petrology, Acta Mineralogica – Petrographica, European Journal of Mineralogy and Minerals.

Starting with 2015, the museum organizes in May, within the "Days of Maramures,", a symposium entitled "Natural Heritage", which aims to promote the results of research on the knowledge, conservation and use of natural heritage, especially the one organized in the national network of natural protected areas.

The museum education is oriented towards collaborating with educational institutions, through the conclusion of partnerships, in order to promote the geological education and the knowledge of the importance of mineral resources among the students. Also, the museum organizes a series of natural science themed educational modules, at its headquarters.

Another direction within the educational programs aims to involve the museum in organizing field trips to the most important geosites in the northwest of Romania. Also, one of the most important educational projects implemented refers to organizing a summer school for students, entitled "Geodiversity in Maramureş", by developing practical geology lessons and trips, in locations with a generous natural heritage.

Management of natural protected areas

For the Mineralogy Museum, the custody of natural protected areas represents an inheritance, considering the initial decision, whereby, at the time of the establishment, the Department of Natural

Sciences was entrusted with the coordination of all the activity in the natural reserves, as well as of all the other natural protected objectives from the Maramureş County.

In this regard, in the current management plan a program that aims to involve the museum in the management of natural protected geological areas was introduced. Following the procedures carried out by the National Agency for Environmental Protection in 2016, the Mineralogy Museum has become custodian for three protected natural areas – the Limpedea Columns, the Ilba Stone Rosette and the Chiuzbaia Fossiliferous Reserve – until the legislation was modified in 2018.

Conclusions

Although, compared to the age of the exhibits in the museum's collections, 30 years may seem a short time, it should be noted the evolution accomplished by the Mineralogy Museum in this relatively short period of time, in terms of the significant increase in the number of mineral samples from the museum's patrimony and also regarding the evolution of the number of visitors and the intensification of the exhibition and scientific research activity.

One of the most important attributes of the Mineralogy Museum is its representativeness at local, national and European level, as the only symbol for the former Baia Mare mining region. The activity of exploitation of non-ferrous and gold-silver ores in Maramureş, with a tradition of over 650 years, was the main pillar around which the region developed. Today, 12 years after the closure of all the underground mining operations in the northwest of Romania, the only institution that keeps the memory of those times is the County Museum of Mineralogy "Victor Gorduza" Baia Mare.

References

Denuţ, I., Sîngeorzan, A., Fodor, E., Cociotă, A., 2016. Muzeul de Mineralogie la 40 de ani de activitate. Revista Muzeelor nr.1/2016, p. 96-100, Institutul Naţional pentru Cercetare şi Formare Culturală, Bucureşti. ISSN 1220-1723.

Muzeul de Mineralogie Baia Mare, 2009: 1989-2009. Editura Eurotip, 68 pp, Baia Mare.

Muzeul Județean de Mineralogie "Victor Gorduza", 2014: 25 de ani de la inaugurarea expoziției de bază. Editura Eurotip, 56 pp, Baia Mare.

NEW MINERALS FROM THE SĂCĂRÂMB ORE DEPOSIT

George DINCĂ^{1,2}, Gheorghe C. POPESCU¹

¹Dept. of Mineralogy, Faculty of Geology and Geophysics, University of Bucharest 1 Nicolae Bălcescu Boulevard, Bucharest, e-mail: georgedinca@rocketmail.com ²University of Bucharest, Research Center for Ecological Services (CESEC)

The mineralogical research from Săcărâmb ore deposit is the longest one in the Romanian territory. It starts in the first half of the 19th century, with the first research performed on the telluride minerals, continuing with the important discoveries regarding Au-Ag-Te compounds. Throughout the last century, mineralogical research at Săcărâmb has received a major upgrade with the advent of spectrometric methods in the chemical analysis of minerals. With these methods, new discoveries have been made, the most notable being telurantimony - Sb₂Te₃ (Popescu and Simon, 1992, Simon and Alderton, 1995), coloradoite - HgTe (Popescu and Constantinescu, 1992), aleksite-PbBi₂Te₂S₂, sadlebackite-Pb₂Bi₂Te₂S₃, tellurobismuthite-Bi₂Te₃ (Cook, et al., 2005), manganoquadratite AgMnAsS₃ and Cd-manganoquadratite Ag(Mn, Cd)AsS₃ (Dincă, Popescu, 2019). Located in the south-eastern part of the Apuseni Mountains, Săcărâmb represents the most complex ore deposit from the South Apuseni Mountains (Metaliferi Mountains). To perform this study, over 150 polished sections of ore samples, collected from the Săcărâmb ore dumps were analyzed by optical microscopy in reflected light. The optical microscope used was a Leitz Wetzlar reflected light microscope. For the determination of the chemical composition, a scanning electron microscope (SEM) Zeiss Merlin with an attached EDS detector was used at the Geological Institute of Romania. The parameters of the SEM analysis were: acceleration voltage raging between 15 and 20 kV, the electron beam intensity of 1-2 nA, background time of 20 s and using the Oxford Instruments X-MAX 50 EDS detector. The chemical composition and back scattered electron images (BSE) were done by a JEOL JXA 8530F field-emission gun electron probe micro-analyser (EMPA), employing JEOL and Probe for EMP analysis software (WDS mode, 25 kV, 20 nA, 2 µm beam diameter).

Over 100 mineral species were described at Sacaramb and 52 new minerals (the majority are sulfosalts) were discovered by Dincă (2019) in his Phd thesis "Mineralogy of Săcăramb Au-Ag-Te deposit, with a special look at sulfosalts". A selection of the new mineral phases discovered are presented in this paper: mimetite, Au-Te oxide, greigite, petrovskaite, staniferous copper, ferdowsiite, andorite, ramdohrite, Ag-Cu-Pb-Mn-Sb-As sulfosalt, pierrotite and boscardinite.

 $Mimetite\ Pb_5(AsO_4)_3CI$ was identified with the reflected light and electron microscope in three samples as secondary mineral on crystals of galena, bournonite and tetrahedrite with inclusions of covellite (fig. 1a). It appears in the form of a crust or nest at the boundary between sulphides and rhodochrosite. The chemical analyzes performed on the mimetite from Săcărâmb showed a deficiency of CI or even its complete lack compared to the normal composition of the mimetite.

An unindentified Au-Te oxide, with a reflection similar to that of tetrahedrite, with low, pleochroic relief, showing colors from orange to brown and having a strong anisotropy with colors from orange to blue was observed in two samples (fig. 1b). This mineral is associated with: krennerite, silvanite, coloradoite and tellurantimony. At the electron microscope, a crystal showed a clear zonation. Zoning is due to two substitutions: the substitution between Au and Te, together with the substitution between Ag, Cu, Fe and Zn. The empirical formula calculated for this mineral takes into account the substitution of Ag, Cu, Fe and Zn and the substitution of Au \leftrightarrow Te resulting in the empirical formula: (Au, Te)₈ (Ag, Cu, Zn, Fe) O₁₁ based on 20 total atoms.

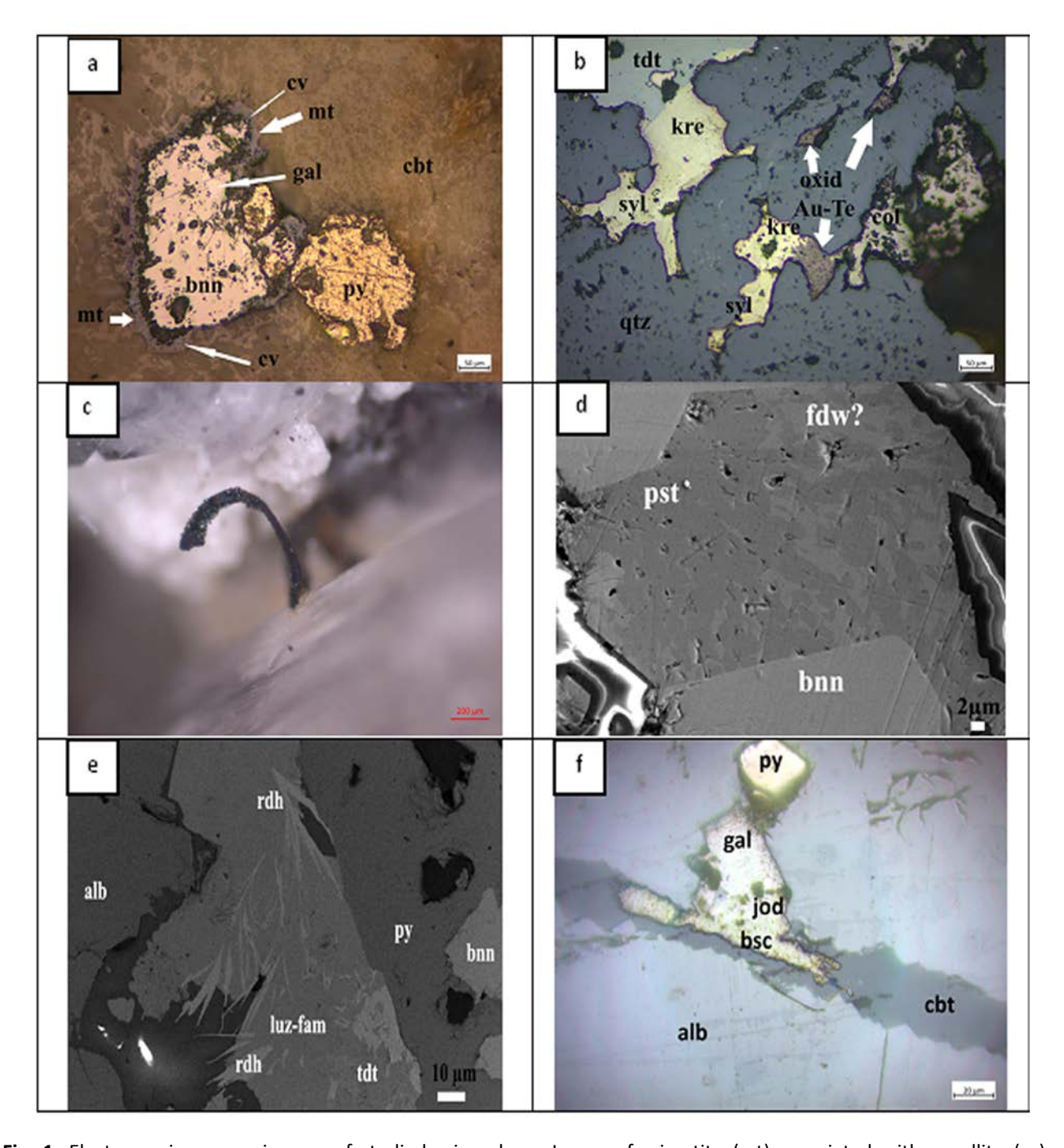


Fig. 1. Electron microscope images of studied minerals. a, Image of mimetite (mt) associated with covellite (cv), bournonite (bnn), pyrite (py) in carbonate (cbt) in reflected light //; b, photomicrograph in reflected light // of the Au-Te oxide associated with krennerite (kre), coloradoite (col), sylvanite (syl) and tetrahedrite (tdt) in quartz (qtz); c, image of the stanniferous copper wire on a gypsum crystal; d, SEM-SE image of ferdowsiite (fdw), proustite (pst) and bournonite; e, SEM-BSE image of ramdhorite(rdh) crystals in luzonite-famatine (luz-fam) with pyrite (py) tetrahedrite (tdt), bournonite and alabandite (alb); f, image in reflected light // of boscardinite (bsc), jordanite (jod), galena (gal), pyrite and alabandite.

Greigite $Fe^{2+}Fe^{3+}{}_2S_4$ has been identified in samples with alabandine, pyrite, pyromorphous pyrite (melnicovite) and sulfosalts. The crystals are of micron size between 1 and 2 μ m, with cubic euhedral shapes that form framboidal structures most often arranged in the center of arseniferous pyrite zoned structures. These structures are magnetic, a property characteristic of greigite. In reflected light greigite appears in a cream-pink color and with a reflectivity similar to that of melnicovite. Chemical analyzes have shown that it does not contain As in the structure, even though it is surrounded by rich arseniferous collomorphic pyrite.

Petrovskaite is a very rare sulfide discovered by Nesterenko et al. (1984) in the Maikain gold deposit, former USSR present Kazakhstan, named in honor of the Russian mineralogist specialized in gold deposits, Nina Vasilevna Petrovskaya. At Săcărâmb, petrovskaite was observed in a sample associated with gold in massive alabandite from the collection of the Department of Mineralogy of the Faculty of Geology and Geophysics. In reflected light and SEM it appears as a halo around the native gold granules, in some cases almost completely corroding the granules. The optical characteristics observed are: reflectivity similar to galena, light gray color, average anisotropy without distinct colors and in some granules simple twins were observed. The empirical formula of petrovskaite from Săcărâmb is Au_{0.99}Ag_{0.87}S_{1.14} calculated on the basis of three atoms.

Staniferous copper was observed macroscopically as wires in a geode together with rhodochrosite, quartz and gypsum, the largest being 10mm long (fig. 1c). Tin copper is almost completely covered with oxides, sulphides and sulphates of Cu, Sn, Zn, Mn; possibly Cu_2S chalcocite; CuSO_4 calcocyanite and chalchantite CuSO_4 • 5H2O. Staniferous copper contains on average 6 wt% of Sn, but is frequently oxidized and tin exceeds 20% in oxidized zones, due to the higher affinity to O, of copper relative to tin. The calculation of the mineral formula resulted in the basic formula $\text{Cu}_{18}\text{Sn}_{1.19}$.

Ferdowsite $Ag_8(Sb_5As_3)S_{16}$ at the optical microscope appears with a light gray color, with distinct anisotropy forming a symplectic texture with a pristine crystal (fig. 1d). From a chemical point of view, this phase is similar to the lead variety of the ferrodowsite described by Mackovicky et al. (2013) in the Barika deposit (Iran). A major difference is observed in Ag, where it appears in a much larger quantity than in the Barika ferrite and another major difference is in Sb / As, where it is lower and a percentage compared to the original ferrite. The stoichiometric formula, calculated on the basis of 32 is $Ag_{10.63}Pb_{0.71}$ ($Sb_{4.77}As_{2.01}$)_{6.78} $S_{13.88}$ with a possible ideal formula of $Ag_{10}Pb$ (Sb_5As_2)₇ S_{14} .

Andorite AgPbSb $_3$ S $_6$ was divided into two distinct species andorite IV and andorite VI by Donnay and Donnay (1954) after discovering that most andorite crystals are actually polycrystals composed of the two species. In the samples studied from Săcărâmb, andorite VI (senandorite) was observed replacing the crystals of bournonite, tetrahedrite and galena together with geocronite, benavidesite and bernarlottiite. The crystals have a prismatic shape, sub-millimetric dimensions and light gray color with a distinct pleochroism. Anisotropy is medium without distinct colors, low relief and with a lower reflectance than galena. From a chemical point of view, the andorite from Săcărâmb has a particularity, the content of Mn that appears predominantly in the crystals of the second crystallization stage. This chemistry indicates the influence of the manganiferous environment from the late hydrothermal fluid. At Săcărâmb, andorite IV (quatrandorite) was observed as a mass of acicular crystals in one sample, developed on the edge of a tetrahedrite crystal. The crystals are light gray and have a distinct pleochroism, average anisotropy and a higher reflectance than tetrahedrite. The quatrandorite from Săcărâmb is similar to the classical quatrandorite, but with Mn and As in the chemical composition.

Ramdohrite $Pb_{5.9}Fe_{0.1}Mn_{0.1}In_{0.1}Cd_{0.2}Ag_{2.8}Sb_{10.8}S_{24}$ is the member of the homologous series of the andorite with 68.75% substitution percentage and may contain Mn, Cd, Fe in the composition. It was observed in two polished sections where it appears in the form of fibrous inclusions in the famatinite (Fig. 1e). The empirical formula calculated based on 44 atoms for manganiferous ramdohrit is $Ag_{3.1}Mn_{1.5}Pb_{5.5}Sb_{11.1}S_{22.8}$.

An unindentified sulfosalt of Ag-Cu-Pb-Mn-Sb-As was discovered in the rhodochrosite secondary veins that cross massive alabandite. The crystals are subhedral, some having an almost tetragonal shape, reflectance below that of the galena, easy to sand, weak pleochroism, gray color, have a distinct anisotropy but without color. The general formula was calculated: (Cu, Ag)_{1.14}PbMn_{2.78} (As, Sb)₅S_{11.11}. There is a clear substitution between Cu and Ag, as well as between Mn and Ag, but the most interesting is the relationship between Mn and Cu, where some crystals are in the form of a substitution and others as enrichment.

Pierrotite $Tl_2(Sb, As)_{10}S_{16}$ was found in a single sample associated with manganoquadratite in the second carbonate veins, crosscuting the massive alabandite. The empirical formula was calculated on the basis of 28 atoms $Tl_{1.72}$ ($Sb_7As_{3.3}$)_{10.3} $S_{16.1}$ is very close to the stoichiometric one, with a deficit in Tl and an excess in Sb + As.

Boscardinite, $AgTI_2Pb_6(Sb_{15}As_4)_{19}S_{36}$ is a rare sulfosalt belonging to the homologous series of sartorite, recently discovered by Orlandi et al. (2014) in material from the Fe mine, Monte Arsiccio (Italy). In

| C: | : | +1 | 21St | |
|-------------|----|-----|------|---------|
| Geosciences | ın | tne | 21 | centurv |

Săcărâmb boscardinite was identified in association with jordanite by substituting galena crystals in the secondary rhodochrosite veins that cross-cut the massive alabandite (Fig. 1f).

In conclusion, Săcărâmb remains one of the most complex epithermal Au-Ag-Te deposit, with an exceptional variety of minerals. It is highly likely that future mineralogical studies could produce even more outstanding discoveries for not only Romania but for the world.

Acknowledgments. The authors are thankful to the Eldorado Gold Corporation for the support provided in the field research, to MICROCOSMOS Laboratory under the administration of the Geological Institute of Romania, for the SEM-EDS chemical analyses and to Dr. Dan Topa from Zentrale Forschungslaboratorien at the Natural History Museum, Vienna, Austria, for electron microprobe measurements and BSE images.

References

Popescu, G. C., Simon, G., 1992. New tellurides from Săcărâmb, Metaliferi Mountains (abs.) Rom. J. Mineralogy, 75, Supplem. Nr. 1 Bucuresti, p. 37-38.

Simon, G., Alderton, D. H. M., Stumpfl, E. F., Bleser, T., 1995. Tellurantimony in Romania: first occurrences in Europe. Mineralogy and Petrology, 53, 1-3, 115-124.

DISCRIMINATION BETWEEN SHALLOW EARTHQUAKES AND QUARRY BLASTS RECORDED IN DEVA REGION DURING 2010-2018 TIME INTERVAL

Raluca DINESCU^{1,3}, Ioan MUNTEANU², Corneliu DINU³, Mihaela POPA^{1,4}

¹National Institute for Earth Physics, 1 Călugăreni St., Măgurele, e-mail: raluca.dinescu@infp.ro

²Repsol S.A., Madrid, UK Exploration team, ioan.munteanu@gmail.com

³University of Bucharest, Faculty of Geology and Geophysics

⁴Romanian Academy of Scientists

The South-West Carpathian Bend Zone (SWCBZ) follows in the western direction the Carpathian Bend from Olt river to Iron Gates. This region is affected by numerous seismic events, mostly shallow and with moderate magnitude. In the region, the number of seismic recordings in the ROMPLUS catalogue is approximately 20 times larger during 2005-2018 time period in comparison with 1639-2004 time period. This large discrepancy has two explanations: the increase in the number of stations covering the region and the increased capacity to detect and locate man-made events from the quarries operating in the region. Thus, approximately 50% of the events recorded between 2005 and 2018 are located around the quarries.

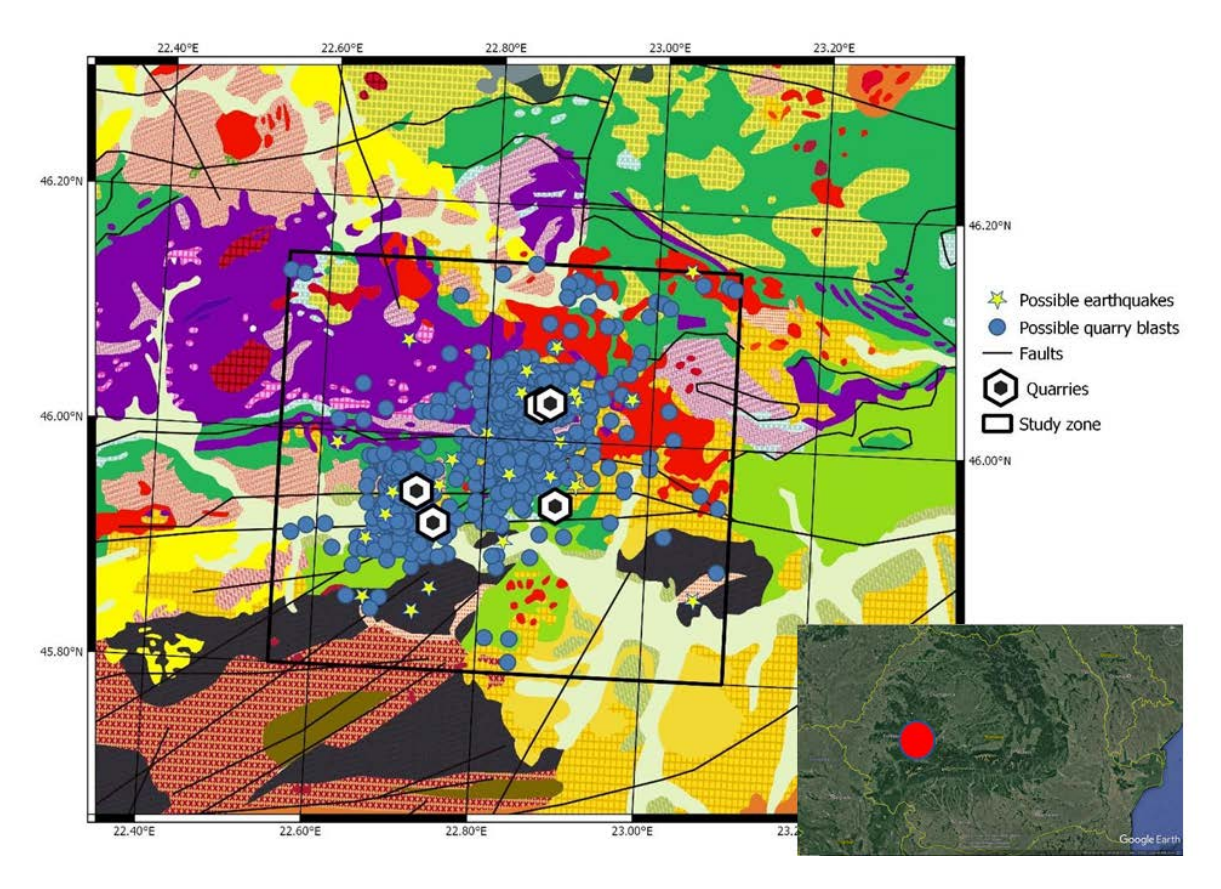


Fig. 1. Geological map from IGR.ro (after Sandulescu et al., 1978) completed with possible earthquake events, quarry blasts events. Inset – localization of the study area within the Carpathian Mountains

The study region, represented inside the black rectangle in Fig. 1, includes the main industrial quarries operating in the Deva region and surroundings extended more than 10 km away from each of the quarries. Distance of 10 km is typical for location errors, especially for small and shallow-depth events.

The strong contamination of the catalogue with anthropic events creates problems in interpreting and modelling the geodynamics of the area. Therefore, a discrimination procedure is required to separate

tectonic from anthropic events. We applied for discrimination cross-correlation technique and check the results using the records of the seismo-acoustic networks of Romania.

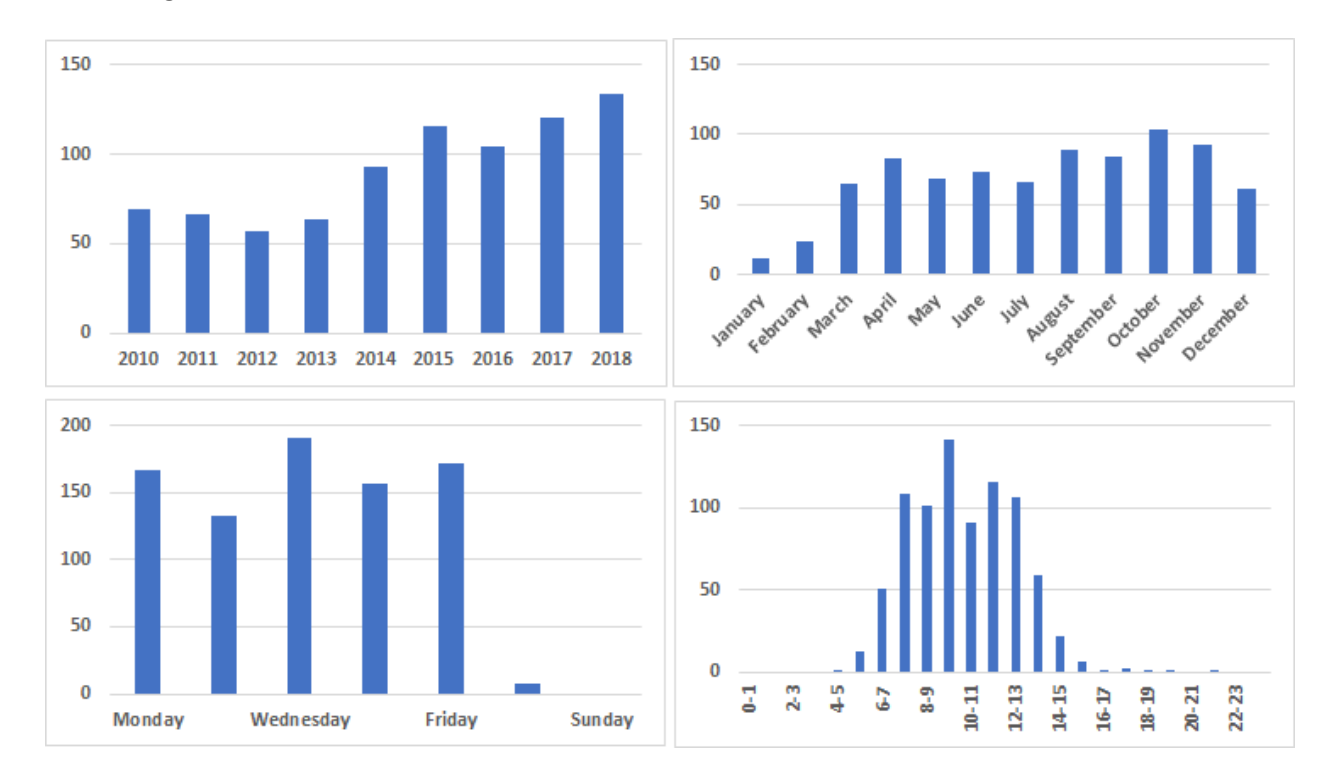


Fig. 2. Events distribution in the Deva study zone: (a) yearly, (b) monthly, (c) daily, (d) hourly (GMT time).

For this study we consider 822 events from the north-western part of Deva city, in the selected time period (Fig. 1). Almost 95% from these events were recorded around 5 quarries near Băiţa, Peştera (known as Băiţa-Crăciuneşti quarry), Păuliş and Sârbi localities.

The statistics in the region shows that yearly number of the recorded events increased with the development of the Romanian Seismic Network reflecting the increase capability of the sensors to record smaller magnitudes, such as the ones related to the anthropic activities, quarry blasts, mining, etc. (Fig. 2). The number of seismic stations increased almost 7 times from 2005 to 2018. The graphs show an increase on the recorded events per year from 5 events in 2005 to 130 events in 2018. The events recorded from Monday to Saturday, from 05 to 15 (GMT time) are considered possible quarry blasts and they will be processed throughout the cross-correlation method.

The events recorded during the night are considered natural earthquakes. The depth criterion is also used: events deeper that 15 km are not used in the cross-correlation method; we assume that these are natural events since the quarries are shallow and error in depth determination is smaller than this depth.

We selected 3 template events, recently recorded which are considered as possible quarry blasts (Fig. 3). All these 3 templates are cross-correlated with the waveforms recorded at Gura Zlata station (GZR) during 2010-2018 time interval. The events with a cross-correlation coefficient greater than 0.7 are considered as quarry blasts.

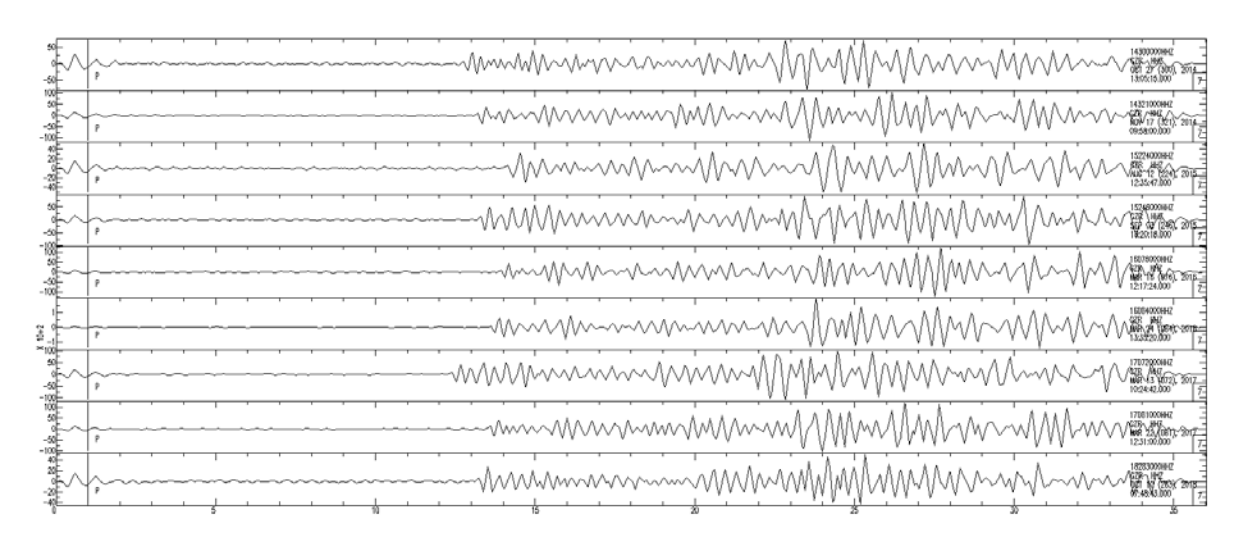


Fig 3. Templates waveform examples

The filtering of the natural events from artificial ones provides a better image of the local seismicity and a better characterization of the input parameters for the neotectonics and seismic hazard assessment in the Deva area. Obviously, evaluation of seismic hazard and the associated risk are better constrained in this way and hence our study is an important step for such evaluations.

Acknowledgments. The data processed in this paper are recorded by Romanian Seismic Network and their locations are taken from ROMPLUS catalogue (NIEP) and SHEEC catalogue. The graphs were created with Microsoft Office and the maps with QGIS application.

References

Lupu, M., Savu, H., Bercia, I., Marinescu, F., 1978. Geological map of Romania. In: Geology Atlas, sheet no 1. IGR, Bucharest.Sandulescu, M., Krautner, H., Borcos, M., Nastaseanu, S., Patrulius, D., Stefanescu, M., Ghenea, C. Edited and printed by the Geological Institute of Romania – IGR, Bucharest.

* * * * *

ROMPLUS catalogue, www. infp.ro SHEEC catalogue, https://www.emidius.eu /SHEEC/

CAPITALIZING ON SOLID MINERAL RESOURCES – ANOTHER LOST CAUSE FOR ROMANIA OF THE 21ST CENTURY?

Dorin DORDEA¹, Anca DOBRESCU²

¹SC Prospecțiuni SA, retiered, e-mail: dorin_dordea@yahoo.com ² Geological Institute of Romania, 1 Caransebeș st., Bucharest, ancadobrescu2003@yahoo.com

In the history of the human civilization, the use of various mineral resources has marked epochs, evolving leaps, growths and decreases of different civilizations, being sources of disputes or conflicts, causes of underdevelopment or prosperity. In the dark ages, mineral resources (like flint, copper, iron, gold-silver, tin, lead-zinc, etc.) have been used accidentally, wherever they were abundant at satisfactory contents. Over time, the increasing need for new resources, apparently diminished quantitatively, required the improvement of selective/ refined extraction of mineral resources, generating specialization and development. In the industrial processes, the use of mineral materials with lower elementary contents diversifies and their extraction requires new mining solutions and metallurgical or chemical preparation of increasing refinement. Tin, zinc, lead, antimony, cast iron and then steel, various salts and aluminium appear in current use successively. The transition to the rare minerals exploitation, difficult to extract, but without which today's economy could not be imagined (heavy metals, radioactive elements, rare earths, antimony, graphite, lithium, beryllium, bismuth, boron, cadmium, cesium, cobalt, germanium, hafnium, indium, niobium, tantalum, rhenium, rubidium, selenium, pure silica, tellurium, thallium, tungsten, vanadium, yttrium, zirconium, etc.) accelerated in the last 60-70 years, generating what today could define the "economic revolution of the 20th century".

Human society has been always worried about mineral resource depletion and consequently interested in new mining technologies and preparation solutions, waste conversion, new discoveries from ocean bottom up to the deep continental crust, increasing quantities of new mineral resources, continuously raising their specific consumption per capita. Besides, people and media concern regarding the pollution generated by the activities around commodities (geological, mining, metallurgical, industrial, domestic or cultural) demands for geological, mining, metallurgical and chemical solutions, in order to reduce the environmental impact and even to restore the affected actual or historical environment.

Extraction of mineral resources on the Romanian territory (Maghiar, Oltean, 1970) has developed beginning with the historical stages of Palaeolithic era (600,000-10,000 BC), Neolithic era (5,500-1,900 BC), Bronze Age (1,900-1,150 BC), Iron Age (12th-5th century BC), the Geto-Dacian stage, the period of Roman and post-Roman dominions (12th-9th centuries AC), the Middle Ages (10th-18th centuries), Romanian capitalism (1848-1944) and the socialist era (1944-1989) up to the recent one, hard to be defined yet. Observed from a historical perspective, Romanian mining has generated specific civilization nuclei marked by periods of economic emulation, sometimes of prosperity, recurrence or ephemeral existence, leaving profound traces that sometimes attract admiration, sometimes critics, but always interesting from historical perspective.

The Romanian socialist mining era began with the 1944-1976 period of continuous increasing production and number of mining objectives followed by the 1976-1989 period of decreasing production, despite increasing investments and extraction units number. Passing into a new political and economic reality of the 1989-2003 period, the Romanian mining industry had to face abruptly the market economy and the technological realities of the capitalist world and, above all, the financial pressure of the World Bank. The Romanian mining industry was constrained by the short-circuiting and the sudden abandonment (in 2003) of the subsidization of the metallic ores, which inevitably led to the cessation of the majority of the exploitations activity. Some (the coal mines in the Jiu Valley, the uranium mines and the Roşia Poieni exploitation) remained active in the same parameters of economic inefficiency and loss incurred by the state budget, besides of consistent subsidies.

The present moment of the international policy on geological research and mining industry, based on efficiency of extraction and preparation, rational use of each gram of mineral product introduced into the world economic circuit, finds Romanian mining in a moment of collapse generated by multiple causes and difficulties, apparently lacking in any prospective project.

The classification of mineral resources according to the US Geological Survey (Kimball, 2017) presents the evolution of reserves and annual consumption for the entire world economy, targets elementary categories (iron, copper, gold, silver, etc.), mineral compounds (iron oxide pigments, phosphate rocks, sodium ash, etc.), as well as industrial products (abrasives, cement, iron and steel, nitrogen, helium, etc.), with the following categories: Aluminum, Antimony, Arsenic, Asbestos, Barite, Bauxite and Alumina, Beryllium, Bismuth, Boron, Bromine, Cadmium, Cement, Cesium, Chromium, Clays, Cobalt, Copper, Diamond (Industrial), Diatomite, Feldspar and Nepheline Syenite, Fluorspar, Gallium, Garnet (Industrial), Gemstones, Germanium, Gold, Graphite (Natural), Gypsum, Helium, Indium, Iodine, Iron and Steel, Iron and Steel Scrap, Iron and Steel, Slag, Iron Ore, Iron Oxide Pigments, Kyanite and Related Minerals, Lead, Lime, Lithium, Magnesium Compounds, Magnesium Metal, Manganese, Mercury, Mica (Natural), Molybdenum, Nickel, Niobium (Columbium), Nitrogen (Fixed)-Ammonia, Peat, Perlite, Phosphate Rock, Platinum-Group Metals, Potash, Pumice and Pumicite, Quartz Crystal (Industrial), Rare Earths, Rhenium, Rubidium, Salt, Sand and Gravel (Construction), Sand and Gravel (Industrial), Scandium, Selenium, Silicon, Silver, Soda Ash, Stone (Crushed), Stone (Dimension), Strontium, Sulfur, Talc and Pyrophyllite, Tantalum, Tellurium, Thallium, Thorium, Tin, Titanium and Titanium Dioxide, Titanium Mineral Concentrates, Tungsten, Vanadium, Vermiculite, Wollastonite, Yttrium, Zeolites (Natural), Zinc, Zirconium and Hafnium.

The document delivered by USGS at the beginning of each year contains information from previous year exercise on the US reserves versus worldwide, the prices of the crude and finite products of various quality standards, consumption, production, import /export relations, prospects and new production units, etc. Regarding the evolution of stock exchange quality, depending on the volume of evaluated resources/reserves, there are no restrictions regarding the publishing information on reserves, extractions, consumption of mineral resources, even on the strategic/critical ones (gold, uranium, molybdenum, lithium, rare earths, antimony, graphite, etc.).

By contrast, the Romanian list of Commodities advanced by The National Agency of Mineral Resources - NAMR (ANRM) lacks in a number of categories, unexploited in Romania; moreover, the Romanian legislation inhibits, by its secrecy, the investments (see the classified information lists advanced by GD – 182/2002 or NARM – Orders of Confidential Information or State Restricted/Secret Information). The Romanian strategy for monitoring the resources / reserves of useful mineral substances elaborated by NAMR aims to hold the annual record on objectives (active or with ceased activity) of reserves evaluated / approved using the following specifications: categories (balance, out of balance, unclassified), groups (A, B, C1, C2), classes (industrial, geological), useful and harmful components (qualitatively presented), geological extraction, industrial extraction, loss, new identification and promotion, recalculation (±), passing from a group / category to another, increases (±), deliveries / takeovers from one unit to another, approvals. It records the following mineral substances: 1. Oil; 2. Natural gas; 3. Coal (Bituminous sand, Bituminous shale, Anthracite, bituminous coal of Banat, bituminous coal of Valea Jiului, Energetic coal of Banat, Energetic coal of Valea Jiului, Brown coal, Lignite, Coal shale, Graphite rock); 4. Ferrous metal ores (Iron ore, Manganese ore, Iron and Manganese ore, Low content iron ore, Metallurgical waste product); 5. Minerals of noble metals (Gold-silver ore, Gold-silver alluvium, Rare and disperse ore, Rare and disperse elements in proper rare and disperse ore deposits); 6. Common non-ferrous metal ores (Base metal ore, Copper ore, Low content copper ore, Copper pyrite); 7. Pyrite; 8. Rare metal ores (Uranium ore, Molybdenum ore, Beryllium ore - Beryllium pegmatites, Boron ore, Heavy ore sands, Rare and scattered elements in other deposits, Tungsten ore, Cadmium ore, ore with Arsen, ore with Antimony, ore with Tin, ore with Germanium, ore with Tellurium); 9. Aluminum ore (Bauxite - exclusively silicon bauxite, silicious bauxite, pyrophyllite shales, Nephelinic sienites); 10. Salts (rock salt, potassium salts), 11. Sulphur rock; 12. Gypsum (Anhydrite, ornamental alabaster, industrial alabaster, celestine, barite); 13. Industrial minerals (Calcite, Disthene rock, Wollastonite, pegmatite with mica, Talc rock, Asbestos rock, pegmatite with feldspar, Quartz, ornamental silicolites, ornamental aragonite); 14. Industrial rocks (basalt, basaltic scoria, diabase, ornamental andesite, Industrial andesite, Industrial dacite, Porphyry, Perlite, Ornamental granite, Granite for buildings,

ornamental granodiorite, granodiorite for buildings, diorite, non-granite sienites for glass industry, amphibolite, serpentinite, magnesite rocks - magnesian serpentinite, green shale, micaschist, gneiss, quartzite, marble, ornamental limestone, industrial limestone, chalk, travertine, dolomite, marl, loess, common clay, kaolin refractory clay, kaolin clay, kaolin-sandy clay, kaolin sand, silicious sand for glass and metallurgical industry, Sand for building materials, Sand and gravel, Industrial volcanic tuff, diatomite, phosphate rock, colored soil, flint +siliceous sand, ornamental sandstone, slate); 15. Sludge (therapeutic sapropel sludge, peat sludge, therapeutic peat, mineral sludge); 16. Mineral waters (carbonated water for food, medicinal carbonated water, medicinal sulphurous water, bicarbonated water, carbonated water, bicarbonated-sulphurous water, chlorinated-carbonated water, chlorinated-sulphurous water, chlorinatedcarbonated water sulphurous and / or sulphurous, Bicarbonated waters with temperature between 23°C-42°C, bicarbonated waters with a temperature above 42°C, bicarbonated-carbonated waters with temperatures between 23°C-42°C, sulphurous bicarbonated waters with temperatures between 23°C-42°C, chlorinated waters with a temperatures between 23°C- 42°C, chlorinated water with temperatures above 42°C, chlorinated-sulphurous water with temperatures between 23°C-42°C, chlorinated-sulfurous water with temperatures above 42°C, sulphurous water with temperatures between 23°C-42°C); 17. MOFETIC carbon dioxide; 18. Heat from hydrothermal systems; 19. Ground waters (drinking and industrial waters, groundwater for irrigation, flat drinking water for bottling directly from sources (Dordea, 2017).

The transition from centralized (state) economy of the extractive industry of mineral resources to free market one was full of efforts and major sacrifices and implied the retreat of the state involvement in the geological research and exploitation but must transfer all the risks (financial, technological and of economic efficiency) to the investors, the state preserving the guaranteed benefit of the taxation (including the specific overcharge - the royalty).

A summary analysis on the exploitation of non-hydrocarbon mineral resources over the last 30 years in Romania reveals some characteristics which can be summarized as follow:

- 1. The delay in privatization the big mining units, initiated between 1998-2001, when the privatization process was exclusively targeted to low-contents resources, some with difficult extraction conditions, out of date technical equipment and major budgetary debts;
- 2. **The number of state exploitation units reduced to one** (Roşia Poieni which becomes a study case for the solutions adopted when the accumulated debts became unpayable), due to loss, debts and cessation of state subsidies (after 2003);
- 3. Mining activity of the coal mines in the Jiu Valley will continue after 2018 (Floruţ, 2015 in Arad et al., 2019) in the state property (with the aid of consistent state subsidies, higher in comparison with the prices for the equivalent imported products of better quality), reduced drastically to 4 economic units of production;
- 4. *The increase of license fees for small and medium-sized exploration operators* for preliminary prospecting and exploration phases and exploitation, plus the necessary investments to reach the efficiency of exploiting the mineral resource;
- 5. The absence of big private Romanian capital capable and willing to take the risk of investments in new major objectives or in the old state objectives functionally blocked;
- 6. **The low level of operating** (production, efficiency) in the units owned by state (of salt and lignite), despite the opportunities and favourable conditions in the international competition;
- 7. *Illegal operations* (lack of license or authorization) of some units, possibly due to the increased levels of taxation and the tolerance of the geo-mining territorial inspection agencies;
- 8. Lack of transparency (on the NAMR policy) regarding the territorial evidence of the licensed areas for exploration / exploitation, inhibiting thus new investments in the rich areas remaining after exploration and exploitation activities (see the transparent operational models in countries with long geo-mining activity, in free market terms);
- 9. *The political and civil society pressure to the increase of the mining royalty* in the absence of a solid analysis of the effects on the budget and investments;
- 10. The numerous myths and mystifications transmitted by the political circles and civil activism (some professionals being equally responsible for such practices) about the exploitation of the mineral resources of Romania, discouraging both national and foreign investments;

- 11. Increasing extraction objectives of non-metallic substances (minerals and industrial rocks);
- 12. Increasing the number and production of mineral water objectives.

Only 2 of the 12 conclusions record emulation in the exploitation of the mineral resources in Romania, the majority and possibly others underline a dramatic decline of the domain.

Some other negative consequences of this decline are the big gaps in the geological and mining education and equally in the research activity for important geological and mining domains.

References

- Arad, V., Arad S., Samoilă L., Teseleanu G., 2019. *The coal exploitation in the Jiu Valley between the strategic resource and social impact.* Journal of Engineering Sciences and Innovation 4, 1, 99-114.
- Dordea, D., 2017. *Resursele minerale ale României o binefacere sau o povară?*. Collegium Mediense VII, Comunicări științifice XVI, Mediaș, 207-218.
- Kimball, S.,M., 2017. *Mineral Commodities Summaries 2017.* U.S. Geological Survey, Roston, Virginia, https://encrypted.google.com/#q=mineral+commodities+2017
- Maghiar, N., Oltean, Şt., 1970. Din istoria Mineritului în România. Editura Ştiinţifică, Bucureşti, 332 pp.

MISSIONS, OPPORTUNITIES AND CHALLENGES OF THE EARTH SCIENCES IN THE 21ST CENTURY: TRENDS IN HIGHER EDUCATION, FUNDAMENTAL AND APPLIED RESEARCH

Mihai DUCEA

University of Bucharest, Faculty of Geology and Geophysics, 1 Nicolae Bălcescu Boulevard, Bucharest, Romania

University of Arizona, Department of Geosciences, Tucson, AZ, USA, ducea@email.arizona.edu

Earth Sciences comprise a number of natural science disciplines historically developed to study the Solid Earth but more recently expanded to understanding the hydrosphere, atmosphere, links between the inorganic and organic realms of our planet's surface, as well as their equivalents on other planets. As such the older sciences of geology and geophysics have seamlessly merged into an ever expanding hybrid and complex array of Earth Sciences. Together, they represent the arsenal of knowledge aiding the discovery of new resources and predicting and mitigating hazards. Geosciences and their ancient forms, have been key disciplines at the core of every civilization throughout the evolution of humanity and will continue to do so into our future. Geoscientists are among the highest paid professionals in the modern world and provide unique skills that are critical for our forward movement and life on this crowded resource-craving planet.

Geology and geophysics are mature sciences that are historically connected to the resource industry (oil and gas, mineral industry, etc.). While these industries continue to employ the majority of geoscience university graduates in the 21st century, the balance of jobs is increasingly tilting away towards newer applications in either unconventional resources or major hazards facing humanity such as the threat represented by the changing of our climate. Aside from the demand provided by our adaptation needs as a society, the overall science of geology and geophysics has seen a "seismic" change in the approaches in which it is being conducted over the past couple of decades. For one, scientific literature doubles every 4 years and 6 months, which in other words means that less than 1.5% of all data anchoring various hypotheses and theories in our field were published prior to 1990. Methodologies of observation as well as experimental and theoretical models have changed dramatically towards a sophistication impossible to have been predicted 3 decades ago. A global shift in funding from public and private agencies have also forced geoscientific research for better or worse into new directions and away from the classic preoccupations universities and research institutions had in the not too distant past. Navigating through such changes has proven difficult for world class institutions in the rich world as much as it is in the developing world. To add to the confusion, most western institutions and guiding professional organizations (geological societies, etc.) have not helped the case of our community by indiscriminately mixing professional issues concerning knowledge with unrelated though otherwise worthy social causes (gender or racial biases, etc.) in their programmatic documents. Consequently, vision and perspective that are constantly needed in our (and any other) professional community to adapt and lead, often lag behind the times or turn into empty ideological slogans. Below, I will present some of the major evolutionary trends in geoscience education, fundamental and applied scientific research, new directions and disciplines and applied geosciences and the rise of artificial intelligence with its opportunities and challenges. A few examples of hot topics will illustrate the fabric of modern preoccupations although of course not exhaustive in nature. Throughout this, examples are drawn from American, Chinese and western European trends and are compared to Romanian realities, often very similar in cause. Proposed pathways forward for the Romanian geoscientific community end this essay.

Academic evolution - Degrees in Geosciences

Most American and European institutions are granting geosciences degrees after essentially 3 years of discipline-specific education, much less than in the past. This in turn translates into offering only basic core classes on geology and geophysics to the new graduate. Courses such as field camp or more in depth

traditional geosciences classes have been limited or disappeared all together even in some high profile institutions. The pressure for more students seeking degrees has turned even basic tasks like conducting a petrology laboratory more difficult given the limited number of microscopes per room. Universities are relentlessly promoting online courses and other forms of cheap and arguably inefficient methods of accommodating larger number of students and fewer educators and resources. This trend connects well with the need of corporate employers who are willing to give the university graduate specific training after employment. More advanced courses are offered for postgraduate degrees of which Master of Science degrees dominate over doctorate degrees (PhD). As a result, the modern geoscientist emerges out of his/her education with only the most limited skills of those that are traditionally thought to be required for a geologist. We focus primarily on passing on basic quest principles to our students – how to find literature, how to ask logical questions, how to present results, how to draw figures or handle large data with modern software. This adaptation is in part driven also by the students themselves – few of them read hard copies of textbooks anymore or have the patience to deal with details that are not obtainable on Wikipedia.

Currently there is a shortage of Romanian geoscience students. This is driven in part by the fact that high-school students in Romania are not exposed to geology, by the *en masse* migration of Romanian high school graduates toward western institutions and by the lack of promotion on the part of the Universities themselves. It is a multifaceted problem with no simple solutions but I strongly believe that while better course offerings and a more modern appeal needs to be built into geology departments here, the "vintage" natural science tradition could be better preserved than in western schools – it is a great opportunity to stand out. Similar geo-educational fabrics in places like Argentina or Turkey have made them highly respected internationally. Forays into climate change sciences, geobiology, modern tectonics and geomorphology, and an increased role of geophysics are an absolute must for the future survival of Romanian school of geosciences.

Basic scientific research and funding

We live in an era of declining support for basic core research funded by governments, a trend that is noticed globally, perhaps with the exception of China. The simple truth is that only around 10-15% of fundamental research proposals get funded and that number is to be found around the world. Basic bottom-up driven research outside of the "hot topics" of the day is a luxury in the 21st century and is afforded only by the most creative minds possessing the highest technology available. Romania's funding for the past decade certainly fits into that trend. Overhead rates are so high in North American institutions that the actual moneys available to the successful researcher are often minuscule, certainly in geosciences. Yet to this date, only governmental agencies provide constant and unbiased support for advances in sciences. Private company support comes primarily from oil and gas and mineral resources industries, both of which have rollercoaster rides in the modern economy and operate on relatively low margins of profit; they are not likely to invest massively in basic research today. Geosciences-related industry is not start-up and innovation driven like biotech or IT industries, but instead is a mature field undergoing relatively little in the way of discovery. Countless private trusts and foundations available (like the Gates or Packard Foundations) in the west provide little to no support in the fields of geosciences, or other physical sciences for that matter. There is little governmental/federal support for traditional geological surveys, who use to provide not only basic geologic mapping until the 1990s, but high quality connected research; these institutions have by and large collapsed as support for this science waned. To make the issue ever more difficult to navigate, funding agencies of the west have migrated toward bigger projects (more moneys but distributed in fewer projects to more researchers under complicated rules and schemes) that are multidisciplinary and geared towards hot topics such as AI or climate change. This top down approach ("we fund topics that we, the agency, think is important and not the individual researcher") has been the norm for the past at least two decades; its success is yet to be quantified. Many researchers find themselves left out in these schemes, often unable to submit proposals that fit the hot topic dejour. Whether the model of science funded primarily bottom up as problems identified solely by the exceptional researcher, will return to us as a society in the future is unclear; it will depend on how we progress as a society for the next couple of decades.

More than 50% of fundamental geo-research funding today goes toward climate change sciences, both predictive and past. Adaptation to current research trends is almost impossible without the inclusion of some climate-related relevance to one's preoccupation. Other hot topics include microgeobiology, life in extreme environments, planetary science geology, and ocean sciences.

The rise of Al-driven science and big data

We are experiencing a massive increase of data and with it one needs to manipulate large datasets in our science. Big data science is a trend away from the basic interpretations that are discipline-specific and into the statistical science of presumably understanding it all. Romania has not yet compiled its various forms of quantitative geoscience data (geochemistry and geochronology for example are the easiest to manipulate) and is in a more general sense (educational for example) completely unprepared for this new hybrid approach to what we do. Big data together with AI are promising a transformative step towards our ability to quickly access and interrogate global sets of data which otherwise would be impossible to handle by the individual researcher. The globality of geological processes at any given time (e.g. was the Ordovician the time of most arc magmatism on Earth? How does one even approach the fluxes of magma given that the exposures of Ordovician rocks are scattered across the continents?) remains one of the biggest limitations in geoscientific endeavors especially those pertaining to deep time. Al and its linguistic tools have the ability to read and examine thousands of manuscripts in a matter of hours and provide summaries of science in ways previously unthinkable. One of the biggest fears that we have is that from data acquisition to interpretations science may be performed by machines alone in the not too distant future; all young scholars interested in research should enjoy the beautiful art of scientific discovery in the old school way while they still can. In the meantime, Romanian universities and geology departments in particular, should brush up on data science and its applications to freely available global databases.

Examples of the new geology: at the interface between fundamental and applied

Below, I present a few examples of modern geoscience topics, in order to illustrate the rapidly changing fabric of our discipline. Of course this list is not comprehensive.

Carbon sequestration. Excess CO₂ from industrial activities can be captured and is ready to be stored somewhere in the Earth's interior. This activity has become one of the most important resource problems of the day – rather than extracting, we are focused on reinserting mass in the Earth's crust. Aside from the engineering aspect of the problem, it is a geological task- where will we find a home that can safely sequester large amounts of CO₂? It appears that peridotites from ophiolites are the ideal material- olivines and pyroxenes react exothermically and quickly at relatively low temperatures to form carbonates (e.g. listvenites). Finding the ideal depths and appropriately fractured materials means a reinvestigation of ophiolites from orogenic belts – a geologic task. Moreover, geo-biologists work with carbonate forming bacteria that can catalyze this process. From field mapping to experimental work and thermodynamic models, the science behind storing carbon is decidedly resource oriented and geologic. In addition, many other geologic formations provide ample evidence that natural capture of carbon through the form of carbonate veins operated in many geologic environments in the past. Accretionary wedge turbidites such as the spatially extensive flysches in orogenic belts contain enormous volumes of carbonate veins. Unraveling the conditions under which they formed diagenetically in the past is a key to future carbon capture in rocks other than peridotites.

Provenance – from rocks and minerals to food and everything else. The science of provenance originates from sedimentary geology. Today, it is a mature field drawing from geochemistry, isotope geochemistry and isotopes as well as the more classical petrographic approaches. The fingerprint of a "place of origin" on planet Earth is now extending to materials other than rock units. The same isotopes and ages that help us figure out if a geologic terrain originated elsewhere are used in tracing materials and trade in archaeology, as well as food and other edible substance. This application is particularly important as humans grow increasingly aware of the importance of knowing the source and the pathways their food supply were involved. As plants inherit the geochemical fingerprints of the rocks and soils they formed on,

the only scientists capable of tracing the origin of these substances are geoscientists. From cocoa, wine, cheese, bottled water, etc., the "tectonics of food" is one critical aspect of the new food science and our increasingly aware consumer willing to invest in safe and clean aliments. This forensic tool is obviously available to a variety of other human artifacts. This field of study is virtually untouched in Romania and a major avenue for multi- and transdisciplinary science in the future.

Anthropocene science. This newly defined epoch spans the time period of industrial Earth. There are new minerals, plastics, industrial metals accumulating downstream from our factories, from rivers and deltas to the Mariana trough. Sediment supplies have changed dramatically along major rivers globally as they have been damned for hydroelectric projects after World War II. Industrialization has literally changed the nature of sediment accumulation and metal and plastic enriched materials return into our food chain enriched tens to thousands of times relative to the pre industrial era. The mineralogy, geochemistry and petrology of the Anthropocene have become among the most important types of studies in Environmental Sciences today and are directly linked to the tools of Earth Sciences. Geological studies of modification of the natural environment in the Anthropocene are few and far between in Romania and have immense growth potential over the next decade.

Applied geoscience

Most applied geoscientists today resides in the oil and gas industry with significantly lesser numbers in the mineral industry. The oil and gas discipline is sedimentology, stratigraphy and seismology-oriented, as well as of course, engineering. Little research comes from these fields as they have a mature technology and depend financially on the ever complicated geopolitics of fossil fuels. However, new plays in shale gas as well as an interest in carbon storage from the oil industry have revitalized some of the applied scientific resources available to universities. In Romania, OMV-Petrom is the single most important employer on the Earth Science market and is a primarily downstream operation not likely to grow in the near future. Nevertheless, it is one of Romania's largest companies and an extraordinary corporate employer of geology graduates of this century.

New industry pertaining to global climate change as CO_2 becomes a marketable commodity is likely to become the major player hiring geology and geophysics graduates. This field is wide open in Romania and has been capitalized so far only by Geography Departments in academia. Otherwise, there are no Faculties of the Earth Science spectrum that are capable of producing geo-graduates with a focus on climate evolution. This is both an opportunity and a challenge for the next decade in Romania.

Romanian geosciences - possible pathways for renewed relevance and success

Geosciences have been among the most successful scientific fields of modern Romania since the early days of our Universities and research institutions. Signs of great collective success were evident to this author as a junior student 30 years ago; some of the great minds of the day, including Professor Constantinescu, in honor of whom this presentation was prepared, are still active today. It only makes sense that this immensely important and strategic science finds continued sustainability and relevance in the 21st century in Romania. Admitting that the past 3 decades were somewhat syncopated in direction and evolution, just as the entire country was due to the massive changes in society, one can strategically outline what needs strengthened, and what needs changed. The admission of "need for improvement "does not take anything away from the many brilliant individuals that continue to function in this community; instead it is a call for strategic improvement.

No individual has all the answers and vision and a strategic planning should be pursued by the Earth Science faculties in Romania in collaboration with the Ministry of Education and that of Research, the Romanian Academy of Science, and outstanding foreign European counterparts with experience in strategic planning. The following are a starting point towards a big picture discussion: Romanian geosciences need better integration with other natural science disciplines, a curricular diversification to expand toward new geoscientific preoccupations, a major upgrade in data acquisition technology, applications to BIG DATA, and

| Geosciences in the 21 st century |
|---|
|---|

massive reintegration and collaborative projects with peers from outside its borders in geology and geophysics.

CARBON CAPTURE AND STORAGE ACTIVITIES OF GEOECOMAR. AN OVERVIEW

Alexandra-Constanța DUDU, Constantin-Ștefan SAVA, Sorin ANGHEL, Corina AVRAM

NRDI GeoEcoMar, 23-25 Dimitrie Onciul St, Bucharest, e-mail: alexandra.dudu@geoecomar.ro

The adoption of the Paris Agreement on reducing greenhouse gas emissions is an extremely important step in limiting global climate change and the disastrous effects that have already begun to be felt. The targets for reducing emissions derived from UNFCC (United Nations Framework Convention on Climate Change) members commitment to limit global warming to less than 2°C (1.5°C) are quite ambitious and, according to emission evolution models, will not be achieved without the widespread implementation of CCS (CO₂ capture and storage technology) (IPCC, 2014; GCCSI, 2016, 2018; IEA; 2016). The latest report of IPCC (2018) recognizes that CCS "play(s) a major role in decarbonizing the industry sector in the context of 1.5°C and 2°C pathways, especially in industries with higher process emissions, such as cement, iron and steel industries." Global CCS Institute (2018) assumes that more than 2500 CCS facilities (with a capture capacity of more than 1.5 million tonnes per annum) would be needed in operation by 2040 in order to achieve emission reduction targets.

CCS was recognized in Romania as an important method of decarbonizing the energy sector within the National Energy Strategy (Ministry of Energy, 2016) and the National Strategy for Climate Change 2013 – 2020 (Ministry of Environment, 2012).

But the research in CCS has started almost two decades ago, in 2001, with the accession of GeoEcoMar to ENeRG (European Network for Research in Geo-Energy) and participation in the CASTOR research program. Subsequently, specialists from the University of Bucharest and GeoEcoMar participated in important pan-European research projects on the geological storage of CO₂ from FP6 (EUGeoCapacity, CO₂ NetEast), FP7 (CGS Europe, CO₂Stop) and Fenco Era "Impact of communication".

In 2006, within EUGeocapacity project, the theoretical CO_2 geological storage capacity for Romania was estimated. Only onshore solutions were taken into account, deep saline aquifers and depleted hydrocarbon reservoirs. The location of the storage solutions can be seen on Fig. 1.

Thus, the theoretical storage capacity of CO_2 in deep saline aquifers has been estimated at 18.6 Gt CO2 (Sava et al., 2006, Sava et al., 2007, Sava et al., 2009), the sedimentation basins hosting the regional saline being divided into four major regions: Moesian Platform and the Southern Carpathian Foredeep, Moldavian Platform and the Eastern Carpathian Foredeep, Transylvanian Basin and the Pannonian Basin (Sava et al., 2009).

The theoretical CO₂ storage capacity in depleted hydrocarbon fields was estimated to 4 GT CO₂ (Sava *et al.*, 2006, Sava *et al.*, 2007, Sava *et al.*, 2009). The estimation was made on separate geological units: Pannonian Depression, Transylvanian Depression, Bârlad Depression, Nord Dobrogean Promontory, Eastern Carpathian, Getic Depression and Moesian Platform.

In 2010, with the preparation for the launch of the NER300 financing program, the Romanian Government started the procedures for implementing a CCS demo project in Romania, signing since February 2010 the memorandum "Action plan for the implementation of a CCS demonstration project in Romania". In August of the same year, the Ministry of Economy contracted within the sectoral plan the research project "National Plan for Carbon Capture and Storage (CCS) with time horizon 2020", coordinated by GeoEcoMar.

For the implementation of a demonstration project, a selection of tenders was made, following which it was decided to apply the CCS technology to the Turceni power plant, specifically to the block no. 6 (existing) 330 MW, rehabilitated, operating on lignite. By order no. 1508 of the Ministry of Economy, Trade and Business Environment, was set up in August 2010 the inter-ministerial committee to lead the project composed of representatives of the Ministry of Economy, Trade and Business Environment, Ministry of

Environment and Forests, Ministry of Public Finance, National Agency for Resources Minerals, of the National Authority for Scientific Research, SC Turceni Energy Complex, of the National Transport Company for Natural Gas "TRANSGAZ" S.A. Mediaş and of the National Society of Natural Gases Romgaz S.A. Mediaş. By the same order, the beneficiaries of the project are designated as S.C. Turceni Energy Complex S.A. (CO₂ capture operator), National Transmission Company of Natural Gas "TRANSGAZ" S.A. Mediaş (CO₂ transport operator) and of the National Natural Gas Company Romgaz S.A. Mediaş (CO₂ storage operator). Responsible for the technical documentation of the project were named the Institute of Energy Studies and Designs - ISPE and the National Institute for Research and Development on Marine Geology and Geoecology – GeoEcoMar.

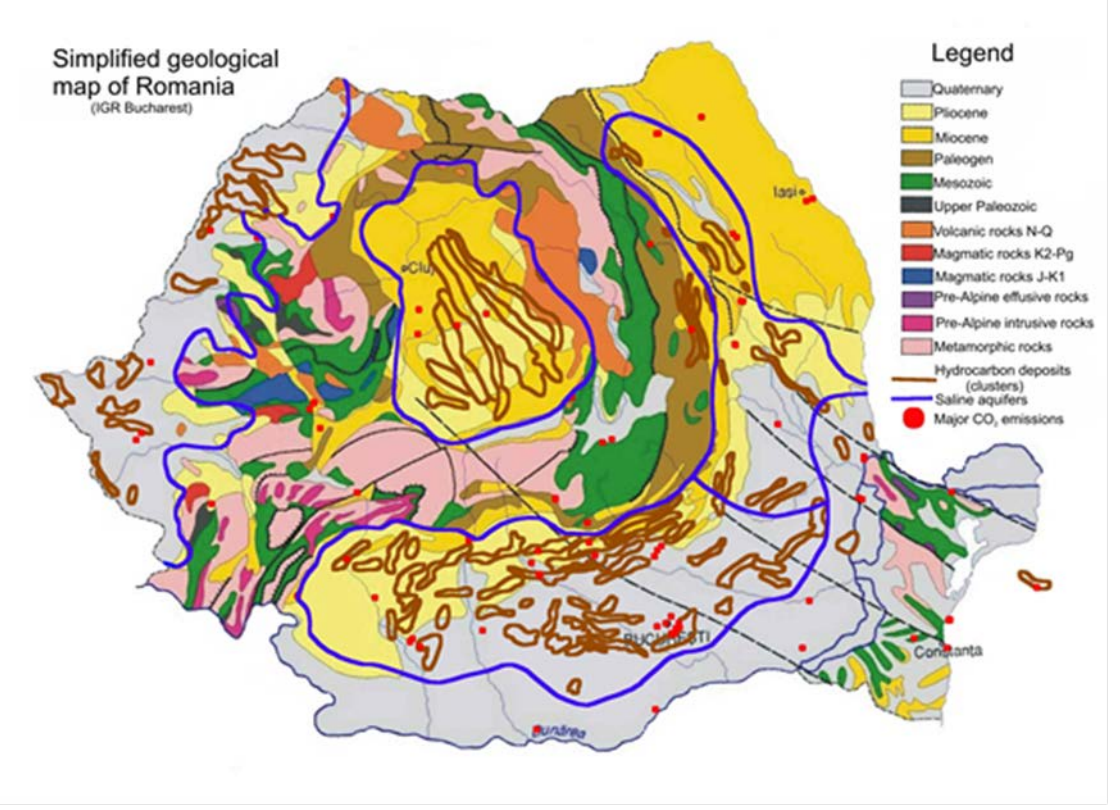


Fig. 1. Location of CO₂ geological storage solutions and major CO₂ emissions (Sava et al., 2009).

The feasibility study of the project was funded by the Global CCS Institute and the Ministry of Economy, Trade and Business and was at the basis of the application form for the NER 300 funds, an application submitted to the European Investment Bank. The demonstration project was due to enter into operation in December 2015. Following the failure of NER 300 program, the refuse of the Romanian government to support GETICA CCS and the impossibility to complete the funding scheme of the project, GETICA CCS was stalled indefinitely.

In the meantime, the CCS Directive was transposed into Romanian legislation (Law No 114/2013) and the specific procedures for granting exploration and storage permit were issued by the Competent Authority for CO₂ geological storage in Romania, National Agency for Mineral Resources (NAMR).

The year 2017 meant starting the assessment of storage possibilities in Histria Depression (Black Sea) and also two new projects, within ACT (Accelerating CCS Technologies) program, ECOBASE and ALIGN-CCUS. The start of ECOBASE project meant the start of CO₂-EOR (Enhanced oil recovery through injection and storage of CO₂) assessment in Romania. Until now, several clusters have been assessed for implementing CO₂-EOR and a study case has been chosen in order to demonstrate the business case for implementing the technology. Within ALIGN CCUS, Romanian consortium has the role in defining a blueprint for Oltenia region, identifying and describing CCUS (Carbon Capture, Utilization and Storage) pathways.

In Horizon 2020, GeoEcoMar participates within two projects: ENOS (Enabling Onshore Storage in Europe) and STRATEGY CCUS. STRATEGY CCUS is focused in Romania for another region with major CO₂ emissions, Galati region.

The most recent research and direction of study for CO₂ geological storage in Romania began in 2019 within GeoEcoMar core program and is focused on identifying natural laboratories for the study of monitoring methods in areas with natural emissions, Harghita and Banat.

References

IEA. 2013. Technology roadmap. Carbon Capture and Storage.

IPCC, 2014: Climate Change 2014: Synthesis Report. Contribution of Working Groups I, II and III to the Fifth Assessment Report of the Intergovernmental Panel on Climate Change [Core Writing Team, R.K. Pachauri and L.A. Meyer (eds.). IPCC, Geneva, Switzerland, 151 pp.

IPCC, 2018: Summary for Policymakers. In: Masson-Delmotte, V., Zhai, P., Pörtner, H.-O., Roberts, D., Skea, J., Shukla, P.R., Pirani, A., Moufouma-Okia, W., Péan, C., Pidcock, R., Connors, S., Matthews, J.B.R., Chen, Y., Zhou, X., Gomis, M.I., Lonnoy, E., Maycock, T., Tignor, M., Waterfield, T. (eds.), Global Warming of 1.5°C. An IPCC Special Report on the impacts of global warming of 1.5°C above pre-industrial levels and related global greenhouse gas emission pathways, in the context of strengthening the global response to the threat of climate change, sustainable development, and efforts to eradicate poverty). In print.

Global CCS Institute, 2016. The global status of CCS: 2016. Australia

Global CCS Institute, 2018. The Global Status of CCS: 2018. Australia.

Ministry of Energy (Ministerul Energiei). 2016. Strategia Energetică a României 2016 - 2030,cu perspectiva anului 2050. 15 noiembrie 2016.

Ministry of Environment (Ministerul Mediului). 2012. Strategia națională a României privind schimbările climatice 2013 – 2020

Sava, C.S, Andrei, J., Heredea, N. 2006. CO2 Emissions and Geological Storage Possibilities in Romania: "The 1st EU GeoCapacity Working Meeting", 31 May-1 June 2006, Toledo, Spain.

Sava, C.S., Georgescu, C., Scrădeanu, D. 2007. State of work in Romania: "The 2nd EU GeoCapacity Working Meeting", 12-17 March 2007, Athens, Greece.

Sava, C.S., Anghel, S., Dudu, A. 2009. CO₂ Storage Possibilities in Romania, Side Event - Prospects and challenges for CCS implementation in the new EU members States and candidate countries, The 5th BGS Congress –Geophysics at the Crossroads, 10-16 May 2009, Belgrade, Serbia.

BRUSHITE FROM SEVERAL CAVES IN SOUTHERN ROMANIA: CRYSTALLOGRAPHIC AND INFRARED DATA

Delia Georgeta DUMITRA޹, Ştefan MARINCEA², Aurora-Măruța IANCU¹ Ciprian CONSTANTINA¹

¹Geological Institute of Romania, 2 Kiseleff Road, Bucharest e-mail: d_deliaro@yahoo.com ²Geological Institute of Romania, 1 Caransebeş Str., Bucharest

Brushite, ideally Ca(HPO₄)•2H₂O, is one of the most important phosphate species occurring in the guano-bearing caves world-wide. Schadler (1929) first mentioned brushite in the bat guano deposit at Cioclovina, Sureanu Mountains, Romania, but number of other occurrences were found (see Dumitraş, (2013) and references therein). The mineral forms at product of reaction between the strongly acidic phosphatic solutions derived from the guano deposits and the carbonate substrate of the cave, or the flows of moonmilk. It generally associates with hydroxylapatite, occurring as nodular masses or as aggregate powders of bright white (snow white) color. SEM examination of micromounts showed that the brushite masses are generally composed by sheaf-, cluster-like or rarely by radiating aggregates of crystals to a diameter of 0.2 mm. Pure micromounts were selected for analysis, after the check for purity based on X-ray powder diffraction analysis.

This paper reports and partially documents the crystallographic parameters and the infrared behavior of brushite from fossil bat guano deposits in fifteen caves from Romania.

The unit cell parameters of a substantial number of samples from the analyzed caves were calculated by least-squares refinement from XRD powder data, using reflections in the 2θ range from 5 to 90° . An extensive collection of such parameters is given in Table 1.

Table 1. Cristallographic parameters of selected samples of brushite from caves in Romania.

| Sample/Cave | a (Å) | b (Å) | c (Å) | 6 (o) | V (ų) |
|--------------------------|----------|-----------|----------|--------------|----------|
| 2214 B, "Dry" Cioclovina | 5.807(3) | 15.186(5) | 6.242(3) | 116.33(2) | 493.4(3) |
| 2217 A, "Dry" Cioclovina | 5.817(1) | 15.187(3) | 6.249(1) | 116.35(1) | 494.8(1) |
| 2217 B, "Dry" Cioclovina | 5.816(1) | 15.195(3) | 6.242(1) | 116.40(1) | 494.1(1) |
| D 2 C, "Dry" Cioclovina | 5.960(5) | 15.163(2) | 6.354(7) | 116.29(9) | 514.9(2) |
| D 7 B, "Dry" Cioclovina | 5.819(3) | 15.181(6) | 6.233(3) | 116.33(2) | 493.4(3) |
| D 9 B, "Dry" Cioclovina | 5.809(3) | 15.168(9) | 6.244(3) | 115.80(3) | 493.5(3) |
| D 13 C, "Dry" Cioclovina | 5.821(2) | 15.149(4) | 6.238(2) | 116.34(2) | 493.0(2) |
| D 13 D, "Dry" Cioclovina | 5.823(3) | 15.174(8) | 6.243(3) | 116.52(3) | 493.5(3) |
| D 14 A, "Dry" Cioclovina | 5.806(3) | 15.163(4) | 6.237(2) | 116.46(2) | 491.6(2) |
| D 17 B, "Dry" Cioclovina | 5.810(3) | 15.170(6) | 6.230(3) | 116.35(3) | 492.1(3) |
| D 17 C, "Dry" Cioclovina | 5.808(2) | 15.174(7) | 6.249(4) | 116.19(2) | 494.2(3) |
| D 19 A, "Dry" Cioclovina | 5.818(7) | 15.206(1) | 6.252(7) | 116.44(1) | 495.2(6) |
| D 19 B, "Dry" Cioclovina | 5.812(3) | 15.167(6) | 6.261(3) | 116.32(2) | 494.7(3) |
| D 19 C, "Dry" Cioclovina | 5.813(2) | 15.158(5) | 6.247(2) | 116.25(2) | 493.7(2) |
| D 30 C, "Dry" Cioclovina | 5.806(1) | 15.174(3) | 6.232(1) | 116.43(1) | 491.7(1) |
| D 33 A, "Dry" Cioclovina | 5.808(2) | 15.168(3) | 6.240(2) | 116.41(1) | 492.4(2) |
| D 33 B, "Dry" Cioclovina | 5.812(2) | 15.178(6) | 6.249(2) | 116.30(2) | 494.2(2) |
| D 35 A, "Dry" Cioclovina | 5.805(3) | 15.189(7) | 6.251(3) | 116.22(3) | 494.4(3) |

| D 35 C, "Dry" Cioclovina | 5.807(1) | 15.179(2) | 6.240(1) | 116.37(1) | 492.9(1) |
|--|----------|------------------|----------|-----------|----------|
| D 36 A, "Dry" Cioclovina | 5.821(3) | 15.151(7) | 6.243(3) | 116.12(3) | 494.2(3) |
| D 36 B, "Dry" Cioclovina | 5.816(2) | 15.186(4) | 6.234(2) | 116.14(2) | 494.3(2) |
| D 38 A, "Dry" Cioclovina | 5.812(5) | 15.191(8) | 6.244(6) | 116.40(1) | 493.8(5) |
| D 38 B, "Dry" Cioclovina | 5.808(2) | 15.169(4) | 6.247(2) | 116.36(2) | 493.1(2) |
| D 38 C, "Dry" Cioclovina | 5.816(2) | 15.168(5) | 6.241(2) | 116.12(2) | 494.3(2) |
| D 39 A, "Dry" Cioclovina | 5.808(1) | 15.177(2) | 6.241(1) | 116.42(1) | 492.6(1) |
| D 39 B, "Dry" Cioclovina | 5.813(2) | 15.165(5) | 6.243(2) | 116.14(2) | 494.1(2) |
| D 40 A, "Dry" Cioclovina | 5.813(1) | 15.190(1) | 6.245(6) | 116.41(1) | 493.9(6) |
| D 41 A, "Dry" Cioclovina | 5.807(2) | 15.167(4) | 6.239(2) | 116.21(2) | 493.0(2) |
| D 41 B, "Dry" Cioclovina | 5.805(1) | 15.175(2) | 6.240(1) | 116.37(1) | 492.5(1) |
| D 41 C, "Dry" Cioclovina | 5.804(2) | 15.179(6) | 6.247(2) | 116.28(2) | 493.5(2) |
| D 42 C, "Dry" Cioclovina | 5.812(2) | 15.179(6) | 6.242(2) | 116.19(2) | 494.1(2) |
| D 43 A, "Dry" Cioclovina | 5.808(1) | 15.176(2) | 6.240(1) | 116.37(1) | 492.9(1) |
| D 43 B, "Dry" Cioclovina | 5.812(2) | 15.160(6) | 6.240(2) | 116.36(2) | 492.6(2) |
| D 52 A, "Dry" Cioclovina | 5.807(2) | 15.167(3) | 6.231(2) | 116.37(1) | 491.6(2) |
| D 52 B, "Dry" Cioclovina | 5.810(2) | 15.183(6) | 6.243(2) | 116.33(2) | 493.6(2) |
| D 59 E, "Dry" Cioclovina | 5.814(2) | 15.172(4) | 6.235(2) | 116.42(2) | 492.5(2) |
| D 61 A, "Dry" Cioclovina | 5.816(2) | 15.159(5) | 6.236(2) | 116.35(2) | 492.6(2) |
| D 62 A, "Dry" Cioclovina | 5.807(1) | 15.166(3) | 6.240(2) | 116.47(1) | 491.9(1) |
| D 63 A, "Dry" Cioclovina | 5.807(3) | 15.163(5) | 6.237(2) | 116.45(2) | 491.7(3) |
| D 63 C, "Dry" Cioclovina | 5.812(2) | 15.172(4) | 6.236(2) | 116.32(2) | 492.9(2) |
| D 64 A, "Dry" Cioclovina | 5.808(1) | 15.160(4) | 6.236(2) | 116.42(1) | 491.8(2) |
| D 64 B, "Dry" Cioclovina | 5.825(2) | 15.163(3) | 6.245(2) | 116.47(1) | 493.8(2) |
| D 64 C, "Dry" Cioclovina | 5.812(2) | 15.187(5) | 6.234(2) | 116.38(2) | 492.9(2) |
| D 65 A, "Dry" Cioclovina | 5.811(1) | 15.172(3) | 6.246(1) | 116.41(1) | 493.2(1) |
| D 65 B, "Dry" Cioclovina | 5.811(2) | 15.159(5) | 6.243(2) | 116.13(2) | 493.7(2) |
| D 66 B, "Dry" Cioclovina | 5.807(1) | 15.178(2) | 6.235(1) | 116.37(1) | 492.4(1) |
| D 68 A, "Dry" Cioclovina | 5.810(2) | 15.186(6) | 6.240(3) | 116.37(2) | 493.2(3) |
| D 81, "Dry" Cioclovina | 5.815(2) | 15.755(5) | 6.238(2) | 116.41(2) | 493.1(2) |
| P 2 A, Peştera Mare from Mereşti | 5.809(2) | 15.172(4) | 6.236(2) | 116.41(2) | 492.3(2) |
| P 3 A, Peştera Mare from Mereşti | 5.814(2) | 15.164(4) | 6.246(2) | 116.35(2) | 493.4(2) |
| P 4 A, Peştera Mare from Mereşti | 5.809(2) | 15.175(3) | 6.236(2) | 116.49(1) | 492.1(2) |
| P 5 A, Peştera Mare from Mereşti | 5.811(1) | 15.171(3) | 6.239(1) | 116.44(1) | 492.5(1) |
| P 6 A, Peştera Mare from Mereşti | 5.814(3) | 15.165(7) | 6.237(3) | 116.23(3) | 493.3(3) |
| P 6 B, Peştera Mare from Mereşti | 5.819(3) | 15.175(5) | 6.241(3) | 116.13(3) | 494.4(3) |
| P 9 A, Peştera Mare from Mereşti | 5.805(2) | 15.163(4) | 6.238(2) | 116.43(1) | 491.7(2) |
| PPL 3 A, Peştera cu Lilieci from Peştera | 5.803(3) | 15.159(5) | 6.235(2) | 116.39(2) | 491.2(4) |
| PPL 3 B, Peştera cu Lilieci from Peştera | 5.802(4) | 15.157(9) | 6.246(5) | 116.07(4) | 493.3(4) |
| PC 1 B, Comana | 5.847(4) | 15.184(8) | 6.265(8) | 116.09(7) | 499.5(3) |
| PM 1 A, Muierii | 5.798(3) | 15.134(7) | 6.229(3) | 116.38(2) | 489.7(3) |
| PM 1 B, Muierii | 5.817(6) | 15.174(9) | 6.234(8) | 116.08(8) | 494.2(8) |
| PM 2 A, Muierii | 5.807(3) | 15.140(7) | 6.231(3) | 116.40(2) | 490.7(3) |
| PM 2 B, Muierii | 5.830(6) | 15.196(9) | 6.231(5) | 116.02(6) | 496.0(6) |
| PM 6 A, Muierii | 5.810(1) | 15.172(2) | 6.241(1) | 116.46(1) | 492.6(1) |
| PM 6 B, Muierii | 5.810(1) | 15.184(1) | 6.239(1) | 116.42(1) | 492.9(9) |
| PM 7 A, Muierii | 5.794(3) | 15.127(8) | 6.231(3) | 116.40(2) | 489.2(3) |
| PM 7 B, Muierii | 5.806(1) | 15.172(3) | 6.239(1) | 116.38(1) | 492.4(1) |
| | -:(-/ | _ == := : = (= ; | | ===:30(=) | |

| PGD 2 A, Grigore Decapolitul | 5.812(3) | 15.164(6) | 6.238(2) | 116.33(2) | 492.8(3) |
|------------------------------|----------|-----------|----------|-----------|----------|
| PGD 2 C, Grigore Decapolitul | 5.802(3) | 15.181(8) | 6.235(3) | 116.15(3) | 492.0(3) |
| PGD 8 A, Grigore Decapolitul | 5.805(2) | 15.157(5) | 6.237(2) | 116.27(2) | 492.1(2) |
| PF 32 A, Făiroagă | 5.818(2) | 15.141(7) | 6.249(6) | 116.03(4) | 494.6(3) |
| L 7 A, Lazului | 5.811(1) | 15.194(3) | 6.247(1) | 116.41(1) | 493.9(4) |
| PT 12 A, Topolniţa | 5.804(2) | 15.155(5) | 6.234(2) | 116.41(2) | 491.1(2) |
| C 14 A, Cloşani | 5.805(3) | 15.174(9) | 6.237(7) | 116.10(7) | 493.4(2) |
| PD 2 A, Podul Natural | 5.816(2) | 15.165(6) | 6.235(3) | 116.23(2) | 493.3(2) |
| PD 2 B, Podul Natural | 5.820(3) | 15.181(6) | 6.234(3) | 116.40(2) | 493.4(1) |
| PD 2 C, Podul Natural | 5.810(3) | 15.181(7) | 6.241(3) | 116.40(1) | 493.1(3) |
| PAA 2 B, Peştera lui Adam | 5.803(2) | 15.179(7) | 6.261(4) | 116.12(3) | 495.1(3) |
| PGP 1 B, Gura Ponicovei | 5.802(2) | 15.162(5) | 6.230(2) | 116.45(2) | 490.7(5) |
| PN 2 A, Nandru | 5.808(7) | 15.183(1) | 6.241(8) | 116.38(6) | 493.1(7) |
| PN 3 A, Nandru | 5.808(2) | 15.165(4) | 6.233(2) | 116.39(2) | 491.8(4) |
| PR 2, Românești | 5.806(6) | 15.153(9) | 6.244(0) | 116.40(5) | 492.1(3) |

The essential of the infrared spectra on a number of samples is given in table 2. Few remarks on these spectra were considered as important: (1) Four distinct bands related to the OH-stretching vibrations of hydrogen-bonded water molecules were observed in all spectra. This agrees with the four bond distances found by structure refinement by Curry & Jones (1971) for the hydrogen bonds implying water molecules in stoichiometric brushite (3.09, 2.83, 2.78 and 2.76 Å). Using the equation of Libowitzky (1999) to calculate the OH stretching wavenumbers as a function of O-H...O bond distances, we obtain, for stoichiometric brushite, theoretical stretching wavenumbers of 3571, 3441, 3372 and 3336 cm⁻¹, which slightly differ from the stretching wavenumbers in Table 2. The differences are clearly due to the strong asymmetry of the H-O-H groups in brushite (Curry & Jones 1971), as well as to the slight non-stoichiometry of our samples. The unusually long bond distance of 3.09 Å between water molecules characterizes very weakly bonded molecular water and fully explains the easy thermal removal of a part of the molecular water reported before. (2) A fifth hydrogen bond is established between OH groups pertaining to the protonated phosphate groups (Curry & Jones 1971). According to the bond distance - wavenumber correlation of Libowitzky (1999), for a O-H...O distance of 2.678(5) Å (Curry & Jones 1971), the corresponding stretching band must be at 3115 cm⁻¹, which could explain the presence, in our spectra, of the shoulder at ~2930 cm⁻¹. (3) The H-O-H "scissors" vibrations are materialized by two bands at ~1725 and ~1650 cm⁻¹, which are, on their turn, split. This agrees with the observation of more than one structural position of water in brushite. The same splitting characterizes the H-O-H librational modes, which are materialized by the bands at ~370 cm⁻¹ and ~390 cm⁻¹ (Berry & Baddiel 1967). (4) The tetrahedral protonated phosphate anion seems to generate eight vibrational modes whose corresponding bands are tentatively assigned in Table 2. Berry & Baddiel (1967) noted that the band recorded by us at ~526 cm⁻¹, materializing a in-plane O-P-O motion, is in fact split, a second band (v_4'') occurring at ~535 cm⁻¹. If this assumption and the assignments in Table 2 are correct, this band multiplicity $(3v_3 + 1v_1 + 3v_4 + 2v_2)$ is consistent with a C_s punctual symmetry of the distorted protonated phosphate anion.

Table 2. Positions of and assignments of the infrared absorption bands recorded for selected samples of brushite from Cioclovina, Mereşti and Româneşti caves ⁽¹⁾

| Structural group | Vibrational mode | Wavenumber (cm ⁻¹) ⁽²⁾ | | Character, intensity ⁽³⁾ | |
|------------------|------------------------------------|---|---------|--|--------|
| | | Cioclovina | Merești | Românești | |
| H ₂ O | ν_3 antisymmetric stretching | 3552(12) | 3558(4) | 3481(8) | vs, sh |
| H ₂ O | ν_3 ' antisymmetric stretching | 3489(5) | 3490(3) | 3459(4) | vs, sh |
| H ₂ O | v_1 symmetric stretching | 3292(10) | 3300(7) | 3278(12) | vs, b |

| H ₂ O | ν ₁ ' symmetric stretching | 3160(6) | 3164(5) | 3160(5) | vs, b |
|--|---|---------|---------|---------|------------|
| (HPO ₄) ²⁻ | (P)O-H stretching | 2931(2) | 2933(4) | 2926(3) | s, shd |
| (HPO ₄) ²⁻ | (P)O-H stretching ⁽⁴⁾ | 2389(5) | 2390(1) | 2368(8) | m, b |
| H ₂ O | ν_4 in-plane H-O-H bending | 1724(4) | 1725(4) | 1769(5) | w, b (shd) |
| H ₂ O | ν ₄ ' in-plane H-O-H bending | 1649(4) | 1648(4) | 1649(1) | s, sh |
| (HPO ₄) ²⁻ | P-O-H in-plane bending | 1210(3) | 1209(2) | 1210(2) | s, b |
| (PO ₄) ³⁻ | v ₃ antisymmetric stretching | 1135(4) | 1138(4) | 1132(3) | vs, b |
| (PO ₄) ³⁻ | ν ₃ ' antisymmetric stretching | 1064(3) | 1063(2) | 1067(2) | vs, b |
| (PO ₄) ³⁻ | ν ₁ symmetric stretching | 1001(2) | 1001(2) | 1000(2) | s, b (shd) |
| (PO ₄) ³⁻ | ν ₁ ' symmetric stretching | 987(1) | 986(4) | 986(3) | vs, sh |
| (HPO ₄) ²⁻ | P-O(H) symmetric stretching | 873(2) | 872(1) | 893(4) | s, sh |
| (HPO ₄) ²⁻ | P-O-H out-of-plane bending | 793(2) | 794(3) | 796(2) | s, b |
| H ₂ O | v_2 out-of-plane H-O-H bending | 671(2) | 672(1) | 672(1) | m, sh |
| H ₂ O | ν_2 ' out-of-plane H-O-H bending | 662(2) | 661(2) | 668(5) | m, shd |
| (PO ₄) ³⁻ | v_4 in-plane bending (O-P-O) | 577(1) | 578(1) | 578(1) | s, sh |
| (PO ₄) ³⁻ | v_4 ' in-plane bending (O-P-O) | 526(2) | 526(1) | 527(2) | vs, sh |
| (PO ₄) ³⁻ | v_2 out-of-plane bending (O-P-O) | 410(1) | 410(1) | 405(5) | m, sh |
| H ₂ O | libration | 391(5) | 394(5) | 388(5) | m, sh |
| (?) | composed mode [Ca-H ₂ O (?)] | 380(4) | 381(4) | 376(5) | m, shd |
| H ₂ O | libration | 369(2) | 370(2) | 368(3) | m, sh |
| [CaO ₆ (H ₂ O) ₂] ¹⁰⁻ | lattice mode (Ca-O) | 357(3) | 359(3) | 356(3) | m, shd |
| [CaO ₆ (H ₂ O) ₂] ¹⁰⁻ | lattice mode (Ca-O) (5) | 307(2) | 307(3) | 310(4) | w, sh |
| [CaO ₆ (H ₂ O) ₂] ¹⁰⁻ | lattice mode (Ca-O) | 282(4) | 287(6) | 282(4) | m, b (shd) |
| (PO ₄) ³⁻ | v_2 ' out-of-plane bending (O-P-O) | 262(3) | 265(5) | 268(4) | m, sh |

(1) assumptions according to Dumitraş et al. (2004) and refered works; (2) standard deviations into brackets; (3) s = strong; m = medium; w = weak; vs = very strong; sh = sharp; b = broad; shd = shoulder; (4) second rank overtone of the P-O-H in-plane bending motion at ~1210 cm⁻¹ or composed with an unassigned band at ~1060 cm⁻¹ (Dumitraş et al, 2004); (5) probably composed with a H-O-H translation.

References

Berry, E.E., Baddiel, C.B., 1967. The infra-red spectrum of dicalcium phosphate dihydrate (brushite). *Spectrochimica Acta*, 23A, 2089 – 2097.

Curry, N. A., Jones, D. W., 1971. Crystal structure of Brushite, Calcium Hydrogen Orthophosphate Dihydrate: a neutron – diffraction investigation. *Journal of the Chemical Society*, (A), 3725–3729.

Dumitraş, D.,G., 2013. Associations minerales dans les sediments de la grotte Cioclovina Uscata. Teza de doctorat. Editura ANRT (Atelier National de Reproduction des thèses) – Thèse à la carte, Lille, Franta, 340 p. Identifiant BU: 09EMSE0022; Cover - Summary: SC-17589.pdf

Dumitraş, D.G., Marincea, Ş., Fransolet, A-M. 2004a. Brushite in the bat guano deposit from the "dry" Cioclovina Cave (Sureanu Mountains, Romania). *Neues Jahrbuch für Mineralogie, Abh.*, 180/1, 45 - 64.

Libowitzky, E., 1999. Correlation of O-H stretching frequencies and O-H...O hydrogen bond length in minerals. *Monatsh. Chem.* 130, 1047–1059.

Schadler, J., 1929. Mineralogisch-Petrografische charakteristik der phosphat-ablagerung in der Cioclovina-Höhle bei Pui. Publicațiile Muzeului Județului Hunedoara, V (XXVII), 1, Deva.

CULTURAL GEOLOGY. INTERLINKING EARTH SCIENCES, HISTORY AND PHILOSOPHY

Dan GRIGORESCU

University of Bucharest. Department of Geology Institute of Advanced Studies in Levant Culture and Civilization e-mail: dangrig84@yahoo.com

The lengthy history of the dawn of human civilization follows the path of using, shaping and processing stone; a path down which primitive man broke away from the rest of the animal kingdom and along which he has continuously sought out a variety of material sources in order to meet the ever more complex and refined requirements of his evolving livelihood. Along the way, the cultural importance of Geology became markedly highlighted through the delineation of the successive stages of human civilization - made on the basis of the primary materials employed, namely stone and metal. The most noticeable expression of the relationship between Culture and Geology can be traced back to the very system classifying historical chronology itself, introduced by the Danish antiquarian Christian Thomsen towards the middle of the 19th century and subsequently taken up by society at large: the progressive chronologies of the "Stone Age" (further subdivided into the Palaeolithic, the Mesolithic and the Neolithic), the "Bronze Age" and the "Iron Age". The evolution of material production within these epochs - divided by scientists into various cultures or industries - closely mirrors the evolution of the Homo genus itself, a sequence in which river stones, most accessible to early man, were gradually replaced by flint, whose hardness and utilitarian modularity allowed for the diversification and refinement of further stone tools. An artistic interest was added later on to the tools which saw the incorporation of bone, wood and ultimately metals with ever more advanced technologies of extraction, tooling and alloy production. From a cultural and artistic perspective, the pinnacle of this evolution was the explosion of parietal art during the Upper Palaeolithic.

The progressive specialization of tools sheds light on the mental development of primitive man, highlighting an ever-expanding pool of knowledge of natural objects leading to the development of comparative analysis and selection processes mandated on specific needs, and later to the capacity of combining different objects altogether in the pursuit of the new ones. The anatomical evolution of humans' mental development has been charted by the paleo- neurological studies carried out on fossilized hominids from *Homo habilis* to *Homo erectus* and *Homo sapiens*, which show an expansion of cranial volume paralleling the development of the cerebral cortex and its functional structuring.

Although Culture and Geology are fundamentally interwoven through natural elements and their significations, ever more intricately interpreted throughout the successive development of human civilization, it was only recently that they came to be studied as a whole, as a new field of geosciences. In recent years the international scientific events dedicated to the geosciences have, almost without exception, included sessions on Cultural geology where numerous interesting papers were presented. The topics and themes of such contributions serve to outline the emerging field of "Cultural Geology", only recently coined, yet one that has already specialized scientific journals, such as the "Geology and Culture" journal in Japan (Huzuki, 2018). Recently, a total of 24 presentations – many by Romanian researchers (Papp et al., 2018; Gál et al., 2018) – were presented during the Cultural Geology - themed session of the 21st International Congress of the Carpathian-Balkan Geological Association, held in Salzburg in September of 2018, titled Composition, technology and provenance of archaeological artefacts.

In our view, the cultural filiation of geology can be approached from a three-fold perspective: 1. Geology taken as the material source of objects and of cultural construction; 2. Geology seen as the

scientific and philosophical foundation of the history of Earth and the history of civilization; 3. Geology as a source of artistic inspiration.

The first perspective represents also the most common approach for the connection between Culture and Geology, the origin and qualities of stones, minerals and metals used in tools, the involved technologies, the rocks and mineral substances used in the construction and decoration of the cultural buildings and historical monuments, representing common research topics.

In the second geo-cultural approach the history of the Earth - encompassing all stages and events occurring over the course of more than 4.5 billion years - represents the basis for both creationist and evolutionist philosophical interpretations. These would come to a head towards the end of the 18th century, when James Hutton launched the idea of an immense geological time needed for the creation of the thick pile of rocks which encompass the Earth history, fundamentally incompatible with the mere few thousand years assumed by creationist philosophers. The entirety Nature philosophy, based on intertwining of phenomena with different origins that are revealed by virtue of a common observable effect, traces its origins to the geological movement, which preceded the biological movement. The knowledge of the past events allows for a better understanding of contemporary ones and for the anticipation of those yet to come, thus opening the way to the elaboration of preventative measures when needed. Thus, the present "global warming", as well as the cooling periods, has many antecedents in the geological past; the knowledge of their cosmic determination may allow a more realistic assessment of the way in which the human factor could intervene. One field wide open to the philosophy of Life at a global scale is that studying the simultaneous disappearance of numerous clades of organisms in the past through mass extinction events, where causes tied to terrestrial dynamics are closely interwoven with the processes of organic evolution.

Ancient civilizations have elaborated innumerable mythologies around geological objects (minerals, fossils, etc), and especially around past catastrophic events (earthquakes, floods, tsunamis); the myths are parts of the earliest human cultures which were studied, and at times confirmed, by historical and archaeological research. An especially interesting collage of such myths was the object of a session on *Myth and Geology* during the International Congress of Geology held in Florence in 2004, the proceedings of which were later published in 2007 by the London Geological Society in a volume bearing the same name. Inside, we may learn of the surprising coincidence between the age of the Earth in Hindu Vedic cosmology on the one hand (4.3 billion years) and in the modern scientific consensus (4.65 billion years) on the other. We may then see how the Vedic estimate is derived from the addition of the duration of the four *yugas*, or aeons: Satyuga, Trethayuga, Daparayuga and Kaliyuga which, when multiplied by 1000, yield one *Brahma* day. The four *yugas* can, therefore, be tentatively equivalated with the geological periods of Precambrian, Palaeozoic, Mesozoic and Cainozoic (Chandrasekharam, 2007).

Overall, the scientific data gathered by the various branches of Geology holds pride of place in the cultural background of those interested in an in-depth knowledge of the world we inhabit. In the third approach, Geology – taken as the inanimate part of Nature – has proven to be and continues to represent an inexhaustible source of artistic inspiration for painting, sculpture and musical composition.

In the work of many master painters, the geological landscape, with or without a particular aesthetic, was one of the predominant themes, with van Ruisdael in the Netherlands, Claude Lorraine and J. B. Corot in France, J. Constable and J.M.W. Turner in Britain, Nicolae Grigorescu and Ion Andreescu in Romania being a few notable highlights of this trend. In music, A. Vivaldi's "Four Seasons", G.F. Handel's "Water Music" collection or Martian Negrea's symphonic suite set "In the Apuseni Mountains" brilliantly evoke their inspirational natural setting. In sculpture, an excellent example is set by the work of Constantin Brâncuşi, founder of the modern sculptural art. Many years ago, I suggested in a conference that the sandstone concretions (*trovants*) found in the Gorj hills around his native Hobiţa served as a powerful inspiration to Brâncuşi to forsake figurative sculpture, that he mastered so well, to dedicate himself to the intuitive representation. This idea was first taken up by journalists, and later by some art critics.

A practical interplay of Geology and Culture may be noticed throughout many of the touristic trails that wind across UNESCO geoparks - protected areas in which the natural and cultural heritage of the region alike are jointly protected and sustainably valorised. The geosites and cultural sites that lie along such trails allow visitors to get in touch with the heritage values of a region in a holistic way; the association

of natural and cultural sites represents an added value which underpins the region's sustainable development.

Cultural geology also bears exceptional educational value, bringing to light the lesser-known aspects of Geology that are closely tied to the emergence and early development of human civilization. Consequently, such an approach serves to bring the field of Geology closer to the general public – which is all the more important today, when, at least in Romania, Geology is rather understood through movies and dinoparks than through courses taught in school. Moreover, Geology's underpinning of cultural developments represents an additional reason to carefully safeguard the geological environment.

In the above spirit, the Institute for Advanced Studies in Levant Culture and Civilization launched the "Dobrogea – Witness to the Millennial Civilizations of the Levant", a multi-annual project, wherein Cultural geology is one of the primary research themes approached through a multidisciplinary partnership of geologists, archaeologists, geo-archaeologists, biologists and historians. Dobrogea is indeed , the ideal location to conduct this manner of research, boasting an impressive number of archaeological sites, cultural/historical monuments and artefacts from successive epochs ranging from the Neolithic and Eneolithic, through the Hellenistic, Roman, Romano-Byzantine, Byzantine and Mediaeval periods , all the monuments within striking distance of stone quarries, specially limestones of various petrographic types and ages, dating from the Sarmatian back to the Eocene, Cretaceous, Jurassic and the Triassic. These ages, representative for the rock sources in the archaeology of Dobrogea, are the distinct chapters of our forthcoming study.

Acknowledgements. The author thanks to Dr. Ana-Maria Răducan and Mr. Maxim Onofrei for the English translation of the article, and to Mr. Ion Scutelnicu for the photos.

References

- Chandrasekharam, D., 2007. *Geo-mythology of India*, in L. Piccardi and W. B. Masse (editors): *Myth and Geology*, Special Publication of the Geological Society of London, 29-37.
- Gál, Á., Benea, M., Silye, L., 2018. *The Emblematical Stone Monuments of Cluj-Napoca, Romania*. XXI. International Congress of CBGA, Salzburg, Austria. Abstracts, p.366.
- Papp, D.C., Milu, V., Cociuba, I., 2018. *Prospects of the Use of Volcanic Geosites from the Carpathian Areas of Romania for Informal Geological Education and Awareness.* XXI International Congress of CBGA, Salzburg, Austria. Abstracts, p.365.
- Suzuki, H., 2018. *Cultural Geology Salzburg to Japan.* XXI International Congress of CBGA, Salzburg, Austria. Abstracts, p.356.

Cultural geology of Dobrogea. Images taken during researches in 2018 and 2019.

Plate I



Fig. 1. Sculptured plates (metopes) from the Tropaeum Traiani monument in Adamclisi, carved in Sarmatian limestones excavated in quarries at Deleni (*Enige*) village, situated at short distance from the archaeological complex.

Plate II



Fig. 1. The "Skulls cave" in Upper Jurassic limestones from Gura Dobrogei includes two archaeological levels with human skeletal remains: a lower one of Iron Age (7th-5th century BC) and an upper one from the Roman-Byzantine epoch (ca. 4th - 5th century AD).

Plate III Engravings in stone



Fig. 1. Stone graffiti in the Lower Cretaceous limestone from Alimanu (South Dobrogea). The engravings dated 9th - 10th century include associated Christian and laic signs: the cross with widen margins (*Malta cross*), symbolic horses and persons mounted on horseback, etc. Similar Medieval engravings are found in many other places from South Dobrogea: Cernavoda, Murfatlar, Dumbraveni, Limanu as well as in Bulgaria and Turkey, most of them linked to limestone quarries.



Fig. 2. Enigmatic writing in Upper Jurassic limestone near Casian village (Central Dobrogea). It is considered to certify the Saint Ioan Casian (c. 360 - c. 435AD) origin in this region. The Saint Ioan (John) Casian is acknowledged in both the Western and Eastern churches as founder of monasticism.

GEOARCHAEOLOGY. APPLICATIONS OF SEDIMENTOLOGY AND SOIL MICROMORPHOLOGY IN ARCHAEOLOGY

Constantin HAITĂ

National Museum of Romania History, 12 Calea Victoriei, sector 3, 030026 Bucharest, costel_haita@yahoo.com

Sedimentology and Soil micromorphology are two domains of scientific research that can bring very important and detailed information for the study of the archaeological sites. Until each of these disciplines has its own methods and concepts, they complete each other.

Sedimentology applied in archaeology may be defined as an interdisciplinary domain, at the border between Sedimentary petrology, Pedology and Archaeology, which studies the natural and anthropogenic deposits from the archaeologically investigated sites transformed by anthropic, physical-chemical and pedological agents. The main characteristics that must be observed for the description and interpretation of the sedimentary units are: texture, structure, composition, color and homogeneity. The main methods of analysis are: grain-size analysis, morphometric and morphoscopic analysis, clays mineralogy, pH and chemical analyses, scanning electron microscopy and microprobe.

The main applications of sedimentology in archaeology can be attributed to the following objectives of research.

- the study of the sedimentary paleoenvironment of the area in close spatial relationship with the site during the period of occupation. This study consists in the analysis of all the sedimentary features in order to reconstruct the paleogeographic background during the occupation, to understand the area's depositional history, and the possible implications for the settlement, and to identify the sources for the sedimentary materials necessary for construction materials, clay, pigments, etc.
- the study of the sedimentary units from the composition of archaeological deposits. The sedimentological study of each unit (context) recognised during the archaeological research is very useful for the understanding of human activities and the spatial organisation of settlement.

The sedimentological research, integrated in the cultural, chronological and geomorphologic context of the investigated archaeological site, which conduct the sampling and the interpretation of the obtained data, can assist the approach of important archaeological themes, like analysis of the activity areas, estimation of site's inhabiting intensity and continuity, and identification of the abandonment causes and conditions.

Soil Micromorphology is a method from the Soil Science domain that consists in the analysis at the microscope of the sedimentary units, in undisturbed and oriented state, with the purpose to understand the formation processes. Micromorphology applied in archaeology allows the study of the anthropic and natural units from the site and of the materials of anthropic origin like daub, mortar, brick, plaster, ceramics and different constituents of organic nature.

The micromorphological analysis of sediments and soils in archaeological context may bring important information that can be considered thus: data about the functionality, role and evolution of the structures made by man, data about the sediments' accumulation mechanisms, determined directly or indirectly by the structures' utilization and abandon, and data about the environment, especially to characterize the natural deposits and recent soils, with natural evolution or cultivated.

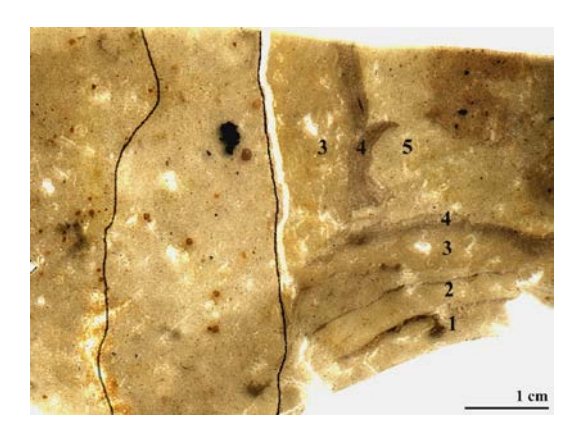


Fig. 1. Image of a micromorphological thin section illustrating the wall and the floor of a dwelling, with successive plasterings.



Fig. 2. Image of an in situ organic accumulation with fish scales. Photo at microscope, PPL, image width 2 mm.

The archaeological problems that are addressed by the micromorphological analysis can be presented as follows:

- the nature of the sedimentary materials that form the archaeological deposits and the source of these sediments;
- the preparation techniques of the building materials used for the construction of the archaeological structures;
- the nature of the constituents accumulated through human activities and the physical-chemical and thermal transformations;
- the human activities that produced these constituents or which determined their transformations and the corresponding environmental conditions;
- the spatial relations between different sedimentary units which form the archaeological structures;
- the construction modality of the sedimentary units in the archaeological structure and their spatial organization;

- the character *in situ* or reworked of the anthropic accumulations, the significance of these deposits from the perspective of human activities, and to establish the activity areas in the inhabited space.

We must note here that the most important element for this type of geoarchaeological research is the collaboration between the archaeologist, who comprehends the site and it is the most suitable to highlight the main questions and hypothesis, and the sedimentologist, who brings more specific information in order to participate in the interpretation of the formation and evolution of the archaeological site.

References

- Bullock, P., Fedoroff, N., Jongerius, A., Stoops, G., Tursina, T., 1985. *Handbook for soil thin section description*, Waine Research Publications, Wolverhampton, Rotterdam, 152 pp.
- Butzer, K.W., 1982. Archaeology as human ecology: Method and theory for a contextual approach, Cambridge University Press, New York, 320 p.
- Courty, M.-A. 1992. Soil micromorphology in Archaeology, Proceedings of the British Academy, 77, 39-59.
- Courty, M.-A, Goldberg, P., Macphail, R., 1989. *Soils and micromorphology in archaeology*, Cambridge University Press, Cambridge, 344 p.
- Goldberg, P., Macphail, R.I., 2006. Practical and Theoretical Geoarchaeology, Blackwell Publishing, Oxford, 455 pp.
- Haită, C., 2003. Micromorphology. Inhabited space disposition and uses. Analysis of an occupation zone placed outside the dwellings, In D. Popovici, C. Haită, A. Bălăşescu, V. Radu, Fl. Vlad, I. Tomescu, *Archaeological pluridisciplinary researches at Borduşani Popină*, Biblioteca Muzeului Naţional, Seria Cercetări Pluridisciplinare, VI, Editura Cetatea de Scaun, Târgovişte, 51-73.
- Haită, C., 2012. Sedimentologie şi Micromorfologie. Aplicații în Arheologie, ediția a II-a, Biblioteca Muzeului Național, Seria Cercetări Pluridisciplinare, XII, Editura Cetatea de Scaun, Târgoviște, 216 pp.
- Miskovsky, J.-C. (coord.), 1987. *Géologie de la préhistoire: Méthodes, techniques, applications*, Association pour l'Étude de l'Environnement Géologique de la Préhistoire, Paris, 1297 pp.

RARE EARTH ELEMENT AND YTTRIUM MINERALS IN THE DITRĂU ALKALINE INTRUSIVE COMPLEX, EASTERN CARPATHIANS, ROMANIA

Paulina HÎRTOPANU

Department of Mineralogy, University of Bucharest, 1, Nicolae Bălcescu Blv., 010041 Bucharest e-mail: paulinahirtopanu@hotmail.com

Abstract

The Ditrău alkaline intrusive complex (DAIC) hosts a rich and diverse mineralization of Nb, Ta, Ti, REE, Th, Zr, Te, and U mostly highly concentrated in two areas: Jolotca and Belcina. The mineralization is polygenetic, being formed in at least 5 important genetical stages, from oldest to youngest: magmatic, magmatic-metasomatic, carbothermal, medium, and low T hydrothermal processes. The multistages mineralizing process is supported by textural relationships, where replacement of earlier rare minerals by later ones is common. The first magmatic stage began with the oldest Nb-rutile, originated from the upper mantle. Primary homogeneous Nb-rutile broke down in secondary rutile, ilmenite, ferrocolumbites, aeschynite-(Ce), aeschynite-(Nd), aeschynite-(Y), and euxenite-(Y). The REE mineralization occurs in the magmatic-metasomatic stage with the following minerals: REE-apatite, monazite-(Ce), zircon and magnetite. In the carbothermal stage the primary LREEfluocarbonates were formed. They follow the primary monazite-(Ce). The LREE fluocarbonates are hosted by calcite, dolomite and siderite carbonatite rocks, all being late carbonatites. The majority of primary REE fluocarbonates, which were determined in the DAIC, have in their compositions the light rare earth elements (LREE) group or Ce group: bastnäsite-(Ce), bastnäsite-(La), parisite-(Ce), parasite-(Nd), synchysite-(Ce), synchysite-(Nd), röentgenite-(Ce), sahamalite-(Ce), and eisenkalkancylite. In the high T stage (contemporaneous / interference) with the carbothermal process appear the new large monazite-(Ce) crystals, new large allanite-(Ce) crystals, törnebohmite-(Ce), chevkinite, and hydrothermal zircon. To the last hydrothermal stage belong the pyrochlore supergroup, fergusonite-(Ce), fergusonite-(Y), euxenite-(Y), fluorapatite, Th rich apatite, many sulfides, Y-fluorite, Ce-fluorite, thorite, xenotime-(Y), Th rich monazit-(Ce), many varieties of secondary REEfluocarbonates and secondary allanite-(Ce). This last stage has a large development in Belcina area. The REE mineralization is associated to alkaline, alkaline-ultrabasic, and carbonatite complex intrusions, the primary LREE-fluocarbonates being a product of carbonatitic hydrothermal activity.

Introduction

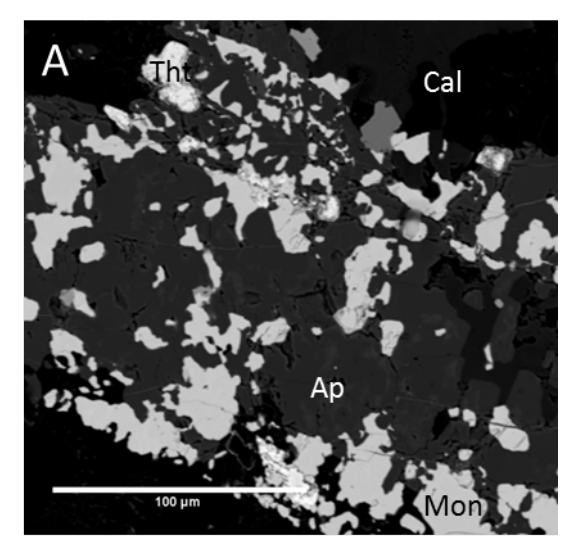
The Ditrău alkaline intrusive complex (DAIC) is situated within the crystalline rocks of the inner part of the East Carpathians, in the Gurghiu Mts. It has a distinct ring structure and a succession of magmatic events ranging from ultramafic, gabbroic, and dioritic magma to syenitic and various postmagmatic events. All these events developed between a Triassic extensional stage and a Jurassic rifting stage. The succession of magmatic events in Ditrău could have been completed with a carbonatite intrusion that followed after the alkaline intrusion and used the same pathways as the previous alkaline silicate melt. It is known that the peralkaline rocks are commonly characterized by extreme enrichment in alkali metals (Na, K) and high field strength elements (HFSE), such as REE, Y, Zr, Ti, Nb, and Ta. The optical and electron microprobe study established the mineralogical and genetical evolution of the Ditrău REE(Y) minerals and their associated minerals.

The evolution of the mineralizing genetic process of DAIC

The Ditrău REE mineralization is polygenetic, being formed in at least 5 important genetical stages, from oldest to youngest (Hîrtopanu, 2019). The multistage mineralizing process is supported by textural relationships, where replacement of earlier REE minerals by later ones is common.

1. Magmatic stage/process began with the oldest exotic homogeneous primary Nb rutile/Nb rutile+Nb ilmenite, originating from the upper mantle (Hîrtopanu, 2019). The later exsolutions of aechynite-(Ce), aechynite-(Nd), aeschynite-(Y), ferrocolumbite, manganocolumbite, yttrocolumbite-(Y), and euxenite-(Y), occur in magmatic niobian rutile from an old common solid solution. Generally, the Ditrău REE content of aeschynite minerals is dominated by the Ce and Nd, and less Y.

2. The magmatic-metasomatic stage is the second mineralizing process. The old magnetite, old apatite, old zircon, and old primary monazite-(Ce) appeared as a younger mineralizing process after the magmatic one. The textural relations of old apatite with its mineral associations are displayed in many optical images and also in many backscattered electron mages. The old apatite is substituted by new monazite-(Ce) and thorite (Fig. 1A) and the old monazite-(Ce) is substituted by allanite-(Ce) and REEepidote (Fig. 1B). The most common substitution in the old apatite is the exchange $Ca^{2+}+P^{5+} \leftarrow REE^{3+}+Si^{4+}$. The incorporation mechanism of tetravalent elements (Th⁴⁺) in the structure of monazite-(Ce) is described by means of coupled substitution Th⁴⁺Si⁴⁺ with Ce³⁺P⁵⁺. The substitution involves a coupled intervalence replacement, which leads to the formation of the cheralite family. The Ditrău old monazite-(Ce) is usually unaffected by metamictization, in spite of its Th and U contents. Strong ionic bondings in the structure of this mineral are very likely responsible for its resistance to metamictization. Also, it has diverse submicroscopic inclusions and its rims are corroded by natrolite. The allanite-(Ce), REE-rich epidote, secondary REE-carbonates, thorite, molibdenite, and other sulfides frequently grow on the cracks and cleavages of the old monazite-(Ce). Therefore, the primary monazite-(Ce) is older than primary allanite-(Ce), primary REE-carbonates, REE-rich epidote and sulfides, and younger than old apatite and old magnetite.



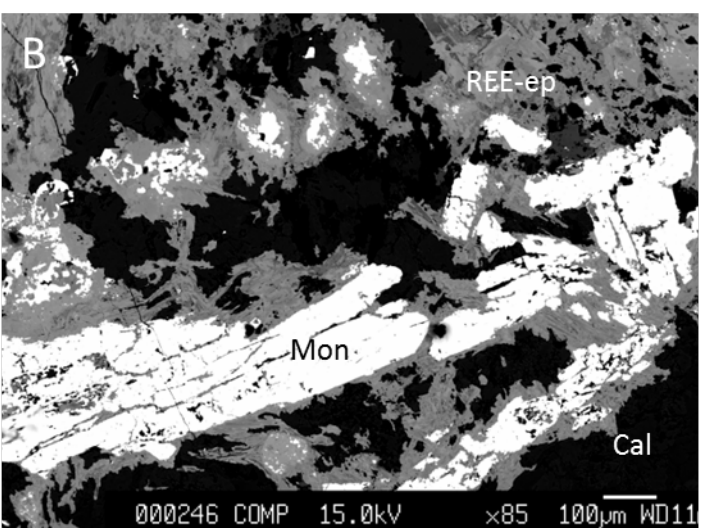


Fig. 1. A, An old apatite (Ap, dark grey) substituted by primary monazite-(Ce)(Mon, white), thorite (Tht, bright white), and calcite (Cal, black); B, Primary monazite-(Ce) (white prisms) substituted by REE-epidote (REE-Ep, grey, oscillatory composition), calcite (Cal, black), Jolotca area.

3. In the **carbothermal** stage, the **primary LREE-fluocarbonates** were formed. They follow the primary monazite-(Ce), or could be interfered with it. The primary REE-fluocarbonates cut through the old magnetite-apatite association being younger than the latter, belonging to a new genetical process. Frequently, primary REE-carbonates mantle old monazite-(Ce), and monazite-(Ce) mantles the old apatite.

The LREE fluocarbonates are hosted by calcite, dolomite and siderite carbonatite rocks, all being late carbonatites. The primary LREE-carbonates were crystallized from the fluids enriched in LRRE linked with the carbonatite magmas and their associated alkaline rocks, fluids which contain complex agents, such as PO_4^{3-} , CO_3^{2-} and F^- . The majority of primary REE fluocarbonates, which were determined in the DAIC have in their compositions the light rare earth elements (LREE) group or Ce group (Fig. 7A).

Bastnäsite-(Ce), (Ce,La)CO₃F, sometimes is zoned with parisite-(Ce) and synchysite-(Ce). The rare **bastnäsite-(La)** occurs intergrown with calcite and rutile and has bastnäsite-(Ce) around it. Because of the absence of Ca layers in its structure, bastnäsite-(Ce) has the highest REE content of any of the fluocarbonate species. The allanitisation of bastnäsite-(Ce) around and inside the grains is widespread (Fig. 2A).

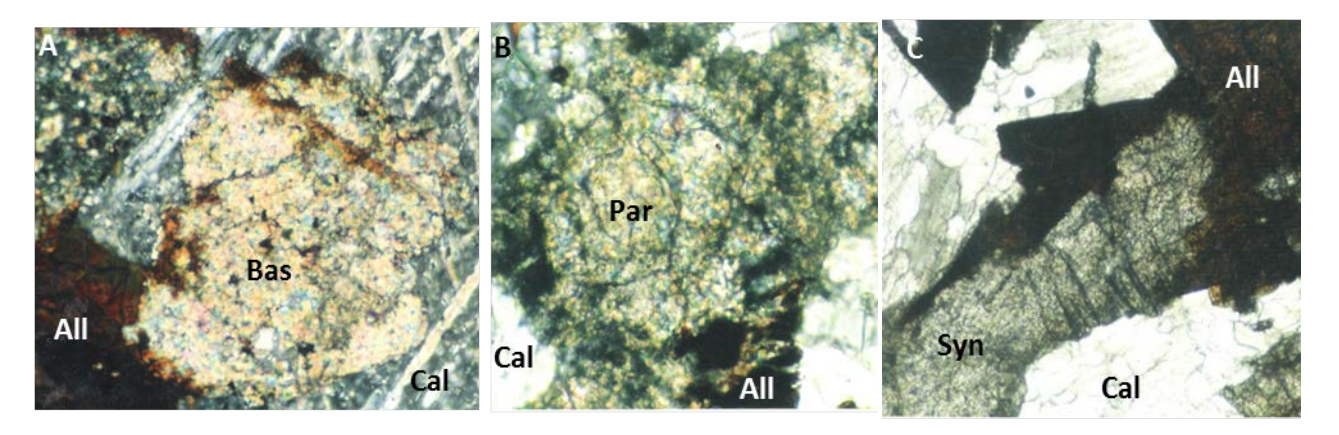
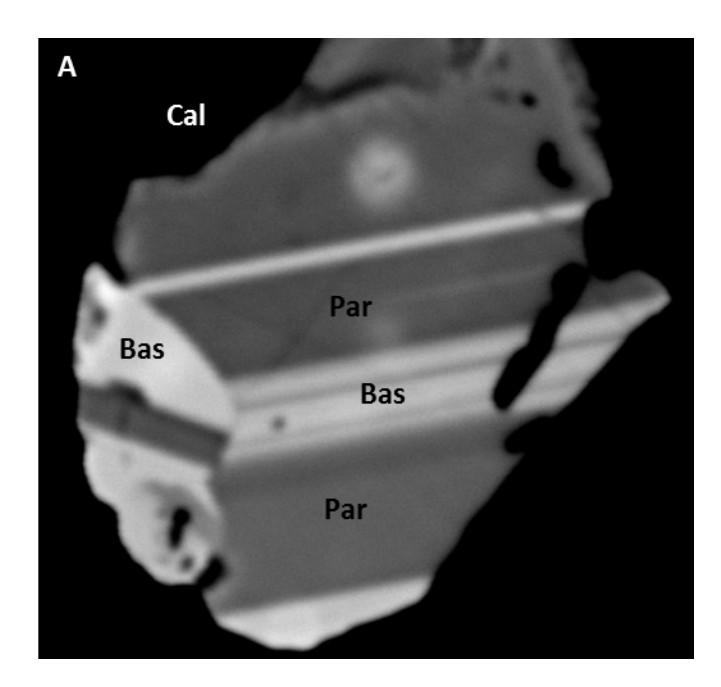


Fig. 2. A, Bastnäsite-(Ce) (Bas, high birefringence) and allanite-(Ce) (All, red) in calcite (Cal, grey), TL, N+, x 25; B, Parisite-(Ce) (Par, concentrically zoned) and allanite-(Ce) (All, black) in calcite (Cal, white/grey), TL, N+,x 25; C, Synchysite-(Ce) (Syn, grey, no cleavage) allanitized (All, brown black) in calcite (white grey), TL, NII, x 25, Jolotca area.

The **hydroxylbastnäsite-(Ce)** with (OH) >F was formed on bastnäsite-(Ce) and has a continuous series with it. Relics of bastnäsite-(Ce) occur in hydroxylbastnäsite-(Ce). The primary **parisite-(Ce)**, Ca(Ce,La)₂(CO₃)F₂ forms prisms with perfect cleavage. It frequently appears zoned/with concentric texture (Fig. 2B). The **primary synchysite-(Ce)** Ca(Ce, La)(CO₃)₂F forms short prismatic crystals, which have no cleavage (Fig. 2C). Often it has an oscillatory zoned composition. The allanitisation process of synchysite-(Ce) began on the edges of grains or on the fractures, changing the shape of the grains, which became rounded, and sometimes remaining as relics in allanite-(Ce) (Fig. 2C). **Synchysite-(Y)**, Ca(Ce,Y)(CO₃)₂F, occurs in Belcina area. A distinct aspect of the Ditrau LREE-carbonates is the anomalously high LREE content. Among them, the bastnäsite-(Ce) is the most abundant. The Ditrau bastnäsite-(Ce) contains up to 70wt% LREE or even more. The Nd₂O₃ and La₂O₃ contents have a high percentage, sometimes of the same level as that of Ce₂O₃, but the latter is usually the dominant LREE (Fig. 7A). The additional natural mixed-layer compounds with compositions between bastnäsite-(Ce) and synchysite-(Ce) and between bastnäsite-(Ce) and parisite-(Ce) have been determined in the Ditrău REE-fluocarbonates by electron microprobe.

The REE carbonates exhibit a pronounced zoning, which is usually seen in backscattered electron images (Fig. 3A and 3B). The very fine scale oscillatory zonings reflect fluctuations in the composition of the carbothermal/hydrothermal fluid, while the T and P are constant during their formation. Sometimes fine scale oscillatory zoning is superimposed on the sector zoning. This complex zoning results mainly from variations in LREE and Ca. The secondary REE-carbonates were formed by the action of late hydrothermal solutions rich in CO₂ and F on some pre-existent REE-phosphates such as monazite-(Ce), REE rich apatite, on some preexistent and diverse REE-silicates, and even on some primary REE-carbonates. The alterations (transformations) among different terms of REE-fluorcarbonates (belonging to the same group) were observed in the Ditrău REE-carbonates: some of the parisites occurring in hydrothermal mineralization were formed by alteration of primary synchysites, and the röntgenites were formed by alteration of primary parisites. These transformations among fluocarbonates very likely result from variations in either Ca²⁺ or CO₃-2 activities in the fluid. The presence of fluorite as secondary mineral, associated to REEfluocarbonates is good evidence for a high fluorine content of the mineralizing fluid. They are a late hydrothermal/ carbothermal product probably resulting from the fractionation of carbonatite and/or alkaline magmas. Because of this abundance of LREE-carbonates and their associations (calcite, dolomite, ferrodolomite, and ankerite) in this carbothermal/hydrothermal stage, as well as the presence of connections with alkaline and ultabasic/basic rocks, that the source of CO2 of Jolotca LREE-fluocarbonates could be related to carbonatite magmas and most probably less to alkaline magmas.



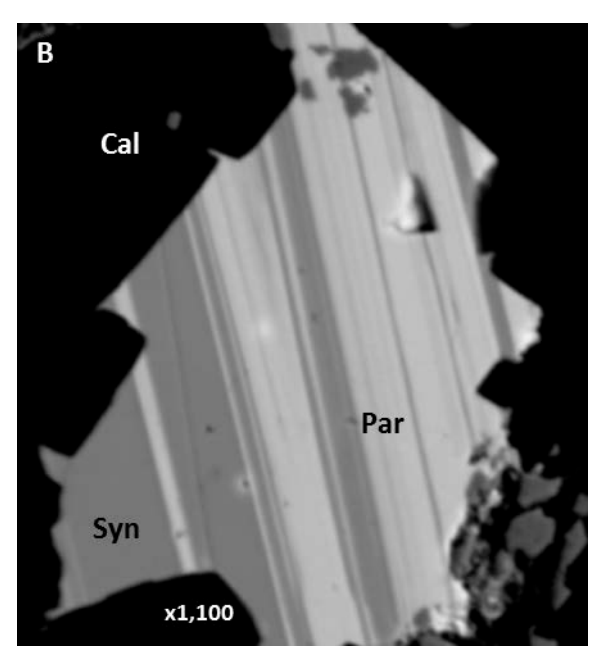


Fig. 3. A, Backscattered electron image of zoned LREE carbonates: A. bastnäsite-(Ce) (Bas, white) zoned with parisite-(Ce) (Par, grey), calcite (black); B, Bastnäsite-(Ce) (white) zoned with synchysite-(Ce) (Syn, grey), Jolotca area.

Besides the bastnäsite-(Ce), bastnäsite-(La), hydroxylbastnäsite-(Ce), parisite-(Ce), synchysite-(Nd), synchysite-(Y), another rare REE-carbonates, such as eisenkalkancylite (carbonate of REE, Fe and Ca), röentgenite-(Ce), and sahamalite-(Ce) also occur infrequently in DAIC.

4. The high temperature hydrothermal process was most probably contemporaneous/interfered with the previous carbothermal process. The new monazite-(Ce) and allanite-(Ce) as main constituents of the ore minerals in the Jolotca vein mineralization belong to this hydrothermal stage. The Jolotca mineralizing veins show a telescoping texture. The medium to low temperature mineralizations, represented by sulphides, are situated outside the vein, and the high temperature mineralizations, represented by new monazite-(Ce)/allanite-(Ce) are situated in the central part of the veins. Between them there are the primary LREE-fluocarbonates. The new monazite-(Ce) has a distinctive paragenesis, with new allanite-(Ce), and they are associated with old REE-fluocarbonates and new sulfides (especially pyrite), which seems to be, amongst them, the oldest mineral. Sometimes the bastnäsite-(Ce)/monazite-(Ce) contact is sharp.

Secondary allanite-(Ce), many secondary REE-carbonates, REE rich epidot, REE low phillosilicates, and REE low chlorites could be formed through replacement of monazite-(Ce). The hydrothermal veins of secondary allanite-(Ce) crystals cut through the pyrite. The mineralization may have been formed by one or a combination of two agents: (1) hydrothermal solutions originating from the nearby syenitic rocks, and (2) residual solutions originated from carbonatite magma. The textural and compositional data indicate replacement and breakdown of primary monazite-(Ce) by H₂O, CO₂ and F rich fluids, released during post-magmatic overprint of the carbonatites rocks. Therefore, the variable breakdown products of monazite-(Ce) from Ditrău depend on the fluid composition, P-T conditions and the character of hydrothermal fluids.



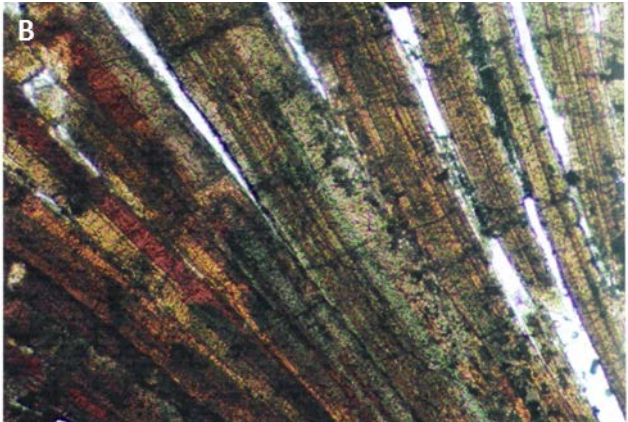
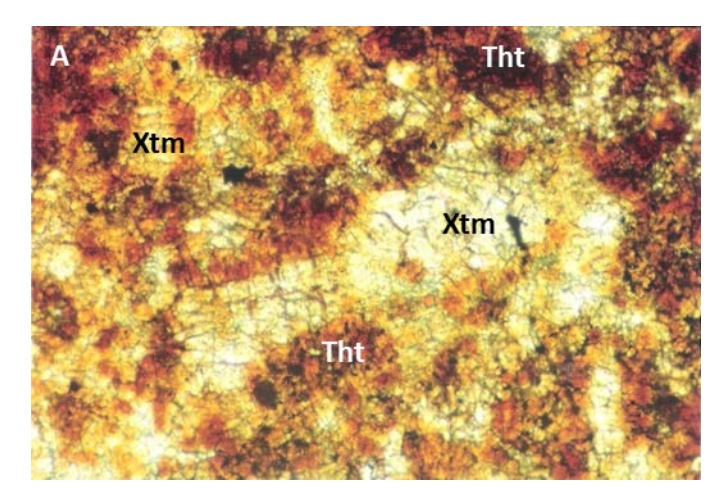


Fig. 4. A, Large hydrothermal monazite-(Ce) crystals; B, Large Hydrothermal X allanite-(Ce) crystals, TL, N+, x 25, Jolotca area.

The hydrothermal monazite-(Ce) crystals are large, prismatic (Fig. 4A), of a few cm in size. They are colourless, light yellow or light brown in transmitted light and have a weak pleochroism. The refringence and birefringence are high and increase with the ThO₂ content (more exactly, with the Th silicate component huttonite) in the monazite structure. The twinning of hydrothermal monazite-(Ce) is common. The (100) twins could be thick or thin. All grains/crystals are free of inclusions at high magnification, differing from old magmatic monazite-(Ce) which has many and diverse inclusions. The chemical composition of hydrothermal monazite-(Ce) determined by microprobe has the following variations of its main REE-oxides (wt%): Ce₂O₃=34.00-35.00, La₂O₃=19.00-20.00, Nd₂O₃=10.00-11.00, and F=0.826. Some contents of ThO₂, Y₂O₃, Pr₂O₃, Ty₂O₃, Dy₂O₃, Er₂O₃, Gd₂O₃, Sm₂O₃, ZrO₂ and PbO were also determined (Hirtopanu, 2017). The hydrothermal REE-fluorapatite has large crystals, grown radially, without inclusions, thus looking different from the old magmatic bearing REE-fluorapatite.

Allanite-(Ce) occurs as a constituent mineral in Jolotca area and as an accessory in the Belcina area. It forms coarse brown to good size black crystals of a few cm in size growing tabular, prismatic to acicular. It may also be granular or massive. In thin sections it has a brown, red or green colour with strong pleochroism (Fig. 4B). The bastnäsitisation of allanite-(Ce) and the reverse processes, the allanitisation of bastnäsite-(Ce) occur frequently. The chemical composition of allanite-(Ce) has a high Fe_2O_3 content showing oxidizing conditions for its genesis. The effect of changing redox conditions could be one possible cause for the neoformation of allanite-(Ce) on the other REE bearing silicates. The allanite-(Ce) can form on monazite-(Ce) and this transformation process is reversible. It is sometimes closely associated with infrequent torneböhmite-(Ce), dollaseite-(Ce), dissakisite-(Ce), as very late-stage minerals, substituting the monazite-(Ce). The chevkinite-(Ce) and its dimorph perrierite-(Ce) are found associated to allanite-(Ce), in a Ti-rich environment of the Jolotca mineralizing area (Hîrtopanu 2014).



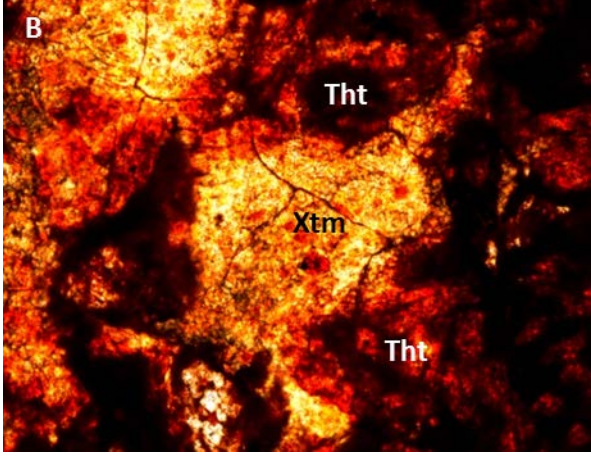


Fig. 5. A, Xenotime-(Y) (Xtm, large grain, white-yellow) intergrown with thorite (Tht, red/brown), TL, NII, x30; B, Xenotime-(Y) (Xtm, yellow, large grain) with thorite (Tht, black-red) around it, TL, NII, x35, Belcina area.

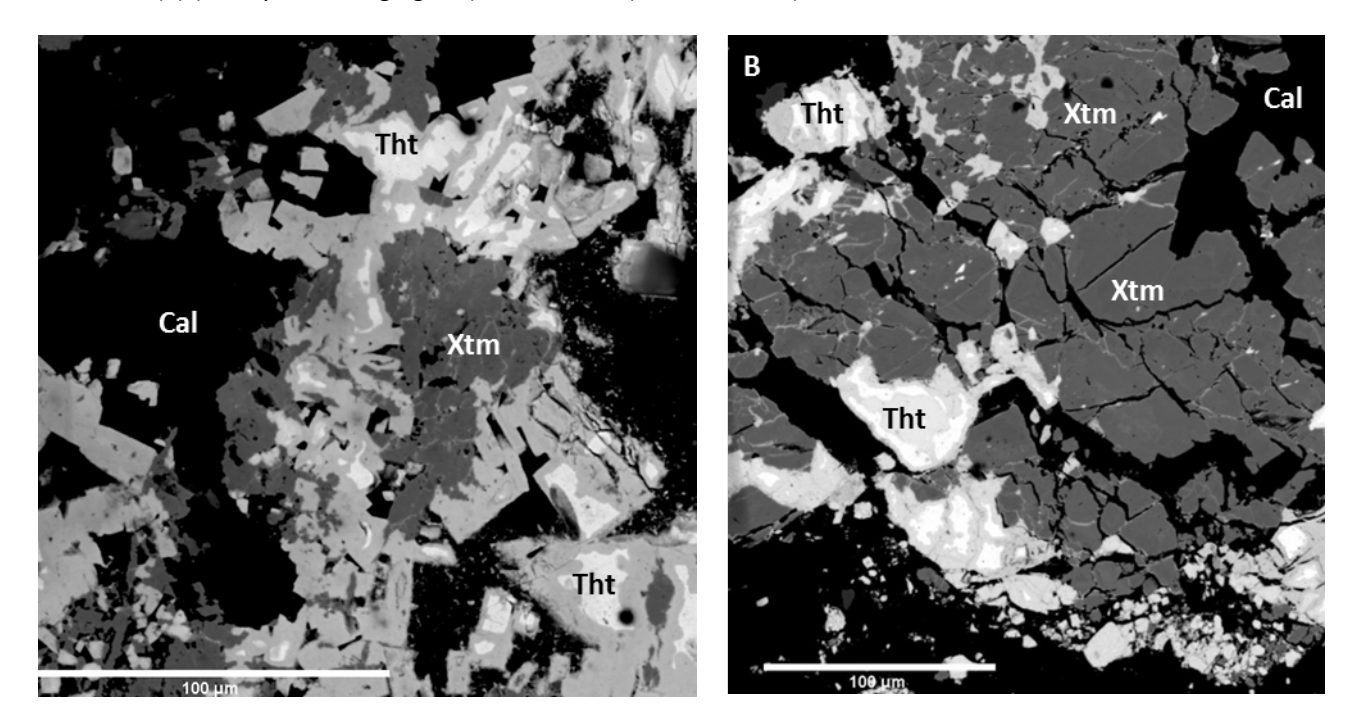


Fig. 6. A, Backscattered electron image of xenotime-(Y) (Xtm, dark grey, centre, core) substituted around by thorite (Tht, oscillatory composition: more Zr white, more Fe light grey), calcite (Cal, black); B, BSE image of xenotime-(Y) (Xtm, big grain, dark grey), thorite/thorogummite (Tht, oscillatory composition: white more Th, grey light more Zr less Th, and grey less Th, less Zr, more Fe), and calcite (black), Belcina area.

5. In the low temperature hydrothermal stage were formed the pyrochlore group (all its terms), betafite subgroup of the pyrochlore group represented by two accessory minerals, yttrobetafite-(Y) and betafite, members of fergusonites [fergusonite-(Y), fergusonite beta-(Nd), fergusonite-(Ce)], and many sulfides. The presence of fluorite, such Y rich and Ce rich varieties in the Jolotca vein mineralization is good evidence for a high fluorine content of the mineralizing fluids, which were also enriched in Y and Ce. The large twinned natrolite hosts the Na rich pyrochlore. More than 40 sulfides, Bi-tellurides, native Hg closely associated with later REE-apatite, and Ba-feldspars occur in this genetical stage in Jolotca area.

The Belcina vein type mineralization belongs to the same low hydrothermal process, but is at its late stage of very low T. It is situated outside the Ditrău massif, in the surrounding metamorphite rocks of the Tulghes Group. The Belcina occurrence (Hirtopanu et. al., 2013) comprises a complex mineralization, different from those previously reported in Jolotca. The large thorite closely associated with the large xenotime-(Y) (Figs. 5A, 5B, 6A, and 6B) represents the characteristic paragenesis of the Belcina type mineralization.

Tht

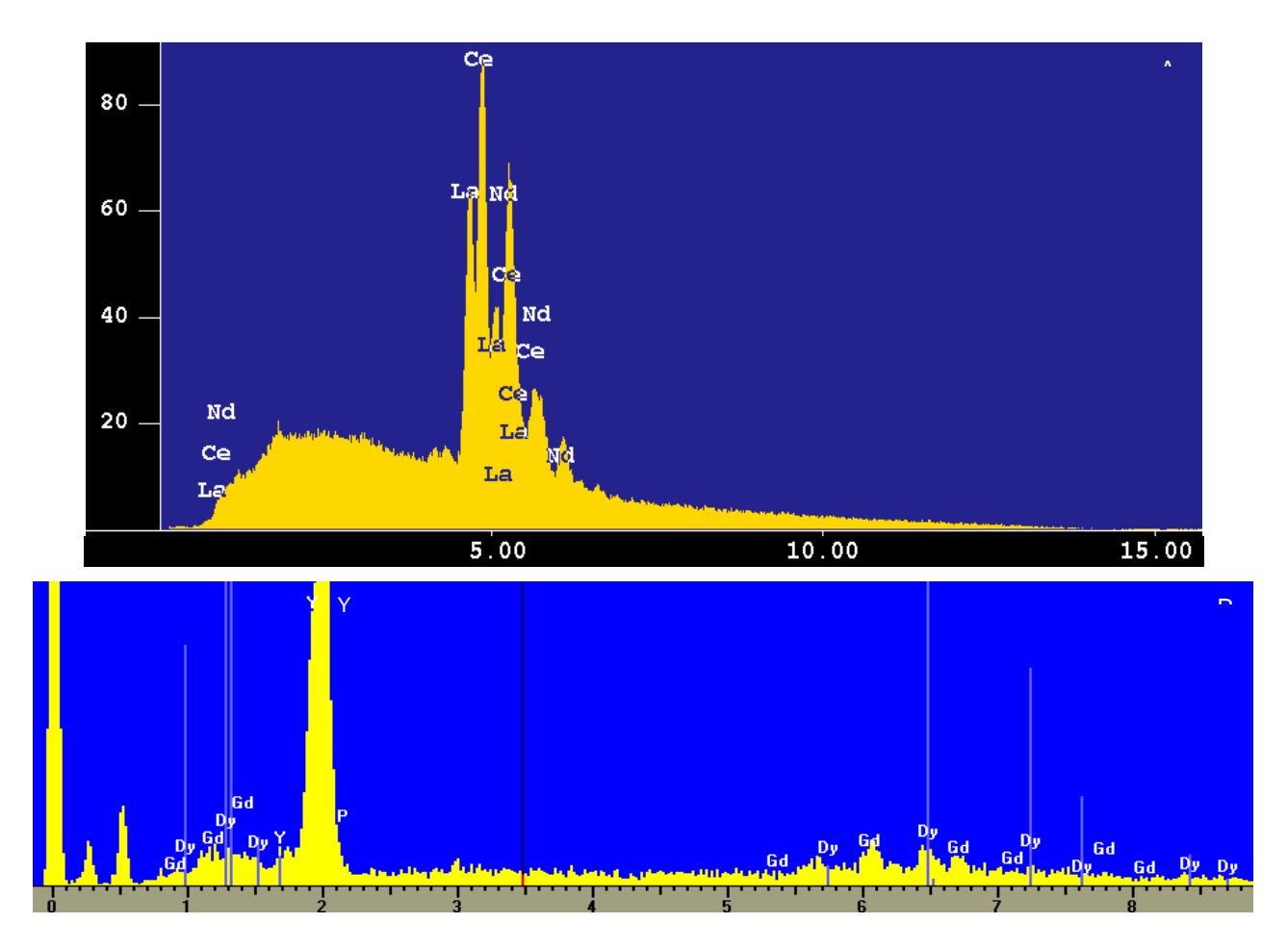


Fig. 7. A. Electron diffractogram spectrum of Nd rich bastnäsite-(Ce), Jolotca area; B. Electron diffractogram spectrum of Dy and Gd rich xenotime-(Y), Belcina area.

The late stage calcite, siderite, ferrodolomite, ankerite, new apatite veins, the development of the Feoxides and hydroxides (colomorph hematite, goethite, and lepidocrocite), and the minor sulfides of Fe, Pb, Zn, Mo and Hg, are all features of the carbonatite mineralization. Also, the development of many apatites (new Th rich apatite and Y bearing apatite) and carbonates of different generations as gangue minerals is specific to some mineralizations generated by carbothermal/hydrothermal carbonatite fluids.

Conclusions

In the Jolotca area are concentrated mainy Light REE/Cerium group minerals: LREE-carbonates, monazite-(Ce), allanite-(Ce), while in the Belcina area are concentrated mainly Heavy REE/Yttrium group minerals represented by xenotime-(Y) closely associated with Th silicates (thorite, thorogummite). The magmatic/metasomatic/hydrothermal differentiation processes are responsible for the in-situ concentration of many varieties of these rare earth element minerals in the Ditrău alkaline intrusive massif. The hydrothermal /carbothermal processes have played the dominant role, being reflected in the common kind of mineral appearances: grains with marginal and sectorial zonations, oscillatory compositions in the same crystal/grain, and the very complicated compositions of some minerals, due to the sudden variation of hydrothermal mineralization solutions. The mineralizing process was multi-staged, having at least 5 stages. The Belcina Y-Th complex mineralization could be the last stage lower temperature carbonatites.

Worldwide the vast majority of RRE-(Y) mineral resources are associated with three minerals: monazite-(Ce), bastnäsite-(Ce) and xenotime-(Y). Bastnäsite-(Ce) and monazite-(Ce) are the primary source of LREE, mainly Ce, La and Nd. Xenotime-(Y) is a primary source for HREE, including Y, Dy, Er, Gd, Yb and Ho. The Ditrau mineralizing area comprises both types of mineralizations with separate localization in space and time: Jolotca, enriched in LREE minerals, and Belcina, enriched in HREE/Y and Th.

References

- Hîrtopanu, P., Jakab, G., Andersen, C.J., Fairhurst, R. J., 2013. Thorite, thorogummite and xenotime-(Y) in Ditrău alkaline intrusive massif, East Carpathians, Romania, Proc. Rom. Acad. Series B, 15, 2, 111-132.
- Hîrtopanu, P., Fairhurst, R.J., Jakab, G., Udubasa, S.S., 2013. Allanite-(Ce) and its associations from the Ditrău alkaline intrusive massif, East Carpathians, Romania, Proc. Rom. Acad., Series B, 15, 1, pp. 59-74.
- Hîrtopanu, P., Fairhurst, R.J., Jakab, G., Udubasa, S.S., 2017. Monazite-(Ce) and its associations from the Ditrău alkaline intrusive massif, East Carpathians, Romania, Rom. J. Mineral Deposits 90, 1-2, 27-40.
- Hîrtopanu, P., 2019. New minerals and mineral varieties for Romania, Ed. Vergiliu, Bucuresti, pp. 263.

TECTONIC INVERSION AND RELATED TECTONO-METAMORPHIC ZONATION IN THE PRE-ALPINE GETIC-SUPRAGETIC AND DANUBIAN BASEMENT OF THE SOUTH CARPATHIANS

Viorica IANCU¹, Gabriel BINDEA¹, Antoneta SEGHEDI²

¹Geological Institute of Romania, 1 Caransebes St., 012271 Bucharest
e-mail: iancuviorica_2000@yahoo.com
²National Institute of Marine Geology and Geoecology – GeoEcoMar, 23-25 D. Onciul St.,
024053 Bucharest

Introduction

In the last decades of the 20th century, the Geological Institue of Romania carried out geological studies in the basement units of the South Carpathians, focused on geological mapping at scale 1:50.000, in order to complete the cartographic network partly published previously. Petrological, mineralogical, paleontological and geochemical studies were were undertaken simultaneously, in order to update the scientific information and correlations at local and regional scale were constantly accomplished for each area mapped. Thus, an important analytical data base (microscopic, geochemical, isotopic, micropaleontologic, microstructural) has accumulated, being used at editing and interpreting geological maps and sections, at the legends accompanying the map sheets, or to various types of atlases. Only a small part of these data were published in specialised journals. A spectacular leap of knowledge in the first decades of the 21st century followed, throu access to advanced microscopic methods and technologies (electron microscope, electon microprobe, isotopic age determinations, etc.), especially in laboratories from abroad. Therefore, it becomes necessary to update and revise the cartographic network, as well as the relationships between various geological entities, through integration of analytical results accumulated in time, especially as the printing of the most map sheets is still in progress.

This paper aims at such a revision and completion of the geological information related to the main lithological units of the Getic-Supragetic and Danubian basements in the South Carpathians. It brings petrological evidence related to the tectono-metamorphic zonality of the South Carpathians basements, based on field and laboratory observations and measurements, with details from key areas providing evidence of tectonic or tectono-metamorphic inversion associated to Variscan events (Fig. 1). These areas expose simple shear zones (with associated dynamic metamorphism) along the contacts of contrasting tectono-metamorphic units, remnants of ophiolitic assemblages and/or high pressure rocks (eclogites). These data complete and support the brief synthesis published recently (Iancu, Seghedi, 2017), related to the inheritance or preservation of basements associated to Variscan and Pan-African events. We have to emphasize that accumulation of a large amount of isotopic ages obtained by various methods imposes this type of integration and reinterpretation not only of the regional geology illustrated on the geological maps, but also of previously elaborated geodynamic models.

The South Carpathians

The Cretaceous nappe pile of the South Carpathians mountain range includes important crustal fragments of pre-Mesozoic metamorphic – magmatic rock assemblages, incorporated in the basement units of the Getic-Supragetic and Danubian nappe complexes. The entire South Carpathian Alpine nappe

stack override to ESE the Moesian Platform, which includes unmetamorphosed Paleozoic and Mesozoic sedimentary sequences.

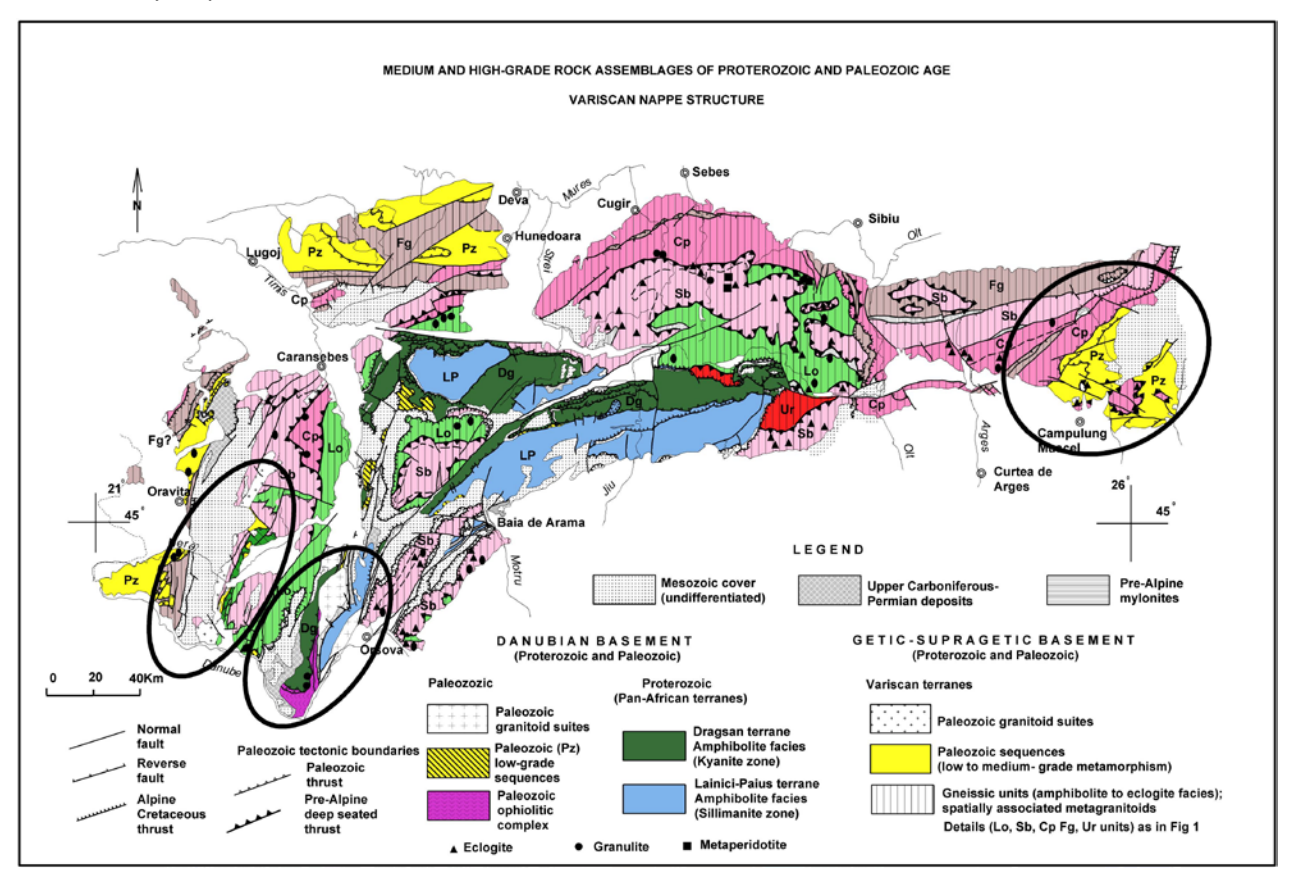


Fig. 1. Inherited Variscan units in the Alpine Getic-Supragetic and Danubian nappe systems, modified from Iancu, Seghedi (2017). Abbreviations: Sb – Sebeş, Lo – Lotru, Cp – Cumpăna, Fg – Făgăraş, Ur – Ursu, Dg – Drăgşan, LP – Lainici-Păiuş, PZ – Paleozoic.

The Danubian and Getic-Supragetic units differ in the geological constitution of their pre-Mesozoic basement, as Neoproterozoic rock-assemblages (protoliths) and Pan-African related granitoids are widespread in the Danubian realm (Liegeois et al., 1996; Balintoni et al., 2014), while their presence in the Getic-Supragetic is poorly constrained. In the Getic-Supragetic basement, pre-metamorphic protolith ages of the widespread medium-high grade rock assemblages ("gneissic units", Ledru et al., 1997) are presumed to be Late Neoproterozoic (Pavelescu et al., 1983; Pană et al., 2002) to Low Paleozoic (Cambrian-Ordovician) (Balintoni et al., 2004, 2014; Iancu et al., 2005; Axente et al., 2008). Scarce Paleozoic (Ordovician to Lower Carboniferous) discontinuous successions in the South Carpathians are metamorphosed in low to medium grade metamorphic conditions (Iancu et al., 2005b) and medium to high grade rock assemblages are widespread, but they are well documented as Neoproterozoic only in the basement of the Danubian units.

The Getic-Supragetic basement

Characterization of pre-Alpine terrains requires the identification and recognition of the pre-metamorphic protoliths, their pre-convergence and/or precollisional evolution, as well as their late collision history.

The Pre-Mesozoic protoliths of the Getic-Supragetic nappes include sedimentary and magmatic rocks with diverse lithologies and depositional environments: oceanic crust and related sedimentary and/or volcano-sedimentary successions (Lotru and Sebeş units); rift related magmatic and sedimentary or volcano-sedimentary rocks and remnants of thin continental crust (Buceava, Caras, Leresti, Călusu units);

continental sedimentary/volcano-sedimentary successions (Făgăraş and Miniş units); magmatic/volcanic arc complexes and volcano-sedimentary or sedimentary sequences (e.g. root zones and in situ anatectic granitoids, preserved in Sebeş 1 unit, Mehedinţi area); post-collisional granitoids (Sicheviţa-Poniasca plutons, dated at 311 Ma by Duchesne et al., 2008). Although preserved in restricted areas within the Getic-Supragetic basement, the highly diversified lithological features of the Paleozoic successions suggest that two major rifting events occured during the Paleozoic, one mainly in the Ordovician and the other during Upper Devonian-Lower Carboniferous (lancu et al., 2005; Balintoni et al., 2014 and references there in).

U/Pb isotopic data of 650-630 Ma, 590-540 Ma and 535-500 Ma on zircon crystals analyzed from orthogneisses and metagranitoids (Balica, 2007) document the preservation of Late Neoproterozoic to Cambrian metamorphosed magmatic and sedimentary rocks, suggesting Gondwana derived terrains and Cadomian magmatic arc activity.

Pre-Alpine tectonic and metamorphic events, identified in the Getic-Supragetic basement rocks based on geological and isotopic data, as well as on structural relationships, are related to the Variscan convergent/collision cycle and can be correlated with coeval metamorphic terrains from the classical Variscan belt outside the Alpine front (lancu et al., 2005). Variscan tectono-metamorphic events include regional, dynamo-thermal metamorphism and shear zone related, dynamic metamorphism.

Regional, dynamo-thermal metamorphism. The Variscan tectono-metamorphic history of the Getic-Supragetic basement is better documented for Early Carboniferous (Neo-Variscan) collision period, but recent U/Pb zircon ages on different granitoids, migmatites and gneisses (Balintoni et al., 2004; Dobrescu, 2005) suggest effects of older tectono-thermal activities in Middle-Lower Paleozoic time. As the result of subduction and contraction related tectono-metamorphic events of Pre-Westphalian age, low-grade (subgreenschist to green schist and epidote amphibolite facies conditions) and medium/high grade (amphibolite and eclogite-granulite facies) rock assemblages were involved in complex nape stacking, tectono-metamorphic inversion and exhumation processes.

Individual tectono-stratigraphic units display different metamorphic and deformational features (S1-S2 foliations and B1, B2 fold systems) as a consequence of contrasting lithologies and metamorphic conditions. Regional deformation gradients inside of the "gneissic units" can be observed on structural maps realized in the Central-South Carpathians (Ledru et al., 1998 and lancu et al., unpublished reports of the Geological Institute of Romania). Apparent transitions from one unit to another are induced by the shear zone related metamorphism, sometimes syn-metamorphic, at amphibolite facies level in the internal, gneissic areas (Lotru-Cibin, Semenic Mts.), while epidote-amphibolite bearing mylonites (including tectonic boudins of eclogites) crop out in external areas (Leaota-lezer Mts.). Extension-related foliations (post-S2, or post nappe stacking) are also present and give a false impression of continuity all over the "crystalline" basement.

The tectono-metamorphic events, as dated up to now, can be attributed to the Variscan orogeny based on isotopic geochronological data: 358-341 Ma, Sm/Nd (Medaris et al., 2003); 357-331 Ma, 40Ar/39Ar (Axente et al., 2008); 354-319 Ma, Sm/Nd, 342 Ma, Rb/Sr and 348-328 Ma, 40Ar/39Ar (Drăguşanu, Tanaka, 1999); 329-323 Ma Dallmeyer et al. (1996), monazite isotopic ages (Săbău et al., 2011). The isotopic data of and 320-309 Ma 40Ar/39Ar (Dallmeyer et al., 1998) and K/Ar ages (Grünnenfelder et al., 1983) represent cooling ages related to Variscan extension and collapse.

The Paleozoic tectono stratigraphic units (lancu et al., 2005 b) are characterized by various tectono - thermal histories (Medaris et al., 2003) and are separated by major tectonic contacts.

Shear zone related, dynamic metamorphism of Paleozoic age is spatially associated to the main tectonic contacts separating the pre-Westphalian litho-tectonic units. Thrust related, strike-slip and extension related fault zones are well preserved on the entire outcropping area of Getic-Supragetic and syn-tectonic blastesis covers large PT fields, from greenschist to amphibolite and eclogite facies conditions.

Some isotopically dated occurrences of mylonites rocks and syn-tectonic pegmatites give Paleozoic, Variscan ages: 342-341 and 332-331 Ma (reinterpreted from Axente et al., 2008) and respectively, 338-332 Ma (Pb/Pb, single crystal zircon ages, Cocherie, in Ledru et al., 1997). The dated minerals are from blastomylonitic rocks (lezer-Leaota) and syn-tectonic pegmatite (Cibin and Lotru), characterizing the tectonic boundaries between the main litho-tectonic units preserved in the Getic-Supragetic basement (lancu et al., 1998).

Tectono-metamorphic zonation. A frequent field feature of the metamorphic terrains is an apparent transition between distinct, even contrasting units, due to progressive changing of mineral assemblages and metamorphic zonation, and a huge volume of literature was published related to terms as metamorphic zonation and inverse (continuous and discontinuous) or inverted metamorphic zonation in the Alps, the Himalayan belt, the French Massif Central or the Bohemian massif. The tectono-metamorphic zonation, illustrated with mapping and petrological data in the Getic-Supragetic basement, is a composite effect of basin or rift/ tectonic/metamorphic inversion processes, as was demonstrated in the most part of orogenic areas: Late Neoproterozoic basin inversion, Antarctica (Goodge, 1997); Late Paleozoic tectonic inversion, Rocky Mountains (Keller, 2005); inverted metamorphic zonation associated to the base of an ophiolitic complex, Oman (Ghent et al., 1981).

In the Getic-Supragetic basement, the largest areas of the "gneissic units", characterized by apparent metamorphic zonation, are an effect of syn-tectonic and/or post-tectonic evolution, as was demonstrated in the French Massif Central (Burg et al., 1985). Such effect can be related to the tectonic superposition of units with different PTt evolution (Medaris et al., 2003). Different by this, a classical, coeval succession of metamorphic zones (sensu Miyashiro, 1975) in a "normal" sequence can be identified inside of some individual units (Godeanu and Mehedinţi areas), related to one regional metamorphic event (Hîrtopanu, 1986).

Shear zone related metamorphic zonation is spatially associated with structural discontinuities and connected to the main tectonic boundaries, of thrust or strike slip type. In such cases, the neoblastic (syntectonic) mineral parageneses mark narrow metamorphic zones, cross-cutting the former, pure shear structures, mainly affected by polystage deformations.

The post-nape metamorphic imprints, generally related to uplift and extension processes, show a uniform distribution of the mineral phases, finally resulting in cooling related recrystallization.

A particular case in some nape pile complexes of the South Carpathians is the *thermal metamorphic imprin*t related to large granitoid plutons of Late Paleozoic age (e. g., Sicheviţa and Poniasca granitoids, Duchesne et al., 2008); steep and narrow temperature gradients are distributed in direct connection with the intrusion of the mentioned post-collisional granitoids.

Effects of *tectonic and metamorphic inversion* processes are suggested by:

- Contrasting regional (dynamo-thermal) metamorphism of the tectono-stratigraphic units and related HP rocks from the Sebeş and Lotru Mountains (lancu et al., 1998; Medaris et al., 2003; Săbău and Massonne, 2003) (Fig 1);
- Contrasting lithologies and regional structural features of the units involving pre-orogenic riftrelated, mafic-ultramafic and bimodal magmatic assemblages (Mărunţiu et al., 1997; Iancu and Mărunţiu, unpublished reports);
- Structural and metamorphic gaps between tectonic units, underlined by simple shear zones and syn-tectonic blasthesis, marking narrow bands with inverted metamorphic zones (e. g., lezer-Leaota Mountains and Sicheviţa-Poniasca area, Zones A and B in Fig. 1).
- The presence of mafic-ultramafic rocks with the highest-pressure parageneses (eclogite, and garnet peridotite in the uppermost geometrical position inside the "gneissic units", lancu et al., 1998; Medaris et al., 2003).
- The lower thermal and higher pressure gradients (Medaris et al., 2003; Săbău and Massonne, 2003) related to the "external" remnants of subducted Paleozoic sequences and their association with exhumed epidote-amphibolite bearing mylonites including tectonic boudins of eclogites croping out in the lezer-Leaota mountains (lancu, 1998; Negulescu, 2006; Săbău, Negulescu, 2015). The previous geological maps of this area are known from Dimitrescu et al. (1986) and Gheuca and Dinică (1986).

The Danubian basement

The main feature of the Danubian basement is the preservation of Neoproterozoic protoliths with Pan-African affinities (780 to 570 Ma cf. Liégeois et al., 1996) related to Drăgşan (rift and oceanic crust

type) and Lainici-Păiuş (continental type crust) terranes (lancu and Măruntiu, 1989; Berza et al., 1994; Seghedi et al., 2005).

The Pan-African tectono-metamorphic evolution is documented by U/Pb, K/Ar and Ar/Ar isotopic data at 580-560 Ma (Grünenfelder et al., 1983; Liégeois et al., 1996; Dallmeyer et al., 1998). Contrasting geothermal gradients are characteristic for the Drăgşan (MP facies series) and Lainici-Păiuş (LP facies series) terranes (Berza et al., 1994). An apparent inverted tectono-metamorphic zonation, but an inverted pressure field gradient (Vannay, Grasemaan, 2001) of these two litho-tectonic units is due to the Paleozoic overthrust of the Drăgşan onto Lainici-Păiuş unit. This is characterised by distinct pre-Ordovician regional tectono-thermal evolution (different PTt paths). The Variscan tectonic boundary separating the Drăgşan and Lainici-Păiuş units was formed in greenschist facies conditions (stilpnomelane/chlorite/biotite zones), suggesting an overthrust emplacement at higher crustal level and late orogenic/collisional environment.

The internal part of the Danubian preserves a key-zone (Zone C, in Fig.1) and remnants of an inverted basin of back arc type, with a Devonian age (Plissart et al., 2017) as a result of a new cycle of crustal expansion and oceanic type spreading affecting the older, Neoproterozoic terranes of the Gondwana supercontinent (Iancu et al., 2005; Balintoni et al., 2010). The ophiolitic paleosuture croppingout in the Danube Gorges (Romania and Eastern Serbia) is represented by Late Paleozoic obducted ophiolites (Mărunţiu et al., 1997), which lately yielded Devonian Sm-Nd ages (380±34 -390±52 Ma) (Plissart et al., 2017).

The subduction of the basin successions was followed by tectonic inversion, nappe stacking and magmatic arc activity during a Late Variscan collisional stage (K/Ar and Rb/Sr ages; Sm-Nd ages, Plissart et al., 2017).

The intrusion of Paleozoic continental arc granitoids of 338, 329 and 320 Ma (Ogradena, Cherbelezu and Sfârdinu) dated by U/Pb zircon ages (Balica, 2007, unpublished PhD thesis) and 310, 314, 328 Ma (Plissart et al., 2017) is documented by magmatic flow fabrics (kfsp and biotite foliation), direct transition to a deep seated shear zone and related arteritic/metasomatic migmatization, LP-HT shear zone related metamorphism which can be connected to the high thermal gradients of the magmatic arc environment (lancu et al., 1997), S-C'-C" structures marking a major thrust fault at the eastern border of the Sfârdinu granitoid massive, and syn-tectonic blastesis of sillimanite-kfsp/cordierite-garnet/andalusite -garnet parageneses in the "thermal" contact zone.

Unconformable Upper Carboniferous-Permian sedimentary cover seals the whole nappe stack, granitoid bodies and their associated HT-LP mylonites.

Our mineralogical-petrographic and structural data suggest the overthrust of the Neoproterozoic gneisses (Poiana Mraconia, of Drăgşan type) onto Low-grade Paleozoic successions and Devonian ophiolite remnants took place as a consequence of the shortening and basin inversion in the Middle-Upper Carboniferous time. A thrust-related inverted metamorphic zonation is directly related to the Sfârdinu granitoids intrusion in HT-LP conditions, as indicated by syn-tectonic parageneses. A downward decrease in syn-tectonic metamorphic degree is documented by the preservation of the following metamorphic zones in mylonites: sillimanite-Kfeldspar/garnet cordierite/garnet-andalusite/garnet-biotite/chlorite, characterising mylonitic zone from the granite border to the low-grade Paleozoic successions (approximately 6-800 meters in a W-E cross-section, on Sfârdinu Valley). The west-dipping mylonitic foliation and lineation of the mentioned mylonites and spectacular syn-tectonic (simple shear) fabrics are illustrated by rotated andalusite and cordierite porphyroblasts and their internal inclusion trails (Mărunţiu, Seghedi, 1983; lancu et al., 1997; lancu, Seghedi, 2017).

The Variscan metamorphic events are registered by regional (dynamo-thermal) and syn-tectonic (dynamic) deformation and metamorphic blasthesis developed at different geothermal gradients as shown by the main tectonic units and protoliths assemblages. The inverted tectono-metamorphic zonation related to the main Paleozoic tectonic boundary from the bottom of the Almăj metamorphic-magmatic complex is related to the final stage of convergent-collisional processes involving Neoproterozoic/Pan-African gneissic-granitic terranes, Lower Paleozoic sedimentary successions, and Late paleozoic ophiolites. The intrusion of the Carboniferous granitoid plutons has a syn-tectonic, late collisional emplacement, along a large continental margin geotectonic context, of orogen paralel type.

Selective references

- Balintoni, I., Ducea, M., Pană, D., Wetmore, P., Robu, I., Robu, L., 2004. Cadomian-Early Palaeozoic ages of the Sebes-Lotru terrane (South Carpathians, Romania). Berichte des institutes für Erdwissenchaften der Karl-Franzens Universität. Graz, ISSN 1608-8166, 9.
- Balintoni, I., Balica, C., Ducea, M.N., Hann, H.P., Şabliovschi, V., 2010. The anatomy of a Gondwanan terrane: the Neoproterozoic-Ordovician basement of the pre-Alpine Sebeş-Lotru composite terrane (South Carpathians, Romania). Gondwana Research 17, 561-572.
- Balintoni, I., Balica, C., Ducea, M.N., Stremţan, C., 2011. Peri-Amazonian, Avalonian-type and Ganderian-type terranes in the South Carpathians, Romania: The Danubian domain basement. Gondwana Research 19, 945-957.
- Balintoni I., Balica, C., Mihai N. Ducea, M.N., Hann, H.-P., 2014. Peri-Gondwanan terranes in the Romanian Carpathians: A review of their spatial distribution, origin, provenance, and evolution. Geoscience Frontiers 5, 395-411.
- Berza, T., Balintoni, I., Iancu, V., Seghedi, A., Hann, H.P., 1994. South Carpathians. ALCAPA II Field Guidebook, Romanian Journal of Tectonics and Regional Geology, Suppl. 2, 37–50.
- Burg, J. P., Delor, C.P., Leyerloup, A. F., Romney, F. (1985). Inverted metamorphic zonation and variscan thrust tectonics in the Rouergue area (Massif Central, France): P-T-t record from mineral to regional scale. In: Daly, J. S., Cliff, R. A., Yardley, B. W. D. (eds), Evolution of Metamorphic Belts, geological Society Special Publication No. 43, 423-439.
- Dallmeyer, R. D., Neubauer, F., Handler, R., Fritz, H., Muller, W., Pana, D., Putis, M. (1996) Tectonothermal evolution of the internal Alps and Carpathians: Evidence from 40 Ar/ 39 Ar mineral whole-rock data. Eclogae geol. Helv. 89/1, 203-227, Basel.
- Dallmeyer, R.D., Neubauer F., Fritz V., Mocanu, V., 1998. Variscan vs. Alpine tectonothermal evolution of the Southern Carpathians orogen: constraints from 40Ar/39Ar ages. Tectonophysics 290, 1-2, 111-135.
- Dobrescu, A., 2005. Buchin and Slatina-Timis granitoids revisited geochemical and isotopical premises genetic and chronologic perspectives.
- Duchesne, J.-C., Liégeois, J-P., Iancu, V., Berza, T., Matukov, D. I., Tatu, M., Sergeev, S.A., 2008. Post-collisional melting of crustal sources: constraints from geochronology, petrology and Sr, Nd isotope geochemistry of the Variscan Sichevita and Poniasca granitoid plutons (South Carpathians, Romania). Int. Jour. Earth Sci. (Geol. Rundsch.) 97, 705–723.
- Frey, M., 2002. The tectono-metamorphic history of the Valaisian domain from the Western to the Central Alps: New constraints on the evolution of the Alps. Geological Society of America Bulletin, 114, 2, 207-225.
- Ghent, E.D., Stout, M.Z., 1981. Metamorphism at the base of Samail ophiolite, southeastern Oman Mountains. Journal of Geophysical Research, 86/B4: 2557-2571.
- Goodge, J.W., 1997. Latest Neoproterozoic basin inversion of the Beardmore Group, central Transantarctic Mountains, Antarctica. Tectonics, 16, 4, p. 682.
- Grünnenfelder, M., Popescu, G., Soroiu, M., Arsenescu V., Berza, T., 1983. K-Ar and U-Pb dating of metamorphic formations and associated igneous bodies from the Central South Carpathians. An. Inst. Geol. Rom. XLI, 37–46.
- Haydutov, I., Yanev, S., 1997. The Protomoesian microcontinent of the Balkan Peninsula a peri- Gondwanaland piece. Tectonophysics 272, 303-313.
- Hârtopanu, I., 1986. Problems of the Metamorphic Zonality in the South Carpathians and Apuseni Mts. (Romania). In: Mineral paragenesis, 735-754, Theophrastus Publications, S. A. Athens.
- lancu, V., 1998. Relatii intre granitoide si metamorfite pre-alpine in Carpaţii Meridionale. Unpublished PhD Thesis, University of Bucharest, 206 pp.
- lancu, V., Mărunţiu, M., 1989. Toroniţa Zone and problems of the pre-Alpine metamorphic basement of the Getic and Danubian realms. D. S. Inst. Geol. Geofiz. 74, 1, 223–237.
- Iancu, V., Mărunțiu, M., Johan, V., Ledru, P., 1998. High-grade metamorphic rocks in the pre-Alpine nappe stack of the Getic– Supragetic basement (Median Dacides, South Carpathians, Romania). Mineral Petrol 63, 173–198.
- lancu, V., Berza, T., Seghedi, A., Mărunțiu, M., 2005b. Palaeozoic rock assemblages incorporated in the South Carpathian Alpine thrust belt (Romania and Serbia): a review. Geologica Belgica 8, 48–68.
- lancu, V., Axente, V., Bindea, G., Ledru, P., Maluski, H., 1997. HT/LP and MT/MP mylonites related to nappe emplacement in a Palaeozoic convergent plate boundary in the Danubian Units, South Carpathians. Intern. Symposium "Geology in the Danube Gorges", Geoinstitut, Special Edition 25, 289–290, Belgrad-Bucharest.
- Ledru, P., Cocherie, A., Iancu, V., Mărunţiu, M., 1997. The gneissic units of the Median Dacides (Getic-Supragetic domain); an exotic segment of the European Variscides. Rom. J. of Mineralogy, vol. 78, Supplem. Nr. 1, p. 48, Bucharest.
- Liégeois et al., 1996; Štipská, P., Pitra, P., Powell, R. (2006). Separate or shared metamorphic histories of eclogites and

- surrounding rocks? An example from the Bohemian Massif. Journal of Metamorphic Geology, 24/3, p. 219
- Mărunțiu, M., Iancu, V., Alexe, V., Stoian, M., 1996. Geochemistry of the metamagmatic rocks in the Getic–Supragetic Domain of the South Carpathians. Inst Geol Roman 69, 225–228
- Mărunțiu, M., Menot, R.P., Țapardel, C., 1997. Cryptic variation and geochemistry of cumulate pile from Tisoviţa-Iuţi ophiolite: preliminary approach of magma chamber evolution and tectonic setting. International symposium "Geology in the Danube Gorges", Geoinstitut, Special Edition 25, 295–299.
- Medaris, G. jr., Ducea, M., Ghent, E.D., Iancu, V., 2003. Conditions and timing of high-pressure metamorphism in the South Carpathians, Romania. Lithos, 70, 141–161.
- Negulescu, E., 2006. Semnificația mineralelor și a asociațiilor minerale în determinarea istoriei metamorfice a cristalinului masivului Leaota. Unpublished PhD Thesis, University of Bucharest, 461 pp.
- Plissart, G., Monnier, C., Diot, H., Maruntiu, M., Berger, J., Triantafyllou, A., 2017. Petrology, geochemistry and Sm-Nd analyses on the Balkan-Carpathian Ophiolite (BCO Romania, Serbia, Bulgaria): remnants of a Devonian back-arc basin in the easternmost part of the Variscan domain. Journal of Geodynamics http://dx.doi.org/10.1016/j.jog.2017.01.00
- Săbău, G., Negulescu, E., 2015. Monazite chemical age and composition correlations, an insight in the Palaeozoic evolution of the Leaota Massif, South Carpathians. EGU General Assembly 2015, held 12-17 April, 2015 in Vienna, Austria. id.12781, 17127815.
- Seghedi, A., Berza, T., Iancu, V., Mărunțiu, M., Oaie, G., 2005. Neoproterozoic terranes in the Moesian basement and in the Alpine Danubian Nappes of the South Carpathians. Geologica Belgica 8, 4, 4–19.
- Vannay, J-C., Grasemann, B., 2001. Himalayan inverted metamorphism and syn-convergence of a general shear extrusion. Geological Magazine, 138/3: 253-276.
- von Quadt A., Peytcheva, I., Haydoutov, I., 1997. U-Pb zircon dating of the Tcherny Vrach metagabbro, the West Balkan, Bulgaria. Comptes Rendues de l' Académie Bulgare des Sciences 51, 1-2, 81-84.

ENVIRONMENTAL PROBLEMS ASSOCIATED WITH THE MINING ACTIVITIES IN THE APUSENI MOUNTAINS, ROMANIA

Elena-Luisa IATAN

Institute of Geodynamics "Sabba S. Ştefănescu" of Romanian Academy, 19–21 Jean-Louis Calderon St, 020032 Bucharest, e-mail: luisaiatan@yahoo.com

Mining is one of the oldest industries, and abandoned mines with the potential to release harmful substances into soil, water and air are found throughout Romanian territory. Due to the mining activity of ore deposits for more than 2000 years, in Romania there are over 550 tailings dumps, covering an area of approximately 800 ha and storing over 200 million cubic meters of tailings and 64 tailings ponds, which covers an area of almost 1350 ha and stores over 350 million m3 of waste.

Mining activities create a potential impact on the environment, both during exploitation and in the years after mine closure. Underground exploitation presents the risk of collapsing galleries and surface overflowing and involves the dislocation of a large amount of rocks. Quarrying is one of the most common forms of mineral extraction, being particularly harmful to the environment, as strategic minerals are often available in low concentrations, which increases the amount of ore extracted.

Although mining activities are currently stopped in most areas, the potential risk of environmental contamination exists due to the huge quantities of tailings in the tailings ponds and the tailings dumps very close to the watercourses. These are permanent sources of pollution for surface and groundwater, soil and air in the area (Fig. 1).

The oxidation of sulphide minerals led to the removal of soluble metal ions from the mineralization found in mining related wastes under the effect of water. As the water takes over the concentrations of minerals and heavy metals, it becomes a contaminant and a source of dispersion that can pollute the region around the mine and for considerable distances from the source.

The South Apuseni Mountains territory is crossed by a dense network of fluvial courses included in the fluvial system of the Mureş and of the Crişul Alb, both of them discharging their waters into the Tisa and implicitly into the Danube.

The Mureş River is the main collector of the waters in the studied region. The main tributaries of the Mureş, from the Southern Apuseni Mountains, are the Aries, the Ampoi and the Geoagiu rivers.

Downstream Câmpeni, the *Arieş River* receives, from the Metaliferi Mountains, a series of right-bank small rills such as Stefanca, Musca, Sesei, which receive the waters from the Roşia Poieni and Baia de Arieş mining perimeter. The Abrud is the most important right-bank tributary of the Arieş (Fig 1. C). It gathers the rills that flow radially around the igneous massif of Detunata and of Izbicioara, Abruzel and Bucumanilor triburaties reciving waters from Bucium Poieni, Bucium Şasa and Bucium Izbita old mining perimeters. The Corna Valley and the Roşia Valley (Fig 1. A) are among the most important tributaries of the Abrud, receiving the waters from the Roşia Montană and Roşia Poieni mining perimeter. The pollution sources of the Arieş basin proceed from the mining objectives of Roşia Montană, Roşia Poieni, Bucium and Baia de Arieş.

The main water collector within the Roşia Montană mining perimeter is the Roşia Valley stream, called Foieş (Fig 1.A), where the hydrographic network has been totally disorganized by mining activities. From the opencast pit, the pluvial waters infiltrate into underground through the old mining galleries, being collected at the level of the transport gallery "Sfanta Cruce din Orlea" from where they are discharged into the Foieş stream (Fig 1. B). Exceeding values are registered for almost all indicators of the mine waters, including very noxious elements and heavy metals such as lead, copper, zinc, arsenic, cadmium and manganese, with strong acidic conditions (table 1).



Fig. 1. Waters affected by mining: A. Foieş stream (Roşia Montană Valley), B. "Sfânta Cruce din Orlea" (Roşia Montană) gallery waters, C. the confluence of Abrud river (reddish-yellowish color) with Arieş river, D. Barza gallery waters, E. Barza Valley, F. Grimm gallery waters (Troiţa).

In the Roşia Poieni mining perimeter, the local hydrographic network, which collects the waters from the opencast pit and the mine waste dumps, is represented by the Steregoi, Ştefancei, Şesei, Muşca and Fîntînilor Valleys, right-bank tributaries of the Arieş River, as well as the Geamăna and Cuibarului Valleys, right-bank tributaries of the Abrud River. The analysis of the collected samples from the area present exceeding values for all the water quality indicators, with highly acidic pH and alarming values of copper, zinc, cadmium and iron contents.

In the Baia de Arieş mining perimeter, the local hydrographic network has been disorganized as result of stream blocking with mine wastes (Hermăneasa and Cioara Valleys) and with processing wastes (Sartăs Valley, Brazesti Valley). Mine waters are collected gravitationally into two basins and the quality of the waters discharged in the Arieş River is influenced by their mineralization degree. Values exceeding the admitted values are registered for suspensions, fixed residuum, sulphides and metallic ions (Cu, Pb, Zn, Fe, Mn, Cd, As) (Duma, 2009).

Several studies have been carried out in order to evaluate the water quality and the level of metal contamination in the Arieş river and its tributaries affected by the mining operations. The physico-chemical parameters indicated the contamination of the water by mining activities. In the tributaries of Arieş, the pH values were in the acid range (Senila et al., 2015). The water of the Arieş river has been found to be mostly polluted with Cu, Mn and Fe (Levei et al., 2014). The concentrations of metals (Fe, Zn, Cu and Mn) were higher in tributaries (Senila et al., 2015). The sediments in the Arieş river were highly contaminated with Cd, Cu and As, considerably with Zn, moderate with Pb and Ni and low with Cr (Levei et al., 2014). Their impact on the water quality of the river is strongly felt along the entire length of the Arieş river, from Câmpeni to the confluence with the Mureş river, and the intensity of pollution varies depending on the flow of the river (Corches, 2011).

Certej-Săcărâmb, Zlatna, Troița-Bolcana and Vorța are the mining units that have affected aquatic environment in *Ampoi Basin*.

In the *Zlatna* mining perimeter, the hydrographic network has been disorganized due to the construction of the tailing ponds on Sfârci Valley and on Valea Mică and through the mine waste dumps blocking the Hanes and Larga rills. The waters flowing from the tailings settling ponds of Zlatna register exceeding values for copper, lead, zinc, iron, manganese and cyanides. The mine water is affected by the presence of metallic ions (Cu, Pb, Zn, Fe) causing an acid pH (table 2).

Table 1. Chemistry data of analyzed waters from Arieş basin (¹Whitehead, 2009; ²Friedel et al, 2008; ³Duma, 2009; ⁴Corcheş, 2011; ⁵latan, 2019).

| Water | Rosia | Valley | Rosia Min | e waters1 | Corna-V | alea Verde | Saliste | | Abruz | el | Abruz | el- | Sesei | | Baia de | Aries | Aries |
|-----------------|--------|--------|-----------|-----------|----------|------------|---------|------|--------|----------------|--------|-------|--------|-------|--------------------|----------------------|--------------------|
| quality | (Foies |)1 | | | waste du | mp | Valley | 1 | Valley | ₇ 1 | Mine | | Valley | 2 | Aries ³ | River- | River- |
| indicators | | | | | waters1 | | | | | | waters | 1 | | | | Campeni ⁴ | Baia de |
| μg/l | Min | Max | Min | Max | Min | Max | Min | Max | Min | Max | Min | Max | Min | Max | 1 | _ | Aries ⁴ |
| As | 2,15 | 46,9 | 361,18 | 1738 | 0 | 684,2 | 0,9 | 42,8 | 0 | 22,1 | 0 | 265 | 0 | 0 | - | - | - |
| Cd | 1,9 | 432 | 331,09 | 875 | 0 | 54,3 | 1,22 | 73,2 | 1,29 | 73,2 | 2,04 | 107,3 | 0.1 | 50.6 | - | 0.3 | 2 |
| Cu | 134 | 1216 | 3361,5 | 12370 | 1,6 | 381 | 14,6 | 211 | 98 | 3175,7 | 107 | 8070 | 0.6 | 14900 | 350 | 23 | 437 |
| Pb | 0 | 16,8 | 59,01 | 266 | 4,4 | 67,9 | 0 | 4,8 | 0 | 6,4 | 0 | 66,7 | 0.08 | 88 | 400 | 2 | 14 |
| Zn | 138 | 14825 | 52288,57 | 169313 | 28,4 | 14590 | 250,3 | 3129 | 45,5 | 3763,5 | 478 | 13090 | 4 | 7190 | 1000 | 88 | 302 |
| Cr | 4,2 | 1438 | 2387,84 | 14650 | 3,5 | 2964,25 | 5,36 | 532 | 3,5 | 278,17 | 6,4 | 954 | 3.33 | 3.33 | - | - | - |
| Mn | 12,38 | 90 | 5381,4 | 77200 | 0,02 | 603000 | 26,6 | 188 | 0,01 | 1121 | 1,13 | 14640 | 0.4 | 3730 | 1300 | 133 | 620 |
| Fe | - | - | - | - | - | - | - | - | - | - | - | - | 64200 | 64200 | 4700 | 240 | 480 |
| pH ⁵ | 3.1 | • | 2.6 | • | 4.5 | ' | 6.0 | • | 4.3 | | 3.5 | • | 3.5 | | 6.9 | 7.2 | 7.0 |

In the Certej – Săcărâmb mining perimeter, waters are collected into the hydrographic basin of the Certej River, a right-bank tributary of the Mureş River. The mine waters run freely into the emissary, the ones from the Bocşa Mine into the Bocsa Rill, the ones from the Hondol-Băiaga Mine into the Certej River, and the ones from the Săcărâmb Mine into the Nojag Rill. The mine and the opencast pit waters are characterized by high contents of solid suspensions, fixed residuum, metallic ions (Cu, Zn, Fe, Mn) and sulphate ions (SO4). The waters flowing from the Mealu Valley tailings settling pond are characterized by exceeding values for suspensions, fixed residuum, metallic ions (Pb, Zn, Mn), SO4, chlorine and cyanides. The waters of the Certej Rill have polluted through infiltrations also the phreatic waters, which, in certain periods of the year become undrinkable (table 2).

The waters from the Troiţa Mine have a discharge of 420 m3/day and run freely at the level of the Grimm gallery (Fig 1. F) into the Bolcana Rill, a left-bank tributary of the Caian Rill, downstream the locality of Şoimus. These waters are characterized by low values for pH as well as exceeding sulphates and metallic ions (Cu, Pb, Zn, Fe). Mine waters have only little influence upon the water quality of the Caian Rill due to their low discharge value, as well as to the share of carbonates containing waters of the Crăciuneşti lime opencast pit that regulate the pH.

Table 2. Chemistry data of analyzed waters from Ampoi basin (Duma, 2009).

| Water quality indicators mg/l | Hanes Mine | Larga Mine | Baiaga | Bocsa | Sacaramb | Hondol- Coranda | Valea Mealu | Caian | Troita | Paraul Baii gallery | Valea Heius gallery | Vorta Valley |
|--|---------------|---------------|--------|-------|----------|--------------------|----------------|-------|--------|---------------------------|---------------------------|-----------------|
| Cu | 17.4 | 1.9 | - | 1.95 | 0.43 | 15.62 | 0.09 | 0.14 | 1.06 | 0.13 | 0.13 | 0.1 |
| Pb | 0.6 | 0.25 | - | - | - | 0.11 | 0.01 | 0.20 | 26.5 | 0.16 | 0.14 | 0.11 |
| Zn | 720.5 | 25.6 | 4.64 | 55.39 | 50.88 | 246.0 | 0.73 | 0.18 | 94.5 | 0.18 | 0.18 | 0.12 |
| Fe | 1695 | 158 | 0.09 | 3.90 | 0.59 | 302.78 | 2.0 | 1.24 | 83.3 | 2.47 | 2.47 | 1.06 |
| Mn | 830 | 20.8 | 7.30 | 36.54 | 39.29 | 150.40 | 5.60 | - | - | - | - | - |
| Ca | 410 | 254 | 527 | 348.0 | 253.3 | 339.2 | 339.2 | - | - | - | - | - |
| Mg | 50 | 62.4 | 102.8 | 92.25 | 121.40 | 64.92 | 43.7 | - | - | - | - | - |
| рH | 2.2 | 2.5 | 7 11 | 4 76 | 5 31 | 2.8 | 7.30 | 8.09 | 2.78 | 8 4 5 | 2.47 | 8 65 |

The waters evacuated from the Vorţa Mine through the two flank galleries from Heius Valley and Băii Creek (table 2) are discharged into the Vorţa Valley, their quality being characterized by the presence of metallic ions (Cu, Zn, Pb, Fe), but their influence upon the waters of the Vorţa Valley is insignificant due to the low discharges of the mine waters (Duma, 2009).

The Crişul Alb River is the main collector of the waters in the northern sector of the Metaliferi-Zarand Mountains. At Criscior it receives the left-bank waters from the Valea Arsului-Valea Morii, Barza and Rovina Mines and at Brad the ones of the Luncoi Valley (Ruda-Brad mine) (table 3).

Cris Alb River Water quality Barza Barza Ribita Arsului Valea Rovina Cris Alb River Valley Mine tailling Valley Ruda tailling indicators before mining after mining $\mu g/l$ sectors sectors 310 190 32000 0.2 Cu 23 50 0.04 Pb <5 <5 0.2 3 4 2200 5700 11000 106 Zn 2 1 11 940 8 <11 Fe 28000 410 190 52 0.06 < 0.05 0.05 0.7 Cd 11 375 100 < 0.01 As 18 10.3 5300 14400 270 18000 110 22 212 Mn 20 4.6 3.2 7.4 7.1 7.8 pΗ 4.0 8.3

Table 3. Chemistry data of analyzed waters from Crisul Alb basin (Sima et al., 2008)

Heavy metal contaminations in the Criş Alb basin (table 3), combined with high sulfate concentrations and low pH values, are found in valleys, Arsului Valley and Barza Valley (Fig 1.E). The outflow of the open pit mined for copper situated in Valea Arsului, exhibits clearly high dissolved metal contents. The drain of underground galleries and waste dumps in Valea Barza, shows high manganese, iron, zinc and cadmium concentrations. Due to the high contents of dissolved iron and particulate Fe, these waters display an ochre-brownish color, the distinct and classical optical sign of mining pollution (Duma, 2009) (Fig 1. D).

Results and conclusions: High values of the contents of metallic ions were recorded for the waters from Roşia Montană, Hanes Mine, Larga Mine, Săcărâmb Mine, Barza Mine and Troiţa Mine (tables 1, 2, 3). In Roşia Poieni, high contents of copper were registered in the waters flowing from the mine waste dumps.

High contents of cyanides were recorded in the waters of the Săliste Valley tailings settling ponds - Roșia Montană (0.32 mg/l), in the Sartăș tailings settling pond - Baia de Arieș (0.75 mg/l) and in the Valea Mealu tailings settling pond of Certej- Săcărâmb (0.040 mg/l) (Duma, 2009).

The potential for acid generation is directly related to the potential oxidation of sulphide minerals to sulphate (sulphuric acid). The experiments made by Jennings et al. (2000) demonstrated that under strongly oxidizing conditions, pyrite, marcasite, pyrrhotite, arsenopyrite, chalcopyrite and sphalerite are acid-producing minerals but chalcocite and galena were found to be non-acid producing minerals. In the studied area, the main sulphide-producing acid is pyrite.

In the Southern Apuseni Mountains, long-term mining activities have caused environmental problems, affecting waters, soils and sediments, which must be remediated. The rehabilitation of the environment in the Southern Apuseni Mountains has to be done, in order to reduce the impact of mine waters and of the ones flowing from the tailings settling ponds and waste dumps, by the construction of water treatment stations.

Acknowledgments. This work was supported by two Romanian Ministry of Research and Innovation grants, CCCDI – UEFISCDI, project number PN-III-P4-ID-PCCF-2016-4-0014 and project number PN-III-P1-1.2-PCCDI-2017-0346/29, within PNCDI III.

References

Corches, M.T., 2011. The Arieş river anthropic pollution due to mining activities, Journal of Agroalimentary Processes and Technologies 2011, 17, 4.

Friedel, M.J. Tindall, J.A., Sardan, D., Fey, D., Poptua, G.L., 2008. Reconnaissance study of water quality in the mining-affected Arieş River basin, Romania: U.S. Geological Survey Open-File Report 2008-1176, 40 p.

Jennings, S, Dolhopf, D, Inskeep, W., 2000. Acid production from sulfide minerals using hydrogen peroxide weathering. Appl Geochem 15, 247–255.

Levei, E., Ponta, M., Senila, M., Miclea, N. M., Frenţiu, T., 2014. Assessment of contamination and origin of metals in mining affected river sediments: a case study of the Aries River catchment, Romania. Journal of the Serbian Chemical Society 79, 8, 1019–1036.

- Senila, M., Levei, E, Senila, L.R, Roman, M., 2015. Preliminary investigation concerning metals bioavailability in waters of Arieş River catchment by using the diffusive gradients in thin films technique. Journal of Chemistry Volume 2015, Article ID 762121, 8 pages http://dx.doi.org/10.1155/2015/762121.
- Sigismund, D., 2009. The impact of mining activity upon the aquatic environment in the Southern Apuseni Mountains. Romanian Review of Regional Studies V, 1.
- Sima, M., Zobrist, J., Senila, M., Levei, E.A., Abraham, B., Dold, B., Bălteanu, D., 2008. Environmental pollution by mining activities A case study in the Criş Alb Valley, Western Carpathians, Romania, Proceedings of the Swiss Romanian Research Programme on Environmental Science & Technology (ESTROM), 14-2008.
- Whitehead, P. G., Butterfield, D., Wade, A. J., 2009. Simulating metals and mine discharges in river basins using a new integrated catchment model for metals: pollution impacts and restoration strategies in the Aries-Mures river system in Transylvania, Romania. Hydrology Research 1 April 2009; 40, 2-3, 323–346. doi: https://doi.org/10.2166/nh.2009.069.

CANNIZZARITE IN ROMANIAN OCCURENCES

Gheorghe ILINCA¹, Dan TOPA²

¹Department of Mineralogy, University of Bucharest, 1 Nicolae Bălcescu Boulevard, Bucharest e-mail: g.g.ilinca@gmail.com

²Naturhistorisches Museum Wien, Burgring 7, A 1010, Vienna, Austria

Samples of cannizzarite have been found in polymetallic ore deposits and mineralized bodies related to the Banatitic Magmatic and Metallogenetic Belt – BMMB (Berza *et al.* 1998), at Băiţa Bihor (Bihor Mts.) and Oraviţa-Ciclova (Southwestern Banat). The belt represents a series of discontinuous Upper Cretaceous magmatic and metallogenetic occurences which are discordant in respect to mid-Cretaceous nappe structures (Cioflica and Vlad, 1973; Ciobanu *et al.* 2002).

General crystal chemistry of cannizzarite

The name "cannizzarite" denotes a variable-fit homologous series of structurally related phases (Makovicky 1988, Ferraris et al. 2004, Topa $et\ al.$, 2010) whose crystal structures consist of an alternation of pseudotetragonal, square-pyramidal (Pb,Bi)(S,Se) layers (Q layers) and double-octahedron (Bi,Pb)₂(S,Se)₃ pseudohexagonal layers (H layers). The layers are commensurate along an intralayer direction, with a periodicity of about 4.1 Å, and *incommensurate* in the perpendicular intralayer direction. Each layer contains well defined subcells: pseudotetragonal in the Q layers (about 4 Å in the direction of the layer) and centered pseudohexagonal in the H layers (about 7 Å along the same direction). These two subperiodicities may match over relatively long ranges, provided that multiples of Q and H subcells add to a common (or close) periodicity: e.g. 3H:5Q (Borisov $et\ al.$, 2012), 7H:12Q (Topa $et\ al.$, 2010), 27H:46Q (Matzat, 1979). Due to the orientation of H and Q subcells along the ($\overline{1}$ 01) direction, the overall c parameter may not add exactly to a multiple of the 4.1 and 7 Å lengths. Other possible H/Q matches are suggested by Makovicky and Hyde (1981). The layer stacking of cannizzarite measures approximately 15.5 Å.

Samples and parageneses

Cannizzarite was found in five samples from across the BMMB: one sample from Baia Roşie area (Băiţa Bihor), three samples from Tâlva Mică area (Oraviţa) and two samples from Lobkowitz waste dump (Ciclova). At Băiţa Bihor, cannizzarite traces the contact between junoite – $Cu_2Pb_3Bi_8(S,Se)_{16}$ and gladite-pekoite exsolutions. Oraviţa records the most abundant concentration of cannizzarite: (a) large patches associated with proudite – $Cu_2Pb_5Bi_{9.33}(S,Se)_{22}$ and pekoite – $Cu_2PbBi_{11}S_{18}$, (b) mixed grains with chalcopyrite in a felbertalite – $Cu_2Pb_6Bi_8S_{19}$ and cosalite – $Pb_2Bi_2S_5$ matrix or (c) symplectitic mixtures with exsolved gladite-pekoite. The most spectacular occurrence is Ciclova where cannizzarite is graphically replaced by a bismuthinite derivative and it associates with junoite, proudite, relics of lillianite – $Pb_3Bi_2S_6$ and tetradymite – Bi_2Te_2S (Figure 1).

Chemical composition

Cannizzarite samples were analyzed using an JXA–8600 Jeol Superprobe electron microprobe, controlled by Probe for Windows system of programs, operated at 25 kV and 20 nA, with a beam diameter of 5 μ m. Wavelength-dispersion data were collected using the following standards (all synthetic except galena) and emission lines: Bi₂S₃ (BiL α , SK α), galena (PbL α), chalcopyrite (CuK α), Ag metal (AgL α), CdTe (CdL β , TeL α), and Bi₂Se₃ (SeL α). The raw data were corrected with the on-line ZAF–4 procedure. The average results of 142 electron-microprobe analyses are compiled in Table 1.

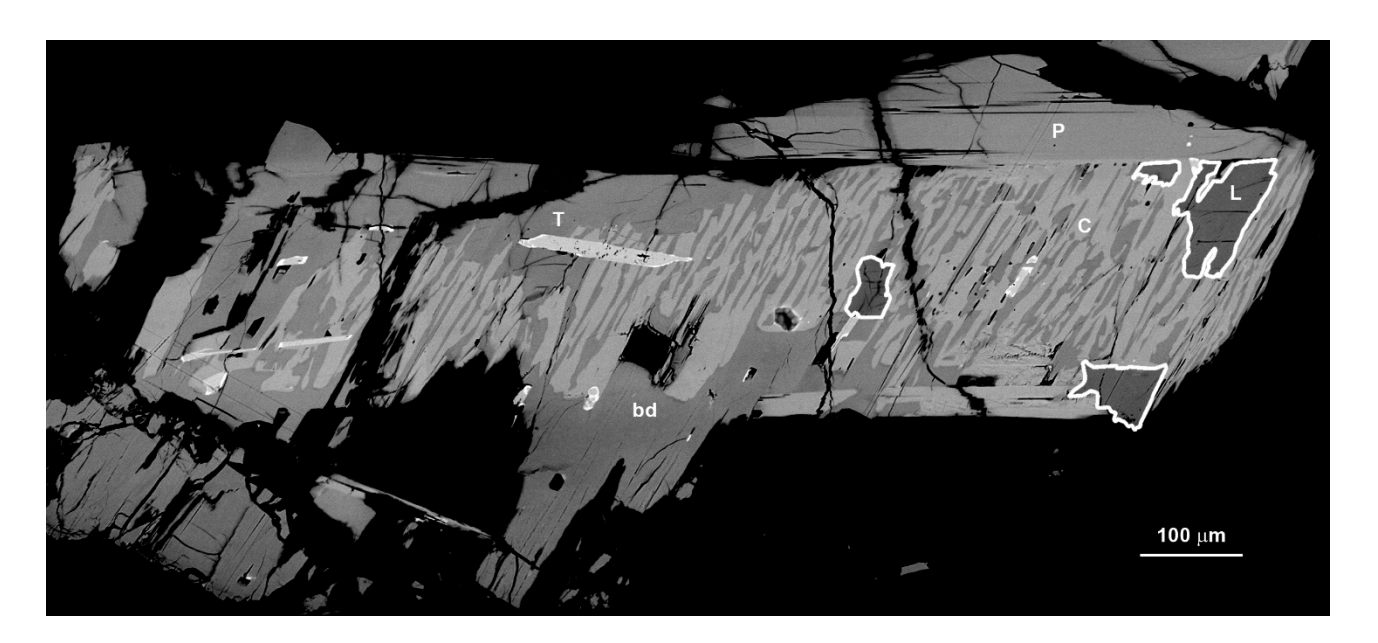


Figure 1. Cannizzarite (c) replaced by a bismuthinite derivative (bd), associated with proudite (p), relics of lillianite (Louthout outlined) and tetradymite. Lobkowitz, Ciclova.

Table 1. Average results of electron-microprobe analyses of cannizzarite from Băița Bihor (BB-192), Oravița (OR12, OR23, OR172) and Ciclova (C25, C65). Compositions are expressed in wt.%; *n*: number of analyses. Standard deviation for the last two digits is shown in parentheses; *Ev* expresses the relative error in the charge balance based on cation and anion charges.

| Sample | n | Cu | Ag | Pb | Bi | Sb | S | Se | Те | Total | Ev |
|--------|----|---------|----------|-----------|-----------|----------|-----------|----------|----------|------------|------|
| BB192 | 35 | 0.28(7) | 1.26(12) | 31.79(76) | 49.53(74) | 0.17(12) | 16.22(15) | 0.61(17) | 0.29(11) | 100.15(49) | 0.59 |
| OR12 | 9 | 0.04(5) | 1.99(20) | 28.72(96) | 51.11(87) | 0.84(26) | 16.63(12) | 0.31(7) | 0.37(13) | 100.01(57) | 0.03 |
| OR23 | 67 | 0.27(5) | 1.22(10) | 32.37(61) | 48.20(55) | 0.79(25) | 16.53(16) | 0 | 0.55(10) | 99.93(55) | 0.01 |
| OR172 | 17 | 0.19(8) | 1.83(11) | 29.82(55) | 50.22(58) | 1.08(36) | 16.91(15) | 0 | 0 | 100.04(56) | 0.03 |
| C25 | 5 | 0.52(4) | 1.02(6) | 31.25(63) | 49.03(33) | 0.78(16) | 16.17(5) | 1.34(16) | 0 | 100.11(43) | 0 |
| C65 | 9 | 0.28(6) | 1.10(15) | 32.38(85) | 49.11(33) | 0.24(14) | 16.20(23) | 0.87(31) | 0 | 100.17(51) | 0.57 |

Empirical formulae calculated for Cu+Ag+Pb+Bi+Sb=100 apfu

| BB192 | $Cu_{1.096}Ag_{2.871}Pb_{37.713}Bi_{58.252}Sb_{0.336}(S_{124.375}Se_{1.909}Te_{0.550}) \\$ | Me=41.681 | SMe=58.588 | (Bi+Sb)/Pb=1.555 |
|-------|--|-----------|------------|------------------|
| OR12 | $Cu_{0.167}Ag_{4.501}Pb_{33.873}Bi_{59.769}Sb_{1.690}(S_{126.792}Se_{0.946}Te_{0.709}) \\$ | Me=38.541 | SMe=61.459 | (Bi+Sb)/Pb=1.817 |
| OR23 | $Cu_{1.053}Ag_{2.759}Pb_{38.202}Bi_{56.391}Sb_{1.595}(S_{126.039}Te_{1.047})$ | Me=42.014 | SMe=57.986 | (Bi+Sb)/Pb=1.519 |
| OR172 | $Cu_{0.718}Ag_{4.099}Pb_{34.853}Bi_{58.196}Sb_{2.134}S_{127.730}$ | Me=39.670 | SMe=60.330 | (Bi+Sb)/Pb=1.732 |
| C25 | $Cu_{2.031}Ag_{2.365}Pb_{37.574}Bi_{58.456}Sb_{1.605}(S_{125.639}Se_{4.221})$ | Me=41.971 | SMe=60.061 | (Bi+Sb)/Pb=1.599 |
| C65 | $Cu_{1.101}Ag_{2.527}Pb_{38.737}Bi_{58.254}Sb_{0.482}(S_{125.224}Se_{2.721})$ | Me=42.365 | SMe=58.736 | (Bi+Sb)/Pb=1.517 |

Empirical formulae recalculated after conversion of Cu^+ , Ag^+ and Sb^{3+} into Pb^{2+} and Bi^{2+} : $2Pb^{2+}=Bi^{3+}+Ag^+$; $Bi^{3+}=Cu^+/3$; $Sb^{3+}\rightarrow Bi^{3+}$; $Se, Te\rightarrow S$

| BB192 | $Pb_{43.46}Bi_{56.08}S_{126.834} \\$ | Bi/Pb=1.29 |
|-------|--------------------------------------|------------|
| OR12 | $Pb_{42.88}Bi_{57.01}S_{128.446} \\$ | Bi/Pb=1.33 |
| OR23 | $Pb_{43.72}Bi_{55.58}S_{127.085} \\$ | Bi/Pb=1.27 |
| OR172 | $Pb_{43.05}Bi_{56.47}S_{127.730}$ | Bi/Pb=1.31 |

C25 $Pb_{42.30}Bi_{56.77}S_{129.860}$ Bi/Pb=1.34 C65 $Pb_{43.79}Bi_{56.09}S_{127.945}$ Bi/Pb=1.28

Without a nominal number of cations derived from the crystal structure, the chemical analyses were normalized for a conventional cation sum of 100. The (Bi+Sb)/Pb ratio ranges between 1.517 and 1.817, *i.e.*, close to that of weibullite – $Pb_5Bi_8S_7Se_{11}$ (1.5), wittite - $Pb_8Bi_{10}(S,Se)_{23}$ (1.25) or galenobismutite – $PbBi_2S_4$ (2.0). The samples contain up to 2.03 wt% Cu and 4.50 wt% Ag, suggesting relatively minor substitution of Pb and Bi with Cu and Ag, but also, some deviation of the Bi/Pb ratios from the ideal stoichiometry. After the conversion of Ag and Cu back into Bi and Pb according to the schemes: $2Pb^{2+}=Bi^{3+}+Ag^+$; $Bi^{3+}=Cu^+/3$; $Sb^{3+}\rightarrow Bi^{3+}$; $Se,Te\rightarrow S$, the Bi/Pb range modifies to 1.27-1.34. The clustering of chemical analyses for cannizzarite in the $Cu_2S+Ag_2S-Pb_2S_2-Bi(Sb)_2S_3$ phase diagram is shown in figure 2.

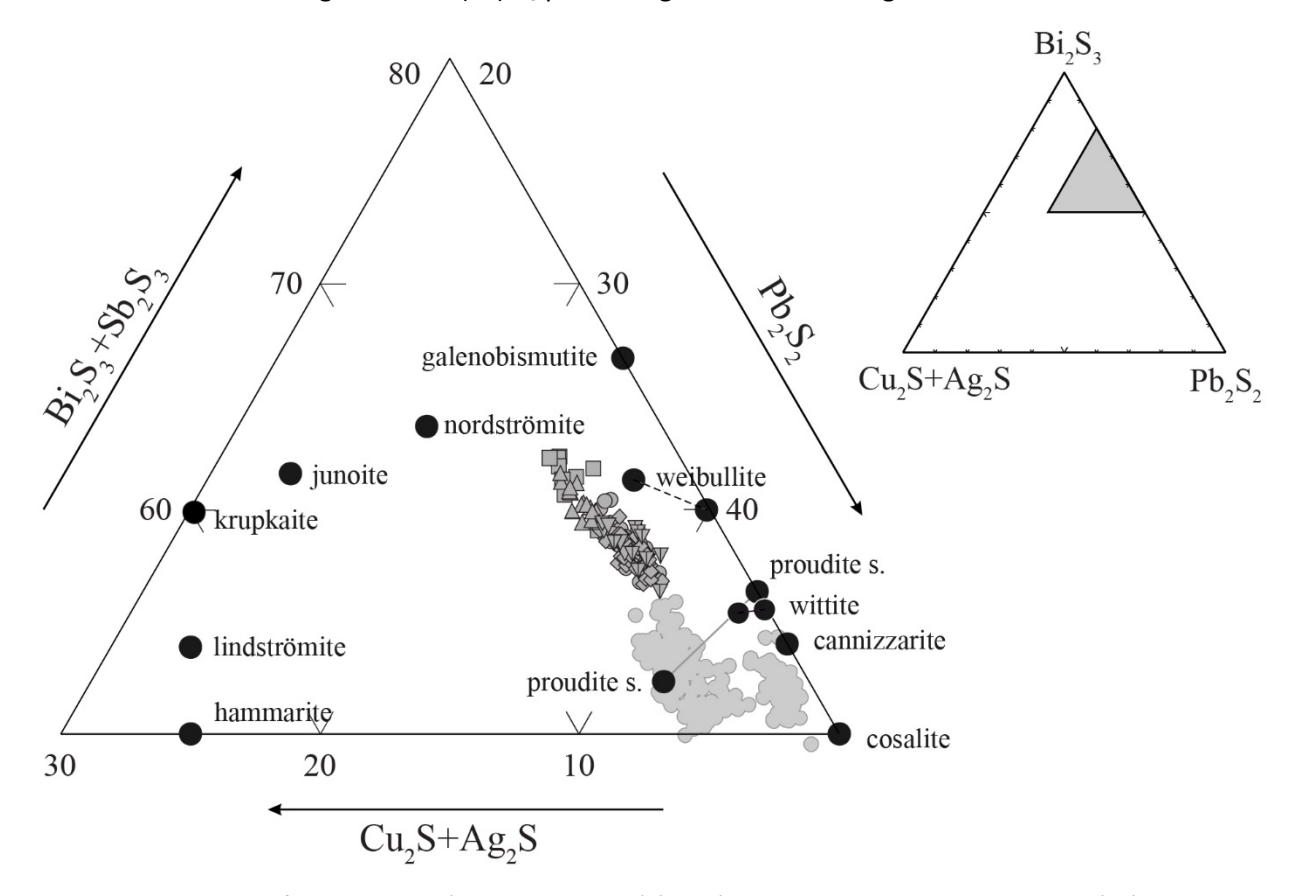


Figure 2. Analytical data for cannizarite (outlined symbols) (at. %) plotted in the $Cu_2S+Ag_2S-Pb_2S_2-Bi(Sb)_2S_3$. Black dots represent ideal, stoichiometric compositions. For comparison, the clustering of cosalite chemical data from the same occurrences is shown in light grey.

Extensive cation substitutions in Pb-Bi (Cu,Ag) sulphosalts may lead to widespread and often to overlapping compositional clusters over the entire area of the $Cu_2S+Ag_2S-Pb_2S_2-Bi(Sb)_2S_3$, thus making it difficult to diagnose cannizzarite (or other Pb-Bi (Cu,Ag) sulphosalts) on the basis of chemical data alone. Even though cannizzarite could be physically distinguished from paragenetic cosalite, proudite and felbertalite, one might not exclude that the observed clustering of chemical data belongs to another phase.

X-ray diffraction

Attempts were made to determine the crystal structure of cannizzarite in the investigated samples, but to no avail. A blade-like fragment extracted from a polished specimen was exposed on a Bruker AXS P3 diffractometer operated at 50 kV and 35 mA, equipped with a CCD area detector using graphite-monochromated MoK α radiation. Collected data allowed the investigation of the reciprocal lattice which confirmed the existence of two subcells measuring $a_Q \approx 15.47$ Å, $b_Q \approx 4.05$ Å, $c_Q \approx 4.07$ Å, $c_Q \approx 98^\circ$ and

 $a_H \approx 15.47$ Å, $b_H \approx 4.05$ Å, $c_H \approx 7.02$ Å, $\beta_H \approx 98^\circ$, respectively. However, the H/Q matching ratio could not be determined on this basis alone.

Discussion

Minerals of the cannizzarite series proved to be unexpectedly frequent in the Bi-sulphosalt assemblages from Băița Bihor, Oravița and Ciclova, despite a strained crystal structure which seems difficult to achieve and stabilize. The incommensurability of the H and Q layers, resulting in long-range matching of the H and Q subcells, leads to fluctuating local charge balance and to tension vs. compression in alternating misfit layers (Makovicky and Hyde, 1981). A solution for relieving such tensions would be to periodically offset the layers in the stacking direction, such as in junoite, felbertalite, proudite or cuproneyite which are relatively common in the sulphosalt assemblages of the mineralized areas under scrutiny.

References

- Berza, T., Constantinescu, E., Vlad, Ş.N., 1998. Upper Cretaceous magmatic series and associated mineralization in the Carpatho–Balkan Orogen. Resource Geology, 48, 291–306.
- Borisov, S.V., Pervukhina, N.V., Magarill, S.V., Kuratieva, N.V, 2012. The crystal structure of (Cd, In)-rich cannizzarite from Kudriavy volcano, Iturup Island, Kuriles, Russia. The Canadian Mineralogist, 50, 387-395.
- Ciobanu, C.L., Cook, N.J., Stein, H., 2002. Regional setting and geochronology of the Late Cretaceous Banatitic Magmatic and Metallogenetic Belt. Mineralium Deposita, 37, 541–567.
- Cioflica, G., Vlad, Ş., 1973. The correlation of the Laramian metallogenic events belonging to the Carpatho-Balkan area. Revue Roumaine de Géologie, Géophysique, Géographie, s. Géologie, 17, 217–214.
- Ferraris, G., Makovicky, E., Merlino, S., 2004. Crystallography of Modular Materials. Oxford University Press, Oxford, U.K.
- Makovicky, E., 1988. Classification of homologous series. Z. Kristallogr. 185, 512.
- Makovicky, E., Hyde, B.G., 1981. Non-commensurate (misfit) layer structures. Structure and Bonding, 46, 101–107.
- Matzat, E., 1979. Cannizzarite. Acta Crystallogr. B35, 133-136.
- Topa, D., Makovicky, E. Dittrich, H., 2010. The crystal structure of 7H: 12Q cannizzarite from Vulcano, Italy. The Canadian Mineralogist. 48, 483-495.

TECTONIC AND GEODYNAMIC MODEL FOR THE VRANCEA SEISMIC ZONE

Dumitru IOANE¹, Irina STANCIU^{1, 2}

¹ Faculty of Geology and Geophysics, University of Bucharest, e-mail: d_ioane@yahoo.co.uk ² National Institute of Marine Geology and Geoecology – GeoEcoMar, 23-25 D. Onciul St, 024053 Bucharest, e-mail: irina.stanciu@geoecomar.ro

Introduction

Due to increased precision in positioning and depth determination of seismicity data recorded since January 2014, (ROMPLUS Earthquake Catalogue of Romania – Oncescu et al., 1996 updated), new possibilities for data processing and interpretation for active tectonics and geodynamics were open. During the last two decades, seismic tomography geophysical technique succeeded to illustrate the in-depth continuation of large geological structures at continental or planetary scale. A new tectonic and geodynamic model for the Vrancea seismogenic zone have been recently built after analyzing and interpreting regional geophysical (gravity, magnetic, refraction seismics, seismic tomography, seismicity), geodetic (gravimetric geoid, GPS) and remote sensing data (loane & Stanciu, 2018).

Tectonic Setting

The Vrancea seismogenic area, characterized by regional crustal and lithospheric seismicity up to 200 km depth, is located in the East Carpathians Zone, between the Transylvanian Depression (NW) and the Moesian Platform (SE). The outcropping geology displays Alpine tectonics, the overthrusted nappes being the result of several tectonic phases: Laramian phase (Late Cretaceous), Early Styrian and Late Styrian phases (Early Miocene) (Săndulescu, 1984).

The main tectonic models built during the last two decades for the Vrancea deep crustal and lithospheric structures were based either on subduction of an oceanic lithospheric slab ended as continental collision and tectonic blocks docking, or lithosphere delamination followed by asthenosphere upwelling. A significant tectonic feature in the Vrancea zone may be considered the quasi-vertical tectonic contact between Tisza-Dacia continental block and the Moesian Platform, shown by refraction seismic data to develop downward for at least 40 km beneath the East Carpathians overthrusted sedimentary nappes (Hauser et al., 2007). A clockwise rotation of the subcrustal geological structures, as compared to the crustal ones, have been interpreted on seismic tomography (Lorenz et al., 1997) and magnetotelluric tomography (Stănică et al., 2004) maps built at different depths.

Wrench Tectonics and Geoidal Anomalies in Romania

Tectonic models involving wrench systems have been already suggested in the region where Romania is located, the S shaped East and South Carpathians structure being attractive to consider it as a result of opposite compressive regimes. A wrench tectonics model in this area was suggested by G. Zolnai (2000), with E-W trending transcurrent faults situated at the northern and southern limits of the South Carpathians.

A wrench tectonics system was recently proposed (loane & Stanciu, 2018), having as starting dataset the EGG 97 geoidal anomalies along TESZ and in the region of the East and South Carpathians. The straight NW-SE lineament crossing Poland and Ukraine, determined by rapid variations of the geoid heights, is changed in Romania to a reversed **S** shaped letter, first displaced eastward and subsequently westward. Since the geoidal anomalies are determined by deeper density inhomogeneities than the gravity anomalies

(loane et al., 1993), the rapid variations in geoid heights are interpreted as being here determined by tectonic contacts of the East European Platform with the European Palaeozoic Platform, the Panonnian Basin and the Tisza-Dacia tectonic block. The thinner crust and lithosphere of the westerly located tectonic blocks, as compared to the East European Platform, determine the sudden increase of the geoidal values over short distances along TESZ, due to an uplifted position of higher density upper mantle rocks. The gravimetric geoidal anomalies were interpreted as associated to the deeply situated western boundary of the East European Platform (TESZ), shifted westward at the East Carpathians Bend zone. The NE-SW trending geoidal anomaly, shifting TESZ within the Vrancea zone, was interpreted as being due to two regionally developed parallel transcurrent faults in a wrench tectonics system (loane & Stanciu, 2018).

The South-Eastern Continuation of the Polish Trough

A component of the newly built tectonic model is represented by the south-eastern continuation of the Polish Trough, a tectonic structure formed by extensional processes, having a particular crustal thickness, a thick pile of Mesozoic sediments and being situated along the western boundary of the East European Platform. In Poland, the Polish Trough was heavily investigated and nicely illustrated by refraction seismic experiments, while in Romania, only the Vrancea 2001 refraction seismic line crossed such a graben-like structure in the East Carpathians Bend Zone (Hauser et al., 2007). After crossing the Vrancea seismic zone, the "Romanian Trough" (Ioane & Stanciu, 2018), concealed beneath the Carpathians, change its trend to south-west up to the Alexandria Depression, considered as the continuation of the Miechow Depression (Sandulescu, 1984).

Lithospheric Thickness and Vrancea Seismicity

Numerous tectonic models built for the Vrancea seismic zone did not use differences in lithospheric thickness between involved continental blocks, due to lack of relevant information or ignoring its importance. Seismic tomography studies, carried out at regional or continental scales, provided since the late 90's good quality data regarding lithospheric thickness of significant geotectonic structures in Europe.

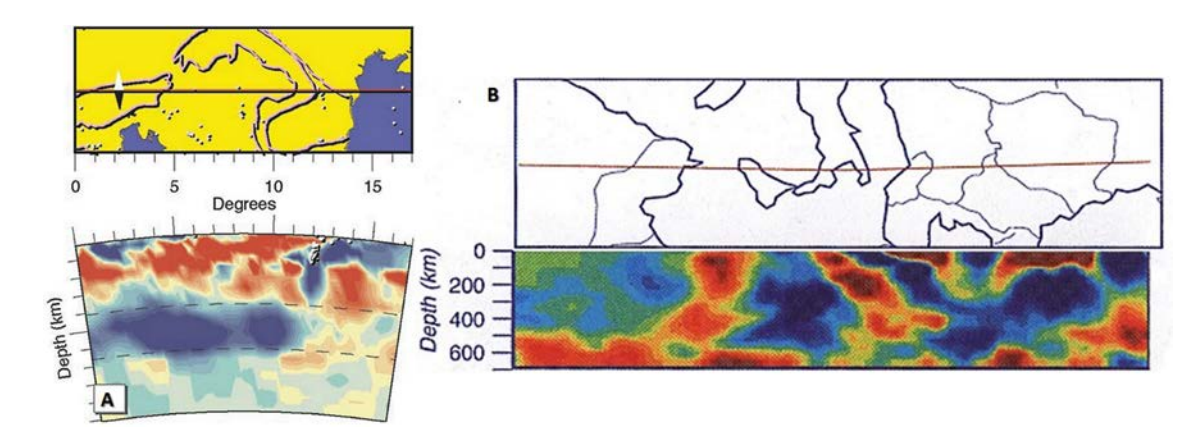


Fig. 1. A: Seismic tomography section crossing the Carpathians Bend Zone (Wortel & Spakman, 2000); B: Seismic tomography section tangent to the Carpathians Bend Zone (Piromallo & Morelli, 1997).

For the Vrancea zone (Fig. 1), it was considered of utmost importance the fact that the East European Platform, involved in subduction processes (Piromallo & Morelli, 1997), was illustrated by seismic tomography (Wortel & Spakman, 2000) to have here the thickness ranging between 200 and 400 km depth (loane & Stanciu, 2018).

Considering that the Vrancea deep seismicity is usually recorded between 70 and 200 km, it results that the earthquakes mainly occur within the East European Platform, situated between 100 and 200 km depth. The lithospheric slab attached to the East European Platform presently displays a vertical position due to break-off processes; it develops between 200 and 400 km and should not be directly involved in the Vrancea seismicity (Fig. 1A – Wortel & Spakman, 2000).

Differences in thickness of platforms situated in the Carpathians foreland may be observed on a seismic tomography section crossing the Vrancea zone, the East European Platform being two times thicker that the Moesian Platform. It may be also interpreted that the oceanic lithospheric slab is here still attached to the platform, preserving an angle close to ongoing subduction processes (Figure 2B – Piromallo & Morelli, 1997).

Extensional Tectonics in the East Carpathians Bend Zone

Present day geodynamic processes, as illustrated by GPS monitoring results, show a SE displacement of the East Carpathians Bend Zone and its foreland (Munteanu, 2009). A consistent displacement of this area towards SE may be also observed on remote sensing imagery data, while a crustal stretching of 10 to 15 km, possibly due to extensional processes, was illustrated in the Vrancea seismogenic zone by refraction seismic data (Hauser et al., 2007).

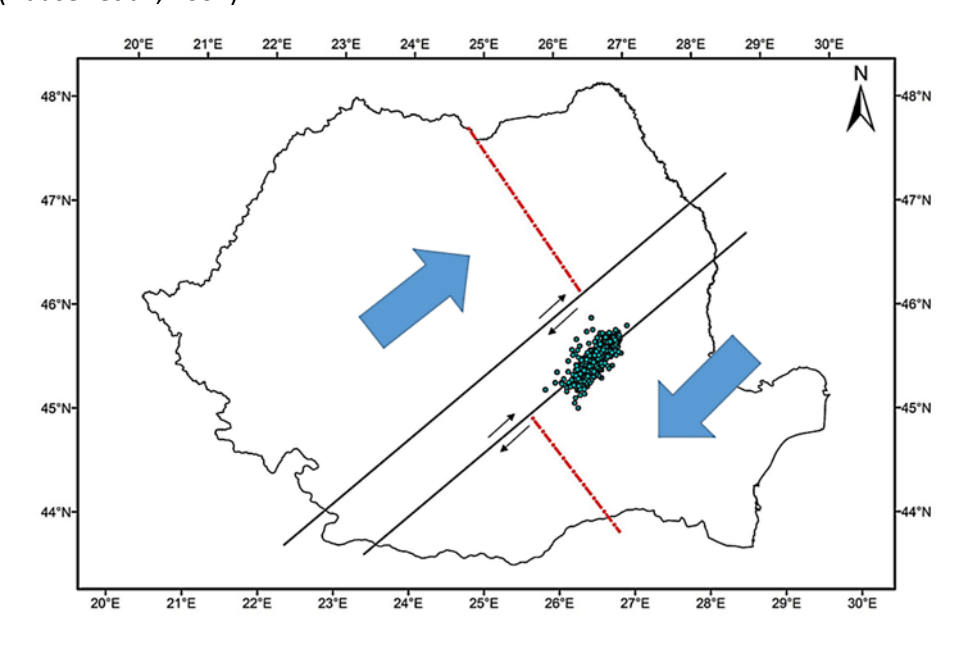


Fig. 2. Regional tectonic and geodynamic model for the Vrancea zone (after Ioane & Stanciu, 2018).

A good possibility for explaining this SE displacement of the East Carpathians Bend Zone foreland would be post-collisional extensional processes, which may be in a large extent responsible for the Vrancea crustal seismicity. Considering the wrench tectonics model (loane & Stanciu, 2018) and the on-going collision directed NE-SW beneath the Moesian Platform (Piromallo & Morelli, 1997), a NW-SE extension may also result in this region.

Tectonic and Geodynamic Model

The regional tectonic and geodynamic data have been integrated for the territory of Romania and represented in Figure 2 (Ioane & Stanciu, 2018). There are two transcurrent regional faults, crossing NE-SW Romania, and developed as a wrench tectonics corridor.

The region situated north of the wrench system (Pannonian Depression, Transylvanian Depression, northern part of East Carpathians and neighboring East European Platform were displaced north-eastward, the red dotted line representing the platform concealed boundaries, as interpreted on gravity and seismic tomography data.

Seismicity and Active Tectonics in Vrancea

The analysis of the recent crustal (1 - 60 km depth) and lithospheric (90 - 160 km depth) Vrancea seismicity (2014 - 2018) led to the following interpretations:

- a) the most active seismicity, both at crustal and lithospheric depths occur in the junction area between the NE-SW transcurrent fault and the NNW-SSE trending "Romanian Trough", meaning the graben-like structure detected by refraction seismics;
- b) seismicity sections, built across the Vrancea zone, illustrate active extensional tectonics, either due to the trans-tensional transcurrent fault at highest lithospheric depths, or to the SE regional drag, at crustal depths. These seismicity sections illustrate the triangular shape of the seismogenic sector, with deep earthquakes generated by the transcurrent fault and shallower ones on normal faults on both sides of the graben-like tectonic structure.

Conclusions

A new tectonic and geodynamic model was built, mainly focused on the Vrancea seismic zone. The wrench tectonics system is composed of two regional transcurrent faults, the blocks displacements towards NE and SW representing effects of the collision between Africa and Eurasia, with a consistent NE lateral escape towards Romania.

Discussing the seismicity in Vrancea, the interpretation of geophysical and geodetic data resulted in the following:

- crustal and lithospheric seismicity occur in the sector where the "Romanian Trough" crosses the southern transcurrent fault;
- earthquakes occur in elongated triangle shaped volumes, the deepest part being along the transcurrent fault and shallower ones on the graben-like structure margins;
- strike-slip movements of the transcurrent fault (transtension) and ruptures on normal faults due to post-collisional processes and the south-eastern regional drag may be the main causes of crustal and lithospheric seismicity.

References

- Hauser, F., Raileanu, V., Fielitz, W., Dinu, C., Landes, M., Bala, A., Prodehl, C., 2007. Seismic crustal structure between the Transylvanian Basin and the Black Sea, Romania. Tectonophysics 430, 1-25.
- Ioane, D., Stanciu, I.M., 2018. Extensional tectonics in Vrancea zone (Romania) interpreted on recent seismicity, geophysical and GPS data, SGEM 2018 Conference Proceedings Albena, Bulgaria,, Vol. 18, Issue 1.1, Applied and Environmental Geophysics, 787-794.
- loane, D., Olliver, J., Radu, I., Atanasiu, L., 1993. Geophysical significances of the geoidal anomalies. Rev. Roum. Geophysique, 37, pp. 9 18.
- Lorenz, F.P., Martin, M., Sperner, B., Wenzel, F., Popa, M., 1997. Teleseismic traveltime tomography of the compressional-wave velocity structure in the Vrancea-Zone, Romania. EOS Trans. AGU, vol. 78, no. 46
- Munteanu, L., 2009. Tectonic blocks movement in and around Vrancea, based on precise GPS measurements in Researches Related to the Disaster Management of Romanian Earthquakes. In: Mărmureanu, G. (Ed.), Editura Tehnopress, Iasi, Romania (in Romanian).
- Oncescu, M.C., Marza, V.I., Rizescu, M., Popa, M., 1996. The Romanian earthquake catalogue between 1984 1996 (*updated*). In: Wenzel F., Lungu D., Novak O. (eds.), Vrancea Earthquakes: Tectonics, Hazard and Risk Mitigation. Kluwer Academic Publishers, 42-49.
- Piromallo, C., Morelli, A., 1997. Imaging the Mediterranean upper mantle by P-wave travel time tomography. Annali di Geofisica XL, 4, 963 979.
- Săndulescu, M., 1984. Geotectonics of Romania. Editura Tehnică, Bucharest, 450 p. (in Romanian)
- Stănică, A., Stănică, M., Picardi, L., Tondi, E., Cello, G., 2004. Evidence of the geodynamic torsion in the Vrancea Zone (Eastern Carpathians). Rev. Roum. Geophysique 48, 15 19.
- Zolnai, G., 2000. Continental wrench-tectonics and hydrocarbon habitat. AAPG Continuing Education Course Note Series, American Association of Petroleum Geologists Education Department, Tulsa, Oklahoma.

| Geosciences in the 21 st century |
|---|
|---|

Wortel, M.J.R., Spakman, W., 2000. Subduction and Slab Detachment in the Mediterranean-Carpathian Region. Science 290, 1910 – 1917.

THE STRUCTURE OF SCLERACTINIAN CORAL SKELETON ANALYSED BY NEUTRON TOMOGRAPHY AND NEUTRON DIFFRACTION

Tatiana I. IVANKINA¹, Sergey E. KICHANOV¹, Octavian G. DULIU^{1,2,†}, Safa YUSUF³, Mohamed M. SHERIF³

¹Joint Institute for Nuclear Research, Frank Laboratory for Neutron Physics, 6, Joliot Curie str. 141980 Dubna, Russian Federation

²University of Bucharest, Faculty of Physics, Department of Structure of Matter, Earth and Atmospheric Physics and Astrophysics, 406, Atomistilor str. 077125 Magurele (Ilfov), Romania e-mail: o.duliu@upcmail.ro

³Cairo University, Faculty of Sciences, Al Orman, Giza Governorate 12613, Egypt

Abstract

Neutron Computed Tomography (NCT) and Neutron Diffraction were used to investigate the internal structure and mineral composition of scleractinian *Favites* sp. coral. NCT evidenced with a spatial resolution of about 0.5 mm the interlocking individual cups as well as the annual periodic variation of density of coral skeleton. At its turn, the ND was used to determine the orientation distribution function of the aragonite fibrils, the main component of coral skeleton. At the same time, the diffraction pattern confirmed that the aragonite represents the excusive mineral component of the coral skeleton.

Introduction

Corals are excusive marine invertebrates belonging to phylium Cnidaria, class Anthozoa (Rupert et al 2004). All genra have the same simple anatomy of which basic unit is represented by sac-like polyp with a radial or radial-bilateral symmetry divided by septs (mesenteries) incompletely dividing the internal (gastrovascular) cavity of polyp in a multiple of six – Hexacorallia subclass, (Chevalier and Beauvais,1987) or eight – Octocorallia sublass (Daly et al. 2007) compartments. Scleractinia order is the most important representatives of the Hexacorallia subclass of which members build a hard aragonite exoskeleton.

Due to their high penetrability, neutrons are intensively used in investigating internal structure of a great verity of materials and objects, which includes, in our case the coral skeletons. Neutron Computed Tomography (NCT) proved its suitability to reveal the internal structure a large category of materials, especially if contain elements such as hydrogen, deuterium or carbon with high scatter or absorption cross sections. At its turn, Neutron Diffraction (ND), due to a higher penetrability of neutrons could furnish more information concerning the reciprocal orientation of aragonite fibrils (Bunge, 1989; Ullmeyer et al., 1998; Keppler et al., 2014), helping to describe the formation of coral skeletons.

Accordingly, one of the best descriptor of the orientation of aragonite fibrils is represented by the Orientation Distribution Function (ODF), better graphically represented by Pole Figures (PF) which in fact represents the stereographic projections of the aragonite main crystalline planes (001), (010), and (100) within coral skeleton (Bunge, 1989).

Both methods were used to investigate o fragment of *Favites* sp. scleractinian coral. The results of this study will be further presented and discussed.

Experimental Data

Corals. A fragments of Favites sp coral (Fig. 1a) manually collected at the depth between 5 and 10 m southern of Al Saleef port (15.308° S, 42.988° E), Yemen Republic, was washed by sea water, airdried and

sent to the Joint Institute for Nuclear Research (JINR), Dubna, Russian Federation, where, by means of a water saw was cut into 6 x 6 x 1.8 cm slabs for further investigations.

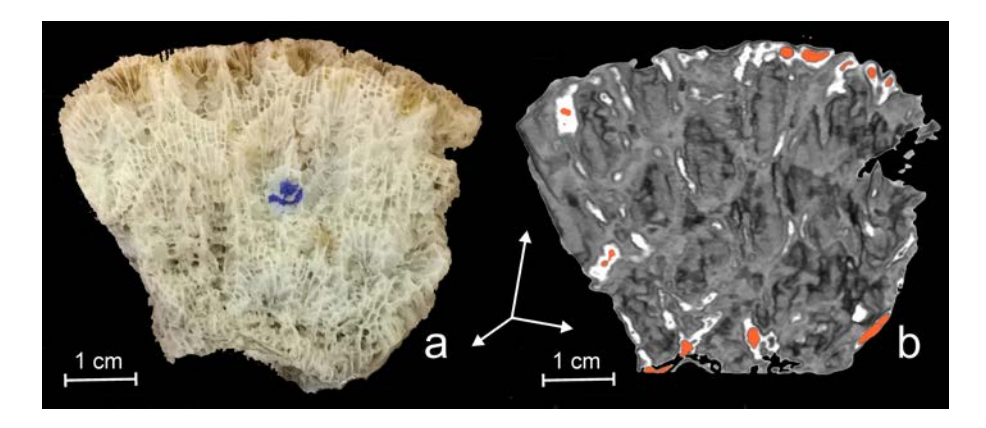


Fig. 1. A photography of *Flavites* sp. fragment (a) and the corresponding NCT 3D image corresponding to a coronal section (b). The orange color corresponds to organic rich residues remained in skeleton. Z axis parallel with the longitudinal axis of the coral skeleton slab.

Neutron computed tomography. The NCT was performed at the Frank Laboratory of Neutron Physics IBR-2 pulsed reactor, Joint Institute for Nuclear Research (JINR), Dubna by a home-made Computed Tomograph (CT). The primary neutron radiographic images with a spatial resolution of about 0.5 mm were used to reconstruct 3D CNT images with the same resolution following a procedure described in detaile by Kichanov et al. (2015) and Kozlenko et al. (2015).

Neutron diffraction. ND investigation was also performed by using the neutron beams produced by the same IBR-2 pulsed reactor as well as the time of flight SKAT neutron diffractometer detailed described by Ullmeyer et al. (1998) and Keppler et al. (2014). It is worth remarking that the SKAT diffractometer uses large neutron beams (up to 5 cm diameter) which significantly increases the instrument accuracy. Starting from the ND spectra, it was possible to reconstruct the ODF of aragonite fibres and represent them by means of corresponding PF (Keppler et al., 2014).

Results and Discussion

Neutron computed tomography. A better interpretation of the information furnished by the NCT images can be done by comparing the optic and the corresponding NCT images (Fig. 1b). On the optic image it can be observed only the lacunars structure of coral colony skeleton with a multitude of small empty spaces allowing different polyps to communicate between them by cenosarc. On contrary, on the corresponding tomographic image (Fig. 1b), internal distribution of aragonite skeleton appears with more clarity together with the images of organic rich matter (orange nuances).

More details of the investigated coral skeleton are provided by the NCT images reproduced in Fig. 2. Here, Figs. 2a and 2b illustrate general 3D images of the coral slab showing with clarity the individual cups which hosted the polyps. The vertical distribution of individual polyps cups are better illustrated on Fig. 2c and 2d. These images illustrates how individual cups are interlocked by forming consecutive layer as the colony grows, this process being well evidenced by an alternation of lighter and dark hues bands which are associated with the annual growth, similar to annual tree ring (LeTissier et al., 1994).

Neutron diffraction. Starting from the neutron diffraction spectra it was possible to recalculate the ODF of aragonite fibrils and to represent them in a system of coordinates of which Z axis lies along the slab height, by means of stereographic projections reproduced in Fig. 3a. Accordingly, the crystallographic texture of aragonite as reflected by the PF (001), (010) and (100) appears well-defined and relatively symmetric. Here, the (100) and (010) planes form two sets of maxima, one consisting of two lobes tangent to the PF equator as well as a stronger single maximum perpendicularly to the previous ones. At the same

time, the PF corresponding to the (001) PF resents two weak two-lobe mutually perpendicular maxima (Fig. 3a).

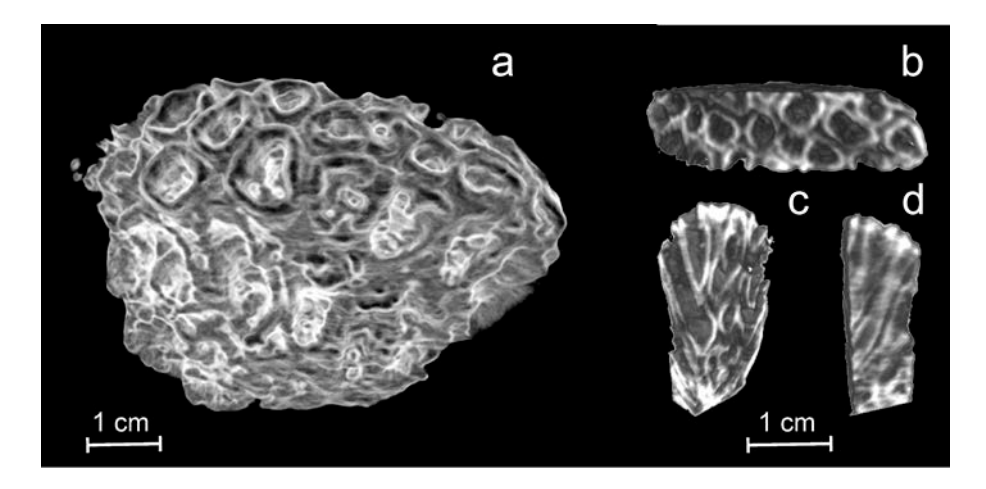


Fig. 2. A general 3D NCT images of the coral slab (a), together with a horizontal (B) and two vertical (c,d) sections. It should be remarked that on (c) and especially on (d) images, the annual growth sections appear in darker hues.

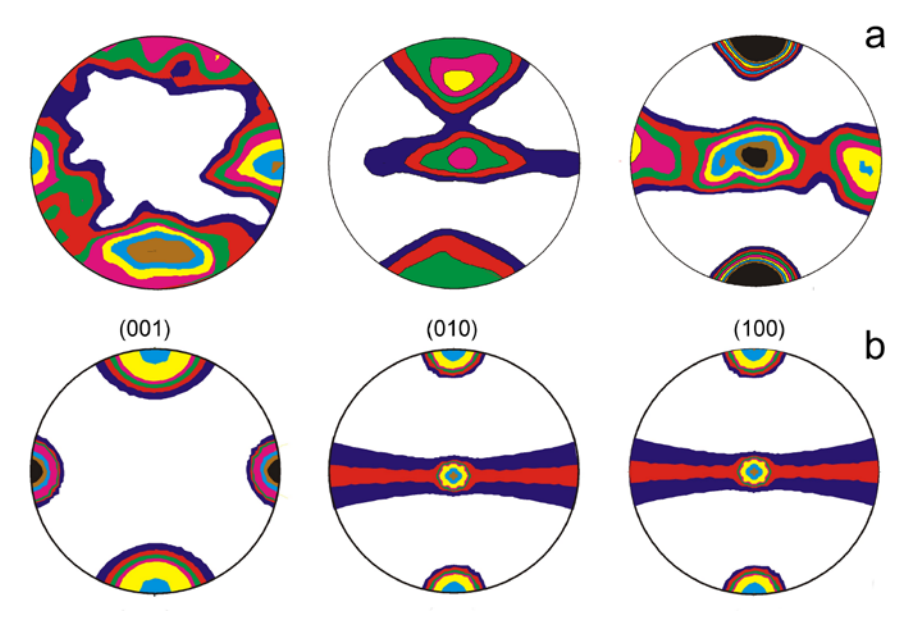


Fig. 3. The principal PF of coral skeleton aragonite representing the stereographic projection the ODF of pole density contours (a) and the model PF of texture components (b) which better approximate de experimental ones.

By following the procedure described above, the ODF allowed evidencing the orientation of aragonite fibres/bundles, regarding to a physical or geometric coordinate system (Ivankina and Matthies, 2015). Accordingly, the experimental PF suggest that the aragonite fibrils distribution follow two main orientations – one parallel to the growth direction of coral, in this case the Z axis direction and the other more or less uniform distributed perpendicular to growth axis in concordance with a model proposed by Barnes and Lough (1993). Moreover, as the degree of crystallographic preferred orientations can be characterised by the texture index *J* (*J* is equal to 1.0 for a random texture), in our case *J* index was found to be equal to 1.33 which signifies a less organised, but not a random texture.

To check this assumption, we have calculated the PF of ODF of aragonite crystallin planes (001), (010) and (100) following the Barnes and Lough (1993) model by considering for the orientation of each of these planes a dispersion of about 30 %. The results of this simulation reproduced in Fig. 3b show a remarkable similitude with the experimental PF ones, in spite some distortions, which is perfectly normal taking into account the fluctuation of marine environment where corals develops. This observation proved that the

aragonite fibers which compose the coral skeleton are not randomly oriented but following a well established pattern as Barnes and Luogh (1993) suggested. At the same time, the real distribution pattern is subjected to local fluctuation, well illustrated by the irregularities in the aspect of the experimental PF, more evidenced in the case of (001) plane (Fig. 3a).

References

- Barnes, D.J., Lough, J.M., 1993. On the nature and causes of density banding in massive oral skeletons. J Exp Mar Biol Ecol 167, 91–108.
- Bunge, H.J., 1989. Advantages of neutron diffraction in texture analysis, Text Microstruct 10, 265-307.
- Chevalier, J.-P., Beauvais, L., 1987. Ordre des scléractiniaires: XI. Systématique. In: Grassé P-P, Doumenc D (eds), Traité de zoologie. Tome III. Cnidaires: Anthozoaires. Masson, Paris, pp 679–764 (in French).
- Daly, M, Brugler. M.R., Cartwright. P., Collins, A.G., Dawson, M.N., Fautin, D.G., France, S., C, Mcfadden, C,S, Opresko, D.M., Rodriguez, E., Romano, S.L., Stake, J.L., 2007. The phylum Cnidaria: A review of phylogenetic patterns and diversity 300 years after Linnaeus. In: Linnaeus Tercentenary: Progress in Invertebrate Taxonomy, Z.-Q. Zhang and W A Shear (eds). Zootaxa 1668: 127–182, https://kuscholarworks.ku.edu/handle/1808/13641 (accessed 09.06.2019).
- Ivankina, T.I., Matthie.s S., 2015. On the development of quantitative texture analysis and its application in solving problems of Earth sciences. Phys Part Nucl 46, 366-423.
- Keppler, R., Ullemeyer, K., Behrmann, J.H., Stipp, M., 2014. Potential of full pattern fit methods for the texture analysis of geological materials: implications from texture measurements at the recently upgraded neutron time-of-flight diffractometer SKAT, J Appl Cryst 4, 1520-1534.
- Kichanov, S.E., Kozlenko, D.P., Ivankina, T.I., Rutkauskasn, A.V., Lukin, V., Savenko, B.N., 2015. The Neutron Tomography Studies of the Rocks from the Kola Superdeep Borehole. Phys Procedia 69, 537-541.
- Kozlenko, D.P., Kichanov, S.E., Lukin, E.V., Rutkauskas, V., Bokuchava, G.D., Savenko, B.N., Pakhnevich, A.V., Rozanov, A.Yu., 2015. Neutron Radiography Facility at IBR-2 High Flux Pulsed Reactor: First Results, Phys Procedia 69, 87-91.
- Matthies, S., Vinel, G., 1982. An example demonstrating a new reproduction method of the ODF of samples from pole figures. Phys. Stat. Sol. 112, 115-120.
- Ullemeyer, K., Spalthoff, P., Heinitz, J., Isakov, N.N., Nikitin, A.N., Weber, K., 1998. The SKAT texture diffractometer at the pulsed reactor IBR-2 at Dubna: experimental layout and first measurements, Nucl Instr Meth. Phys. Res. A 412, 80-88.

CONNECTION BETWEEN SOME OF THE SHEAR ZONES FROM ROMANIA AND MANTLE ANISOTROPY

Denisa JIANU¹, Cezar IACOB², Andra MÂRZA³, Georgian MĂNUC⁴, Vlad Victor ENE⁵, Ema BOBOCIOIU⁶

¹The University of Bucharest, Faculty of Geology and Geophysics, 1 Nicolae Bălcescu Boulevard, e-mail: denisao301@yahoo.com

²DIRAC SRL, Bucharest; ³Hunt Oil Company of Romania; ⁴University of Leeds, UK; ⁵University of Leicester, UK; ⁶Ecole Normale Superieure de Lyon, France

Understanding anisotropy associated with upper crust and the upper mantle, as well as the relationship between the two of them is essential in understanding the plates tectonic. Several studies demonstrate the conection between the shear zones and upper mantle anisotropy determined by the crystallographic preferred orientation of olivine (Katsuyoshi, 2004; Vauchez, 2012).

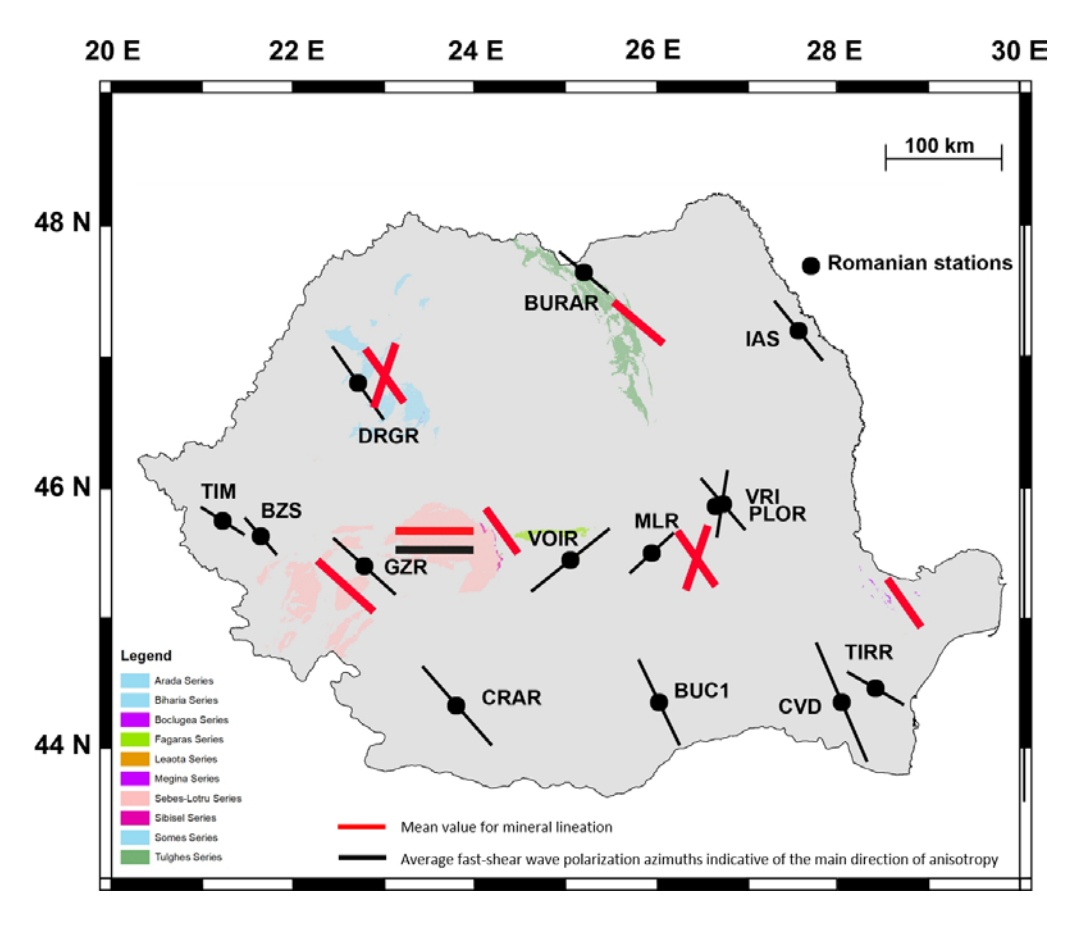


Fig. 1. Map exhibiting the seismic anisotropy associated with the upper mantle (black lines) and the main directions of shear deformation (red line). Modified after Ivan et al., 2008.

This study presents field observations from six basement terranes characterized by ductile deformation in different structural units from the Carpathians Orogen and the North Dobrogea Orogen. These areas are defined as Tulghes Unit from Eastern Carpathians, Leaota Series, Sebeş-Lotru and Făgăraş Units and deformation zone Sibisel from the Southern Carpathians, Bihor Unit from Apuseni Mountains, Megina and Boclugea Series from North Dobrogea Orogen (Fig. 1). Structural elements measured in

metamorphic units characterized by different metamorphic evolutions exhibit parallel trends on the shear deformation and all are parallel with the main anisotropic direction in the seismic anisotropy of the upper mantle, i.e. NW-SE (Ivan, 2008; Russo, 2009). Exceptions is the central part of Fagaras and Sebes-Lotru Metamorphic Series, where the mineral lineation is oriented E-W. In this area, the anisotropy of upper mantle is also oriented E-W (Ivan, 2004 in Russo, 2009). In Leaota Metamorphic Series and Bihor Unit, two shear zones have been recognized: the main is oriented NW-SE and a secondary one on NE-SW direction associated with retromorphism and partial over-print of the pre-existing deformation structures.

Based on seismic investigation studies (S-type waves generated by five earthquakes in Vrancea Zone), Russo (2009) observed two anisotropic directions characterizing the upper mantle underneath the Southern Carpathians: a deeper one oriented NW-SE and a shallower one, NE-SW. He explained that mantle anisotropy coincides with the deformation trends at surface.

The basement units in Romania are considered the result of metamorphism during Ordovician (Balintoni et al., 2014) completed with tectonometamorphic Variscan events (Medaris et al., 2003). Although the age of metamorphism is not clearly established, the community agrees that brittle deformation overprints the metamorphism during Alpine orogeny. The only metamorphic unit currently dated, is Sibisel Shear Zone. Ducea (2019) dated the metamorphism as old as Triassic.

Balintoni (2014) summarizes the complicated history of the metamorphic units representing different terranes (North Africa Orogen affinities, peri-Amazonian) which docked Laurasia during Variscan Orogeny. As previously mentioned, the 'final docking' of Gondwana onto Eurasia is considered Paleogene (e.g. Burchfiel 1980, in Balintoni, 2014). These observations raise many question marks. The shear zones in Eastern and Southern Carpathians, Apuseni Mts and North Dobrogea Orogen might represent fragments of one single shear zone as previously proposed by Pana (2004). However, this model should be supported by age-dating of the shear-deformation in each metamorphic unit. Shear zones were reactivated and placed parallel to the anisotropy direction in the mantle, which raises questions about the factors that influenced the mantle anisotropy.

References

Balintoni, I., Balica, C., Ducea, M.N., Hann, H.P., 2014. Peri-Gondwanan terranes in the Romanian Carpathians. A review of their spatial distribution, origin, provenance and evolution. Geosci. Front. 5, 395-411.

Ducea, M.N., Negulescu, E., Profeta, L., Săbău, G., Jianu, D., Petrescu, L., Hoffman, D., 2016. Evolution of the Sibişel Shear Zone (South Carpathians): A study of its type locality near Răşinari (Romania) and tectonic implications. Tectonics, 35, 1-27, doi:10.1002/2016TC004193.

Ivan, M., Popa, M., Ghica, D., 2008. SKS splitting observed at Romanian broad-band seismic network. Tectonophysics 462 Medaris, G., Ducea, M.N., Ghent, E., Iancu, V., 2003. Timing of high-pressure metamorphism in the Getic-Supragetic

basement nappes of the South-Charpatian mountains fold-thrust belt. Lithos, 70, 141-161.

Michibayashi, K., Mainprince D., 2004. The Role of Pre-existing Mechanical Anisotropy on Shear Zone Development within Oceanic Mantle Lithosphere: an Example from the Oman Ophiolite. Journal of Petrology. 45, 2, 405-4014.

Pană, D., Edmer, P., 2004. Alpine crustal sher zones and pre-Alpine basement terranes in the Romanian Carpathians and Apuseni Mountains. Geology, 22, 807-810.

Russo, R.M., Mocanu, V.I., 2009. Source-side shear wave splitting and upper mantle flow in the Romanian Carpathians and surroundings. Earth and Planetary letters 287, 205-216.

Vouchez, A., Tommasi, A., Mainprince, D., 2012. Faults (shear zones) in the Earth's mantle. Tectonophysics 558-559, 1-27.

SEDIMENTARY HISTORY OF THE ALBIAN CONGLOMERATES FROM THE CARPATHIAN BEND ZONE

Dan C. JIPA¹, Cornel OLARIU²

¹National Institute of Marine Geology and Geoecology, 23-25 D. Onciul St, 024053 Bucharest, Romania, e-mail: jipa@geoecomar.ro

The most important scientific moment for the genetic study of the Carpathian Bend Albian Conglomerates was the understanding of their submarine fan character (Murgeanu et al., 1963). The reconstruction of the Albian conglomerates paleocurrent network (Mihăilescu et al, 1967; Patrulius et al., 1967) provided an important support for this idea. At rather large time intervals the sedimentological studies pointed out the deep water environment of the Albian Conglomerate Fan (Stanley and Hall, 1978), the existence of a shallow water zone at the proximal edge of the Fan (Olariu et al., 2014) and its slope fan nature (Jipa and Olariu, 2018).

The Austrian orogenesis was the engine of the Lower Cretaceous sediment accumulation of the Carpathian Bend Zone. As a consequence of the Austrian orogenesis relief building, the Barremian-Aptian turbidites evolved from silty and fine-grained, to medium and coarse-grained sandstones and conglomerates. The climax of the growing sediment influx was reached during the Albian, when the hundred meters thick pile of Albian conglomerates was formed. The abatement of this impressive sediment flux is marked by the Babele Sandstone accumulation.

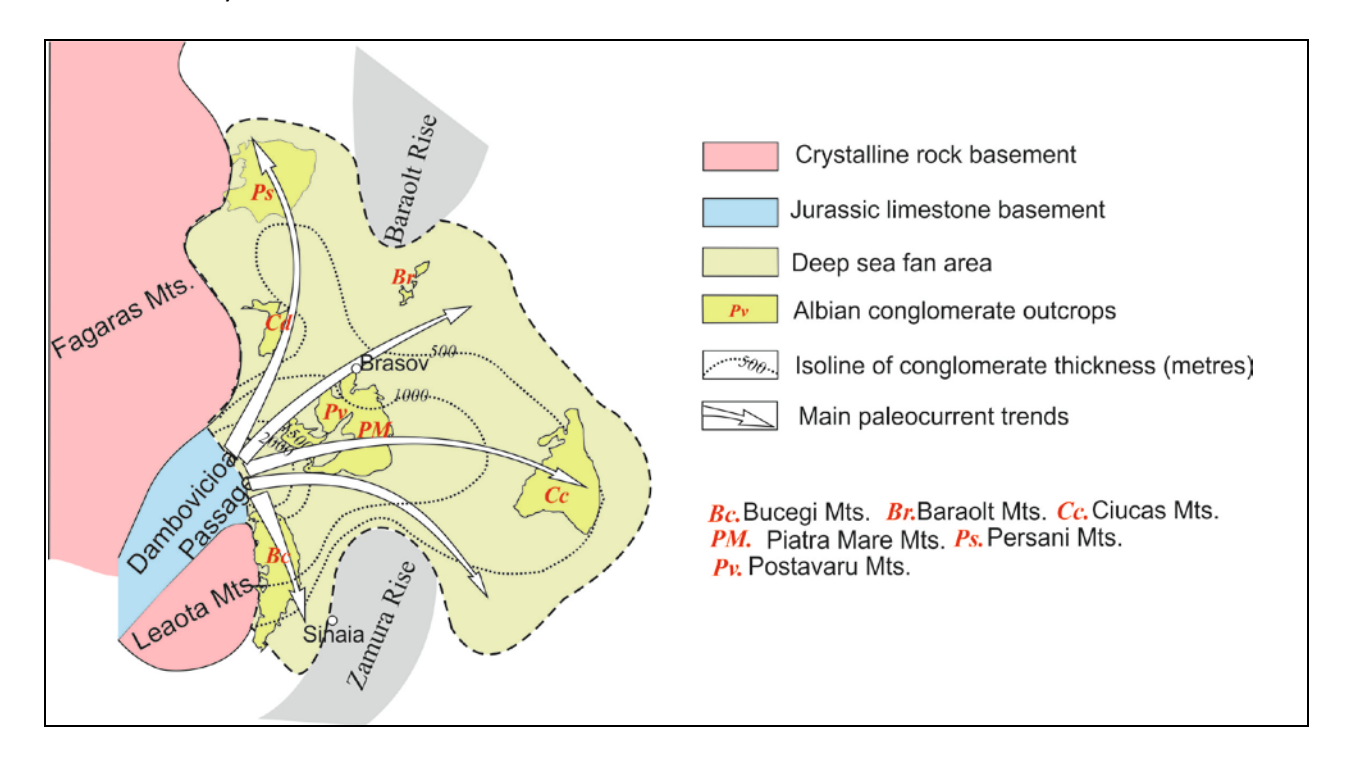


Fig. 1. The Albian Conglomerate Deep Sea Fan in the Carpathian Bend zone.

Most frequently, the sediments of the deep water fans accumulate at the base of the continental slope. Due to the very high sediment influx in the case of the Albian Carpathian Bend Deep Sea Fan, the rudaceous material covered the entire continental slope, building up a slope fan. Consequently, the Albian

²Department of Geological Sciences, Jackson School of Geosciences, University of Texas at Austin, Austin, TX 78712, USA, e-mail: cornelo@jsg.utexas.edu

Fan sedimentary environment varied from deep water in its distal area (Ciucaş and Perşani Mts,) to shallow water in the proximal zone from the northeastern Bucegi Mts. (Fig. 1).

At the apex of the Albian Conglomerate Fan, the thickness of the rudaceous sediments is estimated at 2000 m (Fig. 1). In the lower thickness distal area, two more important sediment accumulations occur in the northern (Perşani Mts.) and especially eastern (Ciucaş Mts.) areas of the Albian Fan.

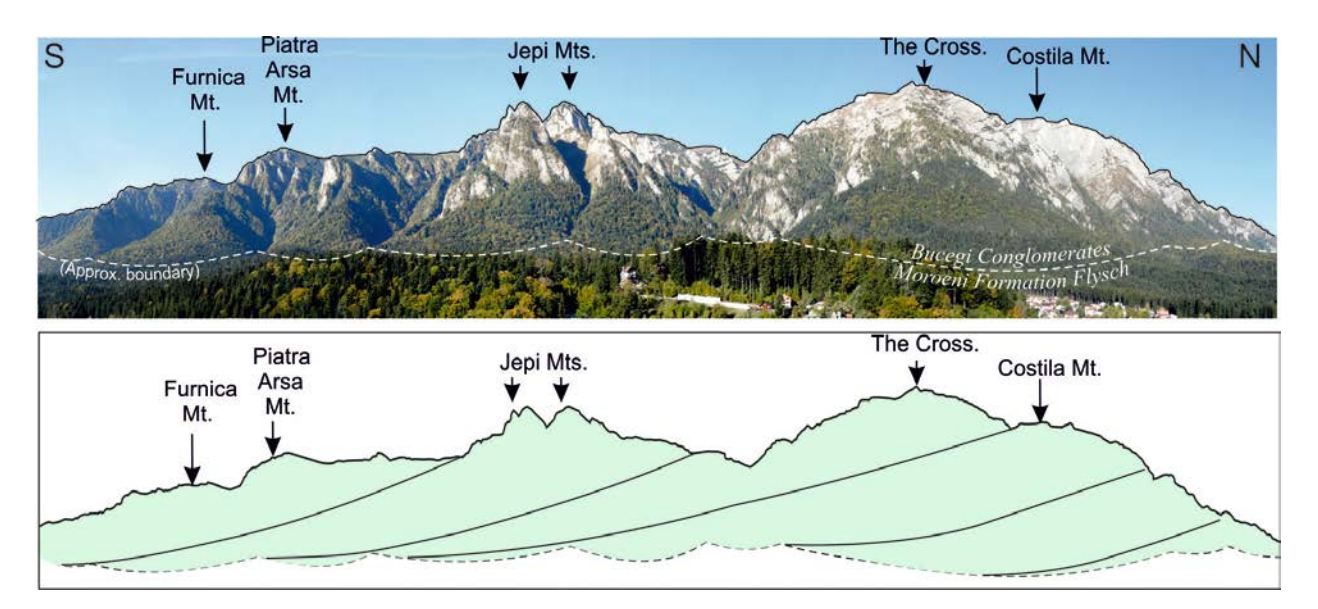


Fig. 2. The large scale internal structure of the Albian Conglomerate Fan in the Bucegi Mts. Area.

The large scale internal structure of the Carpathian Bend Albian Fan is known only from the Bucegi Mountains. Already revealed several decades ago (Jipa, 1984), the inclined bedding of the Bucegi Conglomerates (Fig. 2) reveals the progradation process of the Albian Conglomerate fan development.

Selective references

Jipa, D.C., Olariu, C., 2017. Significance of the Bucegi Conglomerate olistoliths in the Albian sourceto-sink system from the Carpathian Bend basin in Romania

Mihăilescu, N., N. Panin, L. Contescu, and D. Jipa, 1967. Transport and sedimentation of the pebbles from the Albian conglomerate molasse from the Eastern Carpathians (Romania). St. Cerc. Geol. Geofiz. Geogr. 12, 231–237.

Olariu, C., D. C. Jipa, R. Steel, and M. C. Melinte-Dobrinescu, 2014. Genetic significance of an Albian conglomerate clastic wedge, Eastern Carpathians (Romania). Sedimentary Geology, 299, 42–59, doi: 10.1016/j.sedgeo.2013.10.004

Patrulius, D., N. Panin, and S. Panin, 1967. Sedimentogeneza formaţiunilor cretacice din Munţii Perşani si împrejurimile Codlei (Curbura Carpaţilor). D. S. Inst. Geol. Geofiz., LIV/3, 113–141.

Stanley, D. J., and B. Hall, 1978, The Bucegi conglomerates: A Romanian Carpathian submarine slope deposit. Nature 276, 60–64, doi: 10.1038/276060a0.

MIOCENE VOLCANISM IN GUTÂI MOUNTAINS. STATE OF THE ART

Marinel KOVACS¹, Alexandrina FÜLÖP², Zoltán PÉCSKAY³

¹Technical University of Cluj-Napoca, North University Centre of Baia Mare, Baia Mare, Romania e-mail: marinel.kovacs@cunbm.utcluj.ro

²De Beers Canada Inc., Toronto, Ontario, Canada, e-mail: alexandrinafulop@yahoo.com ³Institute of Nuclear Research of the Hungarian Academy of Sciences, Debrecen, Hungary, e-mail: pecskay@atomki.hu

Introduction

Gutâi Mountains represent one of the most studied geological area in Romania. Many researchers conducted numerous studies on the evolution of the volcanism and its coeval metallogeny. In the last two decades, the new geochronological, volcanological, geochemical, isotopical, mineral chemistry and P-T data changed the view on the evolution and petrogenesis of the volcanism from Gutâi Mountains. We conclude on the time and space evolution, volcanological features, geochemical and isotopical characteristics and relationships between the magma source, intracrustal evolution and the volcanic events, presented herein as the state-of-the art, or the most updated summary of the Miocene volcanism evolution.

Gutâi Mountains are located at the eastern tip of ALCAPA, at the contact with the Tisza-Dacia and East European lithospheric plates, as part of the eastern Transcarpathian Basin system belonging to the Neogene-Quaternary volcanic chain of the Carpathians.

Space and time evolution

The evolution of the volcanism had a long time, stage-wise duration in Gutai Mts., from 15.4 to 7.0 Ma (Pécskay et al., 2006). The complex volcanism built up a series of coeval volcanic structures, often overlapping their products. Two types of volcanic activity were defined in Gutâi Mountains (Kovacs and Fülöp, 2003): 1) A felsic (i.e. rhyolitic), caldera-related volcanism, with its onset dated at 15.4 Ma, partially correlated with the widespread rhyolitic volcanism of the Pannonian Basin (Fülöp, 2003). The felsic volcanic rocks (ignimbrites and resedimented counter parts) lie in the southern part of Gutâi Mts. (Fig. 1a). 2) An intermediate (predominantly andesitic) volcanism developed along the 13.4-7.0 Ma time-interval and covers the entire area of Gutâi Mts with its products. The intermediate volcanic activity reached the climax between 11-9 Ma, and comprises four different stages based on temporal evolution (Kovacs et al., 2017a, Fig. 1b). The first two volcanic stages released the highest volumes of volcanic products. They include several volcanic complexes, which group volcanic products with temporal, spatial, and compositional affinities. In the first volcanic stage of the intermediate volcanism, Badenian-Sarmatian (13.4-12.0 Ma) in age, pyroxene andesite lava flows emplaced almost entirely subaqueously in the West and the East of Gutâi Mts. and a dacite extrusive dome grew in the southeastern (Fig. 1a). The second volcanic stage developed during the Pannonian (11.6–9.0 Ma) when a series of intermediate and acidic volcanic rocks were emplaced in the entire area of Gutâi Mts, reaching the highest volume between 10.0-9.0 Ma in the northern part of volcanic area. At this stage, the pile of volcanic products is accompanied by shallow sub-volcanic intrusive bodies (dykes, sills, small-sized laccoliths) dated between 11.8-9.0 Ma (Kovacs et al., 2013) occuring mainly in the southeastern part of the Gutâi Mts. (Fig. 1a). In the third stage of the intermediate volcanism, a small-sized composite andesite-dacite structure (the Laleaua Albă complex, 8.5-8.0 Ma, Pécskay et al., 2006) grew in the central-southern part of Gutâi Mts. (Fig. 1a). Small basaltic intrusions (Firiza basaltic complex, 8.1-7.0 Ma, Edelstein et al., 1993), emplaced in the center of Gutâi Mts. in a fourth stage, ceased the volcanic activity (Fig. 1).

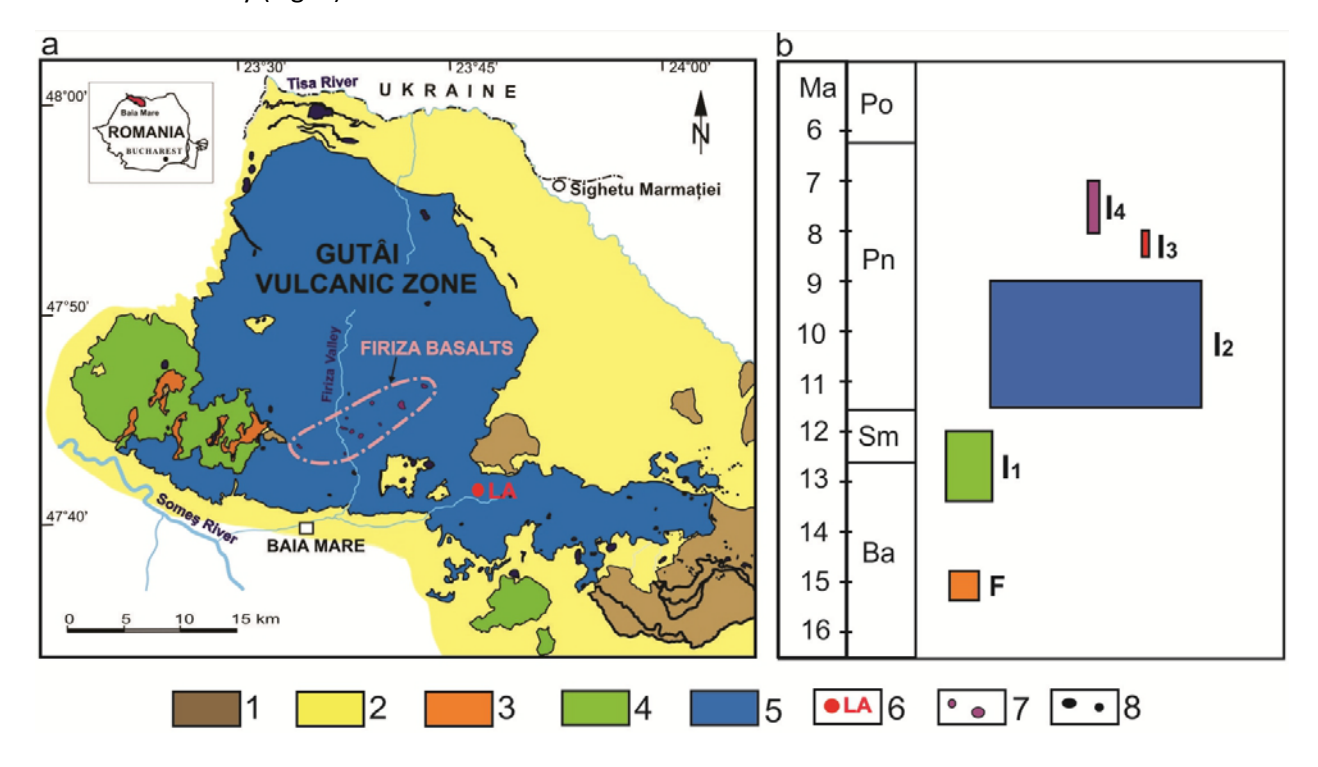


Fig. 1. Simplified geological map (a) and the time evolution of the Miocene volcanism (b) in Gutâi Mountains.

1. Paleogene sedimentary deposits; 2. Neogene-Quaternary sedimentary deposits; 3. Felsic volcanic rocks (F); Intermediate volcanism: 4. First stage volcanic rocks (I₁); 5. Second stage volcanic rocks (I₂); 6. Third stage volcanic rocks (I₃): Laleaua Alba complex (LA); 7. Fourth stage volcanic rocks: Firiza basalts (I₄); 8. Intrusions related to the second stage. Po-Pontian; Pn-Pannonian; Sm-Sarmatian; Ba-Badenian (according to the chronostratigraphic time scale of Harzhauser & Piller, 2007).

Volcanological features

The felsic volcanism is assigned to a caldera activity with an inferred location in the southwestern part of Gutâi Mts. (Fülöp, 2003). Densely welded ignimbrites topped by several meters of ash fall tuffs and a thick and complex succession of resedimented pyroclastic rocks interbedded with deep water sediments accommodate the caldera location, while the ignimbrite outflow lies towards the East, along the southern part of the mountains. The intermediate volcanism denotes high complexity and is difficult to reconstitute. Typical for Gutâi Mts. are composite volcanoes, volcano-tectonic depressions and extrusive domes with volcanic products emplaced both terrestrially and subaqueously, and overlapped volcanic products belonging to different stages and/or to different coeval volcanic structures. The composite volcanoes (e.g. Mogoşa, Igniş, Rotundu, Muntele Bradului) were built during the second stage, some of them connected with extrusive domes. High volumes of lava flows and thick volcaniclastic successions filling volcanotectonic depressions or grabens (due to an active subsidence developed throughout most of the volcanic activity) are well developed in Gutâi Mts. (e.g. northern part of the volcanic area, Lexa et al., 2010). A dome-building volcanic activity is related to the second volcanic stage, when smaller or larger (up to 5 km in diameter) volcanic domes comprised of high-silica andesites and dacites were built as simple, homogeneous domes (e.g. Breze and Gutâi) or compound domes, such as Dănești-Cetățele and Pleșca Mare with an acidic (dacite/rhyolite) central zone and an andesitic marginal zone (Kovacs et al., 2014). Explosive and non-explosive volcaniclastics formed during dome growth indicate fragmental processes triggered by the collapse of the growing structure in subaerial setting (e.g. Vezău and Gutâi), quench fragmentation, or rootless explosions and subsequent resedimentation in subaqueous setting (e.g. Şatra and Dănești-Cetățele).

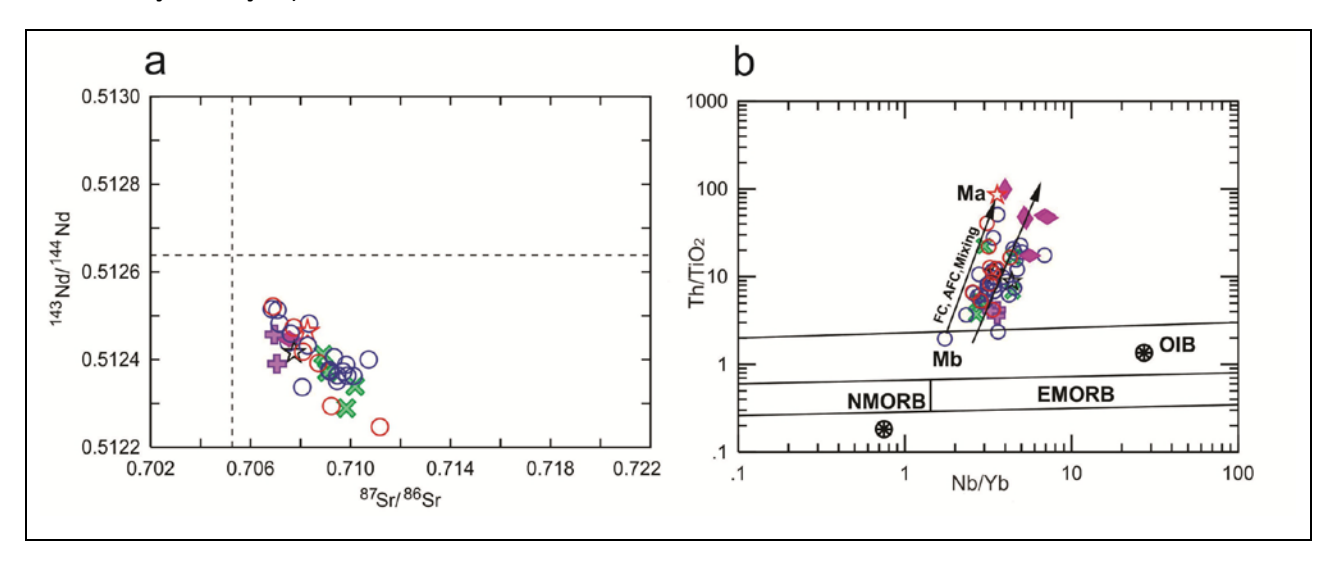


Fig. 2. (a) 143 Nd/ 144 Nd vs. 87 Sr/ 86 Sr diagram displaying typical negative correlation and high 87 Sr/ 86 Sr ratios of the Gutâi Mountains volcanic rocks. (b) Th/TiO₂ vs. Nb/Yb diagram supporting magma evolution by FC, AFC and mixing processes from an enriched magma source. 1. First stage volcanic rocks; 2. Second stage volcanic rocks; 3. Third stage volcanic rocks: Laleaua Albă complex; 4. Mafic enclaves from Laleaua Albă dacite; 5. Fourth stage volcanic rocks: Firiza basalts; 6. Intermediate volcanic rocks from Oaş Mts.; 7. Oraşu Nou rhyolite. Mb, most basic rock-type; Ma, most acidic rock-type. N-MORB, E-MORB and OIB are from Pearce et al. (1990) and Pearce & Peate (1995).

Petrogenesis. The felsic volcanism generated rhyolitic pyroclastic rocks, while the intermediate volcanic activity generated a variety of volcanic rocks ranging from basalts to rhyolites, but predominantly andesites (mostly pyroxene andesites and pyroxene basaltic andesites). The volcanic rocks from Gutâi Mts. indicate subalkaline compositions and a medium to high-K character. They show a typical LREE-enrichment and negative Eu anomalies in the chondrite-normalized REE diagrams, and typical features of subduction-related magmatic arc in the NMORB-normalized diagrams, with strong enrichment in LILE and significant HFSE depletion. The intermediate volcanic rocks show a negative correlation of the Sr–Nd isotopes (Fig. 2a). Major and trace elements geochemistry and the isotopic data constrain the involvement of a strong crustal assimilation by AFC processes during magmatic differentiation testified by the high Rb contents and ⁸⁷Sr/⁸⁶Sr ratios, positive correlation of the LILE elements ratios, or LILE/HFSE elements ratios with differentiation indexes (Kovacs et al., 2017a). Magma mixing/mingling processes are strongly constrained by the mineralogical, textural and geochemical data of numerous volcanics from Gutâi Mts., especially the acidic rocks of the extrusive domes of the intermediate volcanism. In Gutâi Mts. the volcanic rocks were generated from lithospheric enriched mantle-related magma sources (Fig. 2b), previously modified by melted sediment subduction component (Kovacs et al., 2017a).

Conclusions

Newly obtained P-T data based on the new geothermobarometers for amphibole and clinopyroxene constrain a complex volcanic plumbing system, comprised of multi-level, interconnected intra-crustal magmatic reservoirs, for the main volcanic activity in Gutâi Mts. (Kovacs et al, 2017b). Basaltic magmas from the deep magmatic reservoirs (20-25km depth) repeatedly replenished the intermediate and shallow-level reservoirs, mixed and mingled with more evolved magmas, and subsequently triggered volcanic eruptions. Many volcanic phases of the intermediate volcanism (mainly the dome-building activity generating acidic hybrid rocks) can be linked to such magmatic processes.

References

- Edelstein O., Pécskay Z., Kovacs M., Bernad A., Crihan M., Micle R., 1993. The age of the basalts from Firiza zone, Igniş Mts., East Carpathians, Romania. *Révue Roumaine de GÉOLOGIE*, 37, 37-41.
- Fülöp, A., 2003. The begining of volcanism in the Gutâi Mts.: Paleovolcanic and paleosedimentological reconstruction. *Editura Dacia Cluj-Napoca*, 134 pp (in Romanian).
- Kovacs M., Fülöp A., 2003. Neogene volcanism in Gutâi Mts. (Eastern Carpathians). A review. *Studia Universitatis Babeş-Bolyai, seria Geologia,* XLVIII, 1, p. 3-16.
- Kovacs, M., Pécskay, Z., Fülöp, A., Jurje, M., Edelstein, O., 2013. Geochronology of the Neogene intrusive magmatism of the Oaş-Gutâi Mts., Eastern Carpathians, NW Romania. *Geologica Carpathica* 64: 483-496.
- Kovacs, M., Fülöp, A., Pécskay, Z., 2014. Dome-building volcanic activity in the Oaş-Gutâi Neogene Volcanic Area, Eastern Carpathians, Romania. *Buletini i Shkencave Gjeologjike* 1, 230-233.
- Kovacs, M, Seghedi, I, Yamamoto, M, Fülöp, A, Pécskay, Z, Jurje, M., 2017a. Miocene volcanism in the Oaş–Gutâi Volcanic Zone, Eastern Carpathians, Romania: Relationship to geodynamic processes in the Transcarpathian Basin. *Lithos*, 294–295, 304–318.
- Kovacs, M. Fülöp, A., Seghedi, I., Pécskay, Z., Yamamoto, M., Jurje, M., 2017b. P-T evolution of the Miocene magmatic system from Gutâi Volcanic Zone (Eastern Carpathians, Romania). *IAVCEI 2017 Scientific Assembly Portland, Electronical Abstracts*, p. 546.
- Lexa, J., Seghedi, I., Németh, K., Szakács, A., Konečný, V., Pécskay, Z., Fülöp, A., Kovacs, M., 2010. Neogene–Quaternary volcanic forms in the Carpathian–Pannonian Region: a review. *Central European Journal of Geosciences* 2, 3, 207–270.
- Pécskay, Z., Lexa, J., Szakács, A., Seghedi, I., Balogh, K., Konečný, V., Zelenka, T., Kovacs, M., Póka, T., Fülöp, A., Márton, E., Panaiotu, C., Cvetković, V., 2006. Geochronology of Neogene–Quaternary magmatism in the Carpathian arc and Intra-Carpathian area: a review. *Geologica Carpathica* 57, 511–530.

MUSEUM GEOCONSERVATION – PRIMARY ASSESSMENT OF THE CONDITION OF MINERAL SAMPLES CONTAINING PYRITE/MARCASITE WITHIN THE NATIONAL MUSEUM OF GEOLOGY – BUCHAREST

Monica MACOVEI, Dan GRIGORE, Ionut BARBU, Iulia DANCIU

Geological Institute of Romania, 1 Caransebeș Str., Bucharest e-mail: macovei.monica@yahoo.com

Many conferences and workshops are carried out to support the geoconservation of the natural heritage as regarding the geosites. There are fewer the subjects on geological conservation in the museum area; usually they are mixed with other museum themes (as art, history, nature, etc.). The geological museum has its one particularity regarding especially the decay of the exhibits that is generated not only by the environment (humidity, temperature) but also by its one contribution (the decay of FeS_2 is accompanied by H_2S vapours emission that contributes to alteration of other artefacts and the acceleration of the decay process).

It is very important to preserve mineral samples in the museums because of their uniqueness (some of them belong to intensively exploited or even exhausted ore deposits), not to mention their beauty and, why not, their cost.

There is no guidebook regarding the specific conditions of geological samples storage, no international standard for the care of geological collections (Baars, Horak, 2018). There have been a few attempts to establish those conditions but there is not yet a generally accepted opinion. Only for the marcasite and pyrite storage conditions are more than one opinion, for example regarding the relative humidity (under 60% – US National Parks Service, 1998; under 55% – Shepherd, Tulloch, 2007; under 50% – Howie, 1979, 1984; near 30% – Waller, 1992; under 30% – Fellowes, Hagan, 2003; Becherini et al., 2018).

The formation of pyrite is quite diverse in range starting to a very early stage of diagenessis (even on living creatures as recorded on bivalves *Mercenaria mercenaria* and *Geukensia demissa*, Clark, Lutz, 1980) and finishes in harsh conditions of temperature and pressure and temperatures between 250 and 340 °C and pH of 2,5 - 4 (King et al., 2014).

Other environmental parameters that are responsible to the pyrite decay are: temperature, bacteria activity, oxygen concentration, pH, light, exposed surface, other trace elements that are included into the artefact and the vicinity of other pyrite/marcasite samples. Storing more materials which are emanating acid vapours in the same room or in the same drawer represents an important cause that leads to decay, or the so called "pyrite disease". The process is rather simple: (pyrite+oxygen+water \pm bacteria) \rightarrow (ferrous sulphate+sulphuric acid+sulphur dioxide).

There is not a current unitary program in the National Museum of Geology regarding conservation. The only measures that have been taken are to avoid those chambers that are located in the basement that are exposed to water infiltration and the restoration of a few exhibits that deteriorated in time.

The first step for some major conservation measures is the basic assessment of the current situation regarding: the state of the exhibits and artefacts, the environmental parameters and the measures that need to be taken for the future.

First of all, the artefacts are categorised based on their major chemical and structural components (those that are made from the same kind of material need specific environmental control). This paper refers to the artefacts that are comprised of FeS₂ (pyrite - isometric and marcasite - orthorhombic) and refers to some examples of contractions found in the scientific literature.

In a previous study (Waller, 1992) noticed that from a total of 3000 mineral species around 10% could suffer alteration if they were removed from their natural setting. The pyrite and marcasite are among the most common and sensible minerals.

For this study we took notice of the current visible aspect of the samples that are exposed for the public in the National Museum of Geology, Bucharest. We have examined a total of 88 samples of/with pyrite/marcasite.

The samples were observed in their exhibits and photographed. The notes comprised their composition (according to the inventory of the National Geological Museum), the approximate dimension of the artefact and if it is comprised entirely from pyrite/marcasite or another one is the main mineral, the current aspect (integrity, colour and lustre).

As regarding the museum's repository, this wasn't taken into account for the current study due to the great number of artefacts that needed to be observed and due to different environmental storage conditions. In the repository the aeration is reduced, so, the acid vapours weren't eliminated after emission and they contributed to a more aggressive ambiance that accelerated the degradation of samples leading towards integrity lost. In the future, they will be also analyzed.



Fig. 1. Example of an exhibited sample containing large pyrite crystals (inventory number 35285). Deep cracks and newly formed light grey minerals can be easily observed on the surface of crystals; this piece requires restoration.

Observations lead to the conclusion that degradation has started on all the examined samples. Their general degree of alteration is medium.

The lustre of the artefacts varied from nearly shiny to absent. The colour was generally the specific pyrite-yellow with different colouration along the fissures (usually grey), in some cases a lot darker general colour (brown) or with grey areas, one sample developed along the cracking secondary white minerals and one grey (see figure 1); most of the examined objects had rainbow-like surfaces. Every variation in colour signifies a change in the mineral composition, usually when the pyrite weathers are formed:

The intensity of the cracking varied from invisible to the naked eye (figure 2) to disintegrated material (Fig. 1).

The majority of the artefacts were dull (superficial oxidation), with minor cracks on the edges of the crystals or rainbow-like colours especially on the large crystal surfaces (see figure 2). We noticed that the marcasite tends to get darker in colour than pyrite.

In eight cases was noticed a very advanced degradation with integrity lost, when crystals attached no more to the artefact. It has been observed that the condition for the marcasite is overall worse than

pyrite's; the difference in the crystallisation system makes it more vulnerable (pyrite – cubic and marcasite – orthorhombic), the thinner lamellas also increases the surface of contact with the air.

In a previous paper, Macovei et al. (2019), the attention was focused on the paleontological material that was pyritized. In that study the authors presented material found in the museum's repository but also the 8 ammonites that are in the permanent exhibit and which are included in this current paper. There are more mineralogical samples and their degree of alteration varies more due to a greater chemical diversity, age of exposure to free air and their genetic condition.

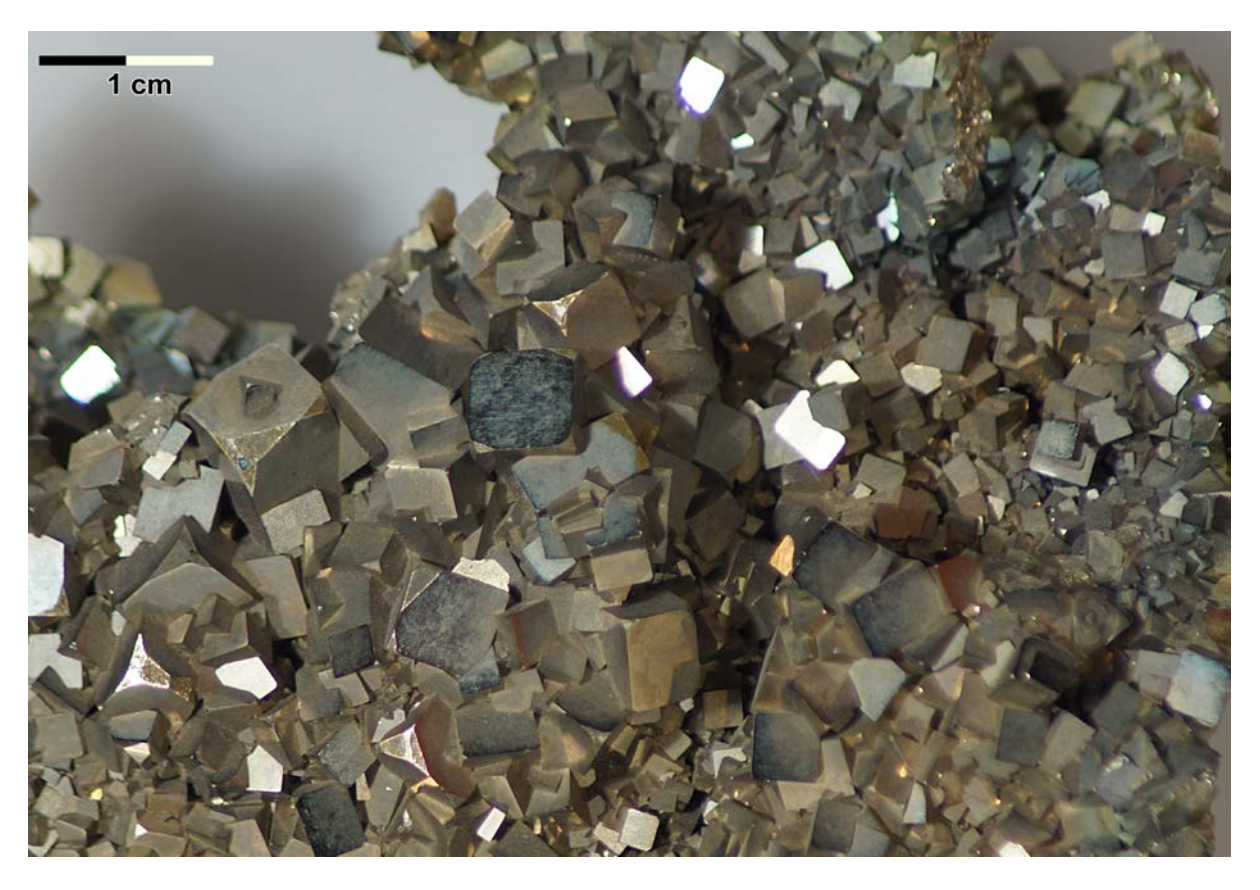


Fig. 2. Part of an exhibited sample containing different sized pyrite crystals (inventory number 21254); alteration minerals (grey and rainbow-like) are visible on the surface of the crystals. This piece requires preservation measures.

In order to stop the weathering of the exhibits, the first step is to properly observe the environmental conditions, which requires specific measuring instruments, so that in the future optimal parameters could be ensured. In the cases where alteration has already started, it will be necessary to recondition those samples and to treat them chemically in order to stop the deterioration process. Treatment should also be applied on all the pyrite/marcasite specimens. Some researchers suggest to clean the surfaces with ethanolamine thioglicollate (Cornish, Doyle, 1984; Cornish, 1986; Cornish et al., 1995), or apply an ammonia vapour treatment (Hodgkinson, Martin, 2004) to prevent further decay. Coating is not a viable solution as presented in previous work (Macovei et al. 2019), the samples continued to decay under the resine/acrylate strata the oil submersion is not an option for such large objects that need to be also presented to the public.

Therefore, from the total of 88 mineral samples exhibited in the Museum, at least 8 necessitate urgent action (restoration and prevention treatment), about 15 require some restoration and the rest should be taken into account for future work of decay prevention. These pieces require further study in order to identify the newly formed secondary minerals, as well as meticulous periodical surveillance of their state of alteration, while placing dehumidifiers and monitoring environmental conditions and keeping them in reasonable limits.

References

- Baars, C., Horak, J., 2018. Storage and conservation of geological collections a research agenda. Journal of the Institute of Conservation, 41, 2, 154-168.
- Becherini F., Del Favero L., Fornasiero M., Guastoni A., Bernardi A., 2018. Pyrite Decay of Large Fossils: The Case Study of the Hall of Palms in Padova, Italy. Minerals, 8, 2, 40.
- Clark, G. R., Lutz, R. A., 1980. Pyritization in the shells of living bivalves. Geology, 8, 6, 268–271.
- Cornish, L., Doyle, A.M, 1984. Use of ethanolamine thioglycollate in the conservation of pyritized fossils, Palaeontology, 2, 421–424. Cornish, L., 1986. The treatment of decaying pyritiferous fossil material using ethanolamine thioglycollate, Geol. Curator, 4, p. 451–454
- Cornish, L., Doyle, A.M., Swannel, J., 1995. The Gallery 30 Project: Conservation of a collection of fossil marine Reptiles. Conservator, 19, 20–28
- Fellowes, D., Hagan, P., 2003. Pyrite oxidation: The conservation of historic shipwrecks and geological and paleontological specimens. Stud. Conserv, 48, 26–38.
- Hodgkinson, S., Martin, S. 2004. History and mineralisation of highly degraded pyrite fossil collection. Curation history and mineralisation of highly degraded pyrite fossil collection Information Management Programme. Internal Report Ir/04/037. British Geological Survey, 30 pp. (http://nora.nerc.ac.uk/, accessed 07.09.2019)
- Howie, F., 1979. Museum Climatology and the Conservation of Palaeontological Material. In: Curation of Palaeontological Collections: A Joint Colloquium of the Palaeontological Association and Geological Curators' Group, ed. Michael Bassett (London: The Palaeontological Association), 103–125.
- Howie, F., 1984. The Conservation and Storage of Geological Materials. In: John Thompson (Ed.), Manual of Curatorship: A Guide to Museum Practice. Severnoaks: Museums Association/Butterworth & Co., 308–322.
- Kesler, S.E., Deditius, A.P., Chryssoulis S., 2007. Geochemistry of Se and Te in arsenian pyrite: new evidence for the role of Se and Te hydrothermal complexes in Carlin and epithermal-type deposits, In: Kojonen, K. K., Cook, N. J., Ojala, V.J. (Eds.), Au–Ag–Te–Se deposits, Proceedings of the 2007 Field Workshop Espoo, Finland, August 26–31, 2007. Geological Survey of Finland, 53, 85–95.
- King, J., A.E., Williams-Jones, V., Van Hinsberg, G., Williams-Jones, G., 2014. High-Sulfidation epithermal pyrite-hosted Au (Ag-Cu) ore formation by condensed magmatic vapors on Sangihe Island, Indonesia. Econ. Geol. 109, 1705-1733.
- Macovei, M., Grigore, D., Sebe-Rădoi, O. G., Dumitraș, D. G., Crușoveanu-Rusu, S., 2019. Degradation of paleontological samples which contain pyrite and / or marcasite considerations on their conservation. Oltenia Studii și comunicări Științele Naturii, (in print).
- Shepherd, P., Tulloch, G., 2007. The Monitoring of Environmental Conditions under which BGS Data and Information (Including Corporate Collections) are managed at Keyworth and Edinburgh 2006. British Geological Survey Internal Report, IR/07/011.
- Waller, R., 1992. Temperature and Humidity Sensitive Mineralogical and Petrological Specimens, in The Care and Conservation of Geological Material ed. F. Howie, Butterworth-Heinemann Publishers, London, United Kingdom, 25-50.

* * * * *

US National Parks Service, 1998. ConserveOGrams - short publications by the offering guidance on the care of museum objects, Storage Concerns for Geological Collections (Washington, DC: National Park Service Museum Management Program), No. 11/2, https://www.nps.gov/museum/publications/conserveogram/cons_toc.html (accessed 04 September 2019)

THE ROLE OF UAV (UNMANNED AERIAL VEHICLE) IN THE STUDY OF LANDSLIDES

Raluca MAFTEI, Radu FĂRNOAGA, Adrian TĂTARU, Constantina FILIPCIUC, Elena TUDOR

Geological Institute of Romania, 1 Caransebes St., 012271 Bucharest e-mail: mafteir@yahoo.com

Landslides are natural disasters with some effects in the natural environment of the Earth. A landslide has a structure that changes the natural topography boundaries by releasing the forest cover and vegetation. Heavy precipitation as well as the mass movement that can be caused by landslides, trigger the possible tendency to move the soil. The formation of the current Digital Elevation model (DEM) of the area subject to landslides is important in terms of determining the direction, character and effects of the landslide. With the help of aerial photographs obtained by Unmanned Aerial Vehicle (UAV), the production of high resolution and accurate DEMs is becoming increasingly widespread.



Fig 1. UAV Hirrus picture of the Fărcașa village landslide.

The Geohazard team at GIR studied these phenomena since the early 2000's. We started monitoring the landslides, that were not always easy to reach ortoassess but due to lack of money and equipment, we weren't to a fault competitive. So, in2015, we purchased a mini UAV System. It offered us the possibility of

having a system that would allow us to obtain high-resolution imagery data on landslides and areas affected by these in real time. UAV-acquired photographs have been merged to an ortho-mosaic by using plane image rectification methods. The generated ortho-mosaic covers the entire studyareas-Slanic Prahova City, Gornet village, Beclean area, Fărcașa village (fig. 1), with a spatial resolution in the range of 1 – 5cm.



Fig. 2. UAV Hirrus 2015 model and louncher

The collection of aerophotogrammetry data is done with UAS (Unmanned Aircraft System) system composed of:

A. UAV (Unmanned Aerial Vehicle) Hirrus model 2015 (fig.2) with the following characteristics:

or width: 3.2 mlength: 1.2 m

- a recovery: with parachute

a propulsion: electricautonomy: 120 min

- maximum speed: 130 km / h

a maximum flight altitude: 4000 ma minimum altitude of flight: 80 m

UAV is equipped with SONY NEX 7 digital camera with the following parameters:

a resolution of 24 Megapixels
APS-C sensor: 23.5 x 15.6 mm
Focal distance: 18 - 55 mm
Shutter: 30 - 1/4000 s

- Pixel: 0.004 mm

- Image resolution: 6000 x 4000 pixels

B. GCS (Ground Control Station)

C. GDT (Antenna): maintains the directional connection between the UAV and the ground station. The surface of interest is covered in parallel phases, the collected pictures with 60-70% overlap on the flight direction and 40-50% lateral overlap.

| Geosciences in the 21 st century | Geosciences | in | the | 21 st | centur |
|---|-------------|----|-----|------------------|--------|
|---|-------------|----|-----|------------------|--------|

According to the results obtained in the study concerning landslides, the production of DEM based on UAV provides higher accuracy at centimeter level. In addition, the method used is more efficient, faster and lower cost than other terrestrial techniques.

Monitoring and analysis of active landslides involves both spatial and temporal measurements and requires continued assessment of landslide conditions, including the extentand rate of displacements as well as changes in the surface topography. Displacement rates are of great interest and can be directly achieved by the comparison of ortho-photographs as well as digital surface models (DSMs) from different dates.

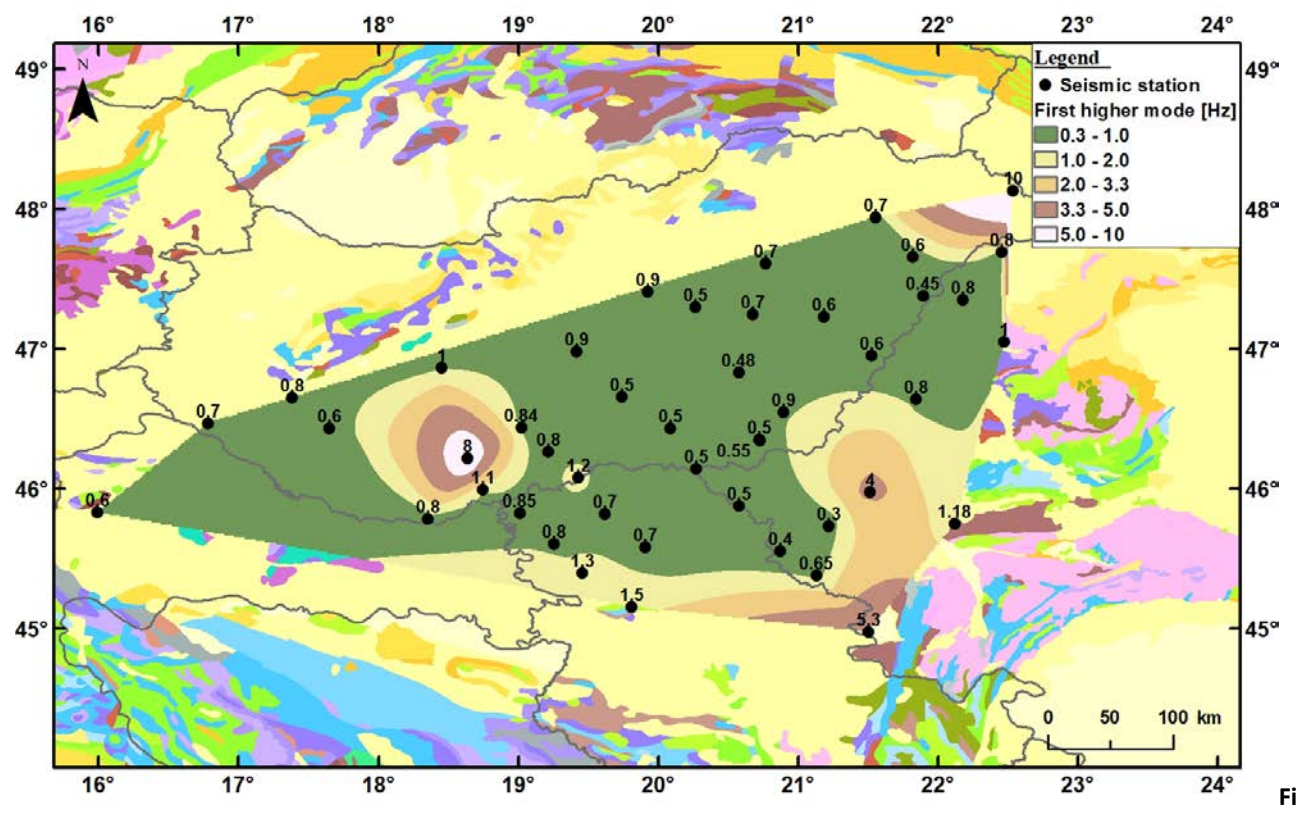
NON-INVASIVE INVESTIGATIONS ALONG THE PANNONIAN BASIN

Elena Florinela MANEA¹, Erzsébet GYŐRI², Alina COMAN^{1, 3}, Carmen Ortanza CIOFLAN¹, Mircea RADULIAN¹

¹National Institute for Earth Physics, 12 Călugăreni St, Măgurele, Romania e-mail: elena.manea@infp.ro ²Geodetic and Geophysical Institute, 6-8 Csatkai E. St., 9400 Sopron, Hungary e-mail: gyori.erzsebet@csfk.mta.hu

³ Faculty of Physics, University of Bucharest, 405 Atomiștilor St, 077125 Măgurele, Romania e-mail: coman@infp.ro

The Pannonian Basin is located in the Eastern part of Central Europe and is one of the largest Neogene sedimentary basins in Europe. The seismicity along this area is moderate and large events do not occur very often, a magnitude 6 earthquake is about once every 100 years, while a magnitude 5 event appears on average every 20 years (Tóth et al., 2008). In the context of rapid urban development of the region, recurrence of similar events would pose a high/significant seismic risk on the exposed communities. Although very strong (M>6) events are rare in this region, estimation of the impact of such events on buildings and life-line systems requires accurate evaluation of local seismic response. In this study, local site investigations were performed along the Pannonian Basin, in order to map and interpret local parameters as fundamental frequency of S-wave resonance by correlating and interpolating the results obtained from single station measurements with the available geological data.



g. 1. Distribution of first higher peak in the Pannonian Basin.

The horizontal-to-vertical Fourier spectral ratio (Nogoshi, Igarashi, 1971; Nakamura, 1989) was primarily applied to assess the variability of the fundamental frequency of resonance over the Pannonian

Basin. These results were interpreted according to the available geophysical/geological information in order to extract essential information and to trace out the geometry of Pannonian Basin. Single station analysis was performed for 73 seismic stations, among these: 26 stations deployed during South Carpathian Project - SCP (2009-2011, Ren et al., 2012), 26 Carpathian Basin Project - CBP (2005-2007, Dando et al., 2011) and the rest of them belong to different countries seismic networks (2 - Slovenia, 2 - Serbia, 6 - Hungary, 1 - Croatia, 1 - Slovakia, 9 - Romania) (Fig. 1).

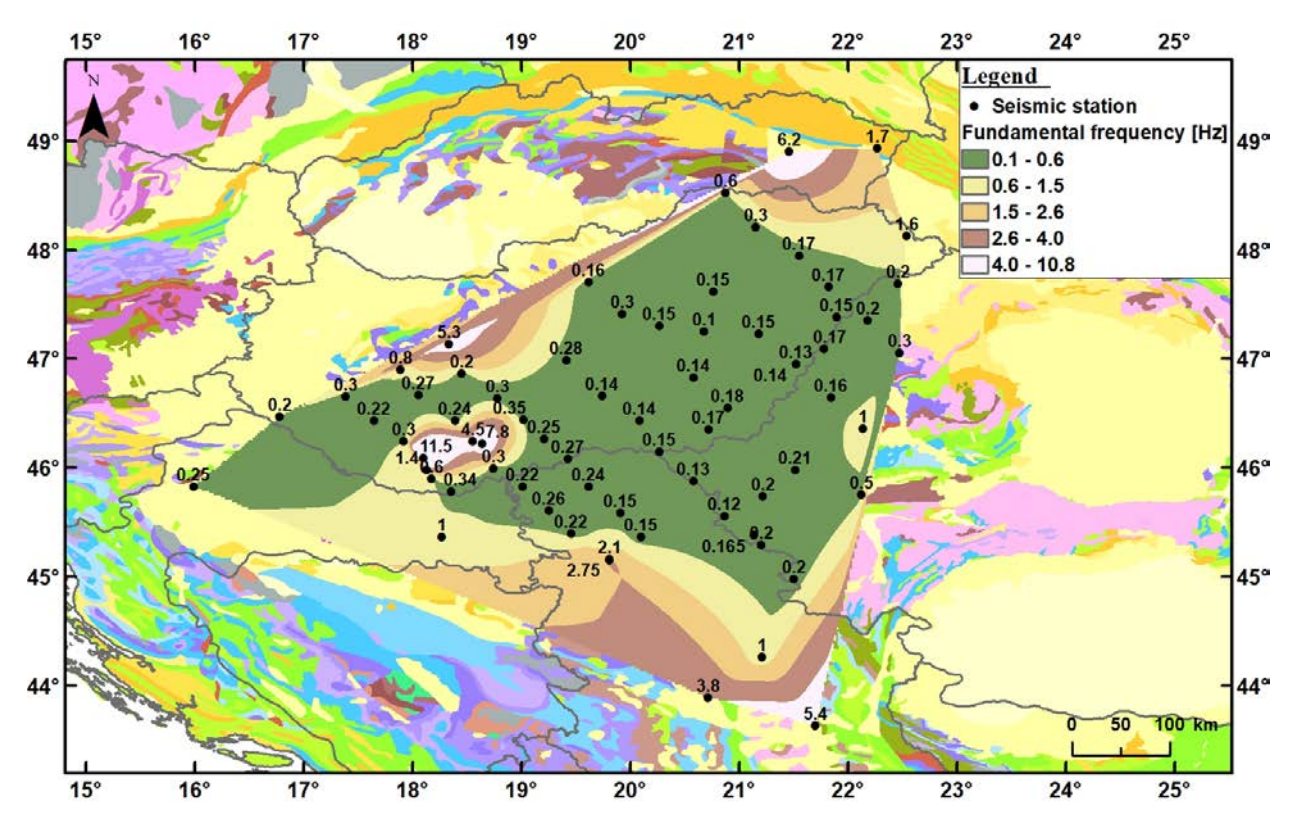


Fig. 2. Distribution of fundamental frequencies of resonance in the Pannonian Basin.

The aspect of the computed H/V ratios over the entire area shows the existence of lateral variations within the subsoil of the Pannonian Basin and exhibit multiple peaks. The fundamental frequency of S waves resonance varies between 0.1 and 6.2 Hz and corresponds to the interface between the Miocene-Pliocene sediments (Horváth et al., 2006; Balázs et al., 2015) (Fig. 2). A second peak in the H/V ratios was observed, between 0.6 and 10 Hz and its depth corresponds to Quaternary-Pliocene interface (Horváth et al., 1999). The information about these interfaces will offer new and significant perspective on the quantification of its influence on the seismic site response on the Pannonian Basin and in this way to minimize their uncertainties in seismic hazard evaluation.

References

Dando, B. D. E., Stuart, G. W., Houseman, G. A., Hegedüs, E., Brückl, E., Radovanović, S., 2011. Teleseismic tomography of the mantle in the Carpathian-Pannonian region of central Europe. Geophysical Journal International, 186, 1, 11-31.

Horváth, F., Bada, G., Szafián, P., Tari, G., Ádám, A., Cloetingh, S., 2006. Formation and deformation of the Pannonian Basin: constraints from observational data. Geological Society, London, Memoirs, 32, 1, 191-206.

Horváth, F., Tari, G., 1999. IBS Pannonian Basin project: a review of the main results and their bearings on hydrocarbon exploration. Geological Society, London, Special Publications 156, 1, 95-213.

Nakamura, Y., 1989. A method for dynamic characteristics estimation of subsurface using microtremor on the ground surface. Rep. Railway Tech. Res. Inst., 30, 1, 25–33.

Nogoshi, M., Igarashi, T., 1971. On the amplitude characteristics of microtremors, Part 2 (In Japanese with English abstract). J. Seism. Soc. Japan, 24, 26–40.

| Geosciences in the 21 st century | Geosciences | in | the | 21 st | centur |
|---|-------------|----|-----|------------------|--------|
|---|-------------|----|-----|------------------|--------|

- Ren, Y., Stuart, G., Houseman, G., Dando, B., Ionescu, C., Hegedus, E., Radovanovic, S., Yang, S., 2012. Upper mantle structures beneath the Carpathian–Pannonian region: Implications for the geodynamics of continental collision. Earth and Planetary Science Letters 349, 139-152.
- Tóth, L., Mónus, P., Bus, Z., Györi, E., 2008. Seismicity of the Pannonian basin. In: E.S. Husebye (ed.), Earthquake Monitoring and Seismic Hazard Mitigation in Balkan Countries. Springer Science + Business Media B.V., Dordrecht. 99-110.

LUDWIGITE IN MAGNESIAN SKARNS FROM ROMANIA: A REVIEW

Ștefan MARINCEA, Delia Georgeta DUMITRAȘ

Geological Institute of Romania, 1 Caransebeş Str., Bucharest, Romania e-mail: smarincea@yahoo.com

Ludwigite, essentially (Mg,Fe²⁺)₂(Fe³⁺,Ti⁴⁺,Al)(BO₃)O₂, is quite a widespread magnesium-iron oxyorthoborate belonging to the homonymous group (orthorhombic, space group *Pbam*), with numerous occurrences in skarn areas. Ludwigite can be a valuable source for boron. In Romania, ludwigite has been reported from magnesian skarns at a number of localities including Ocna de Fier (Tschermak, 1874), Pietroasa (Rafalet, 1963), Maşca-Băişoara (Ionescu et al., 1971), Băiţa Bihor (Stoicovici & Stoici, 1969) and Cacova Ierii (Marincea & Cristea, 1995). Al five occurrences of boron-bearing magnesian skarns mentioned before are related to contact-metamorphic zones of calc-alkaline intrusions, namely the plutons from Bihor, Pietroasa Cacova - Miei and Ocna de Fier – Dognecea. These plutons are of Upper Cretaceous – Palaeogene age, being related to the "banatitic" magmatic event, using the term as first defined by von Cotta (1864) for a consanguineous series of rocks of this age, where calk-alkaline, compositionally intermediate, plutonic and volcanic rocks of magnetite series predominate. The granitoids were emplaced at shallow depths.

| Table 1. Geological fe | eatures of the b | oron-bearing m | agnesian ska | arns from Romania |
|-------------------------------|------------------|----------------|--------------|-------------------|
| | | | | |

| Occurrence | Intrusion | Main intrusive rock | Age of intrusion or mineralization | Protolith | Age of protolith | Structural unit |
|-----------------------------------|---|------------------------------|--|--------------------------|---|---|
| Băiţa Bihor | Bihor batholith | granodiorite | 77 ± 3 to 67 ± 3 Ma ⁽¹⁾ 70 ± 5 Ma ⁽²⁾ 80.63 ± 0.3 to 78.69 ± 0.4 Ma ⁽³⁾ | dolostones | Anisian - Carnian Carnian - Norian | Vălani unit Vetre unit |
| Pietroasa | Pietroasa laccolith | granodiorite | 74 ± 3 to 67 ± 3 Ma $^{(4)}$ | dolostones | Anisian | Ferice unit |
| Cacova Ierii Maşca Băişoara | Cacova – Miei pluton | granodiorite granodiorite | $71.0 \pm 7.8 \text{ to}$ $54.8 \pm 2.1 \text{ Ma}^{(5)}$ | dolomitic marbles | Proterozoic | Baia de Arieş Group |
| Ocna de Fier | Ocna de Fier – Dognecea pluton | granodiorite | 75.5 ± 1.6 Ma ⁽⁶⁾ 76.6 ± 0.3 Ma ⁽⁷⁾ | metasomatic dolomites | Mesozoic | Ezeris - Cârnecea sedimentation zone |

⁽¹⁾ K-Ar ages on whole rock or on "femic" minerals (Bleahu et al., 1985); (2) Rb-Sr isochron (Pavelescu et al., 1985); (3) Re-Os data on molybdenite (Zimmermann et al., 2008) (4) K-Ar age on whole rock (Bleahu et al., 1985); (5) K-Ar ages on whole rock or on biotite (Lemne et al., 1983); (6) U-Pb age on zircon (Nicolescu, 1998); (7) Re-Os data on molybdenite (Ciobanu et al., 2002).

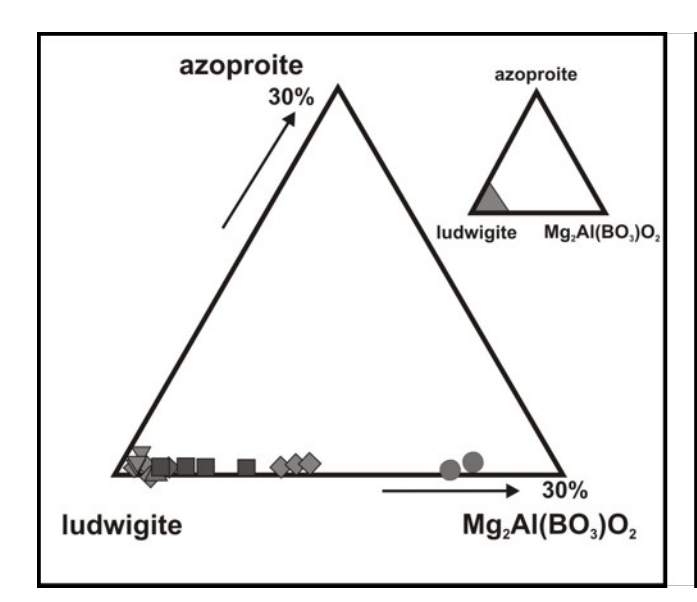
The geological and structural characteristics of these skarn deposits were thoroughly investigated by several authors (Marincea, 1998; Ilinca, 2010 and referred works) and are summarized in Table 1. As common point, a protolithology containing dolomite is common for all the five occurrences. The common treat linking the Romanian boron skarn deposits, as well as other worldwide deposits (e.g., Aleksandrov,

2007) is their occurrence distal from associated igneous rocks. The metasomatism gave metasomatic columns or bands containing magnesian borates (i.e., ludwigite, kotoite, suanite, fluoborite and szaibélyite) in the outer zones, whereas the inner zones typically contain magnesian silicates (e.g., forsterite, humites, diopside, and phlogopite) and spinel.

Ludwigite characteristically associates with kotoite, suanite, szaibélyite, exceptionally with fluoborite and pertsevite, in magnesian skarns containing humites (chondrodite, clinohumite, rarely norbergite), forsterite, magnetite, dolomite, calcite, rarely spinel and fluorite, and retrogressive minerals (i.e., lizardite, chrysotile, clinochlore, brucite, magnesite, pyroaurite, sjögrenite, lepidocrocite, goethite).

In all five occurrences, ludwigite occurs as needle-like, fibrous or prismatic crystals, up to 3.5 cm in length at Ocna de Fier and Cacova Ierii, up to 2 cm at Maşca-Băişoara and Pietroasa and up to 0.8 cm at Băiţa Bihor. Fan-shaped or radiating aggregates of prismatic crystals of ludwigite isolated in a mass of carbonates (calcite, dolomite) and silicates (forsterite, clinohumite, serpentines) are characteristic at Pietroasa and Băiţa Bihor, whereas they are scarce at Maşca-Băişoara and very scarce at Ocna de Fier. Ludwigite from Ocna de Fier, Maşca-Băişoara and Cacova Ierii generally occurs as monomineralic irregular bands of 3 to 20 cm wide, alternating with bands of magnetite having the same thickness, which materialize a metasomatic texture. In the ludwigite bands, the component crystals are disposed in parallel, radiating or interwoven aggregates which sometimes give to the mass a felt-like appearance.

In reflected light, ludwigite from the five occurrences appears to be distinctly bireflectant with pinkish grey (\parallel Z) to dark greenish grey (\perp Z) tints. Under crossed polars, it shows a strong anisotropy in yellowish brown (\parallel Z) to bluish-violet gray (\perp Z) colors. No internal reflections were observed. Ludwigite from Pietroasa and Băiţa Bihor could be translucent.



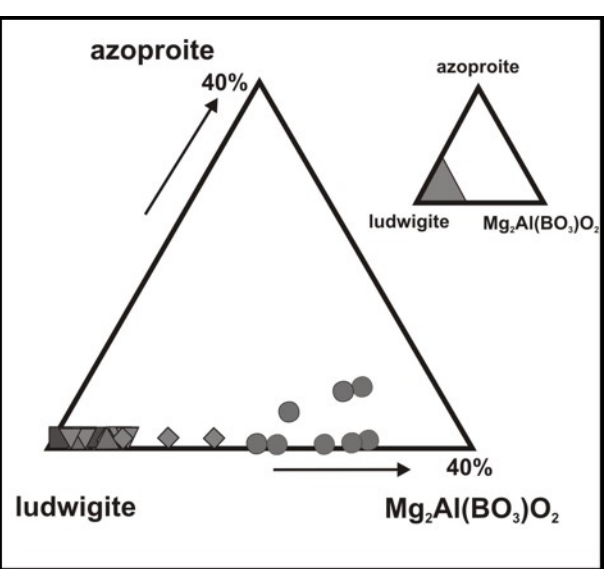


Fig. 1. Ternary diagrams showing the isomorphism of ludwigite from the Romanian occurrences in the azoproite $[Mg_2Fe^{2+}_{0.5}Ti^{4+}_{0.5}(BO_3)O_2] - ludwigite [Mg_2Fe^{3+}(BO_3)O_2] - Mg_2Al(BO_3)O_2$ solid solution series, as illustrated by samples from Băiţa Bihor (solid triangles), Pietroasa (solid circles), Cacova Ierii (solid squares), Maşca Băişoara (diamonds) and Ocna de Fier (inverted triangles). Plots of wet-chemical analyses (left) vs. plots of EMP analyses (right).

The analyzed samples are compositionally variable with vonsenite ranging from 0.74 to 25.95 mol.%, minor azoproite [up to 6.95 mol.% (Mg,Fe $^{2+}$)₂(Ti $^{4+}$,Mg)(BO₃)O₂] and less than 30.01 mol.% (Mg,Fe $^{2+}$)₂Al(BO₃)O₂ in solid solution, generally lower, and with minor Sn, Sb, Cr, Ni, Co, Mn, Zn. The vonsenite contents in solid solution generally define magnesian ludwigite terms. For the analyzed samples, they range from 4.41 to 14.27 mol.% at Ocna de Fier, 5.47 to 23.87 mol.% at Maşca Băişoara, 4.91 to 25.95 mol.% at Cacova Ierii, 5.69 to 14.27 mol.% at Băiţa Bihor, and 0.74 to 6.40 mol.% at Pietroasa. As concerning the substitutions in the M(4) structural site, normally occupied by Fe $^{3+}$, the chemical variations of the analyzed samples of ludwigite from the five occurrences are better depicted in a ternary diagram ludwigite - (Mg,Fe)₂Al(BO₃)O₂ – azoproite (Fig. 1).

Other substitutions, such as those involving Mn, Ni, Co, Ti, Sn, Sb or V are of minor importance.

The average unit-cell parameters, refined on the basis of 35 selected reflections in the X-ray powder patterns, recorded in the 2θ range $10\text{-}120^\circ$, are: a = 9.255(18) Å, b = 12.278(39) Å and c = 3.048(9) Å at Ocna de Fier; a = 9.259(28) Å, b = 12.268(35) Å and c = 3.048(9) Å at Maşca Băişoara; a = 9.246(21) Å, b = 12.274(32) Å and c = 3.051(5) Å at Cacova Ierii; a = 9.268(16) Å, b = 12.262(9) Å and c = 3.052(6) Å at Băiţa Bihor; and a = 9.262(33) Å, b = 12.255(21) Å and c = 3.046(13) Å at Pietroasa.

Generally speaking, it is proven that ludwigite shows a negative correlation between $X_{AI} = AI/(Fe^{3+}+Ti^{4+}+AI)$ and the density, indices of refraction, cell volume and c cell parameter. It is not possible to quantify the variations in the physical and crystallographic parameters by advancing the Al-for-Fe³⁺ substitution because both Fe^{2+} -for-Mg and Al-for-Fe³⁺ substitutions are involved. However, it is clear that Al plays a major role in diminishing the cell volume, c cell parameter, density, absorption coefficient, bireflectance and refraction indices of ludwigite (Marincea, 2000). Because of the influence of Al, natural compositional members of the ludwigite - vonsenite series cannot be unambiguously distinguished neither by their cell dimensions nor by their physical parameters as previously suggested (e.g., Aleksandrov, 1982).

The Mössbauer behaviour of ludwigite was carefully investigated by Marincea (1999). A collection of Mössbauer parameters recorded for ludwigites from Romania is given in Table 2. Part of the samples from Ocna de Fier and Maşca Băişoara show a superparamagnetic behaviour.

Table 2. Mössbauer hyperfine parameters, relative iron distributions (I) and sites assignment fitted to the spectra of Romanian ludwigite

| Crt. no. | Sample | Iron location | I (%) | $\Delta (\text{mm/s})^{(1)}$ | δ (mm/s) ⁽²⁾ | Γ (mm/s) $^{(3)}$ |
|----------|---------|---|-------|-------------------------------|-------------------------|--------------------------|
| | | Fe ²⁺ Fe ³⁺ ₂ O ₄ | 17.70 | - | - | - |
| 1 | 1168 OF | M1 + M2 | 13.80 | - | - | - |
| | | M3 | 21.70 | 2.07 | 1.00 | 0.36 |
| | | M4 | 46.80 | 1.09 | 0.30 | 0.37 |
| | | Fe ²⁺ Fe ³⁺ ₂ O ₄ | 8.00 | - | - | - |
| 2 | 1798 OF | M1 + M2 | 0.00 | - | - | - |
| | | M3 | 19.60 | 2.15 | 0.91 | 0.33 |
| | | M4 | 72.40 | 1.34 | 0.29 | 0.38 |
| | | Fe ²⁺ Fe ³⁺ ₂ O ₄ | 53.30 | - | - | - |
| 3 | 998 CI | M1 + M2 | 5.00 | - | - | - |
| | | M3 | 13.20 | 2.12 | 0.88 | 0.31 |
| | | M4 | 28.40 | 1.35 | 0.30 | 0.35 |
| | | Fe ²⁺ Fe ³⁺ ₂ O ₄ | 23.00 | - | - | - |
| 4 | 1302 CI | M1 + M2 | 0.00 | - | - | - |
| | | M3 | 31.90 | 2.02 | 1.06 | 0.51 |
| | | M4 | 41.10 | 1.07 | 0.30 | 0.50 |
| | | Fe ²⁺ Fe ³⁺ ₂ O ₄ | 19.40 | - | - | - |
| 5 | 1466 CI | M1 + M2 | 0.00 | - | - | - |
| | | M3 | 27.80 | 1.96 | 1.02 | 0.52 |
| | | M4 | 52.80 | 1.06 | 0.30 | 0.51 |
| | | Fe ²⁺ Fe ³⁺ ₂ O ₄ | 33.50 | - | - | - |
| 6 | 1477 CI | M1 + M2 | 0.00 | - | - | - |
| | | M3 | 25.40 | 2.00 | 0.89 | 0.36 |
| | | M4 | 41.10 | 1.30 | 0.32 | 0.36 |
| | | Fe ²⁺ Fe ³⁺ ₂ O ₄ | 45.80 | - | - | - |
| 7 | 1487 MB | M1 + M2 | 0.00 | - | - | - |
| | | M3 | 20.00 | 2.27 | 0.98 | 0.41 |
| | | M4 | 34.20 | 1.48 | 0.33 | 0.41 |

| | | Fe ²⁺ Fe ³⁺ ₂ O ₄ | 24.70 | - | - | - |
|---|---------|---|-------|------|------|------|
| 8 | 1562 MB | M1 + M2 | 0.00 | - | - | - |
| | | M3 | 21.31 | 2.09 | 0.90 | 0.35 |
| | | M4 | 53.99 | 1.33 | 0.37 | 0.30 |

(1) - quadrupole splitting; (2) - isomer shift; (3) - width of the over-all lines.

Investigations of the thermal behavior of ludwigite were undertaken recording the XRD pattern as heating in air progressed up to 1000°C. The main reflections of this mineral may be clearly recognized in the powder patterns recorded at 200, 400, 600 and 800°C. The broadening of peaks occurs at 1000°C, proving an incipient fusion and the amorphization of the mineral. Marincea (1998) listed the complete set of diffraction lines. The assertion of Kissling (1967) concerning the breakdown of ludwigite into kotoite, magnetite and hematite at temperatures lower than 1000°C may be consequently considered with caution.

As expected, the most significant absorption bands in the mid-wavenumber region of the infrared absorption spectra (600 to 1350 cm⁻¹) may be assigned to vibrations belonging to the (BO₃) group. These absorption bands (cm⁻¹) are assigned as follows: (1) 1300-1335 cm⁻¹ and 1260-1268 cm⁻¹: asymmetric stretching; (2) 920-940 cm⁻¹: symmetric stretching; (3) 704-708 cm⁻¹: out-of-plane bending; (4) 622-630: inplane bending. The latter should in principle be doubly degenerated, but the band at 560-570 cm⁻¹ could not be unequivocally assigned because the theoretical superposition of the Fe³⁺-O stretching. The splitting of internal vibrational modes of BO₃ group on the infrared spectra is consistent with its C_{3v} or C_{s} point symmetry, which is characteristic for magnesian ludwigite, in opposition with vonsenite, in which BO₃ has a clear D_{3h} (planar) symmetry.

The compositional data combined with experimental synthesis of borates, accounts for crystallization at temperatures of $600 - 650^{\circ}$ C and oxygen fugacities of $10^{-18} - 10^{-14}$ atm.

References

Aleksandrov, S.M., 1982. Geochemistry of boron and tin in magnesian skarn deposits. Nauka Ed., Moscow, pp. 1-272 (in Russian).

Aleksandrov, S.M., 2007. Endogenous transformation of kotoite in calciphires at magnesian-skarn deposits of boron. *Geochem. Internat.*, **45**, 666-684.

Bleahu, M., Bordea, S., Bordea, J., Istrate, G., Tomescu, C. & Piliuţă, A.M., 1985. Geological map of Romania, 1:50,000, Pietroasa sheet. Explanatory note. Geological Institute of Romania, Bucharest.

Ciobanu, C.L., Cook, N.J., Stein, H., 2002. Regional setting and geochronology of the Late Cretaceous Banatitic Magmatic and Metallogenetic Belt. *Mineralium Deposita*, **37**, 541-567.

Ilinca, G., 2010. Classic skarn localities of Romania: Contact metamorphism and mineralization related to Late Cretaceous magmatism. *Acta Min.-Petr.*, 23, pp. 1-50.

Ionescu, J., Popescu, M. & Întorsureanu, I., 1971. Prezența ludwigitului în skarnele de la Băișoara - Munții Apuseni. *St. Cerc. Geol. Geofiz. Geogr., ser. Geol.*, **16**, 503-509.

Kissling, A., 1967. Studii mineralogice si petrografice în zona de exoskarn de la Ocna de Fier (Banat). Academiei Ed., Bucharest.

Lemne, M., Vâjdea, E., Borcoş, M., Tănăsescu, A., Romanescu, E., 1983. Des datations K-Ar concernant surtout les magmatites subséquentes Alpines des Monts Apuseni. *An. Inst. Geol. Geofiz.*, **61**, 1-12.

Marincea, Ş., 1998. Cristallochimie et propriétés physiques des borates magnésiens des skarns de la province banatitique de Roumanie. Unpubl. Ph. D. thesis, Ecole Nationale Supérieure des Mines de Saint-Etienne, Saint-Etienne, France, 458 pp.

Marincea, Ş., 1999. Ludwigite from the type locality, Ocna de Fier, Romania: new data and review. *Canadian Mineralogist*, **37**, **6**, 1343-1362.

Marincea, Ş., 2000. The influence of Al on the physical and crystallographic properties of ludwigite in three Romanian occurrences. *European Journal of Mineralogy*, **12**, **4**, 809-823.

Marincea, Ş., Cristea, C., 1995. Ludwigite, szaibelyite and pyroaurite at Cacova Ierii (Gilău Mountains): New occurrences in the Banatitic Province in Romania. *Rom. J. Mineral.*, **76/2**, 67-84.

Nicolescu, Ş., 1998. Skarn genesis at Ocna de Fier-Dognecea, South-West Romania. Unpubl. Ph. D. thesis, University of Göteborg, Sweden, 112 pp.

Pavelescu, L., Pop, G.O., Weisz, E., Popescu, G., 1985. La nature et l'âge du batholite banatitique de Bihor. Rep. of the

- XII-th Congress of K.B.G.A. Cracow, 98-101.
- Rafalet, A., 1963. Nota asupra rocilor din aureola de contact a masivelor granodioritice de la Pietroasa si Budureasa. *Asoc.Geol. Carp.-Balc., V-ième Congr., Miner.-Petr.*, **II**, 199-204.
- Stoicovici, E. & Stoici, S.D., 1969. Contribuţiuni la cunoaşterea mineralizaţiei de bor din bazinul superior al Crişului Negru (Băiţa Bihor). *Studia Univ. Babes-Bolyai, Geol.-Geogr.*, **2**, 11-24.
- Tschermak, G., 1874. Ludwigit, ein neues Mineral aus dem Banate. Jb. d. K. K. Geol. R. A., XXIV, 59-66.
- von Cotta, B. (1864): Erzlagerstätten im Banat und in Serbien. W. Braumüller Ed., Vienna, 105 pp.
- Zimmermann, A., Stein, H., Hannah, J., Koželj, D., Bogdanov, K., Berza, T., 2008. Tectonic configuration of the Apuseni-Banat-Timok-Srednogorie belt, Balkans-Southern Carpathians, constrained by high precision Re-Os molybdenite ages. *Mineralium Deposita*, **43**, 1-21.

ELABORATION OF ROMANIAN BLACK SEA GEOLOGICAL AND GEOPHYSICAL MAPS: STATE OF THE ART

Mihaela C. MELINTE-DOBRINESCU, Nicolae PANIN, Gheorghe OAIE, Dan SECRIERU, Gabriel ION, Dan VASILIU, Radu-George DIMITRIU

National Institute of Marine Geology and Geoecology – GeoEcoMar, 23-25 Dimitrie Onciul St, 024053 Bucharest, Romania, e-mail: melinte@geoecomar.ro

Mapping the seafloor remains one of the great challenges in marine geoscience. Generating diverse maps, such as geological and geophysical, may completely change our understanding on various oceanographic issues. During last decades, significant advances in data acquisition, processing, analysis and dissemination have been realized. The mapping is an important tool in the assessment of marine resources and provide the base-maps and support for marine planning activities.



Fig. 1. Research vessel Mare Nigrum of the National Institute of Marine Geology and Geo-ecology used for acquiring data during mapping activities.

Concerning the mapping of the Black Sea, although some progress has been done by the riparian countries, there are still significant gaps in the knowledge and due to the new technologies quite a lot of areas are re-mapped. In Romania, the first detailed geological mapping of the Black Sea has been initiated in 1971, on the continental shelf, by the team of the new established Marine Geology Laboratory belonging to the Romanian Institute of Marine Research, created and headed by Nicolae Panin. Later, in 1975, the entire laboratory was moved to the Institute of Geology and Geophysics. In 1978, besides geological mapping, systematic bathymetric investigation started, and since 1980 magnetometric and gravimetric mapping was added. From 1987, the mapping of the Black Sea continental shelf activities was integrated in the general activity of the aforementioned institute. In 1993, the Marine Geology Laboratory separated from the Institute of Geology and Geophysics and became the Romanian Center for Marine Geology and Geoecology, and later, in 1996, the National Institute of Research and Development for Marine Geology and Geo-ecology (GeoEcoMar). Since then, one of the main activities of GeoEcoMar is producing thematic maps, regarding geological, geophysical, geochemical and biological aspects of the Romanian part of Black Sea.

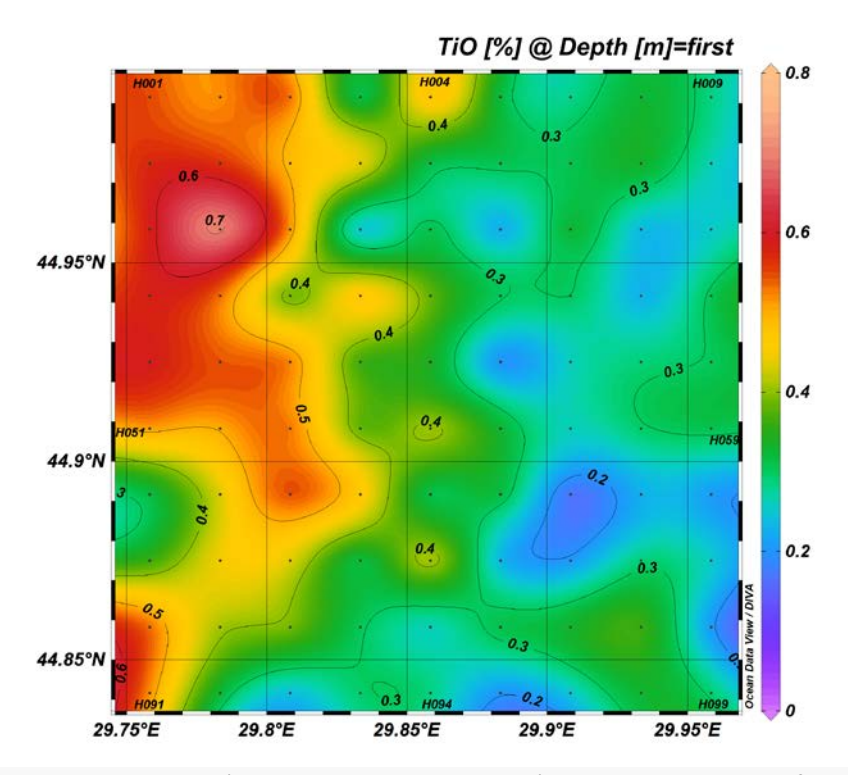


Fig. 2. Geochemistry (team lead by Dr. Dan Vasiliu) – spatial distribution of TiO. Map L-35-120-B, scale 1:50,000 (N Romanian Black Sea region).

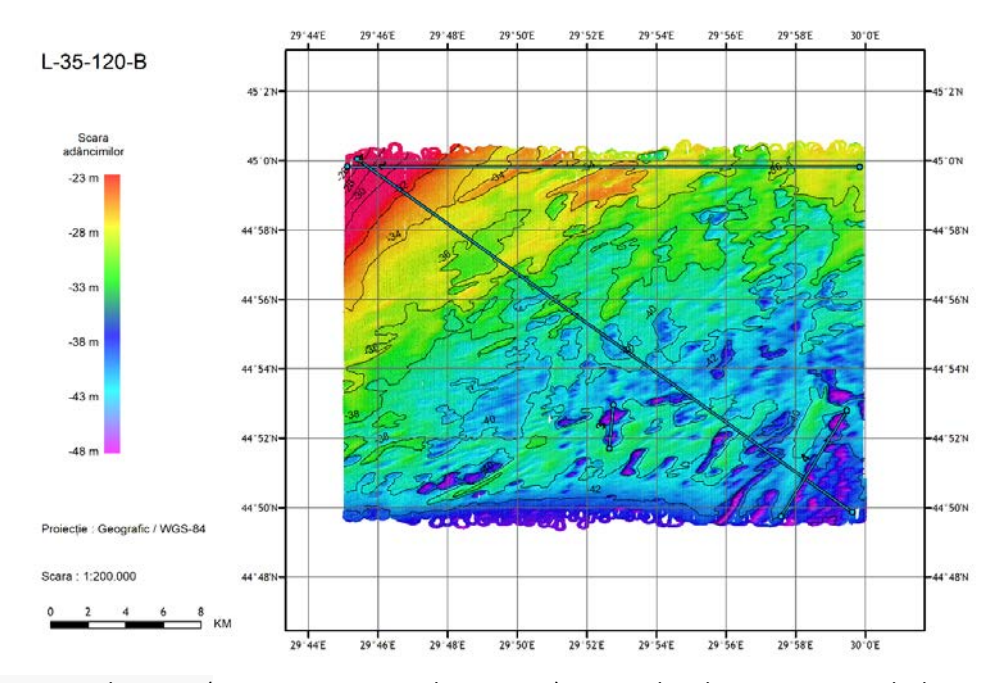


Fig. 3. 3D Bathymetry (Map L-35-120-B, scale 1:50,000), situated in the N Romanian Black Sea region (team led by Dr. Gabriel Ion).

In 2005, after a very long and difficult struggle for funding the Romanian research in the Black Sea region, an ocean trawler became R/V *Mare Nigrum* (Fig. 1). This is the first and the only one Romanian oceanographic research vessel. Continuously improved and outfitted with navigational and scientific equipment, *Mare Nigrum* is one of the main research infrastructures of GeoEcoMar. Over the years, along with mapping projects, the impact of the global changes on the geo-environmental conditions were analysed, along with the study of the past and present-day biodiversity.

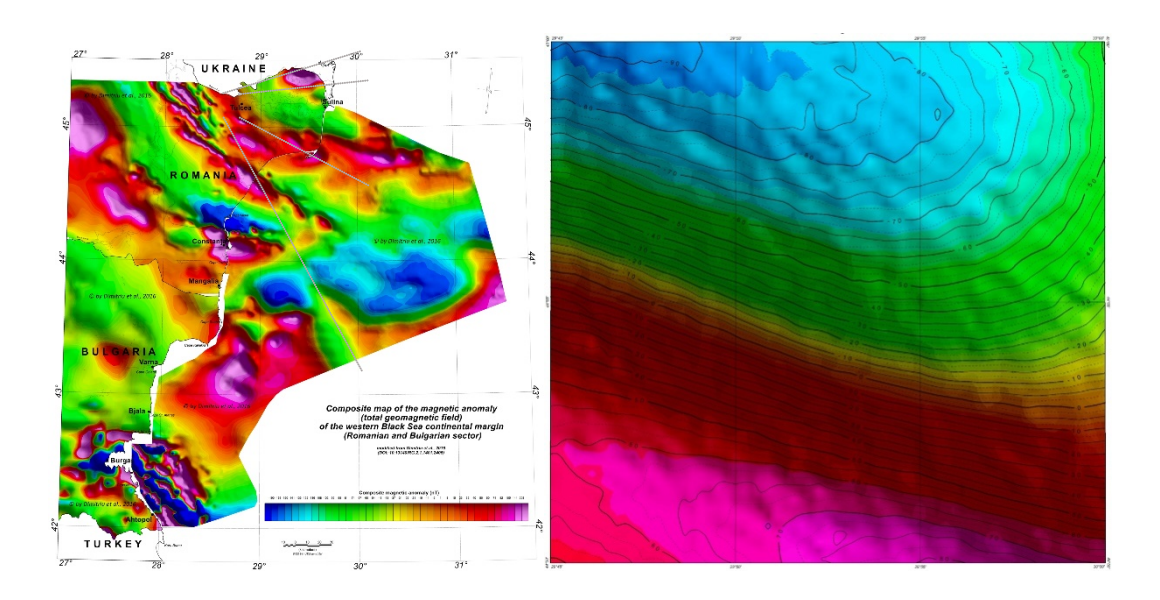


Fig. 4. Left: The composite map of the regional magnetic anomaly of the western Black Sea continental margin; Right: map of the geomagnetic total field (Team led by Dr. Radu-George Dimitriu), corresponding to the Map L-35-120-B, scale 1:50,000, situated in the N Romanian Black Sea region.

The mapping activity on the Romanian Black Sea is focussed on geological and biological sampling (with gravity corers, Van Veen grabs and dredges) and acquisition of seafloor images (by using a ROV). Various analysis, such as sedimentological, mineralogical, geochemical (Fig. 2) and biological (including macro- and microfaunas, along with nannofloras), necessary to compile the thematic maps, are currently performed in GeoEcoMar laboratories. The documentation of very detailed sea bed geology morphology and structure are also based on multibeam, sidescan and sub-bottom profiling data (Fig. 3). Additionally, magnetometric and gravimetric investigations are currently performed (Fig. 4). Therefore, multidisciplinary researches, aiming to achieve the mapping of the Romanian Black Sea region are performed in the National Institute of Marine Geology and Geo-ecology for the last 25 years.

GEOHERITAGE OF THE ANTI-ATLAS (MOROCCO): A NATURAL TREASURE IN SUPPORT OF SUSTAINABLE DEVELOPMENT

Viorica MILU¹, Moha IKENNE², Antoneta SEGHEDI³, Mustapha SOUHASSOU⁴, Nourissaid IÇAME², Mihaela Carmen MELINTE-DOBRINESCU³, Alexandru ANDRĂŞANU⁵, Iuliana LAZĂR⁵

¹Geological Institute of Romania, 1 Caransebeş Street, RO-012271, Bucharest, Romania, e-mail: viorica milu@yahoo.com

²LAGAGE, Faculty of Sciences, Ibn Zohr University, BP. 8106, Cité Dakhla - Agadir, Morocco, e-mail: m.ikenne@uiz.ac.ma, n.icame@uiz.ac.ma

³National Institute of Marine Geology and Geoecology – GeoEcoMar, 23-25 Dimitrie Onciul Street, RO-024053, Bucharest, Romania; e-mail: seghedi@geoecomar.ro, melinte@geoecomar.ro

⁴EGERNE, Polydisciplinary Faculty of Taroudant, Ibn Zohr University, Agadir, Morocco, e-mail: m.souhassou@uiz.ac.ma

⁵Faculty of Geology and Geophysics, University of Bucharest, 1 Nicolae Bălcescu Bd., Bucharest, Romania; e-mail: mesajalex@yahoo.com, iuliana.lazar@g.unibuc.ro

This study is based on an international collaborative project involving four project partners: one from Morocco (Ibn Zohr University) and three from Romania (Institute of Marine Geology and Geoecology – GeoEcoMar, Geological Institute of Romania, and University of Bucarest) (Ikenne et al., 2017-2020).

Morocco is a country with a remarkable geological heritage and outstanding geodiversity. Geology of Morocco consists in rocks whose ages range from Precambrian (> 3 Ga) to Cenozoic. In the Anti-Atlas, the Paleoproterozoic basement is unconformably overlain by Neoproterozoic (Cryogenian and Ediacaran) rocks and then by rocks belonging to the Paleozoic series (Gasquet et al., 2008; Ikenne et al., 2017a). In Southwest Anti-Atlas domain, the quartzite and calcareous series of Taghdoute Group, considered as Cryogenian, was recently dated at ca. 1.7 Ga (Ikenne et al., 2017b).

Morocco is also known for the high number of deposits of mineral resources (e.g. Co-Ni; Ag; Au; Cu-Au; Cu-Pb-Zn-Au-Ag; barite; phosphate etc.), including world-class ore deposits. Located in the Central Anti-Atlas, the Bou Azzer mining district is famous for its important ore deposits (Co-Ni-As-Au-Ag), been one of the main producers of Co in the world (Ahmed et al., 2009). The district is also famous for the mineralogical diversity (more than 220 minerals identified), and as type locality for few minerals as in follow examples: irhtemite (Pierrot et al., 1972); bouazzerite (Brugger et al., 2007); maghrebite (Meisser et al., 2012). In the East Anti-Atlas, the Imiter sillver deposit is a world-class deposit, wide known both for its size and its exceptional mineralogy (e.g. plates of native silver weighing up to several kilograms) (Levresse et al., 2018). Imiter mine is type locality for the mineral imiterite (Guillou et al., 2008).

The aim of our project is:

- a) to highlight the geological heritage, geodiversity and mining richness of the Anti-Atlas region;
- b) to offer to non-specialists a set of data regarding geological phenomena and processes, specially by intermediary of relevant images of geological formations, rocks, minerals, fossils etc.;
- c) to be a step forward in achieving connectivity between natural heritage, cultural heritage, and sustainable development of the Anti-Atlas Region.

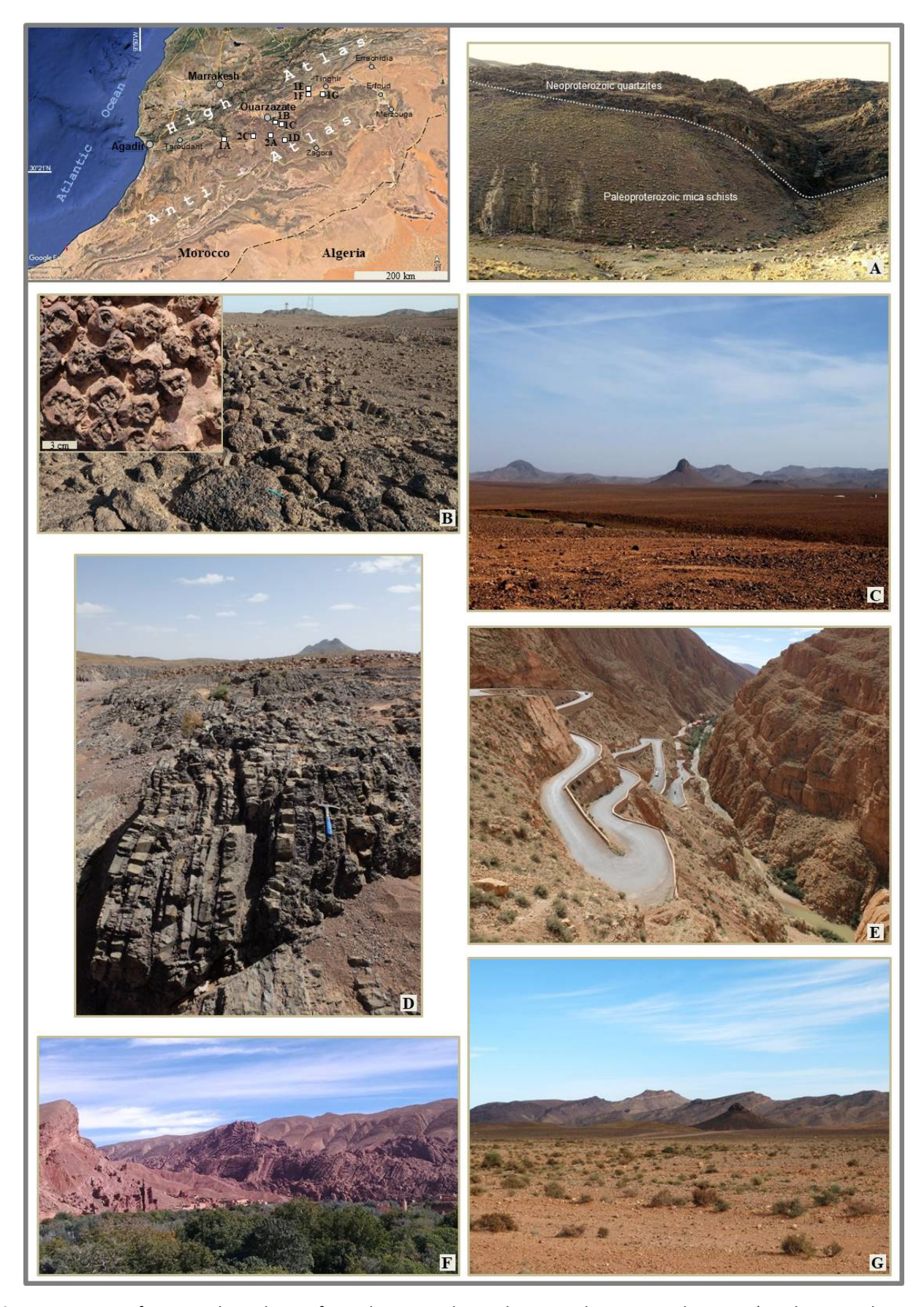


Fig. 1. Some significant geological sites from the Anti-Atlas and surrounding areas. The inset (Landsat Google Earth view) shows the location of the sites presented in images from figures 1 and 2. A) The first main Tizi N'Taghatine unconformity (dotted line) between the Paleoproterozoic (Eburnean) mica schists with pegmatite dykes (~ 2 Ga) and

the Neoproterozoic quartzites. Outcrop on the left side of the road Taroudant – Bou Azzer; **B)** Large outcrop of Late Ediacaran stromatolites on the left side of the road Ouarzazate – Zagora, at about 25 km from Ouarzazate. The formation containing stromatolites belongs to the Ouarzazate Supergroup. The inset shows a detail; **C)** Volcanic structures belonging to the Ouarzazate Supergroup (Late Proterozoic in age) occurring at about 30 km South-East of Ouarzazate. Northeastward view, from the road Ouarzazate – Zagora. **D)** Sedimentary rocks (turbidites) belonging to Tidilline series (Neoproterozoic). Outcrop in the area of the Tidilline village; **E)** Southwestward view of the Dadès Gorges carved out by the Dadès River in Lower Jurassic sedimentary rocks; **F)** Impressive geomorphological features in Dadès Valley (northeastward view, taken from Tamellalt village); **G)** Plio-Quaternary alkaline volcanism (dark brown neck-like structure), consisting in pyroxene nephelinites (Ibhi et al., 2002), outcropping in the area of Foum El Kouss. View from the road Boulmane Dades – Tinghir (at ~ 15 km up to Tinghir).

В D

Fig. 2. Examples of cultural heritage in the studied region. **A)** and **B)** Kasbah Aït Kabot – Village Museum in Tasla: A) Image showing the beauty of the ancient architecture; B) An image of a painted wooden door. **C)** and **D)** Authentic Moroccan carpets and rugs handmade by the women of the Anti-Atlas Region (Taznakht village). For the location of the sites, see figure 1.

The first field mission, conducted in 2018, took place mainly in Central and East Anti-Atlas: Provinces of Taroudant, Ouarzazate, Tinghir and Errachidia. Figures 1 and 2 show images taken from some of the sites / areas of interest for our field mission. Besides these sites, we also mention: the Lower Cambrian sedimentary formations (in Taliouine area); the Bou Azzer mine; the mafic magmatic dykes (recent dated at 1.6 - 1.7 Ga) and their host rocks, in Taghdout village; the Ksar of Ait-Ben-Haddou (in Ouarzazate Province), built on Cenozoic terraces, a UNESCO World Heritage Site (since 1987) etc.

The sites taken in consideration in our study are characterized by one or more of the following values: scientific, educational, and cultural. All the sites have touristic potential.

As one of the results of the project we mention a catalogue containing representative images of the visited sites and offering different levels of information to enable enjoyment by both specialists and non-specialists. The proposed catalogue can be interesting to general public and could contribute to spreading knowledge of natural and cultural heritage of the Anti-Atlas Region. It will contain images: a) of the sites of great scientific interest, b) showing the beauty of the landscape, and c) of the cultural heritage of the region. Examples of this rich natural and cultural heritage respectively are presented in figures 1 and 2.

The geoheritage of the Anti-Atlas could stimulate economic activity and sustainable development through geotourism. The geotouristic routes could include not only the sites from the Anti-Atlas but also the very important sites from the surrounding regions as the amazing landscapes in the Dadès Valley (as in Figs. 1E and 1F) and the Ksar of Ait-Ben-Haddou.

In Taznakht village, "la Coopérative de tissage de tapis", is an association of women of the Anti-Atlas region, worldwide-known for their handmade Moroccan carpets and rugs: a centuries-old tradition (Figs. 2C and 2D). Their association can be considered a model of the role that could play the associations in sustainable development at the local level.

In order to support the local sustainable development, it is important to find the ways to create connectivity between the geological heritage and cultural heritage (e.g. historical, archaeological, architectural, traditional crafts etc.). A better valorization of the natural and cultural heritage of the Anti-Atlas could be obtained by partnerships between the local and regional authorities, tourism stakeholders, scientists, volunteer groups, etc.

Acknowledgements. This work is the result of the joint effort of the affiliated institutions of the authors. Research has been financed by Ibn Zohr University (the above mentioned project – Ikenne et al., 2017–2020) with support from the Romanian Ministry of Research and Innovation (Core Program: Projects PN 18 65 05 01, 19 20 05 02 and PN 19 45 01 03).

References

- Ahmed, A.H., Arai, S., Ikenne, M., 2009. Mineralogy and paragenesis of the Co-Ni arseniade ores of Bou Azzer, Anti-Atlas, Morocco. *Economic Geology*, 104, 249–266.
- Brugger, J., Meisser, N., Krivovichev, S., Armbruster, T., Favreau, G., 2007. Mineralogy and crystal structure of bouazzerite from Bou Azzer, Anti-Atlas, Morocoo: Bi-As-Fe nanoclusters containing Fe3+ in trigonal prismatic coordination. *American Mineralogist*, 92, 1630–1639.
- Gasquet, D., Ennih, N., Liégeois, J.-P., Soulaimani, A., Michard, A., 2008. The Pan-African Belt. In: Michard, A., Saddiqi, O., Chalouan, Frizon de Lamotte, D. (Eds.), Continental Evolution: the Geology of Morocco. *Lecture Notes in Earth Sciences*, 116, 33–64.
- Guillou, J.J., Monthel, J., Picot P., Pillard, F., Protas, J., Samama, J.C., 1985. Imiterite, Ag₂HgS₂, a new mineral; properties and crystal structure (in French with English abs.). *Bulletin de Minéralogie*, 108, 457–464.
- Ibhi, A., Nachit, H., Abia, E.H., Hernandez, J., 2002. Intervention of carbonate components in petrogenesis of the pyroxene nephelinites from the Jbel Saghro (Anti-Atlas, Morocco) (in French with English abs.). *Bulletin de la Société Géologique de France*, 173, 37–43.
- Ikenne, M., Souhassou, M., Arai, S., Soulaimani, A., 2017a. A historical overview of Maroccan magmatic events along northwest edge of the African Craton. *Journal of African Earth Sciences*, 127, 3–15.
- Ikenne, M., Söderlund, U., Ernst, R., Pin, C., Youbi, N., El Aouli, E.H., Hafid, A., 2017b. A c. 1710 Ma mafic sill emplaced into a quartzite and calcareous series from Ighrem, Anti-Atlas Morocco: Evidence that the Taghdout passive margin sedimentary group is nearly 1 Ga older than previously thought. *Journal of African Earth Sciences*, 127, 62–76.

- Ikenne, M., Seghedi, A., Milu, V., Andrășanu, A., Souhassou, M., Içame, N., Melinte-Dobrinescu, M.C., Lazăr, I., 2017—2020. Le patrimoine géologique de l'Anti-Atlas: un trésor naturel au service du développement durable. Projet de coopération Maroc Roumanie.
- Levresse, G., Gasquet, D., Cheilletz, A., 2018. Imiter silver deposit, Anti-Atlas, Morocco (in French with English abs.). *Le Règne Minéral*, 139, 7–20.
- Meisser, N., Brugger, J., Krivovichev, S., Armbruster, T., Favreau, G., 2012. Description and crystal structure of maghrebite, MgAl2(AsO4)2·8H2O, from Aghbar, Anti-Atlas, Morocco: first arsenate in the laueite mineral group. *European Journal of Mineralogy*, 24, 717–726.
- Pierrot, R., Schubnel, H.J., 1972. Irthtemite, a new hydrated calcium magnesium arsenate (in French with English abs.). Bulletin de la Société Française de Minéralogie et de Cristallographie, 95, 365 370.

USEFULNESS OF ROMANIAN GNSS NETWORKS FOR GEOSCIENCE PURPOSES

Alexandra MUNTEAN¹, Eduard Ilie NĂSTASE^{1,2}, Victor MOCANU², Boudewijn AMBROSIUS³

¹National Institute for Earth Physics, PO BOX MG2, 077125, Măgurele, Romania e-mail: muntean@infp.ro

² University of Bucharest, Department of Geophysics, 6 Traian Vuia St, 020956 Bucharest, Romania ³ Delft University of Technology, Faculty Aerospace Engineering, the Netherlands

The first GPS geodetic satellite studies on the Romanian territory were made in 1994 under the auspices of the U.S. National Geodetic Survey (NGS) - and with the participation of the Romanian Ministry of Agriculture (MAA), former Institute of Geodesy, Cadastre, Photogrammetry and Cartography (ICGFC, formerly IGFCOT) and the Direction of Military Topography (DTM) continued in 1995 as part of an international European project, CERGOP (Central European Geodynamic Project) designed for geodynamic studies over Central and Eastern Europe (Schenewerk, 1993). In the following years, another international programme, namely CRC461 - "Strong Earthquakes: A Challenge for Geosciences and Civil Engineering" started; this program involved GPS data acquisition for the region under investigation, starting from 1997, when 28 GPS points were installed, covering an area of 350 x 350 km2 located in the eastern part of Romania, centered on the Romanian most important seismic area. This geodetic network has been measured over the period of time 1997 - 2004 by Dutch specialists from the University of Delft, as well as by specialists from the German Institute of Geodesy from Karlsruhe and specialists of the Romanian National Institute of C-D for Earth Physics (Ghițău et al., 2003). Since 2001 the GPS measurements in the Vrancea network were carried out within the framework of the research project SUBDUCT (Surface Behaviour and Dynamical Units of the Southern Carpathians Tectonics) initiated by the Dutch Centre for integrated research on Solid Earth Science (ISES) and the University of Delft (Netherlands) (Ambrosius et al., 2005). The goals of the project have been fulfilled in collaboration with the Romanian experts from the Faculty of Geology and Geophysics, University of Bucharest and the National Institute for Earth Physics. The main objective of the project was related to the monitoring, analysis, and interpretation of surface movements caused by the dynamics of the lithosphere crust - active in the region of Vrancea (South Eastern Carpathians) (Zoran et al., 2008).

The first Romanian permanent GNSS station was installed in 1999 at the Faculty of Geodesy, the Technical University of Civil Engineering of Bucharest. Since then, the number of stations grew, at present a number of more than one hundred GNSS permanent stations cover the entire Romanian territory. In the following we will make a brief presentation of the actual GNSS networks:

- The *ROMPOS* permanent network has 74 stations, is a commercial network with the goal of providing DGNSS/RTK correction services that are subsequently used for cadastral purposes, represents a project of the National Agency for Cadastre and Land Registration.
- The *GeoPontica* permanent GPS network is developed and maintained by The National Research and Development Institute for Marine Geology and Geoecology (GeoEcoMar). Geopontica (represented by 18 ground settlement stations, 13 in Romania and 5 in Bulgaria) provides data from the West side of the Black Sea geodetic networks concerning the vertical movements of the Earth's Crust (isostasy, elevation, land subsidence, basining etc.)
- The **TGRef TOPGEOCART** permanent GPS network appeared as a natural response to the growing demands of users of the Leica GNSS equipment. TGref is in full development and currently covers RTK 8 cities in central and eastern Romania and provides DGPS corrections for almost the entire territory of the country.
- The *National Institute for Earth Physics (NIEP)* operates a strong regional GPS/GNSS reference network for monitoring the Carpathian-Danubian-Pontic area deformations and the impact of local earthquakes.

The network development started in 2001 when the first permanent station was installed on the Lacauti peak in the mountainous zone of the Carpathian Bending Zone, west of the Vrancea epicentral area. The network was established as a result of an international research project based on a strategic partnership between: the National Institute for Earth Physics (NIEP), the Faculty of Geology and Geophysics – University of Bucharest (FGG), Delft University of Technology, the University of Utrecht and the Netherlands Research Center for Integrated Solid Earth Sciences (ISES). Starting with 2013, the GPS network is maintained and developed by NIEP. With a focus on Vrancea seismic area and the Carpathian Bending Zone (Romania), the network consists of 29 operational stations and another 1 to be installed in 2019. This will provide observations of the crustal motions in order to better understand the surface-to-depth interconnections for intermediate deep earthquakes, improved, reliable and high-accuracy environmental measurements for global weather forecasts, climate monitoring, earthquake precursors (ionospheric studies), coseismic studies, GNSS positioning and navigation, and other types of complementary research. Nowadays, advances in GNSS receivers technology and computational algorithms such as 20 Hz acquisition rate (and even more), that are commonly available, make us search worldwide for systems & algorithms that would make possible a real-time estimation of waveforms and coseismic displacements. Thus, we could support, improve and further analyse the results from the collocated velocity & accelerometers' seismic sensors, particularly atmospheric, magnetic, infrasound, tilt and/or seismic array sensors. So called VADASE (Variometric Approach for Displacements Analysis Stand-alone Engine) does not require either additional technological complexity or a centralized data analysis. Basically, it can be embedded into GPS receiver firmware, thereby providing a significant contribution to tsunami warning and other hazard assessment systems. With the help and support of Leica Geosystem and Topgeocart Company, 7 demo licences were installed on our Leica GR10 & 30 receivers and the system was fully operational in 2019. The approach is based on time single-differences of carrier phase observations collected at a high-rate (1 Hz or more) using a stand-alone receiver and on standard GPS broadcast products (orbits and clocks), which are ancillary information routinely available in real time. In this approach, we primarily estimated the time series of epoch-by-epoch displacements.

Presently, we collect GNSS data from all the above networks. Being networks developed for different purposes we found several limiting factors for data utilization: some of them had no site uniqueness, no file redundancy, no quality control or hardwire web service. Our goal is to collect all those GNSS data in order to standardize, perform quality control and harmonize for creating the metadata and use them for scientific purposes. The involvement in EPOS (European Plate Observing System) project where we are national GLASS (Geodetic Linkage Advanced Software System, an integrated software package to be deployed in a GNSS infrastructure) node, helped us achieve the proposed objectives. GLASS network consists of individual nodes representing a structure for disseminating GNSS data and products. The integration starts from national RIs over national nodes up to EPOS integration service. In the GLASS philosophy, the GNSS raw data (RINEX) are not physically located at the GNSS data gateway, but remain on the underlying data nodes. GLASS offers the means to make this data discoverable at the data portal. The work performed is very important because we managed to create a unique GNSS database from a homogeneous combination of all permanent networks and to create metadata in proper, international standard format, for all stations. We believe that it will be easier for future national and international projects to conduct research studies having all the stations, to promote interdisciplinary interoperability, with special focus on seismology and geology. With GNSS we can study deformation associated with earthquakes. These measurements are complementary to seismological data because they document the full earthquake cycle, including interseismic and transient postseismic processes, as well as coseismic deformations (Boehm et al., 2006).

Monitoring areas with continuous GNSS/GPS measurements to identify episodic changes in the surface motions will enable a better understanding of the dynamics and will allow improved predictions of the future surface motions and the associated hazards in these areas.

The GPS data of all sites were processed with the GIPSY-OASIS v.6.2 software, using the precise point positioning (PPP) strategy (Zumberge et al., 1997), generating position solutions from each individual observation file. This is a unique aspect of GIPSY (in contrast to other software), which makes it possible to analyze fragmented datasets like ours without a need for reference sites. GIPSY is a state-of-the-art analysis tool, which includes a comprehensive suite of models to correct all thinkable effects, ranging from wet and

dry atmospheric distortions of the measurements to ocean loading displacements of the sites. The models are accurate to the 1-mm level. We also used the Jet Propulsion Laboratory (JPL) orbits and clocks products, as well as the widelane ambiguity products, to invoke single-station ambiguity fixing (Bertiger et al., 2010). His results in so-called nonfiducial position solutions, which are in an arbitrary, internally consistent GPS orbit reference frame. These position solutions are then transformed into the latest International Terrestrial Reference Frame, currently ITRF2008 (Altamimi et al., 2011), using a global Helmert sevenparameter transformation also provided by JPL along with the orbits and clocks. Subsequently, the individual site position solutions are grouped into daily combination solutions. In the next steps, these daily solutions are converted to the fixed Eurasian reference frame by subtracting the motion of the Eurasian plate relative to ITRF2008, using the ITRF2008 rotation pole model for this plate. This yields time-series solutions of the position coordinates with respect to stable Eurasia. In the final step, the 3-D velocities are computed by means of linear regression of the position solutions of each individual site. We tested this method for several continuous GPS stations in stable Eurasia, and the resulting motions were found to be close to zero, proving the validity of the method. The results of our studies show that internally the Romanian territory appears to be quite stable, but the whole country tends to move slightly southward relative to Eurasia at velocity rates of about 2.5 - 3.0 mm/yr, especially the southern part. We speculate that this is a far-field effect of slab roll-back due to the subduction of the African plate under the Eurasian plate at the Aegean trench, way to the south. Until now, we did not observe any long-term signals due to the deep Vrancea earthquakes where the effects on surface motion are probably small.

Beside natural seismic activity, Romania can be affected, to some extent, by anthropic activities like mining or oil and gas exploitation. For particular areas, such activities can locally increase the hazard level. We focus on two such areas: Galati region and Petrosani mining area.

In September-December 2013, an unusual seismic swarm was recorded in the north-western part of the Galati city. More than 900 events with local magnitude ranging from 0.1 to 4.0 occurred along a NE-SW alignment in the vicinity of a long-term oil exploitation field. At the same time the region is known as an active tectonic area crossed by a complex system of active faults. On the basis of seismic and GPS measurements (Nastase et al., 2017) we estimate the effects of this activity and the implications on the environment.

The overexploiting mining areas are certainly inducing long-term effects on local topography, infrastructure and human activities. One of the important mining zones with intense past exploitation is located in the South Carpathians, Romania, close to Petrosani city. Once a very dynamic mining area for coal resources, Petrosani represents an area of top interest due to its long-term mining as well as due to a high number of galleries and even mines that were closed in the last several years. The analysis of GPS data from nineteen campaign sites spanning the period 2007–2012 show consistently significant horizontal and vertical surface motions (Muntean et al., 2016). The vertical velocities range from +39 (uplift) in the peripheral area to -263 (subsidence) mm/year in the central sector. The horizontal velocities range from 0 to 260 mm/year (mainly in WSW direction). The consistent WSW motion, in combination with the vertical motions, could induce a massive landslide. We conclude that significant surface deformations can be created locally by human activities that are able to induce serious hazards for particular regions of Romania.

Nowadays, advances in GNSS receivers technology and computational algorithms such as 1Hz acquisition rate (and even more, up to 50Hz), now commonly available; make us search worldwide for systems & algorithms that would make possible a real-time estimation of waveforms and coseismic displacements. Our study also highlights the results obtained in recent years by looking at the Romanian GNSS data over 3 different study cases from another perspective, aims to elaborate on a number of issues and provide some directions for future work that involves nontraditional seismological sensors such as GPS and tiltmeters following the implementation of the new generation of tools into GNSS permanent reference network data processing, in help for a more accurate assessment of the Vrancea earthquakes impact. GPS geodesy and seismology have traditionally been considered distinct tools focused on disparate frequency bands of the deformation spectrum. GPS Geodesy is focused on long-term secular tectonic deformation and static displacements from large earthquakes, while the latter measures dynamic displacements with periods ranging from fractions of seconds to several minutes. High-rate GPS positioning

has been recognized as a powerful tool in estimating epoch-wise station displacement which is particularly useful in seismology. The major advantages of using GPS receivers as seismometers are represented by the fact that they can measure large dynamic displacements without saturation. However, GPS is a few orders of magnitudes less sensitive than seismometers, considering that GPS can only detect movements at the noise level of a few millimeters or accelerations at the noise level of sub-centimeter per second squared (Larson et al., 2003). The goal of our research is to provide 1 Hz position horizontal, vertical and 3D reconstructed velocities in order to see if these can be compared to displacements derived from velocities/accelerations measured at nearly or collocated broadband seismic stations. The high-rate GPS data can capture the rapid co-seismic ground displacements over a range of frequencies and amplitudes that are comparable with those recorded by seismic sensors. High-rate, real-time GPS networks can enhance earthquake detection and seismic risk mitigation (Li et al., 2013).

Acknowledgements. This work was carried out within NUCLEU Program MULTIRISC, supported by MCI, project no PN19080201 and by a grant of the Romanian National Authority for Scientific Research, CNCS/CCCDI-UEFISCDI, project number PN-III-P1-1.2-PCCDI-2017-0266, Contract No. 16PCCDI/2018. We thank the National Research and Development Institute for Marine Geology and Geoecology, National Center for Monitoring and Alarm to Natural Marine Hazards – Euxinus, National Agency for Cadastre and Land Registration, TopGeocart company for providing access to their data.

References

- Schenewerk, MS., 1993. MGPS PAGE4 users manual. OES Internal Document, NOAA, Silver Spring, MD.
- Ghițău, D., Gavrilescu, M., Nacu, V., Dumitrașcu, D., Năstase, F., Mateciuc, D., 2003. National Progress Report of Romania for CERGOP, for the 2nd CERGOP-2/Environment Working Conference, Warsaw, Poland.
- Ambrosius, B.A.C., van der Hoeven, A.G.A., Mocanu, V., Munteanu, L., Spakman, W., Schmitt, G., 2005. Ten Years of GPS Observations in Romania, J. Balkan Geophys. Soc., 8, suppl. 1, 197 200.
- Zoran, M., Mateciuc, D., Neuner, J., Ciucu, C., 2008. Spatial techniques for investigating seismic areas (in Romanian), Conspress Publishing, Bucharest, Romania, 230 pp,
- Boehm, J., Niell, A., Tregoning, P., Schuh, H., 2006. Global Mapping Function (GMF): A new empirical mapping function based on numerical weather model data, Geophys. Res. Lett. 33, L07304.
- Zumberge, J., Heflin, M., Jefferson, D., Watkins, M., Webb, F., 1997. Precise point positioning for the efficient and robust analysis of GPS data from large networks, J Geophys Res, 102, B3, 5005–5017.
- Bertiger, W., Desai, S.D., Haines, B., Harvey, N., Moore, A.W., Owen, S., Weiss, J.P., 2010. Single receiver phase ambiguity resolution with GPS data, J Geodesy, 84, 5, 327–337.
- Altamimi, Z., Collilieux, X., Metivier, L., 2011. ITRF2008: an improved solution of the international terrestrial reference frame, J Geodesy, 85, 8, 457–473.
- Năstase, E.I., Muntean, A., Ionescu, C., Mocanu, V., Ambrosius, B.A.C., 2017. Quantitative and qualitative control for an integrated GNSS study over NW Galati seismogenic area. Conference paper:References: 17th International Multidisciplinary Scientific GeoConference SGEM 2017, SGEM2017 Conference Proceedings, ISBN 978-619-7408-00-3 / ISSN 1314-2704, 29 June 5 July, 2017, Vol. 17, Issue 14, 327-334 pp, DOI: 10.5593/sgem2017/14/S05.041
- Muntean A., Mocanu V., Ambrosius B., A GPS study of land subsidence in the Petrosani (Romania) coal mining area. Nat. Hazards, 80:797-810, 2016
- Larson, K. M., Bodin, P., Gomberg, J., 2003. Using 1-Hz GPS data to measure deformations caused by the Denali fault earthquake. Science, 300, 1421–1424.
- Li, X., Ge, M., Zhang, Y., Wang, R., Xu, P., Wickert, J., Schuh, H., 2013. New approach for earthquake/tsunami monitoring using dense GPS networks. Sci. Rep.

CONTRACTIONAL POLARITY CHANGES, INSIGHTS FROM ANALOG MODELING AND THE BLACK SEA CASE

Ioan MUNTEANU¹, Corneliu DINU²

¹Repsol Exploration, UK Exploration Team, Mendez Alvaro 44, 28045 Madrid, Spain, e-mail: ioan.munteanu@gmail.com ²University of Bucharest, Faculty of Geology and Geophysics, 6 Traian Vuia St, 020956 Bucharest, Romania

In collisional settings, convergence is accommodated by the formation of thin- and thick-skinned thrust and fold belts. The transmission of such deformation over larger distances into orogenic foreland areas is influenced by the inherited rheological characteristics of continental lithosphere. Lateral rheological variations parallel to the strike of continental foreland areas creates contrasting geometries and sequences of deformation that interact during orogenic build-up. A change in contractional polarity occurs when the direction of tectonic transport switches along strike. The parameters controlling and contractional polarity changes are less understood in situations when the strain is transferred at large distances from indenters (far field strain transfer and localization). Analyzing this type of strain transfer is critical for understanding the mechanics of thrusting in fore- or backarc settings of orogenic areas.

We investigate the far-field transmission and localization of strain within a continental lithosphere characterized by a laterally variable rheology through physical analogue modelling. Rheological heterogeneities (weak zones) where introduced at distance from an advancing backstop to study the progressive along strike linkage and interference of structures during contraction The models consist of two mechanically different crustal domains referred to as brittle-ductile (BDD) and brittle domains (BD), respectively, which are floored by the same ductile upper lithospheric mantle (DLM) (Fig 1). Different from the reference model type 1, all other models contain inherited crustal weak zones within the brittle-ductile domain, incorporated by introducing one or more ductile layers with variable thickness and geometries at the base of the brittle crust (Fig 1).

The Black Sea Basin is an example where the lateral change of thrusting direction was controlled by pre-existing extensional geometries (Fig 2., Munteanu et al., 2014). The roll-back associated with the N-ward subduction of Neotethys under the Rhodope-Pontides Arc has opened the Western Black Sea back-arc basin during Early Cretaceous time. The extension continued during latest Cretaceous - Early Eocene enlarging the western part and opening the eastern part of the Black Sea during Paleocene – Middle Eocene (Dinu et al., 2005). Shortly after the extension ceased, inversion of both sub-basins started during late Middle Eocene times due to continental collision recorded in the Pontides.

In the Western Black Sea, the far-field transmission of contractional deformation resulted in the inversion of pre-existing extensional structures and the formation of an N-vergent thick-skinned thrust system (Munteanu, 2011). This system was genetically associated during its late stages with the transpressional activity along the Noth Anatolian Fault starting in Late Miocene – Early Pliocene times. In the Eastern Black Sea, the S-ward thrusting of Crimea and Caucasus created an S-vergent thick-skinned thrust system (Nikishin et al., 2015). A large transfer zone including the Mid-Black Sea High accommodates the overall change in thrusting direction. This NW-SE oriented lineament is the prolongation of the Odessa-West Crimea fault system SE-wards that underwent significant dextral strike-slip movements during Late Eocene – Pliocene times. The total amount of shortening recorded across the entire Black Sea domain is in the order of ~30 km or higher (e.g., Munteanu et al, 2011). These observations document a Late Eocene – Pliocene contractional polarity change driven by the same process of collision.

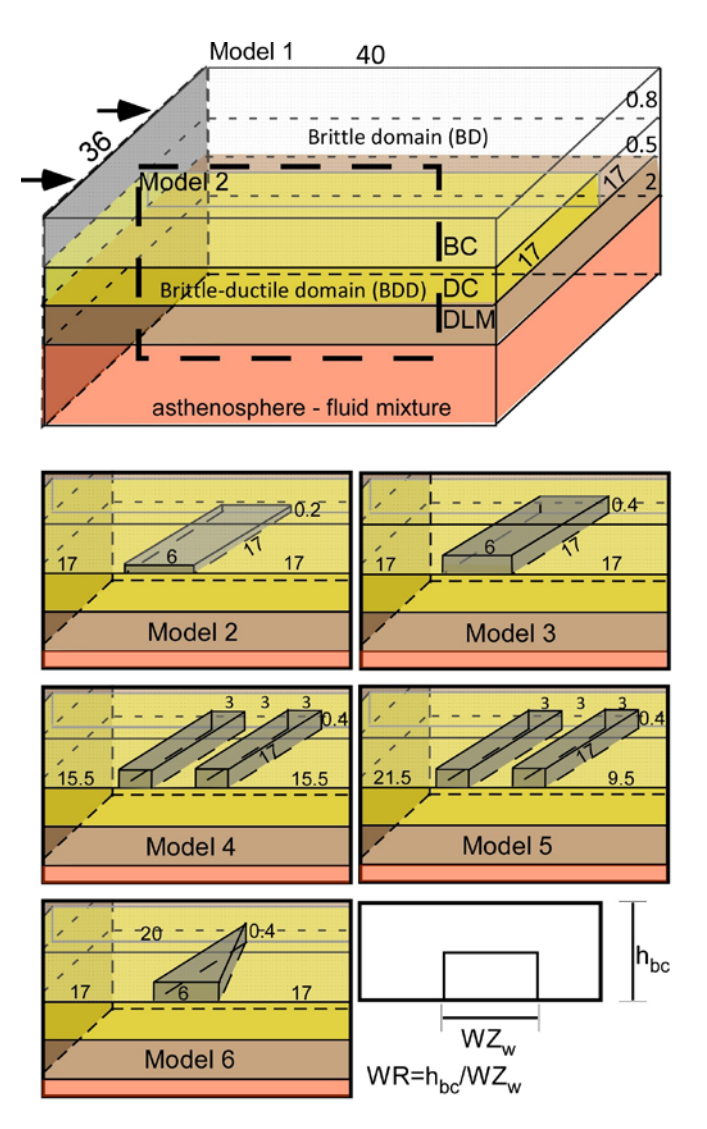


Fig. 1. Sketch illustrating the analogue modelling setup. The model simulates a continental lithosphere composed of two (brittle crust over ductile mantle in the brittle domain – BD) and three (brittle crust over ductile crust and ductile mantle lithosphere – BDD) layers. Note that Model 1 is uniform in the brittle and brittle-ductile domains, i.e. no weak zone. Models 2-6 have a variable geometry of the weak zone in the brittle-ductile domain. The sketch in the lower right corner illustrates the way we calculate the weaknesses ration (WR). The black arrows indicate the direction of contraction. BC – brittle crust; DC – ductile crust, DLM ductile lithospheric mantle, hbc – brittle crust thickness, WZw – weak zone width. The small numbers are illustrating the models and layers dimensions in cm.

Our modelling results reveal that rheological weak crustal zones localize far-field contractional deformation. When the size of weak zones is large, deformation localizes at the boundaries of the weak zone where they lead to the formation of large-offset faults. Subsequently the faults migrate along-strike into areas that are rheologically stronger. When this size is reduced, a large-scale contractional step-over forms in orogenic forelands, where rheological contrasting domains transmit out-of-sequence deformation by a gradual migration of thrust offsets and fold amplitudes along their strike. These results show that crustal scale orogenic step-overs do not always reflect variations in the geometry of plate boundaries or changes in shortening rates. Such features may form in response to variations in rheology, as the ones created by inherited extensional basins situated at large distances from plate boundaries in the orogenic foreland.

The transfer zone situated between the two oppositely acting indenters displays the largest amounts of transmitted deformation. The apparently anomalous shortening is in fact the cumulated shortening from the two indenters moving in opposite sides, even if they do not overlap along strike.

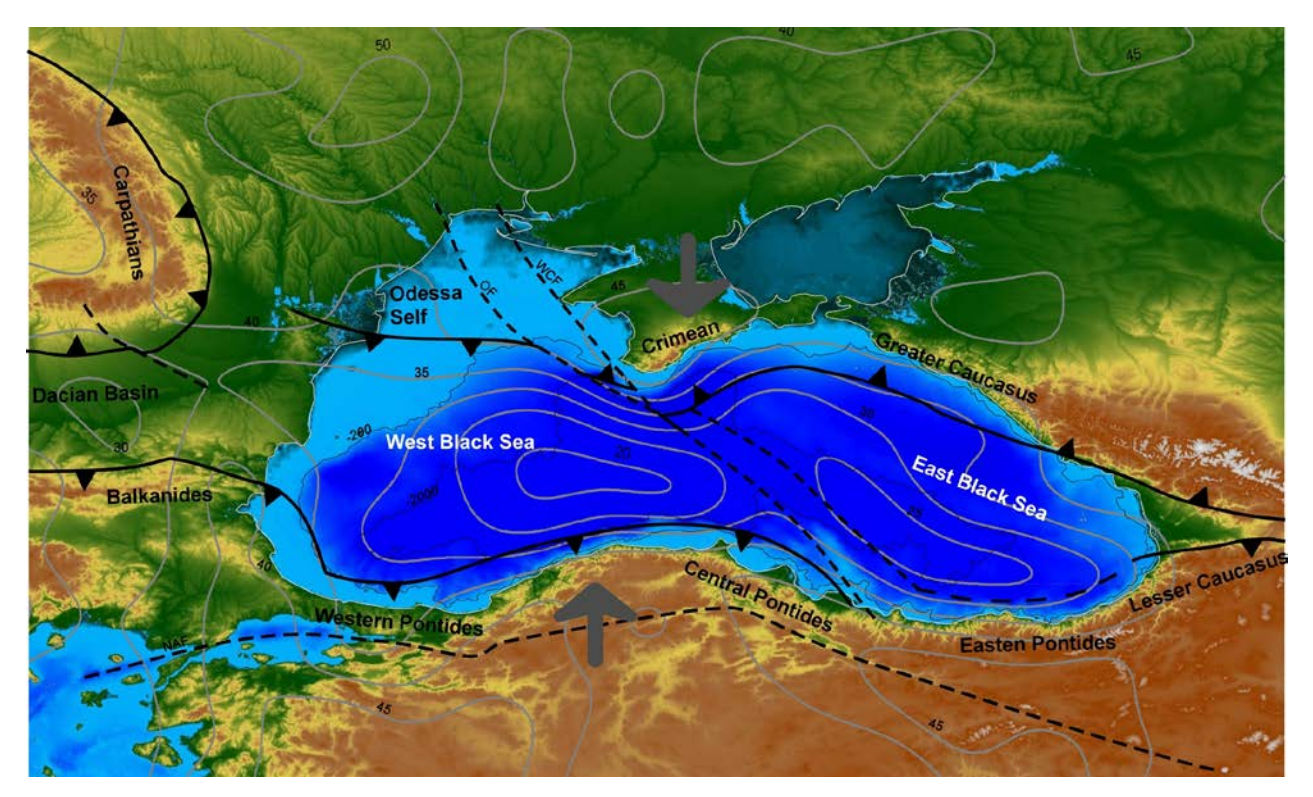


Fig. 2. Tectonic sketch of the Black Sea Basin and adjacent areas (redrawn after, Munteanu et al., 2011) illustrating across strike contractional polarity changes from N-Ward direction, on the Romanian-Odessa Shelf to a S-ward direction, Crimean Caucasus Orogen of the thrusting system. Grey lines represent the dept of crust (after Grad &Tirra, 2009). Grey thick directional arrow indicates the thrusting vergence. OF – Odessa Fault, WCF – West Crimean Fault.

The modelling results suggest that the Western Black Sea is controlled by the Pontides indenter creating a N-vergent thrust system, while the eastern Black Sea is controlled by the Crimean-Caucasus indenter creating a S-vergent thrust system.

References

Dinu, C., Wong, H.K., Tambrea, D., Matenco, L., 2005. Stratigraphic and structural characteristics of the Romanian Black Sea shelf. Tectonophysics 410, 417-435.

Grad, M., Tiira, T., 2009. The Moho depth map of the European Plate. Geophysical Jour. International 176, 279-292. Munteanu, I., Maţenco, L., Dinu, C., Cloetingh, S., 2011. Kinematics of back-arc inversion of the Western Black Sea Basin. Tectonics 30, 21.

Munteanu, I., Willingshofer, E., Maţenco, L., Sokoutis, D., Cloetingh, S., 2014. Far-field contractional polarity changes in models and nature. Earth and Planetary Science Letters 395, 101-115.

Nikishin, A.M., Okay, A., Tüysüz, O., Demirer, A., Wannier, M., Amelin, N., Petrov, E., 2015. The Black Sea basins structure and history: New model based on new deep penetration regional seismic data. Part 2: Tectonic history and paleogeography. Marine and Petroleum Geology 59, 656-670.

Tambrea, D., 2007. Subsidence analysis and thermo-tectonic evolution of Histria Depresion (Black Sea). Implications in hydrocarbon generation, Faculty of Geology and Geophysics. University of Bucharest, Bucharest, pp. 165.

GEOSCIENCES' SUPPORT FOR THE SUCCESS OF OIL & GAS BUSINESS

Pandele NECULAE

WPC CPC Romania Representative, NAMR expert, e-mail: neculae.pandele@petrom.com

This paper represents a Geoscience synthesis with a double focus: the first part has a strong didactic character, with obvious theoretical tendencies; the second part, more developed, more analytical and pragmatic, refers to the Oil & Gas Business approach up to now.

The structure and the modality of approaching the problems reflect, actually, the professional specialization with a consistent stage of working in the Oil & Gas Exploration and Production, focused on Good business, Efficiency, Sustainability, all in one – Success business.

Geosciences deliver detailed insight on the regional geology and petroleum systems prospective basins, providing the critical data for our Oil & Gas businesses as effective prediction of subsurface risk and geological uncertainty. The support of Geosciences consists in potential solutions for challenging current Exploration & Production projects, as the presence of the hydrocarbons in the trap before drilling the well in Exploration and the actual distribution of hydrocarbons inside proved in Production field for appropriate development approach.

The estimation of Resources and Reserves, as core business perspective, is founded on the Geosciences contribution as a major know-how factor related to the real potential of subsurface, the probabilistic estimation in range outcomes sustains in very good conditions the investment value too.

The top current branches of Geosciences developments are accessible as perspective and applications, specific for Oil & Gas industry practice, in connection with the top dedicated services of the company, focused on best result on safety conditions and on competition costs. The methodology of the integrated Risk approach for Oil & Gas business debate starts with negotiation, reserves auditing, subsurface & facilities, E&P and market, and it is connected to the Geosciences' contribution to de – risking, also adds value to the project.

A few success of business measures, using the checking and consolidated input data computing on dedicated for Oil & Gas economics software shows the opportunity to invest and the range of the potential profit. We note for debate the cost of \$ / Boe, profit \$ / Boe, time.

Considering the agreed performance indicators for all projects based on knowledge given by Geosciences, the portfolio is consolidated and ranked and represents the first overview for potential investments, being more valuable after optimization.

How does the phrase *Geosciences as support for a business success* works: anytime it gives us a Chance of Success for each individual project, and if it will be met, we are happy.

The integrated experts team of geoscientists focused on excellence, achieved all on leadership way with top knowledge and skills and appropriate technology do not meet anytime the CoS.

The secret of business success appears simplified as the profit to cover all and finally the economics to be not only positive, however it is necessary to be in line within the company's indicators.

APPLICATIONS OF MODERN BOREHOLE GEOPHYSICAL LOGGING METHODS TO SUBSURFACE CHARACTERIZATION

Bogdan Mihai NICULESCU, Aurelian NEGUŢ, Gina ANDREI

University of Bucharest, Faculty of Geology and Geophysics, Department of Geophysics, 6 Traian Vuia Street, Bucharest 020956, Romania, e-mail:bogdan.nicluescu@gg.unibuc.ro

Background

For oil and gas exploration wells, formation evaluation consists of the analysis and interpretation of borehole geophysical logging data and other types of subsurface information (e.g. well testing, formation testing, and coring) to ascertain if commercially producible hydrocarbons are present and to determine the best means for their recovery. The key properties of reservoir rocks derived through formation evaluation (lithology, porosity, clay content, water and hydrocarbon saturations, hydrocarbons type, permeability, positions of initial fluid contacts, petrophysical cut-offs) are used in further exploration, field development, and resource estimates.

Besides the conventional borehole geophysical methods, modern methods such as the *nuclear magnetic resonance* (NMR) and the *electrical imaging* can provide valuable additional information regarding the characteristics and details of reservoir rocks, as well as the geometry (dip angles and dip azimuths) of the formations intercepted by exploration wells. This enables a better reservoir characterization and reduces the need for costly core data.

The NMR tools use the magnetic moment of hydrogen nuclei in the reservoir fluids to determine directly the porosity and the pore size distribution. The method responds exclusively to protons and the signal amplitude is proportional to the quantity of hydrogen nuclei present in water and hydrocarbons, providing porosity values that are free from lithology effects; porosities are estimated from the rate of decay of the signal amplitude. In the NMR tool, a magnet is used to align the proton spin axis of the hydrogen from the reservoir fluids, then a radio transmitter is used to disturb the spin axis. A receiver records the electromagnetic signal emitted as the protons precess back to the original spin axis. The emitted signals are observed either as parallel (longitudinal) or perpendicular (transverse) to the direction of the applied magnetic field and are expressed as time constants related to the decay of magnetization of the system. The time constant T1 is called the *longitudinal relaxation time* and measures the time taken for polarization (alignment) of the protons in the reservoir fluids. Once the magnet is turned off, the protons lose energy and return to the lower energy state; the time taken to achieve equilibrium is called the *transverse relaxation time* T2. The rate of decay of the emitted signal is converted into a measure of the moveable fluids or free fluid index (FFI). Further processing can determine the volumes of irreducible and clay-bound water (Canon, 2015).

Wireline electrical imaging tools, such as the FMI – *Fullbore Formation Microimager* (Schlumberger) or the CMI – Compact Microimager (Weatherford), produce a high-resolution resistivity image which may cover the entire borehole circumference, due to a total of 192 or 176 button electrodes equally distributed over multiple pads. Measurements are made by causing a current to flow from each electrode button through the formations. As each button touches the formations, the current path is strongly affected by the resistivity variations at the point of contact. Raw data consist of multiple electrode readings, caliper readings from individual pads or pairs of pads, and x-, y-, and z-axis accelerometer and magnetometer readings. Borehole deviation and reference pad #1 (tool) orientation are determined from the magnetometers (Asquith, Krygowski, 2004).

The raw electrical imaging data are processed to create resistivity images, after applying corrections such as filling data gaps, speed correction using the z-axis accelerometer data, gain correction, dead/faulty buttons correction and depth alignment of the pads and buttons. The static and dynamic borehole images

are created from the corrected electrical data by assigning color maps to ranges of resistivity values. By convention, low-resistivity features, such as shales or fluid-filled fractures, are displayed as dark colors and high-resistivity features are displayed as light colors. The static image has a single resistivity/color map contrast setting applied for the entire well. The dynamic image has a variable resistivity/color map contrast applied in a moving window and it provides enhanced views of features such as bed boundaries, fractures, vugs, and sedimentary features. For visualization, the borehole images are split along true north then the cylinder is unrolled, becoming an oriented 2D view (left side – 0° and right side – 360° correspond to true north). Dipping planar features/surfaces that intersect the cylindrical borehole appear as sine waves in the 2D views, whereas the horizontal or vertical features/surfaces will remain horizontal or vertical (Asquith G., Krygowski, 2004; Rider, 2002). An automatic, semi-automatic or manual sine-curve fitting technique is used for obtaining the dip angle and dip azimuth values of the planar features identified on the images.

The primary applications of the electrical imaging tools are: structural interpretations (structural dip, faults and fractures characterization, in-situ tectonic stress orientation), sedimentological interpretations (facies analysis, depositional environments, bioturbation, paleocurrents), and petrophysical applications (thin-bed reservoir analysis, net sand definition, characterization of permeability heterogeneity, identification of flow baffles/barriers) essential to reservoir simulation studies.

Case studies / Examples

Figure 1 illustrates an example of raw data and petrophysical interpretation results for a suite of wireline logs recorded in a gas exploration well from Romania. The well intercepted a gas reservoir hosted in a four-way dip closure structure by Dacian (Early Pliocene) sands. The sands are immature, poorly consolidated (little or no authigenic or diagenetic cement), fine to very fine grained, muddy to silty, sometimes thinly bedded, and bioturbated. In the analyzed well a vertical variability of the reservoir intervals grain size was observed, allowing their separation into a "Sand" upper facies (good reservoir quality, fine sands) of 27 m thickness and a "Silt" bottom facies (poor reservoir quality, silty sands, silts and muddy silts) of 39 m thickness. This upward-sanding succession is interpreted as a progradational parasequence.

The data shown in Fig. 1 are: track 1 – measured depth; track 2 – true vertical depth subsea (TVDSS); track 3 – zonation of the investigated interval; track 4 – total gamma-ray, caliper, bit size and borehole's temperature; track 5 – computed water saturations in the uninvaded and flushed zones (S_w , S_{xo}); track 6 – bulk volumes of formation water, movable and residual (immobile) gas; track 7 – lithology analysis (volume fractions of clay, silt, sand and effective porosity); track 8 – nuclear magnetic resonance (NMR) measured T2 relaxation time; track 9 – processed NMR data showing the computed volumes of clay-bound water, capillary-bound water and free/movable fluids (formation water and gas); track 10 – pressure data measured by a wireline formation tester, computed pressure gradients and computed formation fluids densities. Two distinct gas-bearing reservoirs resulted from conventional logs interpretation in the "Sand" and "Silt" units. These reservoirs are located on the 1391.6–1425.5 m MD (1119.8–1143.6 m TVDSS) and, respectively, 1458.6–1466.7 m MD (1166.7–1172.3 m TVDSS) intervals.

The pressure gradients analysis in Fig. 1 indicates the presence of two fluids and corresponds to the gas and, respectively, formation water gradients. The densities of these fluids, computed from the pressure gradients, are $\delta_{f1} = 0.194$ g/cm³ (gas) and $\delta_{f2} = 0.849$ g/cm³ (water), higher and, respectively, lower than the true densities of gas and formation waters in the studied field (gas -0.08 g/cm³, water -1.01-1.04 g/cm³).

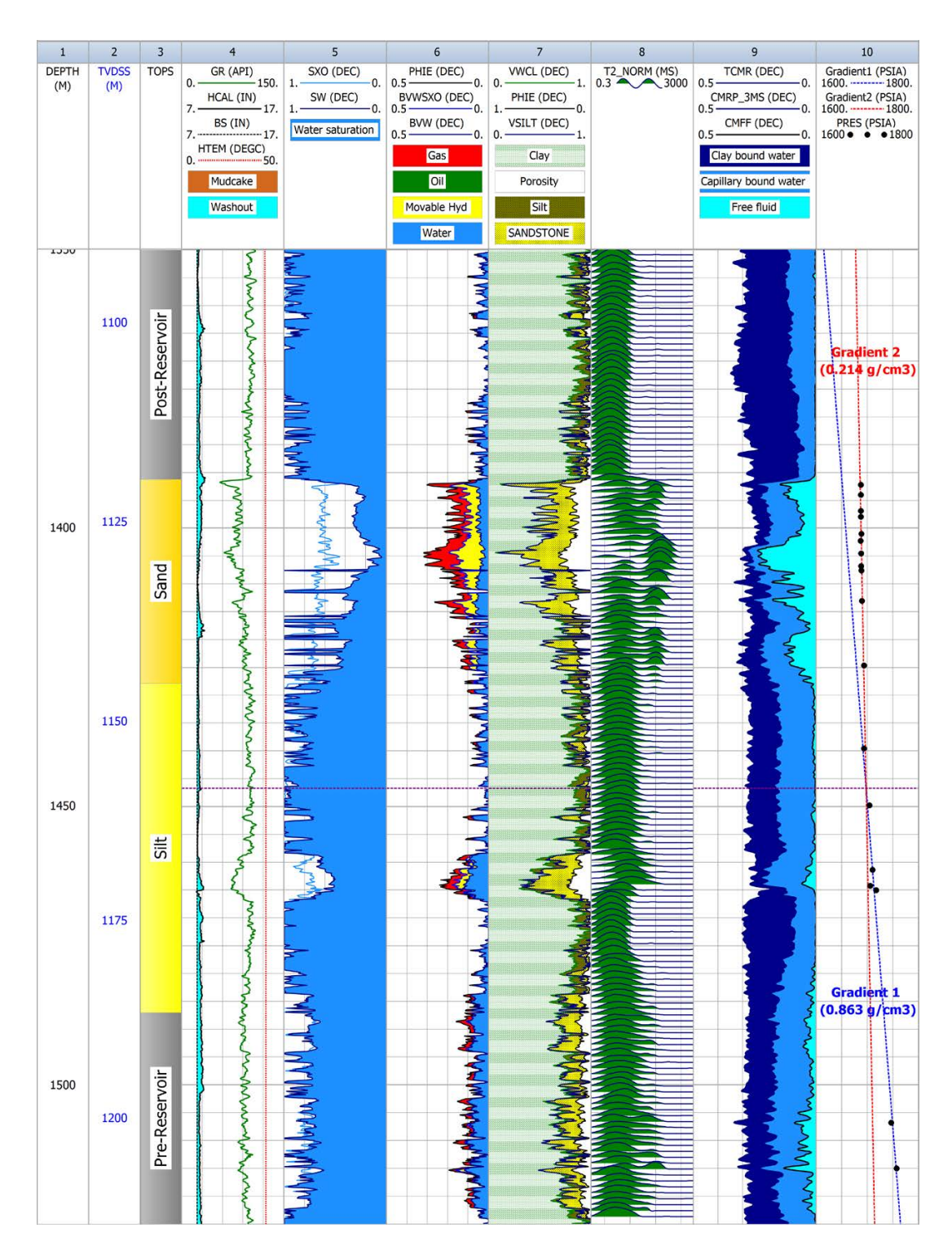


Fig. 1. Petrophysical interpretation of the wireline logs recorded in a gas exploration well from Romania. The GWC level marks the gas—water contact suggested by the intersection of measured pressure data gradients at 1448.4 m (1159.6 m TVDSS). This apparent GWC is located between two gas-bearing reservoirs resulted from log interpretation, at a depth where the processed NMR data show no indication of free fluids, but only bound (immobile) water.

A possible cause for the differences between true and estimated fluid densities may consist in the formation testers not reading pressures corresponding to pure fluids, but to gas + water or water + gas mixtures. In this case, the gas—water contact (GWC) depth inferred solely from the pressure gradients intersection may be inaccurate, leading to errors in the volumetric estimation of gas resources. This GWC uncertainty may also manifest itself in the form of pressure gradients intersection being located at a depth level with no free fluids indications on the results of NMR log, i.e. within an impermeable formation. The unique ability of NMR to distinctly show the intervals with clay-bound water (microporosity), capillary-

bound water (small pore size, related to silt fraction) and free fluids (effective porosity, larger pore size) provides an objective reference for checking the results of conventional log interpretation and can be used to correctly locate the fluid contacts in the reservoirs.

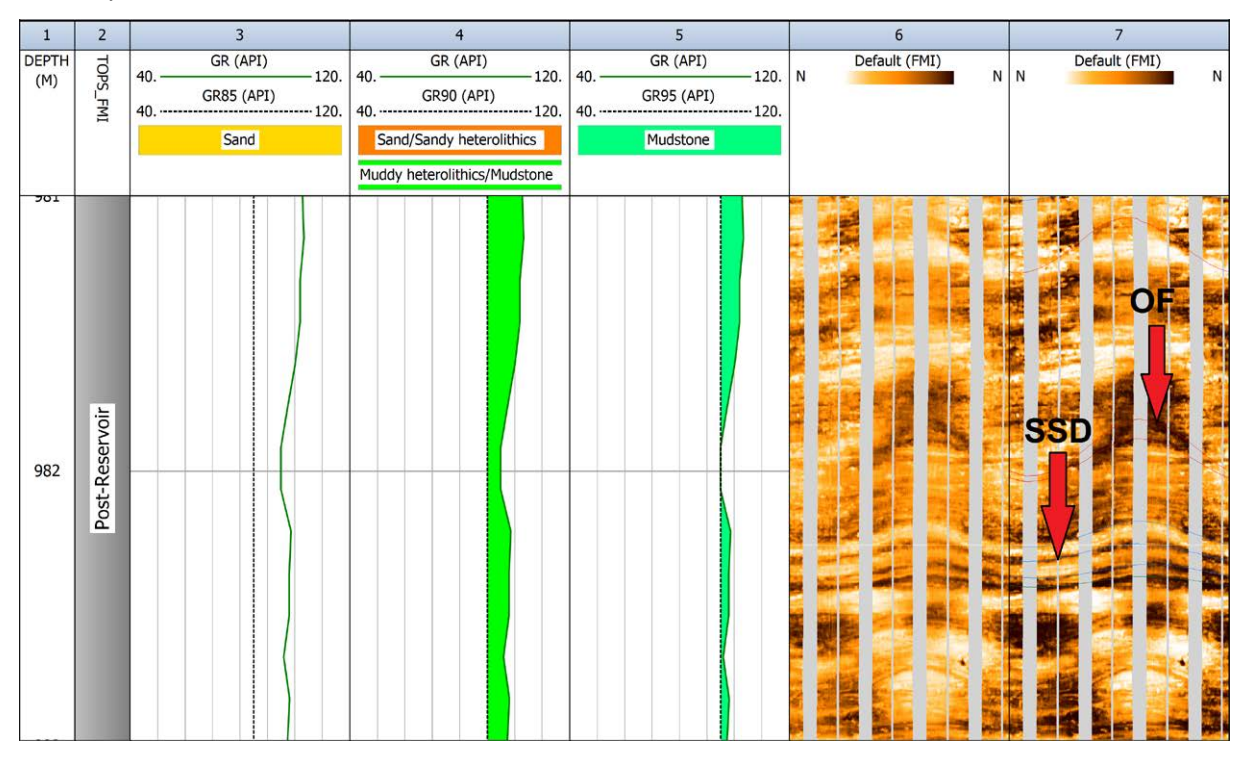


Fig. 2. Static (track 6) and dynamic (track 7) images constructed from borehole electrical imaging data (FMI) recorded in a gas exploration well from Romania: example of open/conductive fractures – OF and soft-sediment deformation – SSD over the 981–983 m depth interval.

Figure 2 illustrates an example of high-resolution borehole electrical imaging (FMI tool) recorded in a gas exploration well from Romania. The static resistivity image is presented in track 6 and the dynamic resistivity image is presented in track 7. The superior contrast of the dynamic image allows a better visualization of the geological features and the fitting of sine wave curves through the dipping planar features that intersect the borehole, in order to compute the dip parameters. On the 981–983 m depth interval (Dacian mudstones/shales) open/conductive fractures with 32° to 40° dip angles and 16° to 37° dip azimuths (ESE–WNW strike) can be identified, together with soft-sediment deformations.

References

Asquith, G., Krygowski, D., 2004. Basic Well Log Analysis, 2nd edition. The American Association of Petroleum Geologists (AAPG), Tulsa, Oklahoma, ISBN 0-89181-667-4.

Cannon, S., 2015. Petrophysics: A Practical Guide, 1st edition. Wiley-Blackwell, ISBN 978-1118746738.

Rider, M., 2002. The Geological Interpretation of Well Logs, 2nd edition. Rider–French Consulting Ltd., Sutherland, Scotland, ISBN 0-9541906-0-2.

COMBINED GEOLOGICAL AND GEOELECTRICAL METHODS IN THE STUDY OF CONVOLUTE FLYSCH NAPPE NEAR THE TECTONIC CONTACT WITH MACLA NAPPE (FIENI, DÂMBOVIȚA COUNTY)

Lidia-Maria NUŢU-DRAGOMIR¹, Florina CHITEA¹,2

¹Institute of Geodynamics "Sabba S. Ştefănescu" of Romanian Academy, Romania, Imnutzu@geodin.ro

²University of Bucharest, Faculty of Geology and Geophysics, Romania

Introduction

The considered region for this case study is positioned in the Carpathian orogen, at the tectonic contact between the Convolute Flysch nappe and the Macla nappe (both belonging to Moldavides system) geographically encountered in the area of Fieni City (Dâmboviţa County). Both nappes, exposed in the outcrops in the area under discussion, had been affected by two important Alpine tectonic phases (Săndulescu, 1984; Ștefănescu, 1995). The first phase (Laramian) generated the thrusting of the Convolute Flysch nappe over Macla nappe while the second phase started later (Styrian), when the Macla nappe and Convolute Flysch nappe, overthrusted the adjoining external nappe, namely Tarcău nappe.

In the confined area covering the trusting zone of the Convolute Flysch nappe and Macla nappe, several shallow depth electrical resistivity profiles (Fig. 1) were executed aiming to decipher the geological structure dawn to 50m deep.

This paper is focused on the sedimentological analyses and ERT data interpretation (made in accordance with sedimentological observations performed in several outcrops and on thin section petrographic analysis) from the Convolute Flysch nappe.

Methods

The sedimentological observations were conducted in 5 outcrop locations (Figure 1) situated in the Convolute Flysch nappe (O_1 , O_2 , O_a , O_b , O_c). Thin section petrographic analysis was performed on 10 new sandstones samples, collected from the outcrops (O_a , O_b and O_c) corresponding to the electrical tomography profiles (Figure 1, blue lines). The thin section were studied with the methodology described in Chitea and Nuţu-Dragomir (2019).

The apparent electrical resistivity data were acquired using Electrical Resistivity Tomography (ERT) technique, which implies the use of multielectrode systems. A large number of electrodes, which acts alternatively as injecting or potential electrodes during measurements, are placed along a straight line, at equal equidistance's. An electrical current is injected into the subsoil and the resulted potential between one (single-channel system) or more pairs (multi-channel systems) of two electrodes, that do not carry current, is determinate. Data processing, by means of inversion algorithms, and its interpretation is done on the basis of electrical DC (direct current). From the resulted resistivity models of the subsoil, geological lithotypes, their distribution and boundaries below the investigated area can be assessed. Inclined or vertical geological discontinuities (faults, dikes) can also be detected when data acquisition is properly projected and well executed.

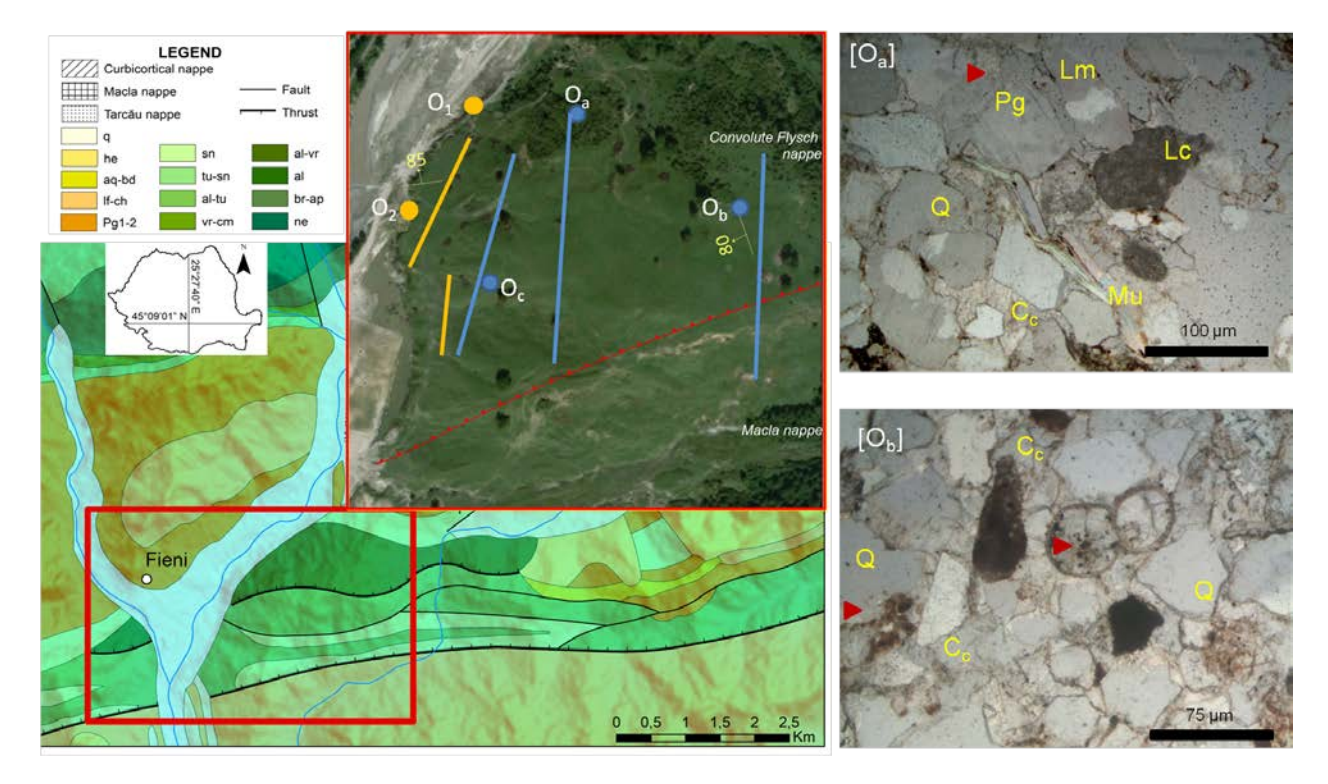


Fig. 1. Geological map within the Fieni area (Patrulius et al., 1968) and the location of the outcrops (dot) and ERT profiles (line) (orange – from Chitea and Nuţu-Dragomir, 2019; blue – this study). Photomicrographs of petrographic and diagenetic features of S_{II} -type sandstones from O_a and O_b outcrops.

Sedimentological observations

The sedimentary succession within the studied area belongs to so-called Convolute Flysch Formation (Săndulescu, 1984) of Albian-Vraconian age, and described as a turbiditic sequence made of sandstones, marls, shales and layers of conglomerates and breccia.

The sedimentary succession that can be seen in O_1 outcrop was described by Chitea and Nuţu-Dragomir (2019) as an approximately 10 m thick sequence of polimictic clast-supported conglomerates and breccias interbedded with thin layers of shales and sandstones. They are followed by alternating thick beds of grey shales, highly porous and moistured sandstones (S_1 -type) and well-cemented sandstones (S_1 -type) (Figure 2, b and c). The sedimentary succession continues for a few tens of meters in O_2 outcrop with only shales interbedded with marls.

Although, O_a and O_c are small-sized outcrops, highly porous and moistured sandstones (S_I -type) or cross lamination well-cemented sandstones (S_I -type) were recognized. On the other hand, in O_b thick layers of highly porous and moistured sandstones (S_I -type) interbedded with massive and cross-laminated well-cemented sandstones (S_I -type) could be observed.

Even if layers dip is similar, there is noticeable differences in layers measured strike between O_{1-2} and O_b outcrops, suggesting the presence of a fault, which could also be recognized in ERT profiles.

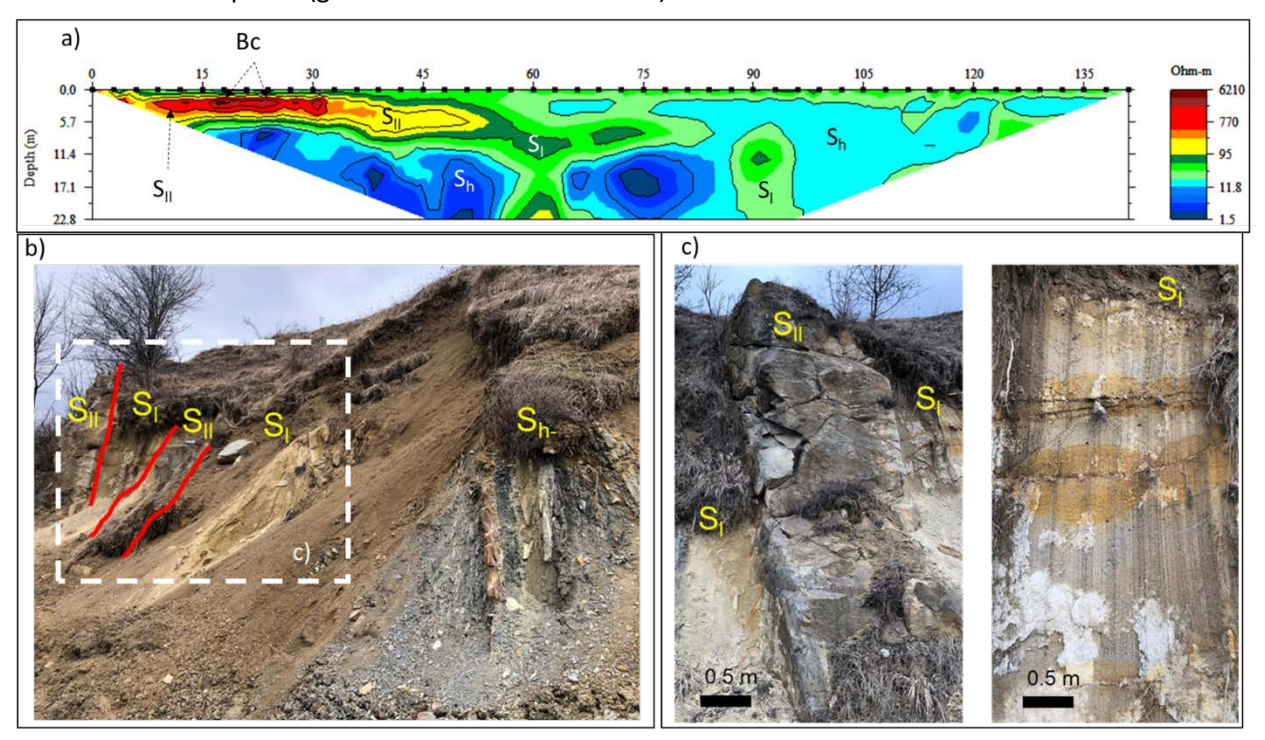
The well-cemented sandstones (S_{II} -type) range from fine- to coarse-grained, and their detrital composition corresponds to sublitharenites (Figure 1). Monocrystalline quartz dominate the detrital constituents. The feldspar content is split between plagioclase feldspar and K-feldspar. Lithic grains occur as sedimentary and metamorphic fragments. Detrital phyllosilicates grains are present with almost equal amount of muscovite and biotite. Few bioclasts (Figure 1) have been found. Mechanical compaction includes plastic deformation of the ductile grains (Figure 1, O_a). The main diagenetic minerals are calcite, hematite and pyrite cements. The diagenetic calcite Figure 1, O_a and O_b) occur as coarse crystalline, poikilotopic, pore-filling masses and partial grain replacement (e.g. detrital quartz, feldspars or lithic grains). Hematite appears as thin grain coating and pore-filling cement (Figure 1, O_a), and occasionally

partially replaces the muscovite and glauconite grains. Pyrite is present as framboidal aggregates. Secondary porosity (<5%) comprises mostly intragranular pores that occur as a result of cement dissolution.

The formation of the diagenetic constituents is related to the interaction between the detrital constituents of the sandstones with diagenetic fluids derived from marine and meteoric solutions. Both compaction and intense cementation were effective in the reduction of porosity of the analyzed sandstones.

ERT data interpretation

In the analyzed perimeter it was noticed a wide ranges of resistivity values (2-15000 Ω hm*m)) that were interpreted according to sedimentological observations and attributed to geological formations investigated down to 50 m depth. The resistivity values which overpassed 7000 Ω hm*m were resulted in areas with river deposits (gravels and limestone blocks).



Legend: S_I – porous sandstone; S_{II} – well-cemented sandstone; Sh – shale; Bc – breccia

Fig. 2. interpretation of the electrical resistivity tomography section (a) and observed lithological succession in the closest outcrop (b), with details on the two types of sandstones (c).

Due to the fact that mineral grains that forms most of the sedimentary rocks are electrically nonconductive, the resistivity of porous -clay free- rocks is governed primary by the rock porosity and permeability, water content and its chemical composition. Considering these, by means of geoelectrical measurement, it was thus possible to differentiate between the two types of sandstones noticed on the ERT profiles measured in Convolute Flysch nappe, close to the O_1 outcrop. An example of the ERT result and its correlation with observed lithotypes is given in Figure 2. The highest resistivity values observed on this ERT profile were associated with breccia (B_c) beds. The transition between well-cemented sandstone (S_{II} -type) and porous sandstone (S_{II} -type) is well illustrated, lower resistivity values being attributed to the S_{II} -type which acts as a groundwater flowpath. The lowermost resistivity values (<15 Ω hm*m) were correlated with shales (S_h). The resistivity values in this formation drops severely at greater depths (below 5 Ω hm*m) in the part of the profile where resistive top formations were detected, suggesting a higher moistened shales in this part than the rest of the profile.

Conclusions

The study of the Convolute Flysch nappe within Fieni area, revealed the fact that by combining sedimentological and ERT data, we can decipher the geological structure down to 50 m depth.

References

- Chitea, F., Nuţu-Dragomir, M.-L., 2019, Electrical resistivity tomography contribution to non-invasive landslide characterization in Dambovita county, Romania, Conference Proceedings SGEM 2019, 19, 1.1, 787-794.
- Patrulius, D., Gherasi, N., Ghenea, C., Ghenea, A., 1968. Geological map of Romania sc. 1:200.000, Târgovişte sheet (L-35-XXVI). Geological Institute, Bucharest.
- Săndulescu, M., 1984. Geotectonica României, Ed. Tehnică, Bucharest, pp. 450.
- Ştefănescu, M., 1995. Stratigraphy and structure of Cretaceous and Paleogene flysch deposits between Prahova and Ialomiţa Valleys, Romanian Journal of Tectonics and Regional Geology 76, 1, 4-49.

OF CROOKED LINE SEISMIC DATA RECORDED FOR HYDROCARBON EXPLORATION

Ionelia PANEA

University of Bucharest, Faculty of Geology and Geophysics, 6 Traian Vuia Street, Bucharest e-mail: ipanea2@yahoo.com

Abstract

Results are presented for seismic reflection measurements performed for hydrocarbon exploration along a crooked line, over an area with rough topography and complex subsurface geology. As an effect, the phase variations on the recorded data were significant. Hard-wired linear arrays were used in the field for data acquisition. Modeling results show that the hard-wired array responses are affected by the presence of irregular spacing between the array elements. A time seismic section was obtained after the processing of shot gathers using a standard flow from industry. The reflectors of interest were characterized by small amplitude, as an effect of the spreading of midpoints over an area with a width of about 900 meters. The time section obtained using a pseudo-3D geometry show improved reflectors in amplitude and continuity. Both time seismic sections were obtained using the same processing steps and parameters, excepting the geometry, in order to allow a fair comparison of the seismic sections.

Introduction

Seismic reflection measurements based on the active method (artificial sources generate the seismic energy) are used for hydrocarbon exploration. These measurements are designed to be performed along linear profiles in order to provide a regular sampling in space and depth of the recorded information. Measurements along crooked lines are performed in areas with rough topograohy or in the presence of various types of obstacles (natural or artificial) in the study area.

The quality of the seismic records is strongly dependent on the data acquisition parameters. Once the data are recorded, the effect of some artifacts of the acquisition cannot be attenuated or removed during data processing. Phase variations on the data are introduced by the irregular spacing between receivers (single sensors or intra-array elements), the rough topography and the lateral variation in velocity in the near surface. Amplitude variations are introduced by the imperfect geophone-soil coupling. These variations are responsible for the presence of spatially-aliased energy on the recorded data, a type of energy that can be partially atenuated during processing.

In this paper, I used modeling to analyse the effect of irregular spacing between array elements on the hard-wired array responses. For the data processing, I defined various types of geometries in order to find the one that improves the amplitude and continuity of the reflectors of interest.

Description of the seismic reflection dataset

The main goal of the seismic reflection survey was to obtain information about the geological structure until depths of about 3000 meters. The seismic measurements were performed along a crooked line with a NE-SW direction (Figure 1). The maximum variation in elevation along the acquisition line was about 300 meters. The recordings were performed using hard-wired linear arrays with 12 elements spaced at about 1.25 meters. The group interval was about 15 meters. Irregular spacing between array elements was obtained due to the rough topography and obstacles met along the line. The seismic energy was generated in 166 points spaced at about 45 meters. Explosive sources and vibratos were used to generate the seismic energy. Time sampling interval was 0.002 seconds. Record length was 5 seconds. The entire dataset contains 166 shot gathers saved in the SEG-Y format.

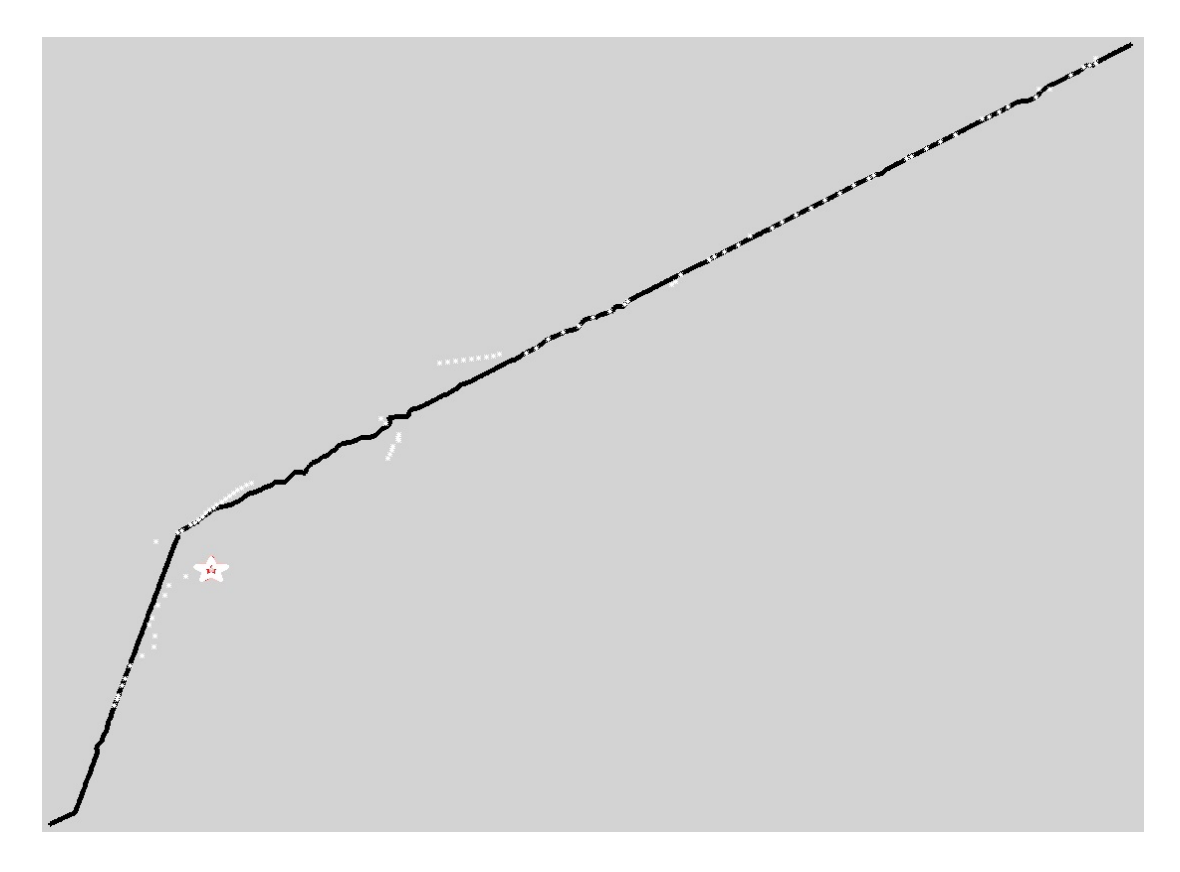


Fig. 1. Map showing the position of sources (white) and receivers (black).

Effect of irregular spacing on the hard-wired array responses

The measurements were performed using hard-wired receiver arrays; each array contained 12 elements spaced at about 1.25 meters. The phase variations introduced by the intra-array variation in elevation and by the irregular spacing between array elements affected the array responses, meaning that the shape of the wavelet was distorted and characterized by smaller amplitude. Seismic modeling was used in order to evaluate the size of the effect of irregular spacing between array elements on the seismic wavelet. A simplified velocity-depth model was built using information extracted from the field seismic data processing. The modeling was done using single sensors spread along the crooked line used in the field for data acquisition (Fig. 1). The modeling was done in the absence of the rough topography in order to analyze the effect of only one disturbing factor. The array responses were computed in two steps. First, groups of 12 traces, 1-12, 2-13, 3-14 etc, were summed into one trace. Then, the summing responses were spatially resampled to 15 meters. An example of synthetic array response is displayed in Figure 2. The distribution of the single sensors and the location of the seismic source used to obtain the displayed response are also shown in Fig. 1. The analysis of the synthetic array response in the time domain shows that the seismic wavelets are destroyed on the trace interval 50-150.

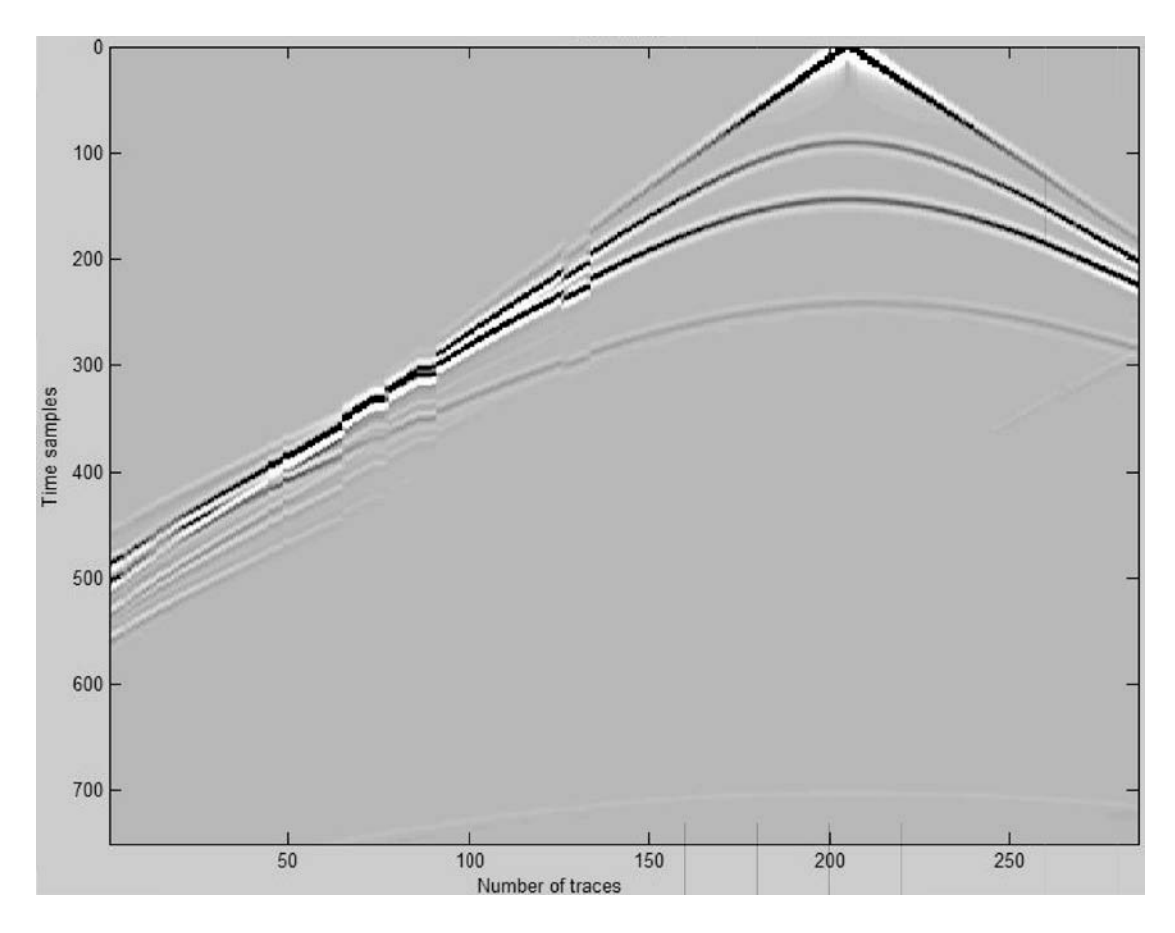


Fig. 2. Synthetic record obtained using receiver arrays with 12 elements; shot location - white star in Figure 1.

Effect of irregular spacing on the stacking of traces

The data processing was done following steps from the standard flow used in industry. The geometry was computed for a crooked profile using a bin size of 900 × 7.5 meters. The irregular spacing between receivers and sources is responsible for the spreading of midpoints outside the acquisition line. The refraction static corrections were computed for a final datum at +1000 meters and using a replacement velocity of 2700 m/s. All records were analyzed in the frequency-wavenumber (f-k) domain. For most of them, the (f, k)-amplitude spectrum displays spatially-aliased surface waves as an effect of the data acquisition parameters (Fig. 3). The frequency filtering was done using the f-k filtering, the predictive deconvolution followed by the band-pass filtering applied for 12-72 Hz. Trace editing was used before and after filtering in order to remove the undesired noise above first arrivals and to kill the noisy traces. Next, the traces from the filtered shot gathers were sorted into common-depth-point gathers, used later for interactive velocity analysis, normal moveout correction, stacking of traces and migration. The reflectors considered of interest seen on the time section displayed in Figure 4 are characterized by small amplitude. Various processing steps and parameters were tested in order to improve their amplitudes. Taking into account the large spreading of midpoints, over an area with a width of about 900 meters, I defined a pseudo-3D geometry with seven lines; the bin size was 127.5 × 7.5 meters. The static correcions were computed for a 3D survey. The rest of the processing steps and parameters were kept the same as those used in the crooked-line data processing. The reflectors of interest appear on the resulted time section with stronger in amplitude.

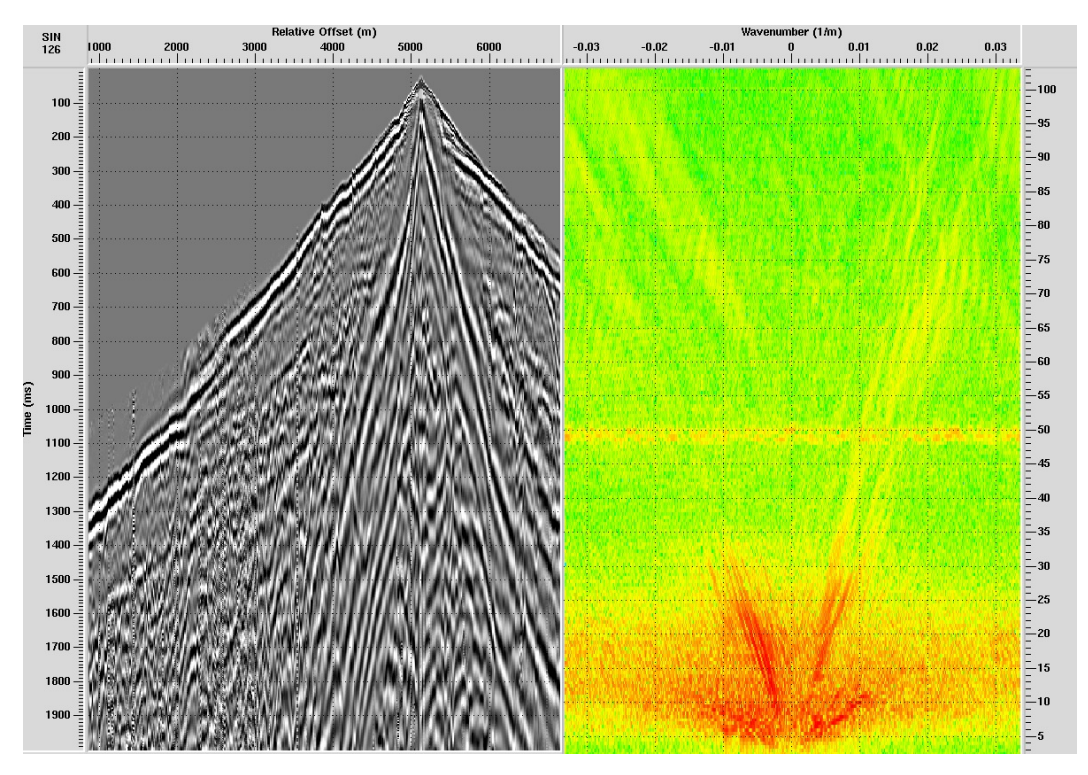


Fig. 3. Example of shot record displayed in (left) the time-distance domain and (right) the frequency-wave number domain.

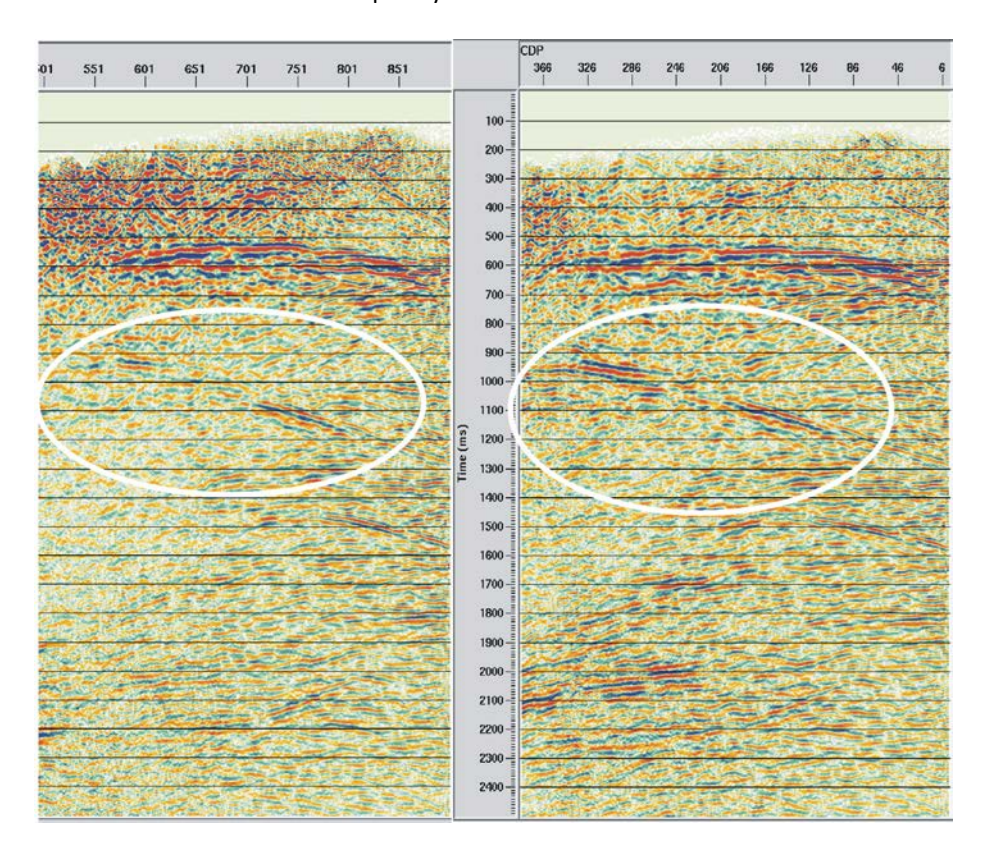


Fig. 4. Time section obtained using (left) crooked-line and (right) pseudo-3D geometries; white ellipse – reflectors of interest.

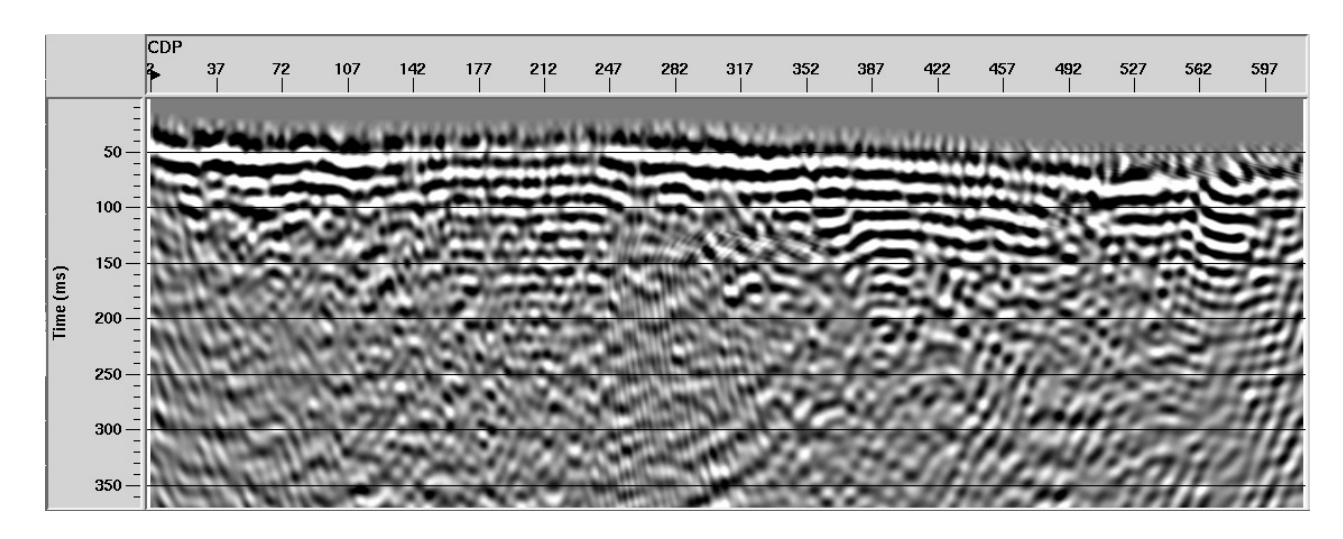


Fig. 5. Time section obtained after the shallow seismic data processing.

The remaining spatially-aliased surface waves after the frequency filtering are seen as dipping events at shallower times on the time section (Fig. 4). A series of small anticlines were interpreted by geologists based on these events. Information about the near-surface geological structure can be obtained using shallow seismic measurements along the seismic line from the survey for hydrocarbon exploration. The time section obtained after the shallow seismic data processing shows the lack of the small anticlines (Fig. 5). The processing of shallow and exploration data was performed using the same steps and parameters in order to allow a fair comparison of both seismic sections.

Conclusions

I analyzed a seismic dataset recorded for hydrocarbon exploration along a crooked line over an area with rough topography and complex subsurface geology. The seismic measurements were performed using irregular spacing between receivers, sources and between the hard-wired array elements. Modelling results showed that the use of irregular spacing between the hard-wired array elements affects the amplitude and shape of the seismic wavelet. The performing of data acquisition along crooked lines is responsible for the spreading of midpoints outside the processing line. After the analysis of the midpoint locations obtained using the field source and receiver coordinates, I defined various types of geometries, crooked and pseudo-3D, during data processing and I compared the time sections. Enhanced reflectors in amplitude and continuity were obtained using pseudo-3D geometries.

THE INVOLVEMENT OF THE ROMANIAN ACADEMY IN THE SUSTAINABLE DEVELOPMENT STRATEGY OF ROMANIA IN THE FOLLOWING 20 YEARS AND IN THE NATIONAL STRATEGY IN THE FIELD OF RESEARCH AND INNOVATION FOR THE ROMANIAN DANUBE REGION

Nicolae PANIN

National Institute of Marine Geology and Geoecology – GeoEcoMar, 23-25 D. Onciul St, 023054 Bucharest, e-mail:panin@geoecomar.ro

Romanian Academy, 125 Calea Victoriei, 010071 Bucharest

Taking into consideration the actual state of the economy of the country and the European and Worldwide current conjuncture, in 2015-2016 the Romanian Academy worked out the "The Sustainable Development Strategy of Romania in the following 20 years" and proposed it in 2017 for guidance to the Romania Presidency and Government.

The Strategy is a very complex and comprehensive document, tackling many scientific and socio-economic domains of the country's life.

The Strategy is structured in 13 chapters (projects) as follows:

- 1. School and Education in the Romanian Academy's conception;
- 2. Natural Resources Strategic Reserves, what and how we should use and what we should leave to the future generations;
 - 3. Energetic Security and Efficiency;
- 4. Informatics safety Protection of cybernetics, protection of the intellectual property within projects and electronic publication;
 - 5. Food security and safety;
 - 6. The economy and life quality;
 - 7. The Health from the molecular biology to the top personalized medicine in Romania;
 - 8. The European Project of the Danube/The National Strategy for the Romanian section of Danube;
- 9. The Romanian Culture among the national, proximal location, and Worldwide multilingual Europe, electronic culture;
 - 10. Romania knowledge based and added value society;
- 11. Romania in the Globalization Era space and tradition for civilizations encounter, in equilibrium and moderation.
 - 12. Public finances and Currency
 - 13. Stable, respected and sustainable public institutions stability of Romanian State

In 2011, the European Council and the European Parliament have adopted the EU Strategy for the Danube Region (EUSDR) and the related Action Plan. The EU Strategy for the Danube Region is a macroregional strategy that aims at the sustainable economic and social development of the EU member countries from the Danube Region, while ensuring greater protection of the environment quality.

The Romanian Academy developed and proposed for adoption to the Government and to the Romanian Presidency the National Strategy in the Field of Research and Innovation for the Romanian Danube Region. This Strategy can ensure better opportunities for Romania in building knowledge-based society through research, education and information technologies, in improving the quality of life, in protecting the environment and the biodiversity, in developing the international cooperation, culture, tourism and international direct contacts, etc. Similar to the EUSDR, the National Scientific Research and Innovation Strategy for the Romanian Danube Region is structured in four main Pillars composed of 11 Priority Areas.

BLUE QUARTZ IN ROMANIA – A PRELIMINARY MINERALOGICAL STUDY

Adrian-Iulian PANTIA, Andra-Elena FILIUȚĂ, Sarolta LŐRINCZ

Geological Institute of Romania, 1 Caransebes St., 012241 Bucharest e-mail: pantia.adrian@gmail.com

Introduction

Despite the fact that the worldwide occurrences of blue quartz have been studied since the end of the XIXth century, the body of literature on the subject is poor, both in extent and detail. Except for the color and, in some cases, mineral inclusions, these occurrences do not vary significantly from regular quartz. Depending on the coloring mechanism, blue quartzes can be classified into two categories: quartzes which owe their color to blue microscopic mineral inclusions and those who are blue because of the scattering of light by nanometer size solid or fluid inclusions. The microscopic blue mineral inclusions are usually magnesio-riebeckite, tourmaline and aerinite, and the most cited nano-inclusions are primarily rutile and ilmenite, but also magnetite, graphite, biotite, zircon or apatite. Some bibliographic sources suggest fluid inclusions as possible causes for the coloration. Blue quartz is mainly found in intermediate and acidic magmatic or volcanic rocks and in their metamorphic equivalents. The global distribution pattern of the occurrences coincides with the major orogenies of every continent and is concordant with the amphibolitic-granulitic metamorphic zones associated with continental collisions. The aforementioned metamorphic grades are common to many occurrences, regardless of age or host rock type. Particularly in the case of hydrothermal blue quartz, the association with Au and U mineralization is often mentioned.

In Romania, the occurrences of Albeşti, Argeş County and Pietrosul Bistriţei, Suceava County, have not been investigated in terms of causes of coloration and their geological significance, and this is true for the overwhelming majority of the global occurrences as well. In fact, the Romanian occurrences are nonexistent in the body of literature on the subject and this is arguably the first dedicated paper on the subject. In the case of the Albeşti blue quartz, the host rock is an Early Ordovician monzogranite, emplaced as stratigraphically concordant lenses within the crystalline formations of the Leaota Massif, South Carpathians. The violet-blue quartz of Pietrosul Bistriţei is part of a Cadomian porphyroid gneiss resulted from the metamorphism of acidic rocks with dacite – rhyodacite composition.

Materials and methods

The Albeşti granite was collected from the villages of Dragoslavele and Albeşti, Argeş County. The Pietrosul Bistriţei porphyroid gneiss was collected from the left bank of the Bistriţa River, Bistriţa Defile, Suceava County. For comparative studies blue quartz samples from Llano (Texas), Milbank (South Dakota) and Rio delle Ossa (Italy) were available, as well as Brazilian amethyst and grey and regular quartz, obtained by correspondence or personally. The samples were studied by optical means, X-Ray powder diffraction (XRD), infrared absorption spectroscopy (FT-IR), thermogravimetry (TGA/DTA) and scanning electron microscopy (SEM-Tabletop) at the Geological Institute of Romania. The microscopic investigations were performed on polished sections, thin sections and grains, both in transmitted and reflected light, dry or immersed. XRD, FT-IR and TGA/DTA investigation were carried out on grains or powdered grains, manually separated from the bulk of the samples by purity and degree of coloration. The FT-IR investigations were performed on pellets containing quartz powder, both heated to 800°C and not heated, and KBr. As a rule, the quartz powders and the KBr were kept in an oven at 60°C in order to limit water adsorption, KBr being especially hydrophilic. The polished sections used for SEM investigations were covered with Cr. In order to study the effects of temperature on the coloration, samples were heated to various temperatures in the 300-800°C range. To facilitate the assessment of the changes, opalescent grains with internal impurities

were chosen. The thermal behavior in terms of mass change was observed with the help of TGA/DTA for temperatures of up to 1000°C.

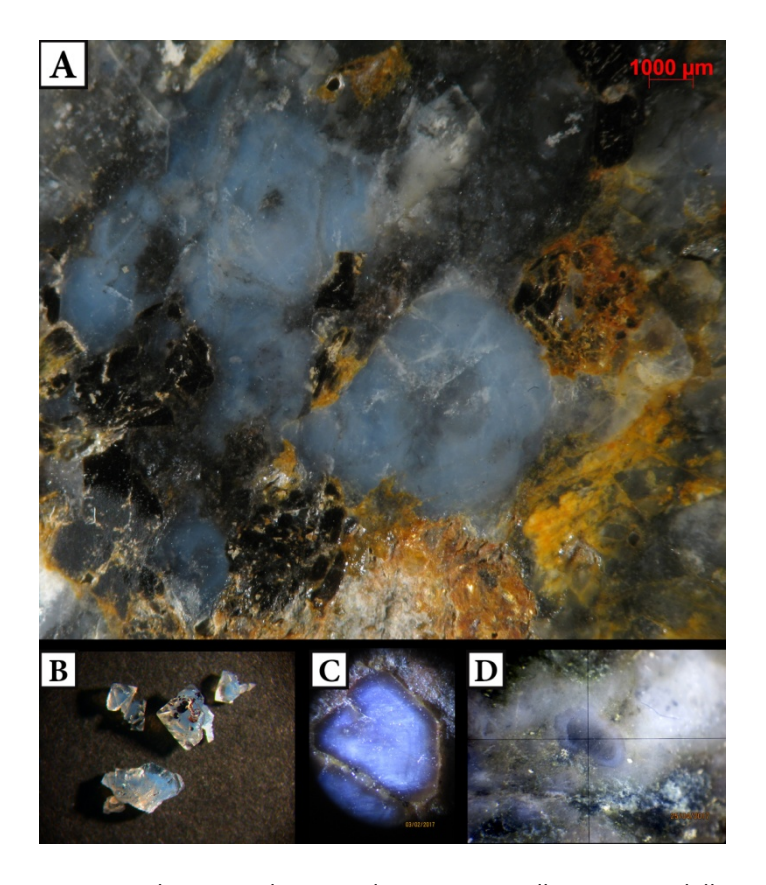


Fig. 1. Blue quartz grains showing a distinct color zoning; A, Albeşti, B, Rio delle Ossa, C, Llano, D, Pietrosul Bistriței.

Results and discussion

The microscopic investigations have shown that the blue quartz grains of Albeşti and Pietrosul Bistriței are blue only in reflected light and brownish-yellow in transmitted light, just like the other studied blue quartz occurrences. The quartzes of Albeşti (Fig. 1) and Pietrosul Bistriței are blue and violet blue, respectively, have an opalescent appearance, more pronounced in the case of the Albeşti granite, and show a circular color zoning, more frequently in the case of the Albeşti quartz and also present in the Llano and Rio delle Ossa occurrences. Therefore, in the case of the Romanian occurrences (and Rio delle Ossa as well), it is possible to separate blue, less blue and even colorless zones within the same grain. While in the Llano and Rio delle Ossa grains the colored zone is located towards the interior and its shape replicates the largely idiomorphic contour of the grains, the Albeşti and Pietrosul Bistriței quartzes show a circular band located, most of the times, towards the exterior, concordant with the apparent orientation of the grains. Unlike the quartz of Milbank or Llano, chatoyance is poor or absent (Albeşti).

Microscopic thin section observations have shown that the grains are single crystals presenting strain shadows, micrometer size secondary fluid inclusions and mineral inclusions, probably biotite, but the quartz grains show no color or zoning of any kind. The dimensions of the identified inclusions range between 1-4 μ m, too large to meet the requirements for light scattering (max 300 nm). No rutile needles were identified, except for the Milbank quartz.

Apart from the Llano quartz, heating the samples in an oven caused an apparent loss of color for all occurrences even at temperatures as low as 300°C. The opalescence described for these quartzes was lost and replaced by a milky appearance. The inclusions taken as reference points before heating were still visible after the fact, suggesting that the whitening of the grains is not caused by internal fractures resulted from thermal structural stress. Also, only the opalescent grains or areas of the grains suffered this

transformation, meaning that colorless grains retained their transparence, while the partially or intensely colored ones turned milky.

TGA/DTA performed on colorless, partially or weakly colored and intensely colored quartz grains, at temperatures ranging between 40-1000°C over a 16 h period did not indicate phase transitions except for α – β Quartz at 573°C. However, the samples vary from a gravimetric standpoint. Measurements performed on Albeşti quartz have shown that when heated, the colorless fraction lost 0.0446 wt%, the partially colored fraction lost 0.0705 wt%, and the intensely colored fraction 0.1351 wt%. The TG curves become steeper beyond 550°C, after which they resume their normal gradient. The mass lost as a result of the α – β Quartz transition accounts for 15.377%, 18.8727% and 40.5194% of the total loss, respectively, over an interval of 75°C, from approximately 550 to 625°C. Similarly, the gray quartz of the Culmea Cernei granite has shown a 0.1515 wt% total loss, with 20.8941% of the total loss between roughly 550 and 625°C.

X-Ray powder diffraction has not detected any inclusions in neither of the investigated samples. Also, there was no difference between unheated samples and the same samples heated to 800°C. The superposition of the diffractograms has shown that from an XRD point of view, all the investigated samples are the same. On the other hand, the powders investigated were identified as fully crystallized low-quartz, ruling out an amorphous or partially crystallized silica phase which would account for the observed opalescence.

For all samples, FT-IR only indicated absorption peaks characteristic for quartz, centered around 1163 cm⁻¹, 1080 cm⁻¹, 796 cm⁻¹, 777 cm⁻¹, 694 cm⁻¹ și 511 cm⁻¹. No differences have been observed between heated or unheated samples or opalescent and non-opalescent ones.

SEM-Tabletop investigations have shown the presence of inclusions loosely compatible with the composition of halite, ranging from 170 to 900 nm (Fig. 2), which have the potential to scatter light. The inclusions themselves have an ordered spatial arrangement, likely the result of healed sets of fractures, although a connection between these solid inclusions and fluid inclusions is yet to be established. Some needle shaped inclusions have also been observed, approximately 3.8 μ m in length and 200 nm wide, but their identity could not be determined.

The preferential scattering of short wavelengths and the transmission of long wavelengths is indicative of a coloration caused by the scattering of light in a colloidal environment and cannot be produced by microscopic or even submicron inclusions. The description of the coloring mechanism in the case of the Albeşti and Pietrosul Bistriţei blue quartz rests mainly on the identification of nanometer scale inclusions. The petrographic microscope investigations have shown the presence of micron size inclusions, too large to cause color by scattering. The same reasoning applies to the rutile needles observed in the Milbank quartz, which are responsible for chatoyance, but not for the blue color as well. The phases observed can only cause scattering if they have nanometer size equivalents, which are well beyond the possibilities of optical detection.

In the case of the Llano blue quartz, the color zoning is caused by the differences in the size and spatial density of the inclusions capable of light scattering. The causes are not fully understood in the case of the other occurrences, since no dedicated studies have been carried out. For the Romanian occurrences, the ordered character of the color zoning may be explained by a crystallographically controlled exsolution or the inclusion of nano-grains during the growth of the quartz crystals.

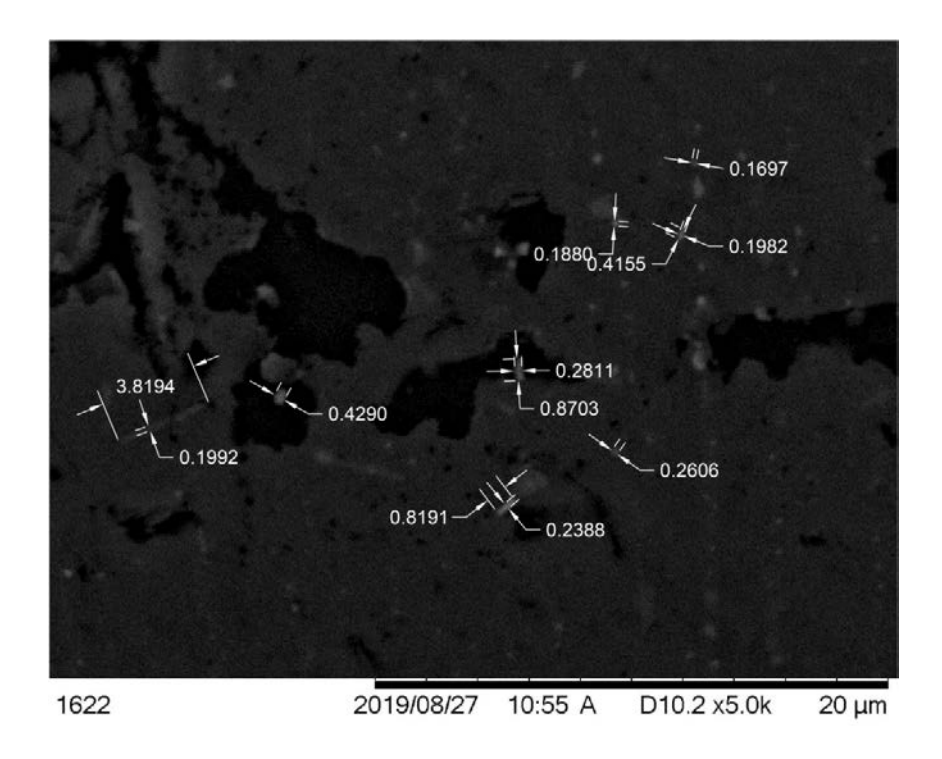


Fig. 2. SEM-Tabletop BSE image of a blue quartz grain from the Albeşti granite showing submicron and nanometer size inclusions.

The loss of the blue color during heating was initially attributed to some transformation suffered by the scattering agents or to the loss of a fluid phase as a result of heating. Since light scattering is mainly dependent on particle size, no phase change will substantially influence scattering unless it is accompanied by a significant increase in dimensions. Even if the coloration is produced by nanometer scale fluid inclusions, these will not decrepitate even at temperatures far exceeding the temperature of entrapment, and even if they do, they will not leave the grain, but rather relocate around the cavity, thus still being able to scatter light and even more so. The whitening caused by heating might be independent of the cause of coloration and it is likely that the blue color is only concealed. Samples which do not owe their color to light scattering, such as amethyst and the grey quartz of the Culmea Cernei granite also turned white as a result of heating. The mass loss accompanying the whitening points to a correlation between the opalescent appearance, a volatile phase and the apparent loss of color during heating.

The fact that XRD was not able to detect mineral inclusions is most likely due to instrument limitations, considering that the microscopic observations have shown rutile in the Milbank quartz and various papers report the presence of ilmenite at Llano. It is therefore possible that mineral inclusions, if they exist, represent less than 2-3 wt% of the samples investigated. The FT-IR results, or lack thereof, could also be attributed to instrument resolution capacity for the same reasons.

The nano-inclusions identified using SEM-Tabletop, while capable of scattering light are poorly described. The ordered pattern and halite-like chemistry hint at a connection with fluid inclusions. Future TEM/STEM investigations may shed new light on the nature and geometric distribution of the solid inclusions.

Conclusions

The results gathered point to a coloration produced through the scattering of light, which rules out microscopic or submicron inclusions as possible causes. XRD and FT-IR produced no results concerning the inclusions themselves, mostly because of the small quantity of inclusions expected. The small scale of the scattering inclusions is also prohibitive for direct optical observations. SEM-Tabletop has identified light scattering capable inclusions within the blue quartz grains of the Albeşti granite, ranging between 170-300

| Geosciences | in | the | 21st | century |
|-------------|----|-----|------|---------|
| Geosciences | ш | uie | 21 | century |

nm, but given the preliminary nature of the results provided by SEM-Tabletop, TEM investigations will be required in order to accurately describe them. Based on the spatial arrangement of the reported solid phases, a possible connection with fluid inclusions can be inferred.

The blue quartzes of Romania are α – Quartz single crystals and not some other variety of SiO₂, such as opal or chalcedony, as shown by XRD, which would explain the observed opalescence more easily. The heating of the samples causes a loss of opalescence, in the sense that the opalescent areas become milkywhite while apparently losing the color in the process. TGA/DTA investigations suggest that the apparent loss of color is accompanied by a loss of mass, but this transformation is likely independent of the coloring mechanism since it has also been observed in quartz grains that are not blue.

The geological significance of blue quartz is difficult to assess without a working understanding of the coloring mechanism. The challenge is not only to determine the causes for the coloration, but also to determine the physical and chemical conditions leading to it. The Romanian blue quartz occurrences, which can be correlated with both high grade metamorphism and U and Au mineralisations, have the potential to become excellent case studies for the poorly understood phenomena of light scattering in blue quartz.

EVALUATION OF THE UNCONVENTIONAL HYDROCARBON RESOURCES FROM ROMANIA

Constantin PENE

University of Bucharest, Faculty of Geology and Geophysics, 6 Traian Vuia St., 70139, Bucharest e-mail: constantin.pene@gg.unibuc.ro

Unconventional hydrocarbon resources typically include:

- (1) coal bed methane (CBM gas), which is methane in coal seams;
- (2) tight sands gas (hydrocarbon gas in tight ultralow-permeability formations);
- (3) shale gas (gas in very-low-permeability shales);
- (4) methane hydrates (methane trapped in crystal structure of water);
- (5) heavy oil (high-viscosity and high-density oil);
- (6) shale oil (kerogen);
- (7) tar sands (containing bitumen which has extremely high viscosities).
- (8) shallow biogenic gas.

The distinction between conventional and unconventional accumulations hinges on whether oil or gas is within a well-defined trap and whether petroleum in a well can be produced economically. The unconventional oil and gas resources cannot be extracted economically by using actually conventional methods and technologies while the conventional petroleum accumulations refer to technically and economically recoverable hydrocarbon. The unconventional accumulations are characterized by large resource but poor reservoir properties. Conventional hydrocarbons only account for lesser than 20% of the world's fossil fuel resources, whereas unconventional hydrocarbons account for at least 80%.

The unconventional petroleum accumulations are obviously different from conventional petroleum deposits in many aspects, including trap, reservoir, configuration of source rocks and reservoirs, migration and accumulation mechanisms, distribution, and occurrence.

Accumulation of unconventional petroleum is performed in unconventional tight reservoirs (very low porosity and permeability) and in atypical trap without obvious trap definition, fluid unit is the basic component element, The limits between fluids (oil-water or gas-water) are not uniform, pressure systems and hydrocarbon saturation varies greatly whereas conventional hydrocarbons are reservoired in ordinary structural, lithostratigraphic, diagenetic and hydrodynamic traps and reservoirs have good properties (good or very good porosity and permeability).

Relationship between source rocks and reservoir is different in many aspects. The reservoirs of conventional petroleum may be far from source rocks whereas for the unconventional hydrocarbons as one or in contact with each other. The production technology is represented by horizontal wells with branches and large-scale hydraulic fracturing with multiple sections for unconventional hydrocarbons whereas conventional petroleum resources are exploited by ordinary vertical wells and conventional fracturing.

On the Romanian territory have been identified 10 petroleum basins with different hydrocarbon richness (Paraschiv, 1974; 1979, Stănescu, 1993): Moesian Platform, Transylvanian Basin, Eastern part of Pannonian Basin, Flysch of Eastern Carpathians, Moldavian Platform, Carpathian Foredeep, Schythian Platform, Maramures Basin, North-Dobrogean Promontory, and Romanian shelf of the Black Sea. In these basins have been identified more than 18 petroleum systems (Popescu, 1995). Almost all these petroleum basins contain unconventional hydrocarbon resources like: tar sands, heavy oil, shallow biogenic gas, shale gas, gas hydrates and coal bed methane (CBM).

The study of rock samples from outcrops and chemical and physical proprieties of oil and gas fields (chemical compositions, pressure, temperature, bubble pressure, formation factor, Gas-Oil Ratio) in correlation with geological and geophysical information from boreholes as well as "hydrocarbon shows" suggest that these basins contain a lot of areas with shale gas, gas hydrates, very heavy oil, tar sands and

coal bed methane (CBM). For the identification of unconventional hydrocarbon resources we analysed outcrops, well logs, seismic profiles and oil and gas production data. We calculated thermal maturity of source rocks, Specific Potential Index (SPI) and estimated the volume of tar sands.



Fig. 1. Tar sand fragment from Sărata Monteoru.

The north-western part of the Moldavian Platform contains gas shales in the Vendian (Ediacaran) Kalius Beds of Nagoriansk Formation and in Silurian black shales of Naslavcea Formation, containing more than 1,2% TOC. Our thermal maturity calculations show that these shales are supermatured in the western part under Carpathian Foredeep and Outer Flysch, matured in the central part of the Moldavian Platform, and they are immatured in the east of the Moldavian Platform where these rocks outcrop on the left shore of the Nistru river (on the Moldavian Republic territory). In some wells at more than of 3950 m depth have been encountered some "gas shows" in the Vendian and Silurian shales.

Gas hydrates were identified on several seismic profiles on Romanian shelf of the Black Sea with very big perspectives for methane.

In the eastern part of Pannonian Basin at Derna-Budoi site is a large tar sands (Pannonian age) accumulation partially exploited by surface mining. Based on analysis of rock samples from outcrops and wells we calculated the unexploited reserves of tar sands as more than 2 billion m³, but their exploitation

will be very difficult because they are under piezometric water level. For a good porosity (20%) it could be calculate a solid bitumen reserve of 400 m³ millions that can be extracted from sands by chemical technologies. For a transformation rate of 50% of the solid bitumens in oil it can infers a petroleum volume of 200 m³ millions, that means a very big oil field = a giant field. The exploitation of these big reserves of tar sands could be profitable in actually technological conditions and at the actually price of oil. In this petroleum basin there is the Suplacu de Barcău field that contains very heavy oil (it density is more than 0,95 g/cm³) reservoired in Pannonian sands that actually is exploited by injection of hot water and chemicals. Tar sands with small reserves are in Sărata-Monteoru (Fig. 1), Matiţa and Buştenari Miocene formations.

The Coal Bed Methane (CBM) was identified in the Petrosani by one well ago 20 years but production had very modest results.



Fig. 2. Dysodile outcrop in Solonţ Valley.

The Flysch of Eastern Carpathians consists of imbricated series of nappes. At least three of them contain rich hydrocarbon source rocks. Tarcau Nappe, Marginal Folds Nappe and Subcarpathian Nappe contain white bituminous marls, menilites and dysodiles (Fig.2) that are very good source rocks. The Total Organic Carbon (TOC) is higer than 1%, up to 9,5%, the kerogen is of Type II or mixed (type II/III) and Hydrogen Index (HI) ranges between 125 and 550 mg Hcs/gTOC. Our calculations in correlations with geological and geochemical data suggest a large perspective for shale gas.

The Audia Nappe of Lower Cretaceous age consists of predominantly Black Shales (Fig.2) with more than 4,5% TOC content (Constantinescu and Anastasiu, 2019). The microspy on the polished sections showed a lot of alginites that in correlation with the elemental chemical analyses (C, H, O) suggest the kerogen is of type I (microbial-algal). After deposition they were buried under the younger thick pile, of Upper Cretaceous and Paleogene Flysch formations. This evolution in a very strong thermal and tectonic regime led to thermal maturation of organic matter and generation and expulsion of hydrocarbons as a result of our estimation. Geochemical and Rock-Eval analyses of the rock samples from outcrops allow us to

calculate the Source Potential Index (SPI). It is defined as hydrocarbon quantity in metric tons that can be generated by a source rock column with height of 1m on 1m² of surface. The potential shale gas reserves from summing of SPI were evaluated as more than 10 billions m³ at STP.

The Bisericani Beds (or Bisericani Formation) is the final formation of the Eocene. It has a thikness usually of 300 – 400 m but it can reaches 800 m in thikness (Bancila, 1958). It have a large areas of development. Bisericani Fm. consists of laminated marls with some intercalations of bituminous shales in the upper part (Băncilă, 1958; Gavăt, 1964). It represents the seal for a lot of petroleum fields in the Eastern Carpathians. Its petrophysical features, in correlation with oil and gas fields suggest the Bisericani Fm. could be a very good deposits for shale gas with large perspectives.

References

Băncilă, I., 1958. Geologia Carpaților Orientali. Ed. Tehnică, București.

Constantinescu, E., Anastasiu, N. et al. 2019. Resursele minerale ale României - Resurse energetice, vol. VIII. Ed. Academiei Române, București.

Gavăt, I., 1964. Geologia zăcămintelor de petrol și gaze din RSR. Ed. Tehică, București.

Paraschiv, D., 1979. Geologia zăcămintelor de hidrocarburi din Romania. Stud. tehn. econ. 10, Institutul de Geologie și Geofizică, București.

Paraschiv, D., 1979. Romanian Oil and Gas Fields. Institute of Geology and Geophysics. Studii Tehnice si Economice, Seria A, 10.

Popescu, M. B., 1995. Romania's petroleum systems and their remaining potential. Petroleum Geoscience, vol.1, 337-350.

Stănescu, V., 1993. Zăcăminte de petrol. Ed. Universității București.

THE CELLULAR CRYSTALLOGRAPHY OF BRAARUDOSPHAERA BIGELOWII

Ion PETREUŞ, Viorel IONESI

Department of Geology, Alexandru Ioan Cuza University of Iaşi, Carol I Blv. 20A 700505 Iaşi, e-mails: opetreus@yahoo.com, vioion@uaic.ro

The cellular crystallography topic introduced in this paper is the last ring of the chain of modern crystallography sciences: molecular crystallography – virus crystallography – cellular crystallography. Cellular crystallography covers the scientific world of fossil and living unicellular plants, animals, spores and pollen.

The single cell exoskeleton of the unicellular *Braarudosphaera bigelowii* alga has a regular pentagonal dodecahedron habit, with a specific symmetry: 15 two-fold rotation symmetry axes, 10 three-fold rotation symmetry axes and 6 five-fold rotation symmetry axes. There is no symmetry planes and symmetry centre. It is a nanobiocomposite regular pentagonal dedocahedron belonging to the iconsahedric system and the 235 (axial) symmetry class. Actually, this exoskeleton is a cellular-capsid constituted of 12 pentasymmetrical, quasiperiodical units and of 60 icosahedric, asymmetric, quasitrapezoidal subunits.

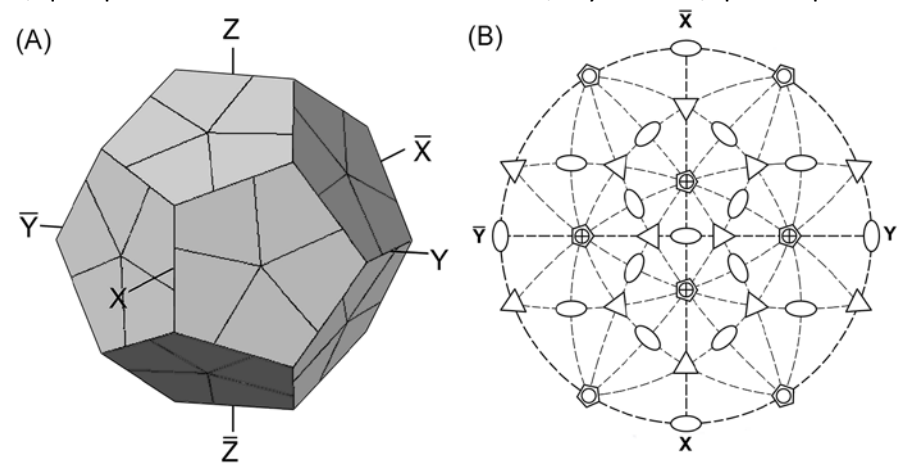


Fig. 1. Positive regular pentagonal dodecahedron of the 235 symmetry class of the icosahedric system: (A) General morphology. (B) Stereographic projection.

Protein regular pentagonal dedocahedron is the extracellular template for proteinaceous biocalcite crystals. The *B. bigelowii* single cell is able to develop a sophisticated biotechnology for constructing a cellular-capsid consisting of a superintelligent nanobiocomposite biomaterial with versatile biologic functionality. The cellular-capsid seems to be the key for solving fundamental problems of the evolution of the cell wall and to inspire new nanobiotechnologies.

Conclusions

The single-cell exoskeleton of *Braarudosphaera bigelowii* has an icosahedral quasicrystal protein habit with a specific symmetry: 15 two-fold rotation symmetry axes; 10 three-fold rotation symmetry axes; and 6 five-fold rotation symmetry axes. No symmetry planes and no symmetry centre are present.

Braarudosphaera bigelowii cellular-capsid is a regular pentagonal dodecahedron belonging to the icosahedral system and 235 (axial) symmetry class. The cellular-capsid of *B. bigelowii* is constituted of 12 icosahedral, pentasymmetric, quasiperiodic units and of the 60 icosahedral, asymmetric, quasitrapezoidal subunits.

The icosahedral protein regular pentagonal dodecahedron is an extracellular template for biocalcite crystal growth, self-assembled under the control of pentasymmetry. The single cell of *B. bigellowii* secretes icosahedral protein and proteinaceous biocalcite nuclei on the base-plate. The biocalcite proteinaceous crystals are then exocytosed outside the cell and inserted in a perfect crystallographic orientation on the icosahedral protein surface of the regular pentagonal dodecahedron extracellular template.

The single cell is able to develop a sophisticated biotechnology including a synchronic intracellular process of icosahedral protein and calcite production, and of an extracellular self-assembling process, controlled by icosahedric symmetry. This natural experiment in two synchronic - intracellular and extracellular - events is repeated 20-30 times during the life of the cell.

The lamellar nanobiocomposite is only the biomaterial able to ensure a versatile functionality and the survival of the *B. bigelowii* cell along some tens of million years.

The *Braarudosphaera bigelowii* exoskeleton is actually a cellular-capsid, constituted of a specific nanobiocomposite biomaterial with icosahedric symmetry. Cellular capside seems to represent a new and important form between virus capside and the Eucarya's cell membrane; we are in front of evolution of the cell wall itself, on the evolutionary natural direction: Archaea \rightarrow Bacteria \rightarrow Eucarya. The cellular icosahedric capsid is the key to solve some fundamental problems of protein crystallography and to inspire new nanobiotechnologies.

FLUID AND MELT INCLUSIONS IN MINERALS: APPLICATIONS IN GEOSCIENCES

Ioan PINTEA

Geological Institute of Romania, 1 Caransebeş St, 012271 Bucharest e-mail: ipinteaflincs@yahoo.com

Introduction

Fluid and melt inclusions in minerals are the only available direct samples of the fluid and melt phases evolved in the Earth Crust and Upper Mantle during the complex geologic Wilson cycles. Its become a separate geological discipline offering the PVTX characteristics of the fluid and melt phases and their evolutionary related processes in time and space.

Brief historcal bacground

Curiosity and conspicuous were the atributes characterizing fluid inclusions in minerals from a long period of time since they were noticed at the beginning of the first milenia (e.g. Pliny the Elder -,,Natural History"- 79AD). In this respect Claudius Claudianus noted a precious historical quote around 400 AD in ,,Carmina Minora" (epigram 33), about a fluid inclusion trapped in a piece of ice crystal (web source):

"Possedit glacies naturae signa prioris et fit parte lapis, frigora parte negat. Sollers lusit hiemps, inperfectoque rigore nobilior vivis gemma tumescit aquis" (This piece of ice still shows traces of its original nature: part of it has become stone, part resisted the cold. It is a freak of winter's, more precious by reason of its incomplete crystallization, for that the jewel contains within itself living water).

Mentioned by Abu Reihan Al - Biruni (Kesler et al., 2013) in the mid 11th century, they become scientific geological objects only in the mid 19th century with the milestone paper published by Sir H.C. Sorby about fluid and stone cavities (1858). Almost forgotten, with some notable exceptions (Touret, 1984), the fluid and melt inclusions from mineral study renewed during the mid 20th century by the contributions of Ermakov (1950), Ermakov and Dolgov (1979), Deicha (1955), Roedder (1962; 1972; 1979; 1984; 1990; 2002; and reference therein), Weisbrod et al., (1976), Clocchiatti (1975) and many others (Zhili et al., 2008). Comercially available microthermometric stages [Chaixmeca - France, Linkam models - UK, USGS and Instec - USA for heating - freezing purposes and Leitz, 1350 (Germany), Linkam TS 1500 (UK), Instec (USA), "Vernadsky" (Russia) for heating at ultra-high temperatures up to 1600°C] coined the modern era of fluid and melt inclusion study with applications in Mineralogy, Geochemistry, Metallogeny, Petrology, Vulcanology, Tectonics, Sedimentology, Gemmology, Oil Industry, and many others. New technique developments notably HDAC and fused silica capillary tubing together with synthetic fluid inclusion methods (Bassett et al., 1996; Chou et al., 2008; Bodnar and Sterner, 1987; Kotel'nikova and Kotel'nikov, 2010) contributed to the modern tremendous evolution of fluid and melt inclusion study. Today there are strong fluid and melt inclusion research teams inside the Universitie's departments or separate Geological Institutes (see "The World of Fluid Inclusions" at http://www.geology.wisc.edu/~pbrown/fi.html) around the world which contribute every year with about 700 published articles on fluid inclusions and other 200 items per year on melt inclusions (Kesler et al., 2013). New books (Roedder, 1984; Shepeherd et al., 1985; De Vivo and Frezzotti (eds.), 1994, Goldstein and Reynolds, 1994; Samson et al. (eds), 2003; Hurai et al., 2015, and the proceedings volumes from the special conferences such as ECROFI, PACROFI, ACROFI, GOLDSCHMIDT, AGU, EGU and other annual or biennial meetings worldwide contain hundreths of new papers released around the world, especially from ore deposit research, petrology, sedimentology, gemmology and many others. The up-to-date development of fluid and melt inclusion study in Romania was summarized recently by Pintea, 2015 (in review).

Fluid and melt inclusion types

Majority of natural minerals, extraterrestrial, industrial or laboratory synthesized contain fluid or melt inclusions function of their original crystallization environment from melt or solution. Based upon their content at room temperature conditions they are monophazic (liquid, vapor or glass), biphasic (liquid-vapor, gas-solid, glass-vapor, glass-solid, liquid-solid), triphasic (liquid - vapor -solid (s), glass-vapor-solid(s), liquid-liquid-vapor etc) and solid multiphase (e.g. nanogranites). Genetically they are primary, pseudosecundary and secondary (Roedder, 1984). A recent paper (Pintea, 2015, in review) present in an atlas form some of the most representative fluid and melt inclusions associations from Alpine magmatic hydrothermal systems, sedimentary and metamorphic formation from the Carpathian area.

Methods of study (the most accessible)

To be interpretable the fluid and melt inclusion must obey at least three of the Roedder's rules as followings: **1.** homogeneous trapping, **2.** constant volume, **3.** none post entrapment modifications (e.g. Goldstein and Reynolds, 1994; Bodnar, 2003; Pintea, 2015 (in review). "To be of maximum value, the analysis of any given inclusion should be complete" (Roedder, 1990): major solvent (H₂O, and sometimes CO₂), major solute ions (Na, K, Ca, Mg, Cl, SO₄, and HCO₃, minor solute ions (Al, Fe, B, Ba, Br, Mn, NH₄, P, F, Si, BO₃⁻³, PO₄⁻³, HSiO₃⁻¹), heavy metals (Au, Ag, Cu, Mo, W, U), the pH and Eh, species with variable valences Fe (Fe²⁺, Fe³⁺), Mn, S (SO₄²⁻, H₂S, HS⁻) carbon (CO₂, CH₄, CO, C_xH_y, H₂CO₃, HCO₃⁻), organic compound (acetate, oxalate, amino acids, aromatic etc), gaseous species (H₂, He, N₂, O₂, Ar), the isotopic composition of the major elements (H, C, N, O, S, Sr, Ar, He).

There are two types of study methods: **1.** Non-destructive, which allow us to analyze one single inclusion without disturbing their sealed volume and chemical composition. The most important techniques include: optical microscopy, microthermometry, CL, IR and Raman spectroscopy, PIXE/PIGE and SRXRF. **2.** Destructive methods which open one or more fluid inclusion at the time, separate for leachates chemical analysis (ions and cations) and bulk analyses of the volatile released phases (Shepherd and Rankin, 1998). The singular methods include: LA-ICP-MS, LA-ICP-AES, SIMS, SEM-EDS, Crio-SEM-EDS, EPMA. The global leachates analysis are based upon AAS, IC, ISE, ICP-MS techniques, and bulk volatile analyses are done by GC and coupled GC-MS. Special techniques have been developed for hydrocarbon-bearing inclusion based upon Grain containing oil inclusions (GOI), Fluid Inclusion Stratigraphy (FIS), and Molecular composition of inclusions (MCI) (Mernagh, 2015).

Data interpretation

The P-V-T-X data of the fluid and melt inclusion assemblages (FIAs and MIAs) are interpreted obviously by the average approach, the high approach and one-by-one approach (e.g. Johnson et al., 1994; Goldstein and Reynolds, 1994; De Vivo and Frezzotti, 1994; Bodnar, 2003, Hurai et al., 2015). These are based on well known master systems such as H_2O , CO_2 , H_2O -NaCl, H_2O -CO $_2$ -NaCl, H_2O -CO $_2$ -NaCl, H_2O -CO $_2$ -CO $_3$ -RaCl-KCl, H_2O -Na $_2$ CO $_3$ -FeCl $_3$ -Side $_3$ -Fe $_3$ -Fe

Available computer programs operating in large P-T-X domains from up to 1500° C and more than 5kbar such as CLATHRATES and FLUIDS packages (Bakker, 2003), MacFlinCor (Bakker and Brown, 2003), SoWat (Driesner, 2007; Driesner and Heinrich, 2007) HokieFinks_H₂O-NaCl (Steele-MacInnis et al., 2012) are frequently used.

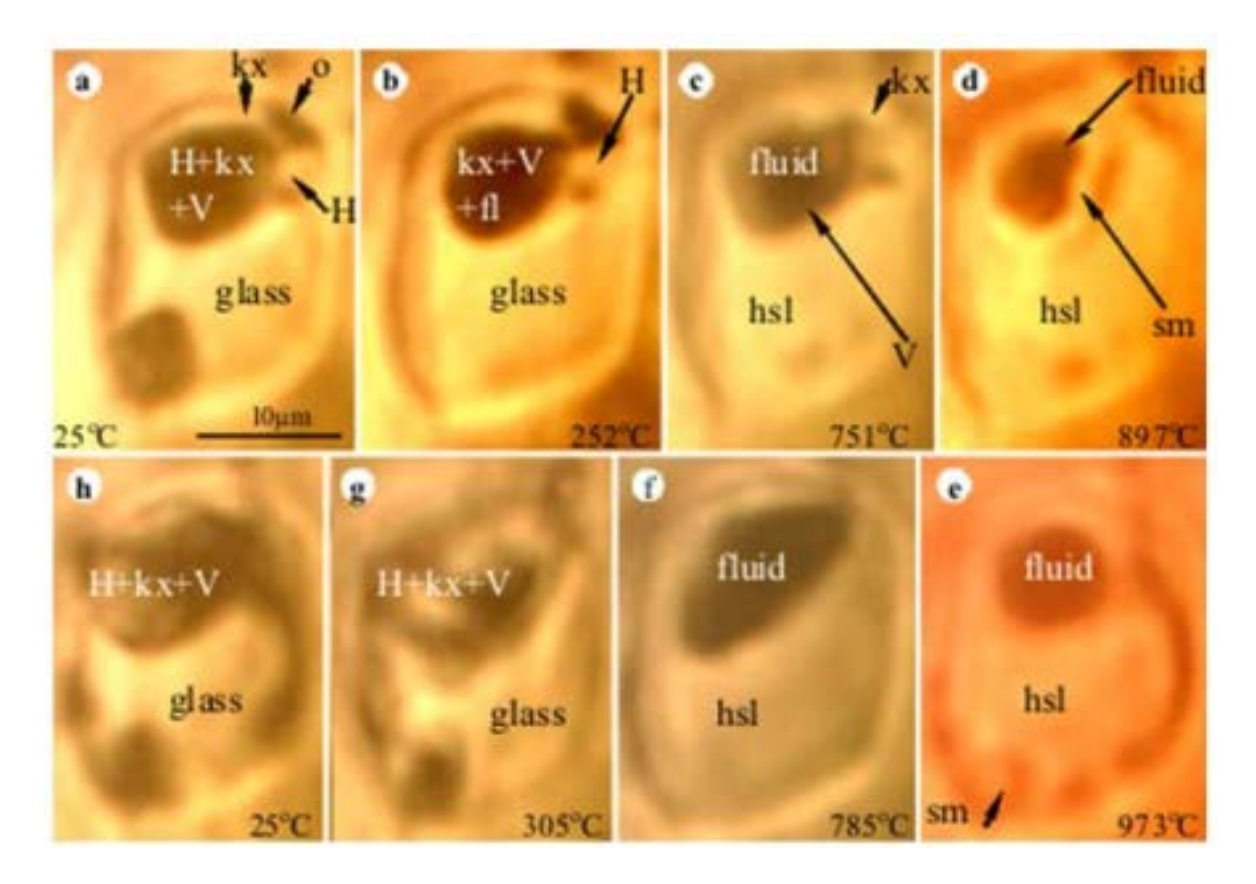


Fig. 1. Melt-melt-fluid immiscibility in a complex silicate melt inclusion from quartz in Upper Cretaceous Moldova Noua porphyry Cu-Mo-(Au) deposit. Microthermometry: Tm halite= 358°C, Th (V) =962°C, Tm (silicate or anhydrite)= 888°C, P= 2036.48bar, Ws=34.0884 wt% NaCl eq., d= 0.762769g/cm³, (L+V) state; Notations: H- halite, kx-silicate/anhydrite/carbonate-?, V- gas bubble, hsl- hydrosilicate liquid, sm-salt melt.

Applications to some case studies in Romania

Alpine hydrothermal deposit in the Carpathian area are fully characterized in the aqueous H_2O -NaCl \pm $CO_2 \pm$ $SiO_2 \pm$ $CO_2 \pm$ $SiO_2 \pm$ CO_3 system (Pintea 2012, Pintea et al., 2018a). Aqueous-carbonic fluids contain a dominated carbonic phase mainly as $CO_2 \pm H_2O \pm CH_4 \pm C_xH_y \pm N_2 \pm NaCl \pm S$ (C-O-H-N-S-salt) heterogeneous systems and were reported in orogenic gold deposits from Southern Carpathians (e.g. Udubaşa et al., 2003), metamorphic fluid in the Eastern Carpathians, Banat, Apuseni Mountains such as pegmatite, low to high grade metamorphic formations (e.g. Pomârleanu, 1971; 1977; 2007), NW - Ditrău alkaline massif and upper mantle fluid in peridotitic nodules from Perşani Mountains (e.g. Pintea and Mârza, 1989, Pintea, 1991), Blazna - Gușet metamorphic Pb-Zn mineralization (e.g. Pintea, 2012).

Pegmatite, porphyry $Cu \pm Au \pm Mo$ deposits, and endogenous skarn associations in alpine Carpathian zone in Romania are characterized by the presence of complex brine inclusions (hydrosaline melt inclusions) associated with hydrosilicate melt-, and vapor-rich "melt" inclusions suggesting immiscibility at the trapping conditions (Pintea, 1996; 2014; 2015- in review and Fig. 1 and Fig. 2).

Foam-like silicate glass inclusion in quartz, plagioclase and zircon from the Dej tuff Miocene formation in the Western Transylvanian basin probably formed by immiscibility in the upper part of the magma chamber at the base of the volcanic conduit offer a unique possibility to study the geodynamic of rhyolite-dacite magma during interaction with mafic influx in the upper mushy layer and the eruptive (explosive) episodes (Pintea, 2013; Pintea 2015 - in review).

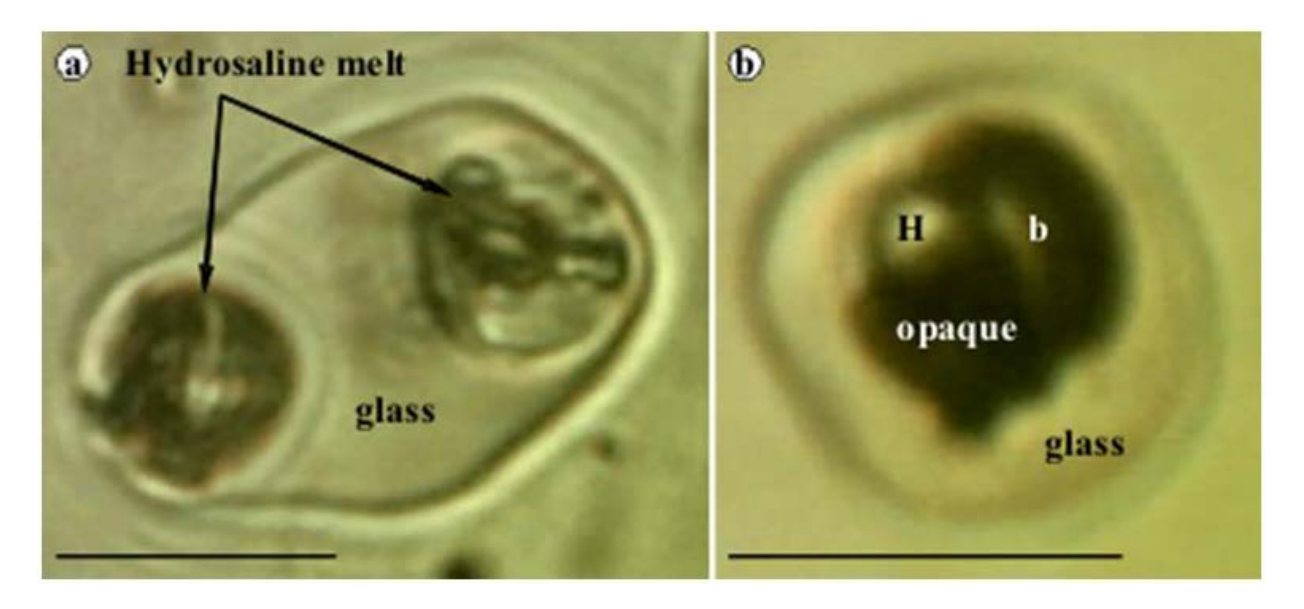


Fig. 2. Melt-melt-fluid immiscibility in reheated complex silicate melt inclusions from quartz from **a.** Valea Morii and **b.** Bolcana Miocene porphyry Cu-Au-(Mo) deposits from Metaliferi Mountains (Golden quadrangle, Apuseni Mountains, Romania). H- halite, b- bubble; Scale bar 10μm.

The recent Raman spectroscopy and high temperature microthermometry data (Pintea et al., 2018ab) shown the presence of multiple daughter minerals in hydrosaline melt inclusions including halite, anhydrite, magnetite and chalcopyrite. Their behavior during heating-cooling microthermometric cycles suggests a fractionation process from a hydrosilicate liquid phase in large P-T-X conditions. The Raman spectra in the same inclusions or contemporaneous vapor-rich "melt" inclusions suggested the presence of H_2O , CO_2 , CH_4 , HCO_3^{2-} , PO_4^{3-} , SO_4^{2-} , sulfides, carbonate, sulphate and a silica-rich compound (clathrasil - like, Pintea et al., 2019).

Conclusions

The fluid and melt inclusion study is relatively new geological domains applied to the geosciences were a fluid and/or a melt phase(s) were involved. They are also applied in industrial related processes including experimental mineralogy and petrology at high temperature and pressure conditions. In Romania, despite the variety of fluid phases involved in very diverse geological environments the application of fluid and melt inclusion study is still at an embryonic stage, rarely being used the most modern analytical possibilities. Nevertheless some recent notable papers were released on fluid and melt inclusions from Ditrau massif (Fall et al., 2007), Neogene dacites (Grancea et al., 2003, Naumov et al., 2014), from epithermal ore deposits in the Baia Mare region (Bailly et al., 1998; Grancea et al., 2002), Rosia Montana (Wallier et al., 2006; Pintea and Iatan 2017; Naumov et al., 2013) and from the porphyry Cu-Au-Mo deposits in Metaliferi Mountains (Pintea, 1996; Damman et al., 1996; Grancea et al., 2001; Kouzamnov et al., 2010; Pintea et al., 2019, in preparation). There is plenty of research work which remains to be done on fluid and melt inclusions in minerals from terrestrial and extraterrestrial environments.

References

Bailly, L.., Grancea. L., Kouzmanov, K., 2002. Infrared microthermometry and chemistry of wolframite from the Baia Sprie epithermal deposit. Romania. Econ. Geol., 97, 415-423.

Bakker, R.J., 2003. Package FLUIDS 1. Computer program for analysis of fluid inclusion data and for modeling bulk fluid properties. Chem. Geol., 194, 3-23.

Bakker, R.J., Brown, P.E., 2003. Computer modeling in fluid inclusions research. In "Fluid Inclusions; Anallysis and Interpretation (I. Samson, A. Anderson and D. Marshall, eds), Short – Course Volume, 32, 175-212.

- Bassett, W.A., Wu, T.-C., Chou, I.-M., Haselton, H.T., Frantz, J.Jr., Mysen, B.O., Huang, W. L., Sharma, K.S., Schiferl, D., 1996. The hydrothermal diamond anvil cell (HDAC) and its applications. Mineral Spectroscopy: A tribute to Roger G. Burns. The Geoch. Soc., Spec. Publ., no.5. (Eds M.D.Dyar, McCammon and M.W. Schaefer, p. 261-272.
- Bodnar RJ., Sterner M.S., 1987. Synthetic Fluid Inclusions. In "Hydrothermal experimental techniques" (G.C. Ulmer and H.L.B., eds), 17, 423-457.
- Bodnar R.J., 2003. Introduction to aqueous-electrolyte systems fluid inclusions. In I. Samson, A. Anderson, & D. Marshall, eds. Fluid Inclusions: Analysis and Interpretation. Mineral. Assoc. Canada, Short Course 32, 81-99.
- Bodnar R.J., Student J.J., 2006. Melt inclusions in plutonic rocks: petrography and microthermometry. In "Melt Inclusions in Plutonic Rocks" (J.D. Webster, ed). Min. Assoc. of Canada Short Course 36, Montreal, Quebec, p. 1-25.
- Chou, I.-M., Song, Y., Burruss, R.G., 2008. A new method for synthesizing fluid inclusions in fused silica capillaries containing organic and anorganic material. Geochim. Cosmochim. Acta, 72, 5217-5231.
- Clochiatti, R., 1975. Glassy inclusions in crystals of quartz: optical, thermo-optical and chemical studies and geological applications. Soc. Geol. de France, Memoires, New Series, 54, no.122, 96p (in French).
- Cruz, M.F., Manning C.E., 2015. Experimental determination of quartz solubility and melting in the system SiO₂-H₂O-NaCl at 15-20kbar and 900-1100°C: implications for silica polymerization and the formation of supercritical fluids. Contrib Mineral Petrol, 170, 35, 17p.
- Damman, A.H., Karis S.M., Touret J.L.R., Rieffe E. C., Kramer J.A.L.M., Vis R.D., Pintea I., 1996. PIXE and SEM analysis of fluid inclusions in quartz crystals from the K- alteration zone of the Roşia Poieni porphyry Cu deposit, Apuseni Mountains, Rumania. Eur. J. Mineral. 8, 1081 1096.
- De Vivo, B., Frezzotti, M.L. eds, 1994. Fluid inclusions in minerals: Methods and Applications. Short course workshop of the working group (IMA) "Inclusions in Minerals" (Potignano-Siena, 1-4 sept 1994), Virginia Polytechnic Inst. and State Univ., 377p.
- Deicha, G., 1955. The crystal voids and their fluid inclusions: significance in ore deposits genesis and rocks. Paris, Masson et Cie., 126p (in French).
- Driesner, T., Heinrich, C.A., 2007. The System H O-NaCl. I.Correlations for molar volume, enthalpy, and isobaric heat capacity from 0to 1000 °C, 1 to 5000 bar, and 0 to 1X. Geochim. et Cosmochim. Acta 71(20), 4902-4919.
- Driesner, T., 2007. The System H O-NaCl. II. Correlation Formulae for Phase Relations in Temperature-Pressure-Composition Space from 0 to 1000°C, 0 to 5000 bar, and 0 to 1 X . Geochim. et Cosmochim. Acta 71, 4880-4901.
- Ermakov, N.P., 1950. Research on mineral-forming solutions. Kharkov Univ. Press, 460p (in Russian).
- Ermakov, N.P., Dolgov Yu.A.., 1979. Thermobarogeochemistry (In Russian), Ed. Nedra, Moscow.271p.
- Goldstein, R.H., Reynolds, T.J., 1994. Systematics of fluid inclusions in diagenetic minerals. SEPM Short Course 31, 199 p.
- Grancea, L., Cuney, M., Leroy, J.L., 2001. Mineralized versus barren intrusions: a melt inclusion study in Romania's gold quadrilateral. C. R. Acad. Sci. Paris, Sciences de la Terre et des planets 333, 705-710.
- Grancea, L., Bailly, L., Leroy, J.L., Banks, D., Marcoux, E., Milesi, J.P., Cuney, M., Andre´ A.S., Istvan, D., Fabre, C., 2002. Fluid evolution in the Baia Mare gold/polymetallic epithermal district (Inner Carpathians, Romania). Miner. Deposita, 37, (6-7), 630-647
- Grancea, L., Fülop, A., Cuney, M., Leroy, J., Pironon, J., 2003. Magmatic evolution and ore-forming fluids involved in the origin of the gold/base metals mineralization in the Baia Mare province, Romania. J. Geochem. Explor., 78/79, 627–630.
- Fall, A., Bodnar, R.J., Szabo, Cs., Pal-Molnar, E., 2007. Fluid evolution in the nepheline syenites of the Ditrau alkaline massif, Transylvania, Romania. 95, 3-4, 331-345.
- Hurai, V., Huraiova, M., Slobodnik, M., Thomas, R., 2015. Geofluids-Development in Microthermometry, Spectroscopy, Thermodynamics and Stable Isotopes. Elsevier, 504 p.
- Johnson, M.C., Anderson, A.T. Jr., Rutherford, M.J., 1994. Pre-eruptive volatile contents of magmas. In Rev. in Mineralogy, 30, "Volatile in Magmas", (Carrol M.R., Holloway J.R., eds), ch. 8, 281-320.
- Kesler, S.E., Bodnar, R.J., Mernagh, T.P., 2013. Role of fluid and melt inclusion studies in geologic research. Geofluids, 13, 398-404.
- Kotel'nikova, Z.A., Kotel'nikov, A.R., 2010. Experimental study of heterogeneous fluid equilibria in silicate-salt-water systems. Geology of ore deposits, 52, 2, 154-166.
- Kouzmanov, K., Pettke, T., Heinrich, C.A., 2010. Direct analysis of ore-precipitating fluids: combined IR microscopy and LA-ICP-MS study of fluid inclusions in opaque ore minerals. Econ. Geol., 105, 351-373.
- Mernagh, T.P., 2015. A review of fluid inclusions in diagenetic systems. Acta Geol. Sinica, 89,3, 697-714.
- Naumov, V.B., Prokofiev, V.Yu., Kovalenker, V.A., Tolstykh, M.L., Damian, G., Damian, F., 2013. Unusual acid melts in the area of the unique Roşia Montană gold deposit, Apuseni Mountains, Romania: Evidence from inclusions in quartz. Geochem. Internat., 51, 11, 876-888.
- Naumov, V.B., Kovalenker, V.A., Damian, G., Abramov, S.S., Tolstykh, M.L., Prokofiev, Yu. V., Damian, F., Seghedi, I., 2014. Origin of the Laleaua Alba dacite (Baia Sprie volcanic area and Au-Pb-Zn ore district, Romania): evidence from study of melt inclusions. Centr. Eur., Geol., 57/1, 83-112.
- Pintea, I., 1991. Fluid inclusion studies on quartz crystals associated to the REE and sulphide ore body from Jolotca (NW-Ditrau masiff, Transylvania, Romania). ECROFI XI, Plinius, 5, abstr. p. 175, Firenze. Italy.
- Pintea, I.,1996. Fluid inclusions study with special view on fluid phases immiscibility associated to porphyry copper genesis from Metaliferi Mountains. Ph D thesis, Univ Bucharest (in Romanian). 172 p.
- Pintea, I., 2012. Fluid and melt inclusions: a precious tool in selective exploration strategy. Rom. J. of Min. Dep., 85, 1, 85-89.
- Pintea, I., 2013. Melt inclusions texture and thermal history in minerals from the Dej Tuff, Transylvania basin, Romania. Rom. Jour. of Earth Sciences. 87, issue 1-2, p. 29-47.

- Pintea, I., 2014. The magmatic immiscibility between silicate-, brine-, and Fe-S-O melts from the porphyry (Cu-Au-Mo) deposits in the Carpathians (Romania): a review. Rom. Jour. of Earth Sciences vol 87, issue 1, 32 p, online first.
- Pintea, I., 2015. Fluid in the earth crust and upper mantle: an atlas of the fluid and melt inclusions from Romania. Romanian. Jour. of Earth Sciences (in review).
- Pintea, I., Mârza, I., 1989. Preliminary observations on the CO₂-bearing fluid inclusions in the olivine and pyroxene peridotitic nodules at Hoghiz (Perşani Mountains). D. S. IGG (IGR), 74/1, (1987), 1989, 107-116.
- Pintea, I., latan E. L., 2017. The magmatic-hydrothermal history of the <beta>-quartz polymorphs from Rosia Montana dacite inferred by solid-, melt, and fluid inclusion assemblages. Rom. J. Mineral Deposits, 90, 1-2, 46-61.
- Pintea I., Nutu-Dragomir, M.-L., Udubasa, S.S., Birgaoanu, D., Iatan, E.L., Berbeleac, I., Ciobotea-Barbu, O.C., 2018a. Hydrosilicate aqueous-, and vapor-"melt" inclusions in some specific rocks and minerals from Romania. Rom. Jour. of Mineral Deposits, v. 91, no 1-2, p.13-18.
- Pintea, I., Udubasa, S.S., Birgaoanu, D., Iatan, E.L., Barbu, O.C., 2018b. Microthermometry and Raman spectroscopy of fluid and melt inclusions in the alpine porphyry copper deposits from Romania: insights on micrometallogeny. Goldschmidt 2018 Conference, Boston, USA., abstract volume online.
- Pintea, I., Udubasa, S.S., Nutu-Dargomir, L.M., Iatan, E.L., Berbeleac, I., Petrescu, L., Ghinescu, E., 2019. Clathrasil compound evidence in fluid and brine inclusions by microthermometry and Raman spectroscopy. Goldschmidt 2019, Barcelona, abstract.
- Pomârleanu, V., 1971. Geothermometry and their application to somes minerals from Romania. Edit. Acad. Române, 158 p (in Romanian), Bucharest.
- Pomârleanu V., 1975. Decrepitometry and their applications in mineral prospection. Edit. Tech., 180p (in Romanian), Bucharest.
- Pomârleanu V. (2007) Microinclusions in minerals from extraterrestrial and terrestrial environments. Ed. AGIR, 173 p (in Romanian), Bucharest.
- Roedder, E., 1962. Studies of fluid inclusions I: Low temperature application of a dual-purpose freezing and heating stage. Eco. Geol., 57, 1045-1061.
- Roedder, E., 1972. Composition of fluid inclusions. Chapter JJ., in Fleischer M., ed., Data of geochemistry, 6th Edition: U.S. Geol. Survey Prof. Paper 440 JJ, 164p.
- Roedder, E., 1979. Origin and significance of magmatic inclusions. Bull. Mineral., 102, 487-510.
- Roedder, E., 1984. Fluid Inclusions. Min. Soc. Am. Rev. in Min. 12, 644 pp.
- Roedder, E., 1990. Fluid Inclusion analysis-prologue and epilogue. Geochim. Cosmochim Acta, 54, 495-507.
- Roedder, E., 2002. Significance of melt inclusions. In Workshop- Short Course on Volcanic systems Geoch. And Geophys. Monitoring Melt Inclusions: methods, applications and problems (B.De Vivo and R.J. Bodnar, Edts. Proceed., sept 26-30th, 2002, Grand Hotel Moon Valley, Seiano di Vico Equense (Sorrento Peninsula)- Napoly, Italy, Abstr. Vol, p. 11-12.
- Samson, I., Anderson, A., Marshal, D. (eds), 2003. Fluid Inclusions: Analysis and Interpretation. Min. Assoc. of Canada, Short Course volume, 32, 384p.
- Shepherd, T.J., Rankin, A.H., Alderton, D.H.M., 1985. A practical guide to fluid inclusion studies. London, Blackie, 239 p.
- Shepherd, T.J., Rankin, A.H., 1998. Fluid Inclusions Techniques Analysis. In "Techniques in hydrothermal ore deposits geology" (J.P. Richards, B.P. Larson, eds), vol. 10, 125-149.
- Sorby, H.C., 1858. On the microscopical structure of crystals, indicating origin of minerals and rocks. Quart. J. Geol. Soc. London 14, 453-500.
- Steele-MacInnis, M., Lecumberri-Sanchez, P., Bodnar, R.J., 2012. HOKIEFLINCS_H₂O-NaCI: A microsoft Excel spreadsheet for interpreting microthermometric data for fluid inclusions based on the PVTX properties of H₂O-NaCI. Computers & Geosciences, 49, 334-337.
- Steele-MacInnis, M., Ridley, J., Lecumberi-Sanchez, P., Schlegel, T.U., Heinrich, C.A., 2016. Application of low temperature microthermometric data for interpreting multicomponent fluid compositions. Earth-Sci. Rev., 159, 14-35.
- Student, J.J., Bodnar, R.J., 1999. Synthetic fluid inclusions XIV: coexisting silicate melt and aqueous fluids inclusions in the haplogranite-H₂O-NaCl-KCl system. Jour. of Petrol., 40, 10, 1509-1525.
- Touret, J.L.R., 1984. Fluid Inclusions: a paradox history. Bull Mineral, 197, 125-137 (in French).
- Touret, J.L.R., Visser, R.P.W. (eds), 2004. Dutch pionneers of the earth sciences. Edita KNAW, Amsterdam, 200p.- (p. 87-107): Touret J.L.R.: Hermann Vogelsang (1838-1847) « European avant la lettre ».
- Udubaşa, S.S., Lespinasse, M., Udubaşa, G., Popescu, C.G., Leroy, J., Bilal, E., 2003. Fluid inclusions data on quartz samples from Costesti gold mineralization, southern Carpathians, Romania. ECROFI XVII, Budapest, 2003, Acta Min.-Petrogr. Abstract Series 2, Szeged, p. 220-221.
- Wallier, S., Rey, R., Kouzmanov, K., Pettke, T., Heinrich, C.A., Leary, S., O'Connor, G., Tămaş, C. G., Vennemann, T., Ullrich, T., 2006. Magmatic fluids in the breccia-hosted epithermal Au-Ag deposit of Roşia Montană, Romania. Econ. Geol., 101, p.923-954.
- Weisbrod, A., Poty, B., Touret, J., 1976. Fluid inclusions in geochemistry-petrology: actual tendence. Bull Soc fr. Mineral Cristalogr, 99, 140-152 (In French).
- Zhili, H., Akbanov, H.A., Diquing, Z., 2008. In memory of Fluid Inclusion Research Pionneers E. Roedder, N.P. Ermakov, H.C. Sorby and Aly Raichan Beruny. Proceed. of XIIIrd International conference on thermobarogeochemistry and IVth APIFIS symposium. Vol. 1. abstract RMS DPI 2008-1-139-1.

MICROPLASTICS IN SURFACE WATERS FROM THE NORTHWESTERN BLACK SEA. AN ABUNDANCE AND COMPOSITION APPROACH

Iulian POJAR¹, Friederike STOCK² and Christian KOCHLEUS²

¹National Institute of Marine Geology and Geoecology – GeoEcoMar, 23-25 D. Onciul St, Bucharest e-mail: iulianpojar@geoecomar.ro

² The German Federal Institute of Hydrology – BfG, e-mail: stock@bafg.de

Plastic products have found a wide applicability in almost all sectors of human society due to their versatility and light-weight nature. With the benefits offered by this commonly used material, the negative impact of the plastic waste over the nature environments is critical, especially to the marine species. In the last two decades the scientific community has intensively investigated microplastics in different environments (Crawford and Quinn, 2017; Wagner and Lambert, 2018). Plastic research has become interdisciplinary with various papers published about marine and freshwater environments including water and sediment (Blettler et al., 2018; Mani et al., 2019; Peng et al., 2018; Schwarz et al., 2019), organisms (Besseling et al., 2018; Triebskorn et al., 2019), soils (de Souza Machado et al., 2018; He et al., 2018) or methodological approaches (Mai et al., 2018; Prata et al., 2019; Stock et al., 2019).

Considered to be Anthropocene "sediments", plastics and microplastics – particles that have a dimension lower than 5 mm (Thompson et al., 2009) – are found in high amounts in divers environments such as river banks, deltas, beaches, shelf areas and other marine domains. Plastic is known for a light density that permits an effortless and fast transport of the particles in particular where are present high velocity fluvial currents, strong marine waves and currents or high wind regimes. Due to these natural agents, the plastic particles are more and more encountered in isolated places from arctic areas to abyssal plains.

Being an eastern border between two continents, the Black Sea is an important basin for aspects such as ecology, geology, tourism, economic or international affairs. The Black Sea drains 21 countries with a total population of ca. 170 million and is a narrow semi-enclosed basin characterized by a high disposition for multiple pollution forms (Bakan and Büyükgüngör, 2000; Topçu et al., 2013; Tuncer et al., 1998), including plastic debris.

The high rates of microplastic particles discharged into the Western Black Sea could be a result of critical level of pollution related to harbors, dense localities and touristic resorts from the western Black Sea coast and from the Danube River - one of the most navigated waterways inside EU. Unfavorably, the Black Sea did not have a decent characterization on microplastics degree pollution; alone one study describes the South-Eastern coast (Aytan et al., 2016).

The present study aims for microplastic abundance and characterization in western Black Sea surface waters. Furthermore, the abundance of the particles identified in sample stations could be associated with surface currents of the Western Black Sea, described in the past (Shapiro, 2019) as a North to South movement of both water body and floating particles.

Floating microplastic particles were sampled with a Neustonic Net (HydroBios, 200µm mesh size) from the surface water along Western Black Sea coast. A total of 12 samples were collected from 2 main areas: south-east of Danube Delta and east of populated coast area (Constanta-Mangalia). For the samples, the organic matter was digested using a reagent composed of equal volumes of 10 M KOH and 30 % H2O2, then, the (micro)plastic particles were isolated from the supernatant by pressure filtration. Analysis was done by visual inspection and selected particles (PP, PE, PAN and PS) were measured with pyrolysis GC-MS.

The first results of the water samples reveal an average concentration of 9 particles per m3. Among microplastic particles 74.6% are identified as fibers, foils represent 13% and 10.85% are fragments (Fig. 1). Fiber clumps and spherules are also present in low amounts. Qualitative analyses show a high presence of

low-density polymers: PE (polyethylene) and PP (polypropylene), and less PP (polypropylene) and PET (polyethyleneterephthalate).

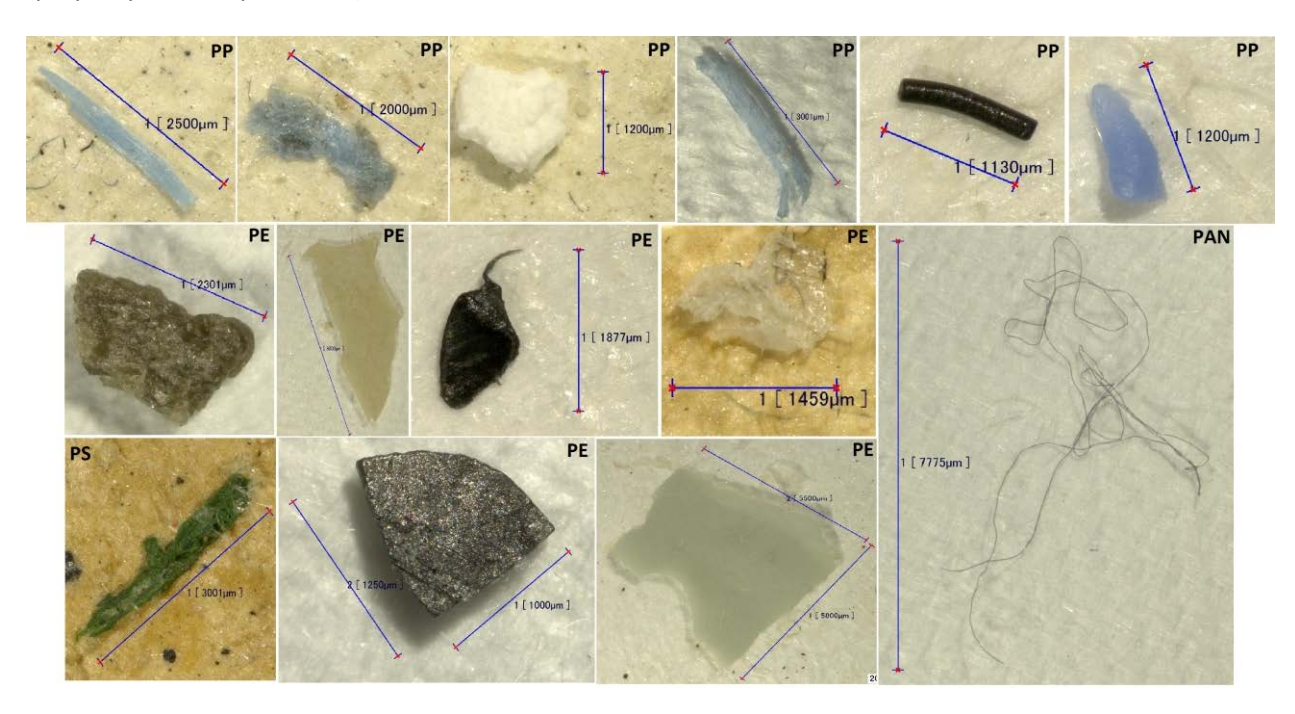


Fig. 1. Microplastic particles identified in Western Black Sea surface water layer (Keyence VHX 2000 imaging, 200x lens).

Due to the high discharge of Danube into the Black Sea it was obvious that the samples collected close to the mouths of Danube Branches could be a considered hotspot for microplastic particles. Also, southern samples adjacent to Mangalia town and harbor are distinct with an important abundance in microplastic particles.

Although a multitude of analytical methods and sampling techniques for MP quantification and characterization (Miller et al., 2017) were tested and described by several authors, the absence of a standardized methodology frequently obstructs the comparison and correlation of the results from different studies.

References

Aytan, U., Valente, A., Senturk, Y., Usta, R., Esensoy Sahin, F.B., Mazlum, R.E., Agirbas, E., 2016. First evaluation of neustonic microplastics in Black Sea waters. *Mar. Environ. Res.* 119, 22-30.

Bakan, G., Büyükgüngör, H., 2000. The Black Sea. Marine Pollution Bulletin. 41, 1-6, 24-43.

Besseling, E., Redondo-Hasselerharm, P., Foekema, E.M., Koelmans, A.A., 2018. *Quantifying ecological risks of aquatic micro- and nanoplastic. Critical Reviews in Environmental Science and Technology*, 1-49.

Blettler, M., Abrial, E., Khan, F., Sivri, N., Espínola, L., 2018. Freshwater plastic pollution: Recognizing research biases and identifying knowledge gaps. *Water Res.* **143**, 416–424.

Crawford, C.B., Quinn, B., 2017. Plastic production, waste and legislation. Microplast. Pollut. 30, 39–56.

de Souza Machado, A.A., Lau, C.W., Till, J., Kloas, W., Lehmann, A., Becker, R., Rillig, M.C., 2018. Impacts of Microplastics on the Soil Biophysical Environment. *Environmental Science & Technology*. **52**, 9656-9665.

He, D., Luo, Y., Lu, S., Liu, M., Song, Y., Lei, L., 2018. Microplastics in soils: analytical methods, pollution characteristics and ecological risks. *TrAC Trends in Analytical Chemistry*. **109**, 163–172.

Mai, L., Bao, L.-J., Shi, L., Wong, C.S., Zeng, E.Y., 2018. A review of methods for measuring microplastics in aquatic environments. *Environmental Science and Pollution Research.* **25**, 11319-11332.

Mani, T., Blarer, P., Storck, F.R., Pittroff, M., Wernicke, T., Burkhardt-Holm, P., 2019. Repeated detection of polystyrene microbeads in the Lower Rhine River. *Environmental Pollution*. **245**, 634-641.

- Miller, M.E., Kroon, F.J., Motti, C.A., 2017, Recovering microplastics from marine samples: A review of current practices. *Marine Pollution Bulletin.* **123**, 6–18.
- Peng, G., Xu, P., Zhu, B., Bai, M., Li, D., 2018. Microplastics in freshwater river sediments in Shanghai, China: A case study of risk assessment in mega-cities. *Environmental Pollution*. **234**, 448-456.
- Prata, J.C., da Costa, J.P., Duarte, A.C., Rocha-Santos, T., 2019. Methods for sampling and detection of microplastics in water and sediment: A critical review. *TrAC Trends in Analytical Chemistry*. **110**, 150-159.
- Shapiro, G.I., 2019. Black Sea circulation. *Encyclopedia of Ocean Sciences*, **3**rd Edition, 303-317.
- Schwarz, A.E., Ligthart, T.N., Boukris, E., van Harmelen, T., 2019. Sources, transport, and accumulation of different types of plastic litter in aquatic environments: A review study. *Marine Pollution Bulletin.* **143**, 92-100.
- Stock, F., Kochleus, C., Bänsch-Baltruschat, B., Brennholt, N., Reifferscheid, G., 2019. Sampling techniques and preparation methods for microplastic analyses in the aquatic environment A review. *TrAC Trends in Analytical Chemistry.* **113**, 84-92.
- Triebskorn, R., Braunbeck, T., Grummt, T., Hanslik, L., Huppertsberg, S., Jekel, M., Knepper, T.P., Krais, S., Müller, Y.K., Pittroff, M., Ruhl, A.S., Schmieg, H., Schür, C., Strobel, C., Wagner, M., Zumbülte, N., Köhler, H.-R., 2019. Relevance of nano- and microplastics for freshwater ecosystems: A critical review. *TrAC Trends in Analytical Chemistry.* **110**, 375-392.
- Thompson R.C., Moore C.J., vom Saal F.S., Swan S.H., 2009. Plastics, the environment and human health: current consensus and future trends. *Philos. Trans. R. Soc. B.* **364**, 2153-2166.
- Topçu, E.N., Tonay, A.M., Dede, A., Öztürk, A.A., Öztürk, B., 2013. Origin and abundance of marine litter along sandy beaches of the Turkish Western Black Sea Coast. *Marine Environmental Research*. **85**, 21-28.
- Tuncer, G., Karakas, T., Balkas, T.I., Gökçay, C.F., Aygnn, S., Yurteri, C., Tuncel, G., 1998. Land-based sources of pollution along the black sea coast of Turkey: Concentrations and annual loads to the black sea. *Marine Pollution Bulletin.* **36**, 409-423.
- Wagner, M., Lambert, S., 2018. Freshwater Microplastics: Emerging Environmental Contaminants? Springer International Publishing, Cham. DOI 10.1007/978-3-319-61615-5.

HABITAT MAPPING ON THE ROMANIAN SHELF BASED ON MULTIBEAM BATHYMETRY AND SIDESCAN SONAR MEASUREMENTS, INTEGRATED WITH GEOLOGICAL AND BIOLOGICAL DATA

Adrian POPA^{1,2}, Adrian TEACĂ³, Mihaela MUREŞAN³, Gabriel ION¹, Begun TATIANA³, Mihai Emilian POPA²

¹National Institute of Marine Geology and Geoecology – GeoEcoMar, 23-25 D. Onciul St, Bucharest, e-mail: adrian.popa@geoecomar.ro

²Faculty of Geology and Geophysics, University of Bucharest, 1 Nicolae Bălcescu Bd., Bucharest ³National Institute of Marine Geology and Geoecology – GeoEcoMar, 304 Mamaia Boulevard, Constanța

Introduction

The shelf represents a very large part of Romanian Black Sea and has significant ecological, touristic and comercial value. As in other marine regions, the Black Sea shelf in general and the Romanian one in particular contain diverse marine habitats; noteworthy the shelf region, along with the coastal area are the most impacted. Presently, the Black Sea ecosystems are under pressure and mirror different stress factors, such as natural and/or antropic: coastal erosion, climate changes, pollution and fishing. Today's policies at national and European levels require the sustainable development of the marine space and coastal areas.

In recent years, the NIRD GeoEcoMar developed several projects regarding the habitat mapping on the Black Sea shelf. These projects are part of a national multianual project, financed by the Minister of Research and Innovation; their main objectives are ellaboration of marine habitat maps and to assess the impact of stress factors and the changes of marine habitats in time. The final scope of the research is to provide a complete picture of areas of interests for realizing a long-term protection and for minimizing the negative anthropogenic effects on them. Additionally, the economic resources represented by various marine species are important and must be kept in line with the sustainable development.

| No. | Year | Cruise ID | Work Area | Area cover |
|-----|------|-----------|--|----------------------|
| 1 | 2017 | MN-164 | ROSCI-0293 Costinești-23 August | 18,5 km² |
| 2 | 2018 | MN-175 | ROSCI-0281 Cape Aurora | 21,0 km ² |
| 3 | 2018 | MN-175 | ROSCI-0094 Sulphide springs from Mangalia and ROSCI-0281 Cape Aurora | 25,5 km ² |
| 4 | 2018 | MN-179 | Front of Constanța town and Siutghiol Lake | 53,0 km ² |
| 5 | 2019 | MN-198 | ROSCI-0066 - Danube Delta - Marine Area | 59,0 km ² |

Table 1. Areas studied between 2017 and 2019 for habitat mapping in the projects of NRDI GeoEcoMar

For most of these projects the target regions were protected areas, parts of the Natura 2000 network, along with an area situated north to the Constanța harbour. This particular area was under a severe stress, as a large quantity of sand was extracted for the beach nourishment in Constanța, Mamaia and Eforie beaches. Regarding the Natura 2000 network, this incudes both marine and terrestrial protected areas that have an ecological coherence and contribute significantly to the maintanance of biological diversity within the biogeographic region concerned. It is comprised from Special Protected Areas (SPA) which are designated under Birds Directive (Directive 2009/147/EC of the European Parliament and of the

Council) and Sites of Community Importance (SCI), which are designated under Habitats Directive (Council Directive 92/43/EEC).

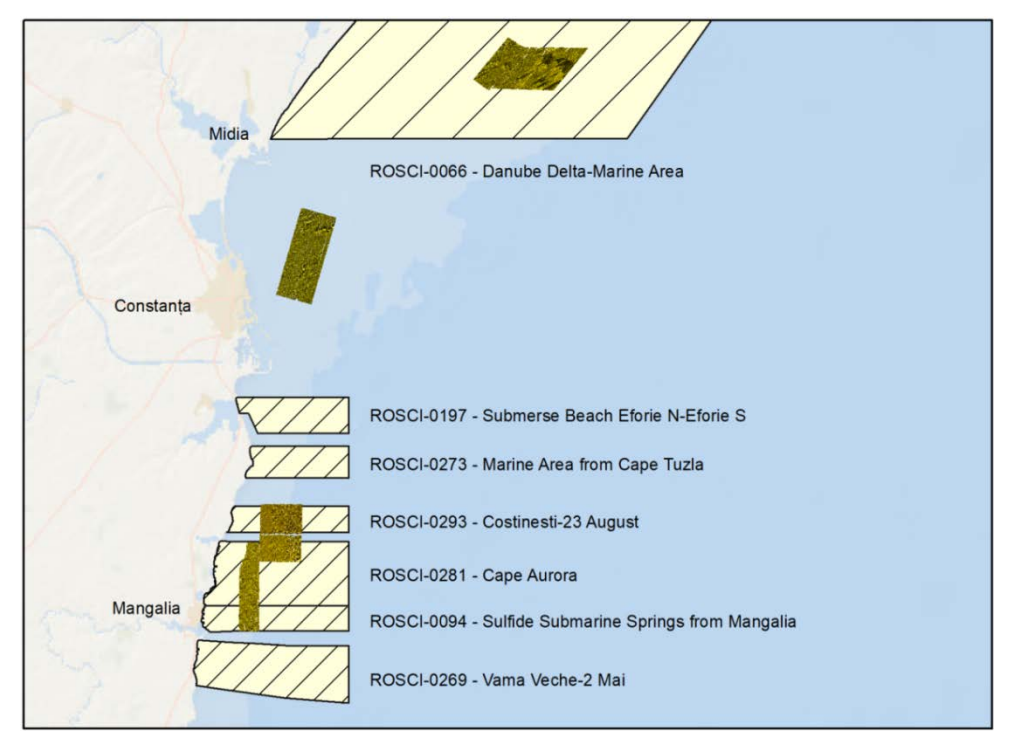


Fig. 1. Study areas investigated between 2017 and 2019 – in brown; Natura 2000 protected areas – in yellow.

This paper aims to present the method used for habitat mapping and the achivements made in this field. These specific research projects began in 2017 and continued in 2018 and 2019. Until now, investigations have been realized in 5 areas from which 4 are included in protected areas. In total more than 177 km² were covered in 3 years (Table 1 and Fig. 1).

Materials and Methods

The researches integrate geophysical methods for acoustic seabed classification with a systematic sampling for biological and sedimentological analysis. In this integrated approach, a multibeam sonar is used, along with a sidescan sonar; the results are correlated with the sedimentological and biological obtained data.

Acoustic seabed classification was first developed in 1960s and 1970s when first multibeams were available. The developments in marine acoustics hardware in 1990s and 2000s made the method much more used. Presently, the acoustic classification of marine sediments has a broadscale use in the world, and, coupled with sediment sampling (for groundtruthing) and biology, gave the best results for habitat mapping on large areas (Anderson et al., 2008). This method has limited use in Romanian and Bulgarian waters in recent years but we do not have knowledge of other countries bordering Black Sea that have done work in this area.

Concerning the methodology employed in our research, first, the data from sidescan and multibeam is processed and sidescan mosaics and bathymetric maps are made. The data is then analyzed by a multidisciplinary research team including geophysicists, biologists and geologists. After analyzing the data, samples are taken from each representative areas and grain size and biology analysis is done. Grain size is determined in the laboratory, from samples collected with a Van Veen grab, while for biological investigation the samples are washed, sorted and preserved on spot, being subsequently studied in the laboratory. The final results are the habitat maps in which, one large studied region is divided in smaller areas, according to each found habitat. The habitats are classified using EUNIS classification system

(European Nature Information System) (Populus et al., 2017), while the identified species nomenclature is in agreement with the World Register of Marine Species (www.worms.org).

Marine habitats may be defined on 3 levels. The first level is the geomorphological one, pointed out based on bathymetric investigation. The bathymetric maps may show the bottom morphology, the depth and slope of terrain, or a depth profile. The second level is the sedimentological one, which is best evidenced based on sidescan sonar. By analyzing the backscatter of the sidescan sonar sonograms is possible to point out the grain size of the sediment: finer sediments as mud have a smaller backscatter value resulting in a darker image on sonogram, while coarser sediments have bigger backscatter value resulting in luminous image. The very coarse (shelly) sediments appear even more luminuos on sonograms and rocks appear very clear and distinct. From the final mosaic resulting from processing all sidescan sonar sonograms, the biological sample locations are choosed. The samples are needed for ground truthing. The 3rd level is the biological one. The same samples which are analyzed for grain size are also analyzed for biology. The classification scheme for habitats take into account the ecological significance, abundance, frequency and average density. By means of GIS technology all information, acoustic, sedimentologic and biologic is fuzioned as a habitat map, where the investigated area is split into specific regions according to EUNIS classification scheme.

Constanța Area Survey

In 2018, a site of 52,5 km² in front of Constanţa city and Siutghiol Lake was studied. This survey was a followup of a survey made in 2016, in which bathymetry was recorded and samples were taken. The depth within the whole study area is between 22 m and 28 m. The whole area is under severe stress from two main reasons. First, in more than 2/3 of the area, bottom trawling is very active for *Rapana venosa* and for *Mytilus galloprovincialis* mollusk species. The trawling traces are 4-5 m wide and are seen very clear on sidescan sonar sonograms. The by-catch is estimated by some studies at 30%, formed mainly by other mollusks (*Spisula, Abra, Pitar* and *Acanthocardia*), crustaceans and fishes (mostly juvenile specimens). Another stress factor is represented by the extraction, in the year 2015 of sand on an area of 2.5 km² for Constanţa, Mamaia and Eforie beaches nourishment. Ditches of 1-3 m depth have been evidenced based on bathymetric investigations; besides, a severe disturbance in benthic fauna has been found in the collected samples. Significant changes in terms of diversity and abundence of species and dominance of some functional grups were recorded (Teacă et al., 2019, Mureşan et al. 2019).

In all, four broadscale marine habitats were identified whitin this area, as follows (Fig. 2):

- circalittoral mud have the largest spreding, aprox. 31.5 km²
- circalittoral mixed sediments between mud, sand and coarse sediments areas: 15 km²
- circalittoral sand mostly in dredged area, 2.6 km²
- circalittoral coarse sediments (shell debris): 3.4 km²

In the circalittoral mud habitat, the dominant taxa belong to the Annelida Phyllum (oligochaetes and polychaetes), including *Mellina palmata, Nephtys hombergii* and *Heteromastus filiformis* and bivalves, such as *Abra nitida, Spisula subtruncata* and *Acanthocardia paucicostata*. The bivalves represent 92% of the biomass, the annelids represent 4% of biomass and 68% of total density, while the rest are crustaceans or other marine organisms. The marine habitat is named after the dominant species: *Mud sediments with Mellina palmata* (Teacă et al., 2019).

In the circalittoral mixed habitat, the main groups of identified marine taxa are similar with the ones found in the circalittoral mud habitat aforedescribed; the difference is given by the dominant species. In the circalittoral mixed habitat, the annelids are dominated by *Prionospio multibranchiata*, *Pygospio elegans*, *Mellina palmata*, while *Nephtys hombergi* and *Micronephthys stammeri* shows a low abundance. The most numerous bivalves are *Abra nitida*, *Spisula subtruncata* and *Pitar rudis*, but they represent only 76% of biomass (Teacă et al., 2019).

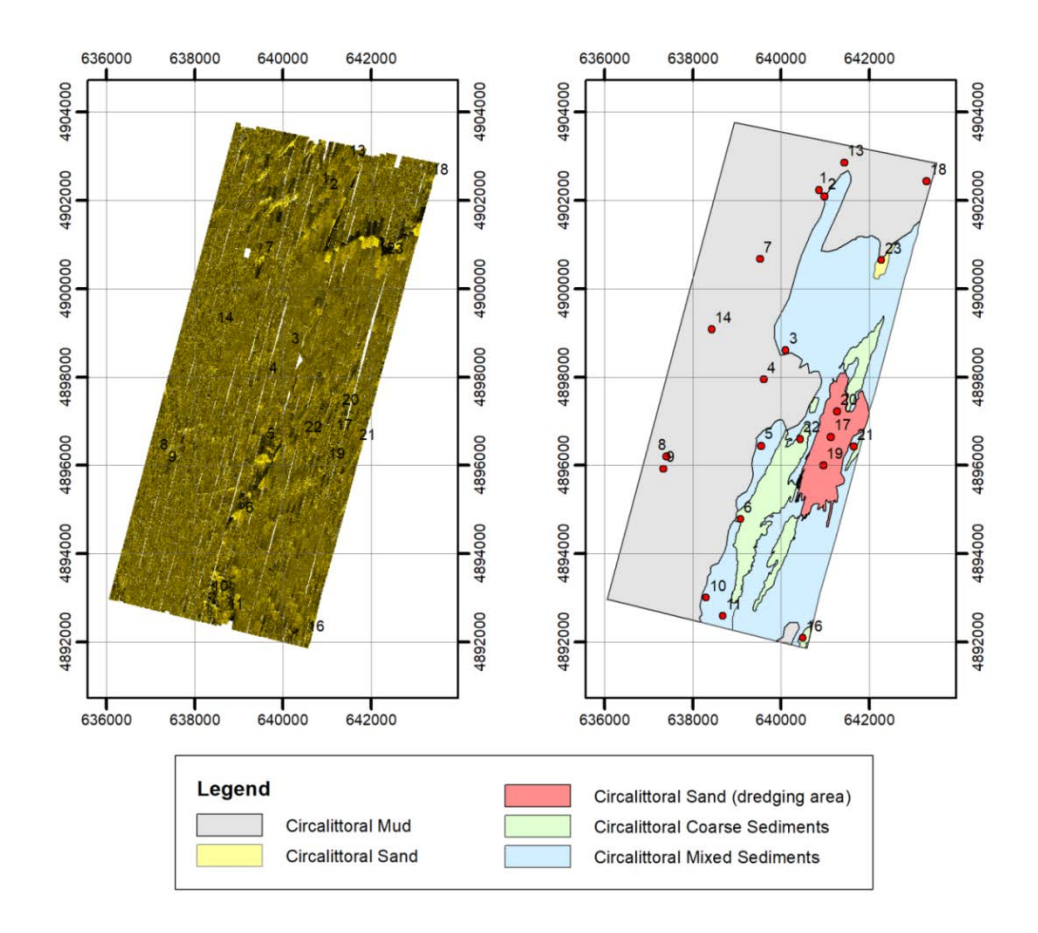


Fig. 2. Sidescan sonar mosaic and the map with the identified habitats in the Constanta-Siutghiol Area.

Most of the circalittoral sand habitat was found in the area where the dredge for sand was done, but also in a small region situated in the central-northern part of study area. A clear difference could be seen between the area affected by the sand extraction and the one that was not affected. In the affected area, the number of species were 17 and 24 in the samples taken, while in the northern area was 31. Besides, the biomass is six times larger in the norther area. The affected area is dominated by annelids, i.e., *Mellina palmata*(58% in station 17), while in the northern part (station 23) the mollusks (6 species, 77% biomass) and crustaceans (5 species, 4% biomass) are dominant (Teacă et al., 2019).

The circalittoral coarse sediments habitat is formed mainly from dead shells, which in some areas formed dunes, with a width of 1-1.5 m. The fauna is less numerous, the main present species, such as *Microphthalmus sczelkowii, Prionospio multibranchiata, Polydora cornuta* and *Alitta succinea*, belonging to the annelids (Teacă et al., 2019).

Summary

In the study area, the bottom trawling activities were and still are done in more than 2/3 of the total area, causing siltation which affect the structure of benthal communities. These are also affected by bycatch. Besides, bottom trawling was done north of the investigated area inside NATURA 2000 sites, activity that is forbidden in such areas. The dredging for sand extraction also caused siltation and a total reworking of the sea bottom. It also caused the disappearance of some species in the dredged area, while some opportunistic species like *Mellina palmata* spread in this area.

References

Anderson, J. T., Van Holliday, D., Kloser, R., Reid, D. G., Simard, Y., 2008. Acoustic Seabed Classification: current practice and future directions. *ICES Journal of Marine Science*, Volume 65, Issue 6, September 2008, Pages 1004–1011. https://doi.org/10.1093/icesjms/fsn061

- Mureşan, M., Teacă, A., Popa, A., Begun, T., 2019. Free-living marine nematods community structural changes within a post-dredging site at the Romanian shelf. Journal of Environmental Protection and Ecology 20, No 2, 753–760.
- Populus, J., Vasquez M., Albrecht, J., Manca, E., Agnesi, S., Al Hamdani, Z., Andersen, J., Annunziatellis, A., Bekkby, T., Bruschi, A., Doncheva, V., Drakopoulou, V., Duncan, G., Inghilesi, R., Kyriakidou, Ch., Lalli, F., Lillis, H., Mo, G., Mureşan, M., Salomidi, M., Sakellariou, D., Simboura, M., Teacă, A., Tezcan, D., Todorova, V., Tunesi, L., 2017. EUSeaMap. A European broad-scale seabed habitat map. https://doi.org/10.13155/49975
- Teacă, A., Mureşan, M., Begun, T., Popa, A., Ion, G., 2019. Marine benthic habitats within a physical disturbed site from the Romanian coast of the Black Sea. Journal of Environmental Protection and Ecology 20, 2, 723–732.
- WoRMS Editorial Board, 2019. World Register of Marine Species. Available from http://www.marinespecies.org at VLIZ. doi:10.14284/170. www.marinespecies.org

PRELIMINARY APPROACH FOR FINE INSIGHTS IN CYCADOPTERIS OBTUSIFOLIA FROM ROMANIA, USING TRANSMISSION ELECTRON MICROSCOPY, CHEMICAL ELEMENTS AND EPIFLUORESCENCE

Mihai Emilian POPA^{1,2}, Gaëtan GUIGNARD³

¹University of Bucharest, Faculty of Geology and Geophysics, Laboratory of Palaeontology 1 N. Bălcescu Ave., 70111, Bucharest, Romania, e-mail: mihai@mepopa.com

²Southwest Petroleum University, School of Geosciences and Technology, 8, Xindu Ave., 610500 Xindu, Chengdu, China

³Université Lyon 1, F-69622, Lyon, France. CNRS, UMR 5023 LEHNA, 7-9 rue Raphaël Dubois 69622 Villeurbanne cedex France. Centre technologique des microstructures Université Lyon 1 France e-mail: guignard@univ-lyon1.fr

Genus *Cycadopteris* Zigno emend. Barale 1982 is represented by Jurassic foliage belonging to seed-ferns (Class Petridospermopsida) with peculiar characters, such as the lack of forked fronds and abaxially folded pinnules. The leaves are hypostomatic and coryaceous, with stomata confined to abaxial areas partially covered by lamina folds. Barale (1982) emended the genus, demonstrating the junior synonymy of genus *Lomatopteris*, with key species such as *Cycadopteris brauniana*, *C. jurensis* and *C. moretiana*.

Cycadopteris obtusifolia (Andrae) Popa 2000 is a representative from Anina, formerly known as Steierdorf, Reşiţa Basin, South Carpathians, Romania, belonging to the Tâlva Zânei Formation, Middle Jurassic in age (Upper Toarcian – Callovian). It was defined, described and illustrated by Andrae (1855) as Sphenopteris obtusifolia in his monograph dealing with the fossil flora of Anina (Steierdorf). The holotype was lost, but Semaka (1972) described a historical material also collected in the XIX-th Century from Anina, Caraş-Severin County, as Sphenopteris obtusifolia, and established a neotype on a single hand specimen available, now stored at the Geological Museum, Geological Institute of Romania in Bucharest. This sample was studied by Popa (2000) who assigned it to genus Cycadopteris and described its cuticles, comparing the material with similar species such as Cycadopteris jurensis and Pachypteris gradinarui. A second sample belonging to Cycadopteris obtusifolia with the same geographical and stratigraphical occurrence was found by Popa in 2008 (Popa and Meller, 2009) within the palaeobotanical collections of the Geological Survey of Austria (GBA) in Vienna.

The sample curated in Bucharest is now subject of a new study, as the cuticle of *Cycadopteris obtusifolia* was analyzed using epifluorescence microscopy, transmission electron microscopy (TEM) enabling 70 nanometers sections (Fig. 1). Chemical elements were also analyzed through TEM and scanning electron microscope SEM.

For epiflorescence, the samples were first treated with HCl and HF and studied using a Carl Zeiss Axioscope microscope with ultraviolet reflected ligh, digital camera and Carl Zeiss Axiovision software for enhancing the image quality (z-stacking).

The samples for transmission electron microscopy (TEM) were prepared following Lugardon's technique (1971). Pieces were embedded in Epon resin, then 70 nanometers ultrathin sections were achieved, as transversal sections (i.e. perpendicular to the leaf length) or as longitudinal sections (i.e. parallel to the leaf length). Sections were collected on uncoated 300 Mesh copper grids, they were observed and photographed with a Philips CM 120 at 80 kV, at the Centre de Technologie des Microstructures ($CT\mu$) of Lyon-1 University, France.

The EDS analysis was performed on both TEM and SEM. The TEM system is a SIRIUS SD ENSOTECH with IDFIX software, acceleration voltage 120kV, spot sizes 1-3, processing time 120 seconds, constant of time 4 μ seconds. Measurements (5 for each check) are evaluated with Mann Withney test, using XLSTAT version 2019.1 software. The SEM system was used with resin blocks used for TEM sections, 10 nm of

thickness carbon-coated, with a BALZERS MED010. The SEM equipment is a Zeiss Merlin compact 10 kv, where EDS analysis is using Oxford X-max 50 mm2, AZTEC software. For TEM and EDS statistics, XLSTAT 2019.1 was used (Addinsoft (2019). XLSTAT statistical and data analysis solutions were used.

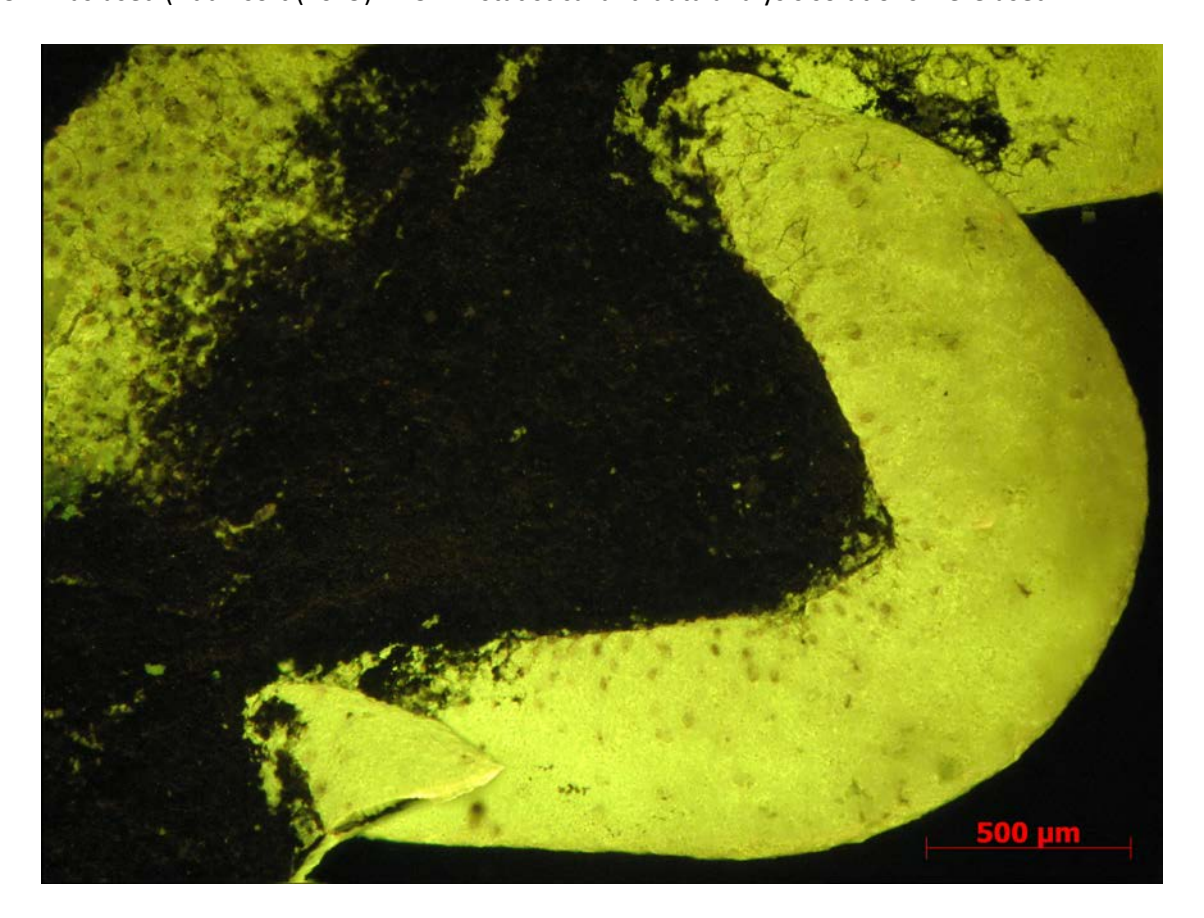


Fig. 1. Pinnule of Cycadopteris obtusifolia, abaxial view in epifluorescence showing the abaxial fold.

As first results, this complementary approach shows the excellent quality of the material, therefore allowing to state that *Cycadopteris obtusifolia* cuticular membrane CM is made with A2 granular layer of the cuticle proper CP, and B1 and B2 layers of the cuticular layer CL. Comparing with other Pteridospermopsids where cuticle details are known (Guignard 2019), *Cycadopteris obtusifolia* has some affinities with *Pachypteris*, which has a much more complex but also « partly » made with A2 and B1 layers (Guignard et al. 2004). Also, its cuticle is very different from *Komlopteris* and *Dichopteris*, which have very simple cuticles that have only the A2 layer (Guignard et al., 2001; Thévenard et al., 2005).

The chemical elements analysis reveals that, although both upper and lower cuticles have many affinities, some differences between the upper and the lower cuticles occur, and a relation with their functions can be demonstrated.

References

Andrae, C., 1855. Fossile Pflanzen der Tertiarformation von Szakadat und Thalheim in Siebenburgen und der Liasformation von Steierdorf im Banate. Zeitschr. Naturwiss. Halle: 201-207.

Guignard, G., Boka, K., Barbacka, M., 2001. Sun and shade leaves? Cuticle ultrastructure of Jurassic *Komlopteris nordenskioeldii* (Nathorst) Barbacka. Review of Palaeobotany and Palynology 114, 191–208.

Guignard, G., Popa, M.E., Barale, G., 2004. Ultrastructure of Early Jurassic fossil plant cuticles: *Pachypteris gradinarui* Popa. Tissue and Cell 36, 263–273.

Guignard G. (in press) Thirty-three years (1986–2019) of fossil plant cuticle studies using transmission electron microscopy: a review. Review of Palaeobotany and Palynology, special issue on "Plant cuticles, fine details", edited by Gaëtan Guignard, Erwin Zodrow and Georgina Marisa Del Fueyo.

- Lugardon, B., 1971. Contribution à la connaissance de la morphogénèse et de la structure des parois sporales chez les Filicinées isosporées (Unpublished Thesis). Toulouse University, France (in French).
- Popa, M.E., 2000. Early Jurassic land flora of the Getic Nappe, University of Bucharest, Bucharest, 258 pp. PhD thesis.
- Popa, M.E., Meller, B., 2009. Review of Jurassic plants from the Anina (Steierdorf) coal mining area, South Carpathians, in the collections of the Geological Survey of Austria. Jahrbuch der Geologischen Bundesanstalt 149, 487-498.
- Semaka, A., 1972. Einige Bemerkungen zu *Sphenopteris obtusifolia* Andrae. Palaontologische Abhandlungen B, 3: 861-866.
- Thévenard, F., Barale, G., Guignard, G., Daviero-Gomez, V., Gomez, B., Philippe, M., Labert, N., 2005. Reappraisal of the ill-defined Liassic pteridosperm *Dichopteris* using an ultrastructural approach. Botanical Journal of the Linnean Society, London 149, 313-332.

THE ODYSSEY OF MINERALS RESOURCES VS. NECESSITIES, POSSIBILITIES AND REQUIREMENTS

Gheorghe C. POPESCU¹, Antonela NEACŞU²

Dept. of Mineralogy, Faculty of Geology and Geophysics, University of Bucharest e-mail: ¹gheorghec.popescu@yahoo.com, ²antonela.neacsu@gmail.com

Introduction

The relationship between man and mineral resources has developed under auspices of the interaction between the needs, possibilities and requirements. These factors have acted in a historical succession: necessity, imposed by the feeding and protection requirements of the primitive man, followed by the possibilities of obtaining resources and ultimately, by the modern demands and limits according to which society had to take into account the natural framework (Fig. 1).

Raising requirements have imposed an extension of the interaction between humans and minerals. At first, man used stone, most likely for defense and hunting, thus acting alone. Then, by appreciating other benefits of rarer materials, humans began to use metals such as gold, copper, tin, iron, which, certainly, required a collective will and action for discovering, mining and processing.

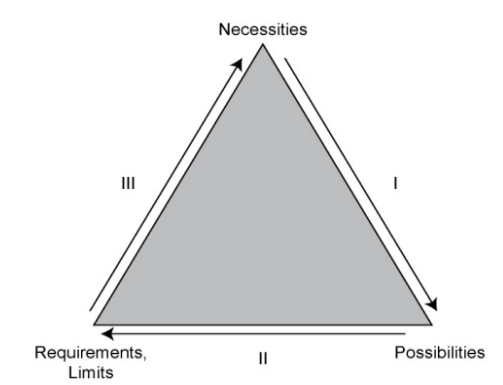


Fig. 1. Diagram of interactions between necessities, possibilities and requirements in the process of usage of mineral resources. I — the primary stage when necessities determined the usage of unprocessed or slightly modified raw materials; II — the secondary stage when resources were processed without inflicting a bad influence over the environment; III — the tertiary stage when resource processing and consumption tend to overcome the supportability of nature. For this reason, the resource consumption needs to be rationalized.

In this context, man has certainly noticed the minerals with aesthetic features, which he used as adornments, and in magic; later, the useful properties of such minerals were understood and man's life witnessed a significant improvement. Besides, the name 'mineral' comes from minera = ore, which underlines that ever since the beginning, man has regarded minerals from a utilitarian point of view.

The most of the tools and weapons used by prehistoric man were manufactured from broken and later chiseled flint. This signified the exercise of a choice, the knowledge of properties yielded by certain stones, from the many occurring on Earth's surface. After "testing" other stones such as granite, quartzite, hard limestone *etc.*, the prehistoric man noticed the advantages of flint and started to look for it that is they *surveyed* and exercised for the first time *economic geology*. The extraction of flint has meant digging galleries and pits, thus putting the man in the posture of *mining*. These activities developed over a long period, until approximately from 2500 B.C. Later, metals began to be used on a current basis. The first 'geologists' and miners have surveyed and extracted ores, from which copper was firstly obtained, followed by bronze, and eventually by iron.

Metals in human society

The first metal observed and used by man – mainly due to its native color, was gold. Owing to its remarkable malleability and ductility, gold was easy to distinguish from hard and brittle stones. Gold could easily be processed and shaped, which helped in developing a specific processing technique long before its extraction from ores.

Its unique properties conferred gold a value which surpassed the simple status of a raw material, and has often been assigned with mystical properties, qualifying it as a symbol of wealth and power; however, gold has not left its sign over an entire epoch of the human history as other metals did (e.g., copper-bronze, iron, aluminum).

In native and unoxidized form, copper was equally shinning as gold, but harder and more abundant, and has been intensely used for manufacturing tools and weapons. For this reason, copper was heavily extracted especially from the oxidation zones of superficial ore deposits, which drew attention by their vivid colors. Owing to the genetic association between copper and tin in several metallogenic districts (e.g. Erzgebirge or Cornwall), the primitive man has probably accidentally produced *bronze* (Popescu, 2002, Laznicka, 2006), which marked an entire epoch of the human history.

The manufacturing of tools from metals or alloys represented an obvious technical progress. Metal weapons also proved to be more efficient both in hunting and war. On the other hand, metals were rare and difficult to get, hence very expensive; as a matter of fact, the word *metal* derives from Greek and means *to search*. For this reason, metals were often used to manufacture luxury objects. Thus, for a long time, farmers and craftsmen have continued to use stone tools and objects. Bronze was most durable than stone and began to be used for large scale production of tools and weapons. Even before 3000 B.C. the metal production raised to several tons of Cu (Sn)/year, and several kilograms of Au/year. A special situation occurred on the present day territory of Romania, where tin was absent. Thus, tin was *imported* from the Erzgebirge area (Macovei & Popescu, 2011). Slowly, bronze has replaced stone, and the Bronze Age took the place of the Stone Age.

In the early times, iron was as rare as copper, due to the difficulties raised by its extraction. Iron was obtained through ore melting in clay furnaces with air bellows. In fact, owing to the poor quality of pure iron which was soft and oxidable, the new metal was also an alloy of iron and carbon, most probably obtained accidentally through contamination with charcoal. In time, man has learned how to obtain cast iron and steel and a new occupation of blacksmithing has emerged.

Starting with 1751 and until the end of the 19th century, 49 new elements were added to the Mendeleev Table, while during the 20th century only two new elements were added: hafnium in 1922 and rhenium in 1925 (Laznicka, 2006). In this context, aluminum discovered in 1808 by Davy, was only used in 1880 when the industrial demand for this metal raised considerably, qualifying it as the second industrial metal after iron. Uranium is another example of a large time interval between its discovery and industrial use. Discovered in 1789 by Klaproth, it began to be used only after 1890, when its radioactivity was firstly observed and allowed its usage in energetic and weaponry.

The present metal demands refer mainly to the major industrial elements, *i.e.*, iron, aluminum, copper and gold, followed by zinc, nickel, lead, PGE, silver, manganese, cobalt, magnesium, tin, uranium and molybdenum. The mining sector delivers the raw materials to sustain the *Fourth Industrial Revolution*: there are some metals which became of strategic importance in the decades, especially for the top industries, such as IT, aeronautics and defense, new energy sources, energy storage solutions: lithium, beryllium, REE, niobium, tantalum, germanium, cadmium, gallium, tellurium, rubidium, yttrium, and hafnium. Their annual output ranges from several millions USD/year to zero in some countries (Laznicka, 2006). Their impact on the Top 40 financial performance will be *incremental rather transformational*, as production volumes will continue to be dwarfed by the dominant commodities for many years to come (PwC's Mine Report, 2019).

Gold transactions increased from 8% on the total Top 40 global mining companies deal value in 2017 to 25% in 2018, and are tracking at close to 95% in 2019 (as at end of April 2019). In 2019, the top five companies make up 50% of total Top 40 market capitalization: BHP Group *Ltd.*, Rio Tinto *Ltd.*, Vale S.A., Glencore *Plc.*, China Shenhua Energy Company *Ltd.* There are four new entrants in Top 40 in 2019: in gold,

Kirkland Lake Gold *Ltd.*, AngloGold Ashanti *Ltd.* and Polymetal International *Plc.*; in coal, PT Bayan Resources Tbk. Over half of the Top 40 produces 55% of global copper production. The decline in 2019 of the copper production, after the past year on year grew of almost 7% for the Top 40, is not yet reflected in the copper price. Coal is very important, supporting 38% of global electricity generation (PwC's *Mine* Report, 2019).

A present feature of the industrial metal production is that more than 95% of them are mined in giant ore deposits (Fig. 2). Mining facilities have grown to huge proportions and focused especially on open pit mining.

The philosophy of mineral resources

Adam Smith's economic theory pleaded for free market, commerce and trade. It is the beginning of the conventional economy, for which natural resources are infinite, because they are not bounded or limited in any *economic* sense (J L Simon, 'The ultimate resource' 1981, 'The Ultimate Resource 2' 1996).

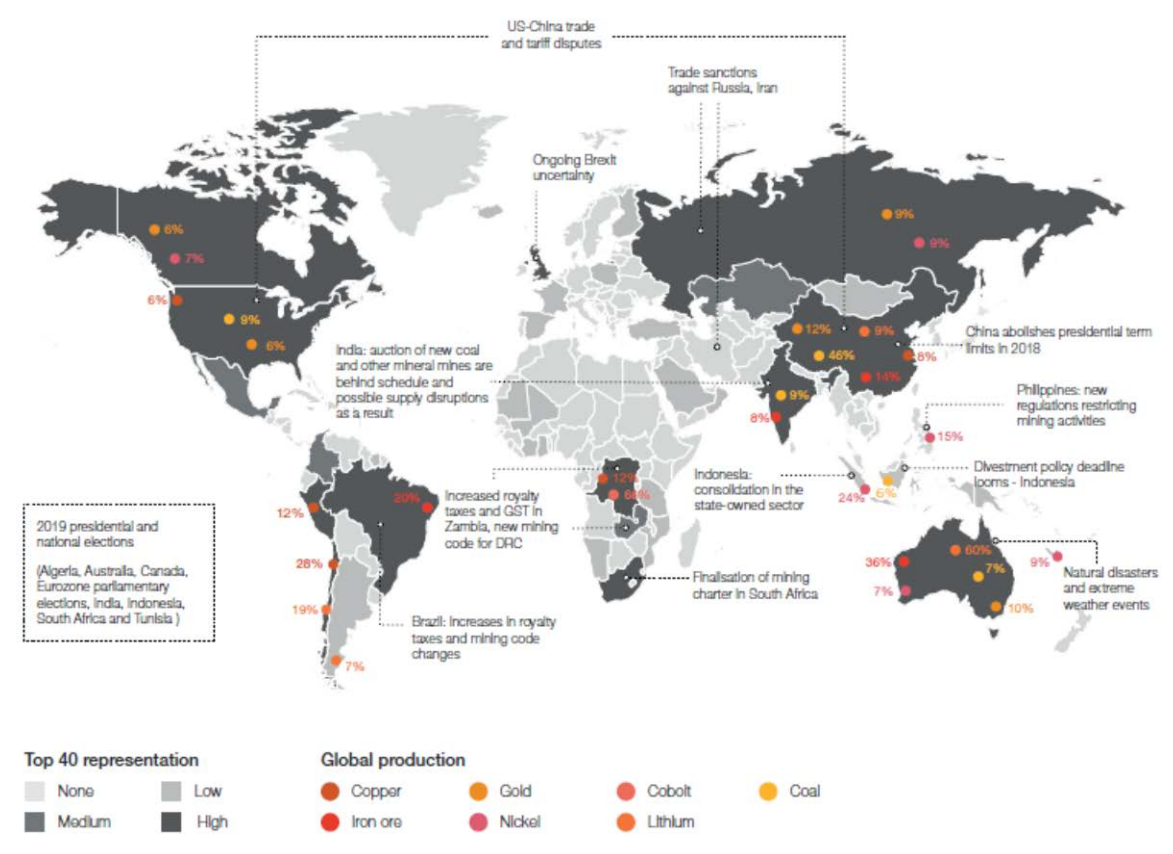


Fig. 2. Top 40 reach and external market drivers (USGS, PwC analysis, in Mine Report, 2019)

During the industrial revolution, the empirical approach of ore deposit surveying could no longer meet the demands. Thus, the need for mineral resources involved a step by step search of the deposits, according to the *centrifugal* principle *ore deposits are found near other ore deposits*. Mining prospectors were focused on ores and their association with certain rocks, so they were not interested to give any explanation looking ore genetic models, and much less about Earth's structure and past evolution.

A.v. Humboldt was the first scientist who presented observation data on the link between igneous rocks and metallic concentrations. Such observations were later explained by Elie de Beaumont in his theory regarding the volcanic and metallic emanations. In fact, his theory materialized two principles which govern the modern metallogeny: the actualism-uniformitarianism principle (as long as metals occur in the modern volcanic terrains, especially in the form of sulfides, the old time ore deposits must have formed in the same way) and the similarity principle (the rocks and ores have formed through the same geological

processes). Such considerations were consistent with the distribution of metallic deposits, most often found in volcanic rocks. This kind of thinking had a guiding role in the discovery of ore deposits and has been fundamenting for a long time the exploration activities.

In our Metaliferi Mts. the gold ore deposits have become more numerous over the time, owing to the discovery of new ore veins near the known ones, or of new ore deposits near the already mined ones. An example is that of Roşia Montană where this kind of discoveries has maintained one of the longest mining activities known in Europe. Moreover, during the 70's, the *porphyry copper* deposit of Roşia Poieni was uncovered in the vicinity of the gold ore deposits. This is just an example of the many pairs of Au-Cu deposits in Metaliferi Mts.: Roşia Montană – Roşia Poieni, Bucium – Tarniţa, Musariu Vechi – Musariu Nou, Troiţa – Bolcana, *etc.* In the Baia Mare district, the eastern extension of the main vein of Baia Sprie outlines the gold ore deposit of Şuior.

The crises of modern Economic Geology

Ever since its foundation at the beginning of the 20th century (Skinner, 2005), several crises occurred in the Economic Geology. It is in fact the consequence of the evolution of geology in parallel with the assumption of the linear or conventional economic model, based on the continuous exploitation of mineral resources.

One of the crises was triggered by the Club of Rome Report in 1972, which stated the intense consumption of metal by emerging industries vs. the limited amount of ore deposits in the Earth's crust.

| Elements | USA crust | Earth's crust | | | |
|----------|-----------|---------------|--|--|--|
| Pb | 1 | 10 | | | |
| Mo | 1 | 23 10 | | | |
| Cu | 1.6 | | | | |
| Ag | 3.2 | 18 | | | |
| Au | 4.1 | 14 | | | |
| Zn | 6.3 | 42 | | | |
| Sb | 11 | 5 30 | | | |
| Hg | 15 | | | | |
| U | 20 | 11 | | | |
| Th | 31 | 22 | | | |
| W | 37 | 4 | | | |
| Ni | 830 | 3 | | | |
| Sn | Very high | 12 | | | |

Table 1. Resources/reserves ratio for some elements (Popescu, 1974).

The report has alerted the governments and suggested an imminent crisis of metallic and energetic raw materials. The solution from the geological point of view came quickly stating that there exist a direct correlation between crustal abundance of the elements and the reserves (McKelvey, 1973). For example, in 1973 the gold reserves were estimated at 0.002 metric tons, with 0.0086 metric tons of potential resources (Erickson, 1973). The resource/reserve ratio was therefore of 4.3, which equaled the odds of discovering new ore deposits. For the entire Earth's crust (minus USA), the reserves amounted 0.0011 metric tons and the resources, 0.15 metric tons, thus yielding a resource/reserve ratio (*i.e.*, ore deposits discovery odds) of 14 (see table 1). Thus, the lower the geological knowledge, the greater the chance of discovering new ore deposits. With the advent of the global tectonics concept, at the beginning of the 70's, exploration works were spectacularly stimulated. The new discoveries have grown the reserves to such an extent that in 2003 the deadline envisaged by the Club of Rome Report was considerably delayed (Schode, 2003).

Concepts as *Material Growth Myth*, *Linear Economy* – based on the continuous exploitation of resources, *Dutch Disease*, GDP as an exact measure of welfare, and *boomerang effect* were vehiculated in the economic literature, all of them meaning finally an increase of demand of resources. In the same time, the world should face the unprecedented rise of pollution, including mining wastes, inequity in mining

policy, the problem of countries rich in mining resources that have become failed states, paralle with mining countries lacking resources that can get to control ore recovery activities, with maximum profit only for their citizens. All these anomalies generating global economic crisis (*i.e.*, '70, 2008, 2011), including also a serious period of stagnation in 2012-2015 in the world wide mining industry.

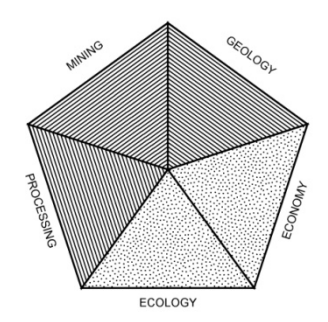


Fig. 3. Diagram of the specific activities involved in the extraction of mineral resources

The last crisis faced by the mineral resource industry was of ecological nature. The negative impact over the environment may be directly related both to the actual mining and to supporting activities which ensure the mining logistics.

The mineral resources represent *geological entities* formed as a result of geological processes. *The issue of how and where ore deposits can be found, may only be solved on the basis of geological principles and by exercising geological sagacity* (Brobst & Pratt, 1973). However, in the present days, a special attention must be given to this issue by the geologists, miners, processing engineers, economists and ecologists (Fig. 1, 3). Based on their expertise, the governmental factors have to decide on the viability of the exploration projects.

A reconciliation of the needs, possibilities and requirements in the process of using mineral resources is imperative nowadays by limiting industrial growth on account of mineral resource extraction. For miners in particular, unconventional economy will be equally focused on managing resources in the market and digging to extract additional resources where needed. Mining companies need to embrace digital technologies to make the transition (S Thimmiah, 'Sustainability in mining: Q &A' 2015). But for technological development, the modern humans need the metals of the Fourth Industrial Revolution. We go back to... economic geology.

As Pricewaterhouse Coopers' 2017 and 2018 Mine Reports stated, recovering from 2015's race to the bottom, the members of the Top 40 paused and drew breath in 2016, obtening a stellar performance in 2017 for global mining industry. But mining requires far more than good financial performance in order to realize value in a sustainable manner (J O'Callaghan, Global Leader, Mining & Metals, PwC Australia) (Pwc's Mine, 2019).

THE NEPHELINE SYENITIC INTRUSIONS IN SOUTHERN BANAT: AGPAITIC CHARACTER, EVOLUTION TRENDS AND QUALITATIVE HFSE AND REE BUDGET

Gavril SĂBĂU

Geological Institute of Romania, 1 Caransebeş St, Bucharest, e-mail: g_sabau@yahoo.co.uk

Several small bodies of nepheline syenite occur in the Late-Variscan-consolidated Ogradena Unit of the Alpine Danubian nappe system of Southern Banat. The identification, locations and a short description are first reported in Streckeisen & Giușcă (1932), who mention characteristic features like the presence of melanitic garnet, strongly zoned clinopyroxene and coarse, abundant poikilitic cancrinite. Anastasiu (1973) describes the main petrographic types and their distribution in three larger sized intrusions, Cărbunăria, Strineac and Dealu Rău. Ifrim and Croitoru (2003) identify optically variable eudialyte supporting an agpaitic character, and the presence of radiometric and geochemical anomalies located both inside the intrusions and at their margin. Ifrim (oral comm.) recognized fenitic alteration zones, indicating a peralkaline character of at least part of the intrusions.

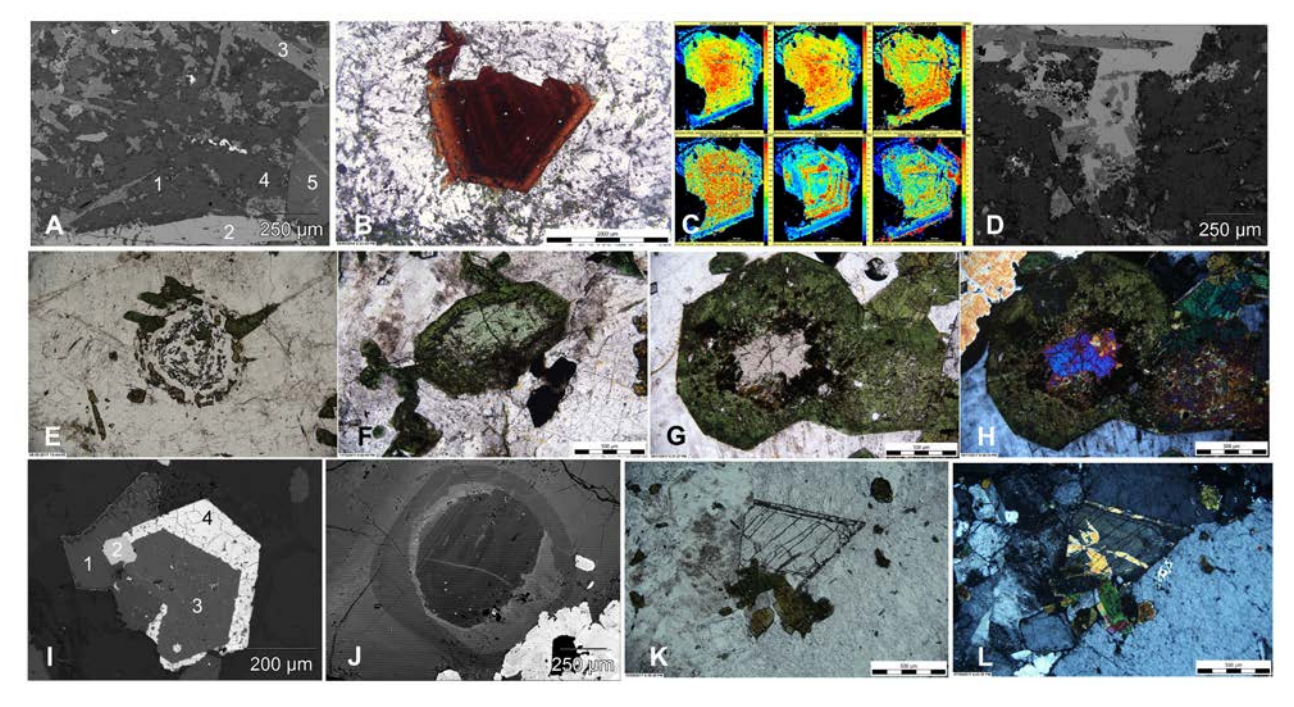


Fig. 1. Mineral composition of the South Banat syenitic rocks A) Back-scattered electron (BSE) image of a garnet ijolite: 1 – nepheline, mostly altered, 2 – garnet, 3 – diopside, 4 – stronalsite, 5 – K-feldspar; B) Microphotograph of a garnet exhibiting concentric zoning and marginal lighter-coloured "spikes"; C) Examples of elemental zonation in a garnet grain, in order Y, Zr, Nd, Eu, Ta, U. Note marginal U-rich overgrowths; D) BSE image of a garnet marginal spike with diopside inclusions; E) Resorbed garnet location with circular shape, isolated garnet relics, the centre being occupied by secondary titanite with circular layout in cancrinite host; F) Diopside antecryst partly rimmed by biotite included in acmite; G) Corroded titanaugite antecryst outlined by biotite and iron oxides, included in acmite; H) The same image with crossed polarizers. Upper left corner sodalite-rimmed cancrinite, lower margin nepheline; I) Accessory minerals in the biotite foyaite: 1 – biotite, 2 – pyrochlore, 3 – apatite, 4 – britholite; J) BSE image of zoned K-feldspar displaying oscillatory zoning, resorption, overgrowth and inclusion in larger phenocryst; K) Photomicrograph of marianoite – wöhlerite grain in association with acmite penetrating in a twinned K-feldspar grain; L) The same field under crossed polarizers, showing twinning and compositional zoning of the grain.

We sampled two syenite occurrences with the best exposures in the area, Strineac and Cărbunăria, with strikingly similar lithologies. The main petrographic types present are foyaite, ijolite and alkali syenite from the marginal facies of the intrusions. Ijolite is quantitatively subordinated, appearing early in the crystalization sequence and contains relatively abundant melanitic garnet. The rock is composed by nepheline, mostly replaced by liebeneritic muscovite, melanitic garnet, diopside, stronalsite and rare epidote (Fig. 1A). Garnet is strongly zoned from andradite to the andradite-schorlomite-morimotoite boundary and contains besides up to 10% Ti a few percents of Zr and Nb. It concentrates most of the trace elements and displays a spectacular zonation with oscillatory concentric, fractionation and patchy patterns, strongly reflected also in the colour of the grains (Fig. 1B). It behaves compatibly for LREE, which amount to hundreds of ppm each, at the same time fractionating Y and HREE. The outer zones or intergranular xenomorphic grains are strongly enriched in U and Th, frequently amounting several hundreds of ppm (Fig. 1C, D). Digested relics of garnet appear in most of the more evolved foyaitic terms.

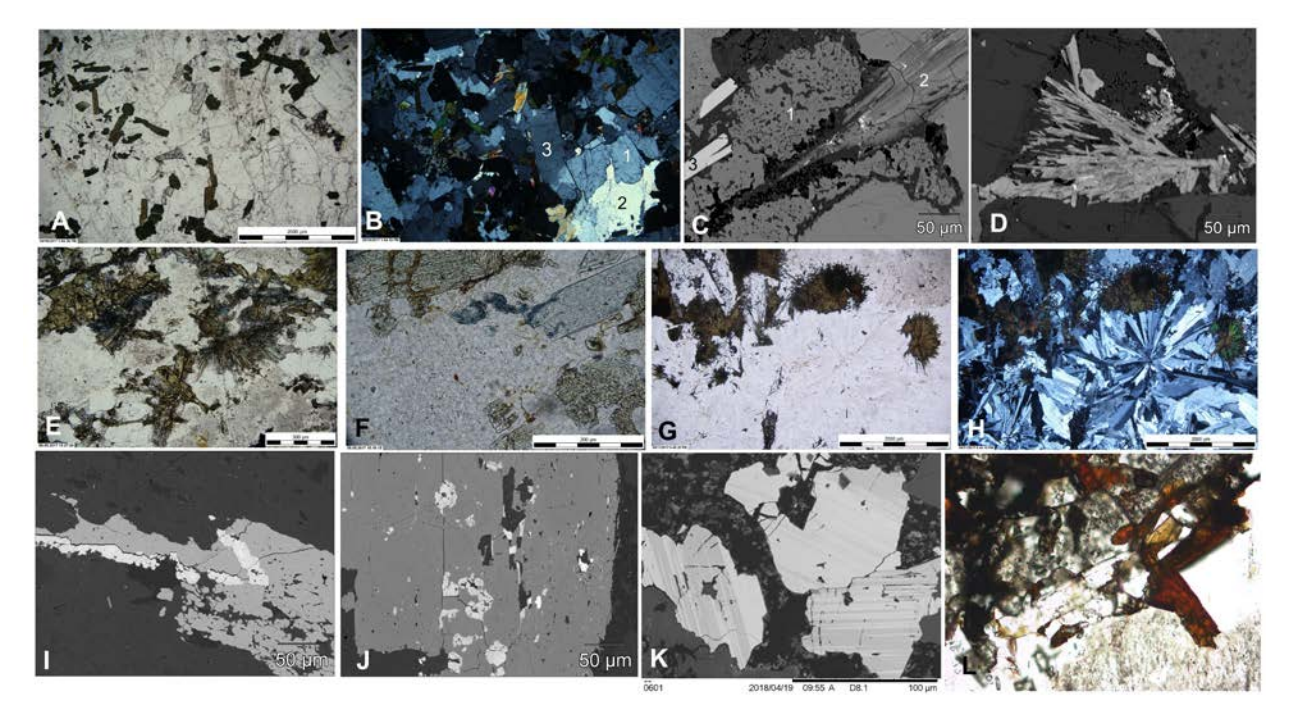


Fig. 2. HFSE and REE minerals in acmite syenite and fenites A) Marianoite – wöhlerite grains in association with acmite in a fine grained syenite; B) The same field under crossed polarizers showing the groundmass consisting of nepheline (1), cancrinite (2) and K-feldspar (3); C) BSE image of a polyphase inclusion in large acmite containing stronalsite (1), an astrophyllite supergroup mineral (2) and marianoite (3); D) Radiating aggregate of rosenbuschite intergrown with "astrophyllite"; the rouded zoner grain in upper central position is kentbrooksite; .E) Microscopic image of a fenite containing acmite rosettes and blue amphibole; F) Alkali amphiboles in fenite; G) Acmite suns set in a groundmass of albite. High relief grains are zircon and acmite is dusted by oxide minerals; H) The same field under crossed polarizers displaying the radiating structure of albite; I) Pyrochlore (bright) intergrown with zircon; J) Pyrochlore and columbite inclusions in manganoan ilmenite; K) REE fluorocarbonates in oriented intergrowt. Brighter is bastnäsite, medium grey parisite and darker grey is synchysite. L) Aeschynite-(Ce) intergrown with zircon.

The sequence of rock types evolves from ijolite to biotite foyaite and finally acmite foyaite to nepheline syenite, as K-feldspar becomes gradually more abundant. The role of main carrier of HSFE and REE, assumed by garnet in ijolite, is taken over by several other phases. The foyaitic rocks start to crystalize as biotite-rich varieties, containing besides nepheline and biotite alkali pyroxene, cancrinite and K-feldspar. Garnet is spectacularly resorbed (Fig. 1E), leaving irregular to atoll-shaped relics in an aggregate formed by cancrinite, titanite and subordinate zircon. Biotite appears often corroded, indicating disequilibrium and resorption after its formation. Pyroxene compositions evolve towards titanian augite and finally acmite. Larger acmite crystals display concentric (continuous to sharply discontinuous) compositional variations, frequently containing corroded antecrysts of different compositions from diopside to titanian augite, sometimes corroded and rimmed by biotite (Fig. 1F-H). Titanite is a major phase, displaying complex

zoning, and is rich in Zr and Nb. Cancrinite develops abundantly in the rock; its the coarse grain size, poikilitic appearance, frequent textural equilibrium and the role in the intergrowths replacing earlier garnet indicate a primary character. Relatively abundant accessories concentrate HFSE (besides titanite) and REE, consisting mainly of pyrochlore often displaying concentric zonation (Fig. 1I), and britholite as independent grains or overgrowing apatite, subordinately zircon, occasionally gasparite-(Ce).

As biotite disappears from the assemblage, K-feldspar becomes more abundant, sometimes inducing porphyric or pegmatoid aspects. In this stage the agpaitic line of crystallization becomes apparent, HFSE being incorporated in phases like terms of the wöhlerite-marianoite series (Fig. 2A), rosenbuschite, kentbrooksite and other eudialyte group minerals (Fig. 1 K-L, 2A), together with an astrophyllite-supergroup mineral similar to sveinbergeite, but containing essential Al, usually associated with rosenbuschite (Fig. 2 C,D). Most of the grains of the wöhlerite solid solution have Zr>Nb (wöhlerite), but some of the grains and zones have Nb>Zr (marianoite).

The important mineral and whole-rock compositional shifts, disequilibrium and corrosion of earlier assemblages, besides indicating the evolution trend, represent evidence for the existence of an intermediate magma reservoir, intermittently replenished with magma batches of different compositions. On the other hand, the similarity of the rock types in different occurrences, extensive recurrent zonation of minerals like garnet and pyrochlore, as well as overgrowth and corrosion episodes of pyroxene and K-feldspar (as indicated mainly by Ba zonation) implies a larger magma chamber with compositional gradients and relatively long residence of the crystals in the parent magma.

The fenitic alteration of the host rocks indicate also larger volumes of peralkaline material as noticed in the field, where ijolite is largely subordinate as compared with other rock types. Fenites appear as fine-grained rocks consisting of albite and acmite rosettes. Alkali amphibole is present, but subordinate (Fig. 2 E-H). Zircon is relatively abundant and well developed, while a large variety of other minerals hosting HFSE and REE appear in smaller quantities. The most frequent is pyrochlore (Fig. 2I), accompanied by britholite, REE fluorocarbonates appearing in oriented intergrowths of bastnäsite to synchysite compositions (Fig. 2 K), manganoan ilmenite, columbite, aeschynite-(Ce) (Fig. 2L), crichtonite, aluminocerite-(Ce).

The diversity and frequent distribution of HFSE and REE in both the syenitic rocks and especially the fenitic alteration zones, poorly known to date, may indicate an interesting potential for these elements.

References

Anastasiu, N., 1973. Corpurile de roci sienitice din cristalinul seriei de Neamţu, Analele Univ. Bucureşti XXII, 54-72. Ifrim, V., Croitoru, Gh., 2003. On the presence of eucolite and eudialyte in the syenites from the south-eastern part of Banat (Almăj Mountains). Petrology – Global context, Anniversary symposium dedicated to acad. Dan Rădulescu, Abstracts, 33-34

Streckeisen, A., Giușcă, D., 1932. Der Nephelin-Cancrinit-Syenit von Orșova (Rumänien) *Bul. Soc. Rom. Geol., Tome I,* 1930, 176-193.

FLUIDS STRIKE BACK – ALKALINE AUTOMETASOMATISM AND PERALKALINE MELT GENERATION AT THE CONTACT OF THE MĂGUREAUA VAȚEI PLUTON, SOUTH APUSENI MOUNTAINS

Gavril SĂBĂU, Elena NEGULESCU

Geological Institute of Romania, 1 Caransebeş St, Bucharest, e-mail: g sabau@yahoo.co.uk

The Măgureaua Vaței pluton is dominantly represented by Ypresian quartz monzodiorite intruded in various lithologies of the Cretaceous Căpâlnaș-Techereu Unit of the South Apuseni Mountains, among which Neojurassic limestone is widespread. The level of erosion corresponds to the apical zone of the pluton, materialized in the outcrop of discontinuous hypabyssal bodies. The contact is outlined by calcic skarn containing high-temperature assemblages with gehlenite (Ștefan et al., 1978), spurrite and tilleyite (Istrate et al., 1978). Detailed accounts of the mineralogy of the skarns are given in Pascal et al. (2001) and Marincea et al. (2001). Associated to the skarn boundary, Pascal et al. (2001) mention alkaline pegmatoids, syenite-like rocks and possible contamination of the marginal part of the intrusion. Săbău & Negulescu (2014) identify the genuine syenitic nature of the rocks referred to by the mentioned authors and their agpaitic character, giving a brief account of the corresponding mineralogy. The present contribution provides more details of the setting, mineralogy and evolution of these agpaitic syenites.

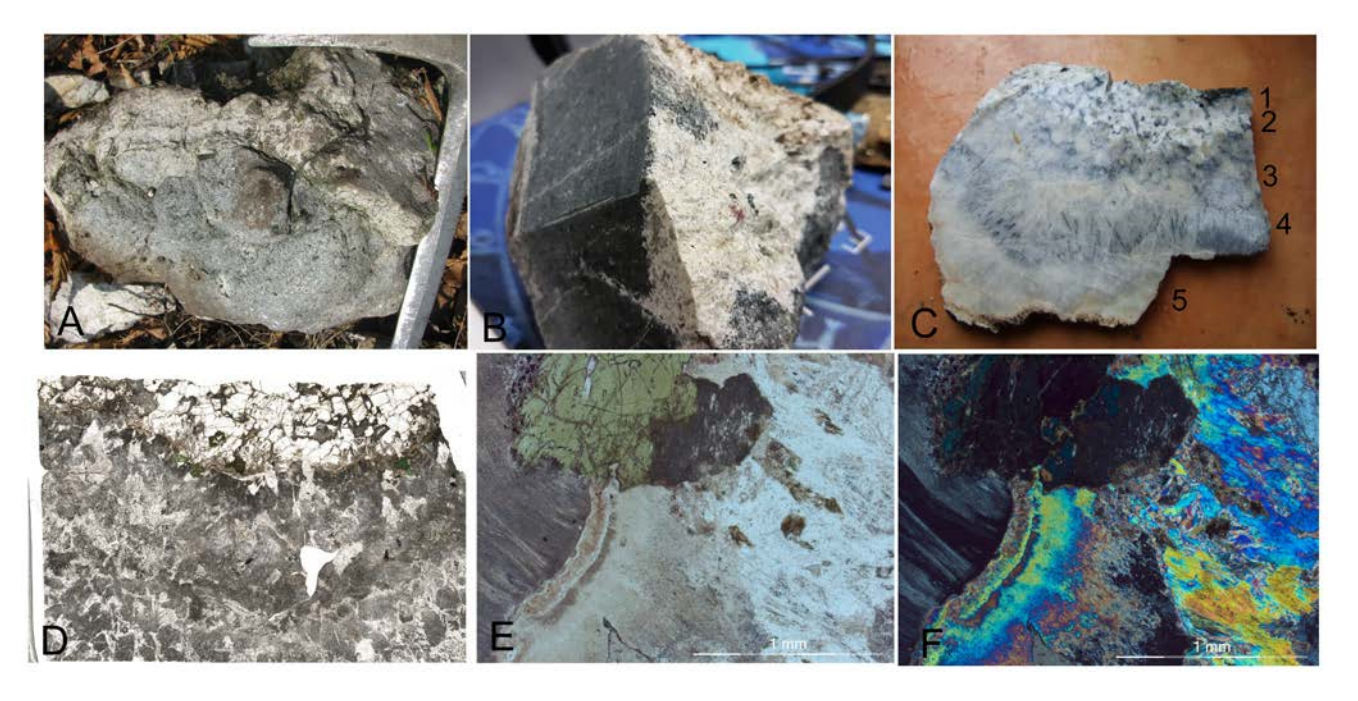


Fig. 1. The occurrence and structure of the agpaitic syenites related to the Măgureaua Vaței intrusion. A) syenite crust on monzodiorite, B) acmite and eudialyte in syenite forming a surface layer and insinuating on veinlets in the monzodiorite. C) The zonality of the syenite: 1- fresh syenite, 2 – diffusion front with incipient transformation in skarn, 3 – skarn with relict structure, 4 – spinifex wollastonite, 5 – altered calcic skarn. D) microscopic image of the syenite/skarn transition with a diffusion front and acmitic pyroxene relics behind the front. In the skarn mass dark lozenge-shaped pseudomoprhs after titanite are recognizable. E) Microphotograph of the diffusion front rich in pectolite extending past an acmite grain. The distal part of the grain is corroded with formation of small sulfide grains. F) The same field under crossed polarizers.

The medium-grained syenite appears at the margin of the intrusion, forming a discontinuous veneer, up to a few centimetres thick, as well as veinlets penetrating the monzodiorite (Fig. 1A, B). The contact is sharp towards the fine-grained, porphyric monzodiorite containing vacuoles, in which amphibole and pyroxene phenocrysts are increasingly replaced by acmitic clinopyroxene and subordinate biotite towards

the contact. The distal contact is diffuse, the syenite grading into fine-grained wollastonitic skarn which contain phantom microtextures indicating former crystals of the same size as those of the syenite, some of which can still be identified as former syenite minerals (Fig. 1C). The main constituents are wollastonite and grossular garnet, along with minor aluminous phlogopite, foshagite, xonotlite, pectolite, prehnite, apatite with limited Cl-ellestaditic substitution and Al, Fe-bearing titanite + wollastonite phantoms with clusters of small perovskite grains. The skarn to syenite boundary is marked by a fine-grained, axiolitic intergrowth of Ca-Si-(Al)-(Na) phases which indicate a diffusion front propagating from the skarn into the syenite, leaving behind more or less decomposed relics (titanite, acmite, eudialyte) (Fig. 1C-F, 2A). The outer boundary of the phantom-bearing skarn is marked by spinifex wollastonite in a fine-grained intergrowth (Fig 1C), in contact with the spurrite and tilleyite calcic exoskarn.

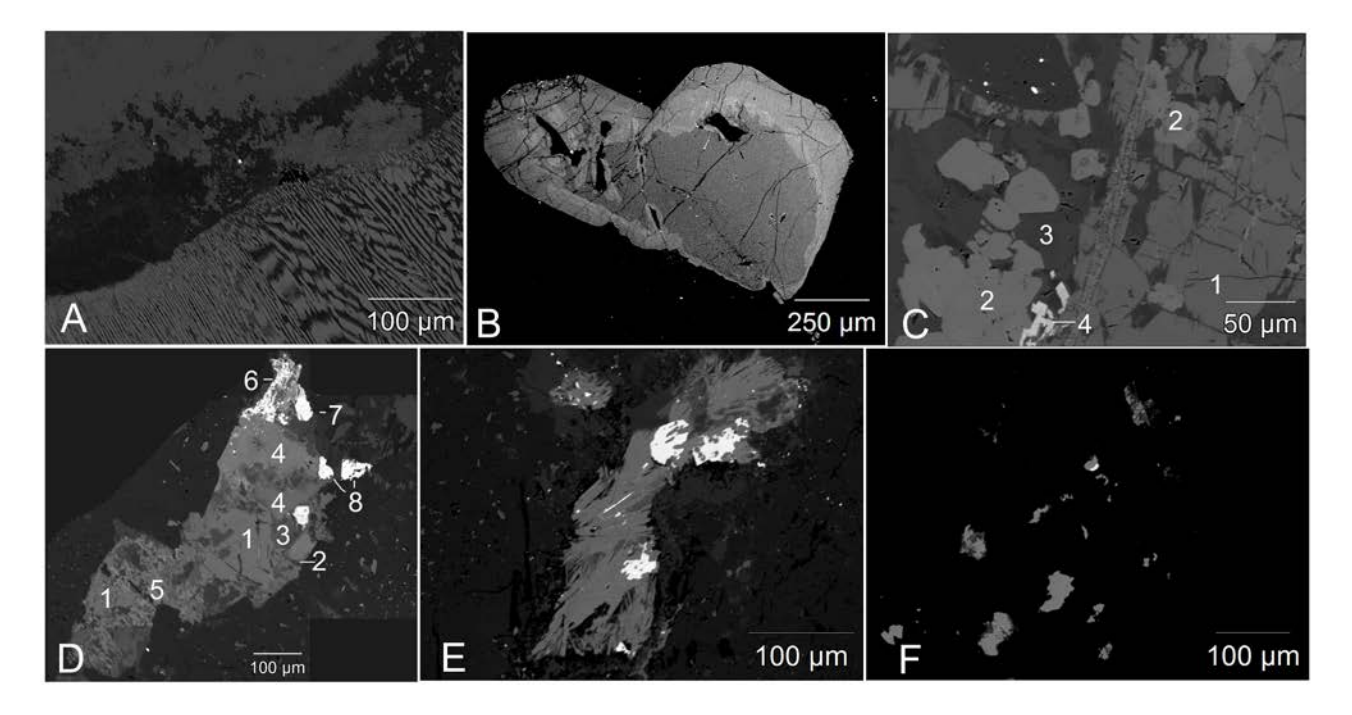


Fig. 2. A) Backscattered electron (BSE) image off the diffusion front displaying fibrous wollastonite, pectolite (grey) and Na-Ca zeolite minerals (dark). B) BSE image of a zoned eudialyte shoving resorption followed by concentric growth. C) Eudialyte (1) overgrown and corroded by dalyite (2), undetermined Fe, Al, Zr, K, Na silicate (3) and turkestanite (4). D) Pseudomorph after eudialyte containing central relics (1), replaced by elpidite (2), pectolite (3), Na zirconosilicates with variable composition (4), gittinsite (5), overgrown and partly replaced by arapovite (6), burbankite (7) and strontianite (8). E) Secondary gittinsite associated with pyrite. F) Cluster of sulfide grains formed around digested pyroxene. Brightest grain is Tl, Fe, Cu djerfisherite.

The primary mineralogy of the syenite is relatively simple, the main primary phases being represented by K-felspar, acmite, titanite, eudialyte, apatite, quartz and minor phlogopite. Eudialyte indicates the agpaitic character of the syenite, displaying limited chemical variation in the pristine grains (not more that a few wt% per element), yet allowing moderate lanthanide substitution and displaying sometimes a zonality given mainly by variations in the moderate Ti contents (Fig. 2B). The zonality indicates resorption of Ti-richer terms and subsequent oscillatory Ti zonation. Apatite appears as a accessory phase and is strontian; some of the grains have micronic stronadelphite crystals perched on the surface. Pectolite appears as coarse-grained crystals in apparent textural equilibrium, but also in replacement aggregates after eudialyte and as rims around quartz, indicating a secondary nature.

The secondary phases display a wide mineralogical diversity, in apparent contrast with the small volume of the syenitic rock and the skarn formed from it. The primary phases undergo a variable degree of alteration, eudialyte being the most sensitive. The intensity of eudialyte grains breakdown ranges from lack of almost any alteration to complete replacement by secondary phases. Fresh grains start to alter forming overgrowths and vein-shaped replacements by dalyite and/or gittinsite, accidentally accompanied by U-

poor terms of the turkestanite-arapovite series, undetermined Zr-poor, Al- and Fe-bearing K, Na zirconosilicates or low-K/Zr K-Si-Zr phases (Fig. 2B). More altered grains preserve central relics surrounded by a polygranular pectolite-elpidite + other undetermined, possibly hydrous, Na-Si-Zr phases with variable, generally low Na/Si and Na/Zr ratios or Ca-Si-Zr phases with low Ca/Si and Ca/Zr ratios. Arapovite, strontianite and burbankite appear also on the margin of the replacing aggregate or in association with pectolite penetrating it (Fig. 2C). Replacement aggregates with no relics preserved, also probably originating from former eudialyte contain various associations like calciocatapleiite-pyrite (2D), zircon - titanite (+Nb, Zr, Na) -pyrite – wollastonite - pectolite, pyrite-chalcopyrite-baddeleyite, gittinsite-pectolite-baddeleyite.

Acmite is stable in the fresh syenite but is decomposed during skarn formation. Typically, acmite grains are not altered by the hydrous Ca-Na front advancing from the skarn but break down once engulfed in the skarn mass. The corroded margins are outlined by a sulfide-rich aggregate containing, alongside with common sulfides, frequent grains of djerfisherite group minerals (Fig. 1E, 2F). Remarkable is the abundance of TI in these minerals, the grains having often a TI-dominant composition like in thalfenisite, but the order of abundance of the most TI-rich grains is Fe>Cu>>Ni.

Titanite is the phase most refractory to alteration, persisting in the hydrous alteration front, but breaking down gradually in the skarn. Initially it alters to pseudomorphs containing Al- and Fe-rich, zoned neoformed titanite intergrown with wollastonite and perovskite "dust" and later on neoformed titanite is resorbed, the contours of the old idiomorphic titanite grains remaining outlined by the perovskite clusters, which may eventually recrystalize. The titanite phantoms, together with the partly obliterated and overprinted inherited coarse-grained structure indicate proximal skarn formation from syenite. Inside the skarnified mass, a very diverse association of opaque grains appears, corresponding to the most advanced alteration stage of the syenite: vaesite-millerite composite grains, vaesite-cattierte + pyrite + chalcopyrite, chalcocite associated with "thalfecusite" and thalcusite, baddeleyite, thorianite.

The relationships of the syenite with the enclosing rocks indicate its emplacement after the consolidation of the monzodiorite intrusion, but coevally with skarn formation. Because such a peralkaline composition cannot represent a differentiation residue of the calk-alkaline pluton, it must have originated from partial remelting under particular conditions. On the other hand, an influx of fluid with alkaline composition is documented by the diffusion front and Na-metasomatism that acted in the monzonite. SUCH an alkali enrichment is not recorded in any part of the system, except the monzonite/skarn interface. Therefore the most probable mechanism lies in creation of an alkaline environment by Al and partially Si discharge in the fluid during precipitation of phases like gehlenite, grossular garnet and vesuvianite. Because peralkaline melts have a very low solidus temperature the fluid could have a composition effective enough to trigger partial melting with formation of a peralkaline syenitic melt consolidated subsequently in situ. Such a mechanism is likely to be more common than presently considered, and peralkaline melts are possibly frequent at the margin of high-temperature intrusions producing aluminous skarns.

References

Istrate, G., Ștefan, A., Medeșan, A., 1978. Spurrite and tilleyite in the Cornet Hill, Apuseni Mountains, Romania. *Rev. Roumaine Géol., Géophys. et Géogr., Géologie 22, 143-153*

Marincea, Ş., Bilal, E., Verkaeren, J., Pascal, M.-L., Fonteilles, M., 2001. Superposed Parageneses in the Spurrite-, Tilleyite and Gehlenite-Bearing Skarns from Cornet Hill, Apuseni Mountains, Romania. *The Canadian Mineralogist* 39/5, 1435-1435

Pascal, M.-L., Fonteilles, M., Verkaeren, J., Piret, R., Marincea, Ş., 2001. The Melilite-Bearing High-Temperature Skarns of the Apuseni Mountains, Carpathians, Romania. *The Canadian Mineralogist* 39/5, 1405-1434

Ştefan, A., Istrate, G., Medeşan, A., 1978. Gehlenite in calc-skarns from the Măgureaua Vaței–Cerboaia (Apuseni Mountains – Romania). *Rev. Roumaine Géol., Géophys. et Géogr., Géologie 22, 155-160*

VESUVIANITE IN HIGH-TEMPERATURE SKARNS FROM ROMANIA: A REVIEW

Cristina SAVA, Ştefan MARINCEA

Geological Institute of Romania, Bucharest, Romania, 012271 e-mail: ghinet.cristina@yahoo.com

Vesuvianite is a relatively common mineral within the metasomatic systems with calcium dominance, being reported in 13 of the 33 skarn occurrences of the Banatitic Province. Mentioned for the first time by von Zepharovich (1859), the mineral has been the subject of numerous investigations over the time, occupying a special place within the paragenesis of the four high-temperature skarn occurrences known so far in Romania, i.e., Oraviţa and Ciclova in Banat (Constantinescu et al., 1988), Măgureaua Vaţei (Ştefan et al., 1978) and Dealul Cornet (Istrate et al., 1978) in Apuseni Mountains. In all four occurrences the contact metamorphism is related to various shallow level magmatic basic-intermediate intrusions of Upper Cretaceous age, pertaining to the Banatitic Magmatic and Metallogenetic Belt, which can be defined as an extensive suite of consanguineous magmatic and metallogenetic events extended from Srednogorie (Bulgaria) to Apuseni Mountains (Romania): Berza et al. (1998). The investigated calcic skarns occur at the very contact between dioritic or monzodioritic bodies and sedimentary carbonaceous sequences of Mesozoic age. In Table 1 are summarized the mineral species identified so far in the four deposits.

Table 1. Associations of minerals in the high temperature skarns occurrences from Romania *

| Mineral species | Ciclova and Oraviţa | Măgureaua Vaţei | Dealul Cornet |
|---------------------|---------------------|-----------------|---------------|
| gehlenite | | | |
| spurrite | * | 坐 | |
| diopside | • | • | • |
| tilleyite | | 坐 | |
| afwillite | | | |
| grossular | • | • | • |
| Ti-andradite | | • | • |
| andradite | * | 坐 | |
| spinel | | | |
| magnetite | | | |
| monticellite | • | • | |
| wollastonite | * | | • |
| perovskite | | ٥ | * |
| vezuvianite | | • | • |
| clintonite | • | | 坐 |
| phlogopite | | | 坐 |
| hydroxylellestadite | | 0 | |
| calcite | | | |
| aragonite | | | |
| pyrrhotite | | | |
| djerfisherite | | | ? |
| cuspidine | ? | | ? |
| scawtite | | | • |
| thaumasite | | | |
| clinochlore | * | | |
| chrysotile | + | | |
| hibschite | • | • | • |
| kamaishilite | | ? | |
| bicchulite | 主 | ? | ? |

| xonotlite | | • | * |
|--------------|----------|---------|----------|
| thomsonite | • | • | • |
| gismondine | 坐 | | • |
| mountainite | | | ? |
| foshagite | | | ? |
| plombièrite | | • | * |
| tobermorite | | | * |
| riversideite | 坐 | | • |
| portlandite | 坐 | | |
| allophane | • | • | • |

^{*} Symbols: ■ major; • common; • minor; ■ rare; □ very rare; ? doubtful identification; [±] not found.

In all four calcic skarn deposits, vesuvianite is particularly abundant in the internal exoskarn area. At Ciclova – Valea Ţiganilor skarn occurrence, and in the outer zone of the metasomatic zone from Oraviţa - Ogaşul Crişenilor, the mineral compose over 95% of the volume of the rock, that can be define as vesuvianitite. The two occurrences are the most spectacular appearance of the mineral in Romania. The monomineral masses of vesuvianite are composed by tetragonal - bipyramidal crystals up to 5 cm across. The morphology of crystals is often complicated by the appearance of vicinal faces, corrosion figures, steps, regular and irregular concretions easily observed in the samples from Ciclova (Valea Ţiganilor).

In the four occurrences, vesuvianite is present both as "primary" mineral, with no apparent (substitution) relations with other mineral phases, and as "secondary" mineral, pseudomorphic on gehlenite (Marincea et al., 2011; 2013). In the outer skarn zone vesuvianite crystals can engulf calcic garnet, wollastonite, diopside, monticellite, hydroxylellestadite, clintonite, okenite and thomsonite. The macroscopic color varies from yellowish green in the endoskarn area to brown in the exoskarn area (outermost). In most cases the mineral is uniaxial negative and has low or even anomalous birefringence, going toward Prussian blue, violet or brown hues.

Chemical profiles performed using EMPA on "primary" vesuvianite crystals sporadically indicated a slight tendency of enrichment in Al and depletion in Fe towards the peripheral areas of the crystals. This particularity has been noticed also in the case of the vesuvianite pseudomorph on gehlenite, but in this case the differences of chemistry between the centers and the peripheries of the crystals are much attenuated. Optical zoning can be observed in the both cases and could be correlated with the zonal variations of (Fe³⁺+Ti) vs. Al ratios (Vanheyste, 2014). Some of the samples from Ciclova are biaxial and optically positive, probably indicating higher boron contents, as observed by Oftedal (1964).

Vesuvianite formulae were normalized to 50 cations and 76 (O,OH,F,Cl) pfu, as recommended by Groat et al. (1992). As in the case of vesuvianite from Cornet Hill (Marincea et al., 2001), electron-microprobe profiles across crystals of both vesuvianite without reciprocal relationships with gehlenite and vesuvianite from replacement pods on gehlenite reveal a slight increase in Al/Fe from core to rim. Deviations from stoichiometry in vesuvianite [ideally $Ca_{19}(Al,Mg,Fe^{3+})_{13}(Si_2O_7)_4O(SiO_4)_{10}(F,OH)_9$], i.e., Si < 18 apfu (atoms per formula unit) of 50 cations and Ti + Al + Fe + Mg > 13 apfu (Table 2) were recorded in all but one samples and are characteristic of boron-bearing vesuvianite (Groat et al., 1992). As it can be seen, from chemical point of view, most of the analyzed samples can be circumscribed to type 2 (vesuvianite from skarns area) after Fitzgerald et al. (1992): Mg contents between 2.29 and 3.79 apfu, Fe contents between 0.86 and 2.00 apfu and minor Ti contents (> 0.5 apfu).

Vesuvianite is present as a main phase or accessory mineral in all four areas of high temperature skarn investigated and the tendency of polytipism results from the different arrangement of the structural "chains" around the c axis (columnary polytipism or "rod polytypism" in the acceptance of Gnos and Armbruster, 2006). Gnos and Armbruster (2006) noted a systematic dependence between the point symmetry of the mineral and the crystallization temperature, which translates into the dominance of the P4np0 polytype at temperatures below 300° C, of the P4/p0 polytype at temperatures between 300 and 500° C and of P4/p1 polytype at temperatures higher than 500°C. As expected, the 8 structural refinements on vesuvianite monocrystals allowed the identification, in almost all situations and within all the four occurrences, of the P4/p1 polytype, characteristic for high crystallization temperatures, specific to the

investigated skarn. The mean unit-cell parameters, considering the P4/nnc symmetry, are: a = 15.595(4) and c = 11.824(4) Å at Dealul Cornet; a = 15.602(3) and c = 11.812(4) Å at Măgureaua Vaței; a = 15.605(3) and c = 11.333(5) Å at Ciclova; and a = 15.577(3) and c = 11.830(4) Å at Oravița.

Table 2. Representative electron-microprobe analyses of vesuvianite from Oraviţa (Ogaşul Crişenilor), Ciclova (Valea Ţiganilor) and Dealul Cornet (Marincea et al., 2001; 2015)

| Sample | 2302 | 2307 | 2312 | 2339 | 2358 | 2259 | 2173 | 2305 |
|---------------------------------|--------|-------------|--------------|----------------|--------------|---------------|-------------|--------|
| Location | | Oraviţa | | Cicl | ova | D | ealul Corne | t |
| N ⁽¹⁾ | 11 | 3 | 5 | 11 | 5 | 5 | 5 | 5 |
| SiO ₂ | 36.05 | 36.89 | 36.77 | 36.73 | 36.90 | 36.26 | 37.12 | 36.38 |
| TiO ₂ | 0.08 | 0.00 | 0.01 | 0.67 | 0.05 | 0.04 | 0.00 | 0.05 |
| Al ₂ O ₃ | 17.51 | 17.30 | 17.26 | 16.03 | 17.79 | 18.42 | 17.66 | 18.59 |
| FeO ⁽²⁾ | 2.88 | 2.74 | 2.11 | 3.06 | 1.85 | 2.06 | 0.65 | 0.88 |
| MnO | 0.05 | 0.07 | 0.03 | 0.07 | 0.04 | 0.04 | 0.01 | 0.04 |
| MgO | 3.68 | 2.94 | 3.48 | 3.89 | 3.84 | 3.45 | 4.23 | 4.69 |
| CaO | 36.06 | 36.67 | 36.41 | 36.08 | 36.33 | 37.14 | 37.41 | 36.86 |
| Na₂O | 0.03 | 0.01 | 0.01 | 0.02 | 0.02 | 0.02 | 0.42 | 0.07 |
| K₂O | 0.01 | 0.01 | 0.00 | 0.00 | 0.00 | 0.00 | 0.01 | 0.01 |
| F | 0.14 | 0.10 | 0.01 | 0.18 | 0.44 | 0.00 | 0.07 | 0.06 |
| Cl | 0.02 | 0.00 | 0.00 | 0.02 | 0.01 | 0.00 | 0.09 | 0.05 |
| H ₂ O ⁽³⁾ | 2.14 | 1.95 | 2.00 | 2.01 | 1.82 | 2.23 | 2.31 | 2.25 |
| | 98.65 | 98.68 | 98.09 | 98.76 | 99.09 | 99.66 | 99.98 | 99.93 |
| O=F,Cl | - 0.06 | - 0.04 | - 0.00 | - 0.08 | - 0.19 | -0.00 | -0.05 | -0.04 |
| Total | 98.59 | 98.64 | 98.09 | 98.68 | 98.90 | 99.66 | 99.93 | 99.89 |
| | N | umber of io | ns on the ba | sis of 50 cati | ons and 76 (| O, OH, F, Cl) | | |
| Si | 17.434 | 17.850 | 17.828 | 17.789 | 17.711 | 17.311 | 17.559 | 17.204 |
| Ti | 0.029 | 0.000 | 0.004 | 0.243 | 0.018 | 0.014 | 0.000 | 0.018 |
| Al | 9.980 | 9.866 | 9.863 | 9.154 | 10.062 | 10.364 | 9.846 | 10.361 |
| Fe ²⁺ | 1.165 | 1.109 | 0.856 | 1.239 | 0.742 | 0.822 | 0.257 | 0.348 |
| Mn | 0.020 | 0.029 | 0.012 | 0.029 | 0.016 | 0.016 | 0.004 | 0.016 |
| Mg | 2.653 | 2.121 | 2.515 | 2.807 | 2.747 | 2.455 | 2.983 | 3.306 |
| Са | 18.684 | 19.011 | 18.914 | 18.719 | 18.685 | 18.998 | 18.960 | 18.676 |
| Na | 0.028 | 0.009 | 0.009 | 0.019 | 0.019 | 0.019 | 0.385 | 0.064 |
| К | 0.006 | 0.006 | 0.000 | 0.000 | 0.000 | 0.000 | 0.006 | 0.006 |
| F | 0.214 | 0.153 | 0.015 | 0.278 | 0.675 | 0.000 | 0.105 | 0.090 |
| Cl | 0.016 | 0.000 | 0.000 | 0.017 | 0.008 | 0.000 | 0.072 | 0.040 |
| 1 | 6.000 | | | | | | | |

^{*} results expressed in wt.%. (1) N = number of point analyses; (2) total iron as FeO; (3) as calculated for charge balance *apfu*: atoms per formula unit.

The mineral associations occurs in a classic metasomtic contact aureole in which elements such as Si, Al, Fe and Ti, were introduced into a calcic marble protolith from the intrusive body, at very high temperature and low pressures (Katona et al., 2003), conducting to the formation of a specific paragenesis for each stage of evolution of the skarnification process.

The crystallization of vesuvianite is coincident with an essentially hydrothermal event, when calcite in excess recrystallize to form calcite I and the relatively high Fe³⁺contents in vesuvianite chemical composition, as well as high Fe³⁺/Fe value in clintonite and the presence of hydroxylellestadite highlights the oxidation character of it.

The replacement of gehlenite by vesuvianite along the metasomatic front was possible due to the presence of a fluid enriched in silicon and iron; the aluminum resulted from the breakdown of gehlenite was capted by the network of clintonite. The wide development of the vesuvianite-bearing skarns as compared to the gehlenite-bearing ones is a clear evidence that the late metasomatism is essentially hydrous. The peak temperatures are estimated at up to 600° C and correspond to those estimated by Katona et al. (2003).

References

- Berza, T., Constantinescu, E., Vlad, S.N., 1998. Upper Cretaceous magmatic series and associated mineralization in the Carpatho-Balkan Orogen. *Resource Geol.*, **48**, 291-306.
- Constantinescu, E., Ilinca, G., Ilinca, A., 1988a. Laramian hydrothermal alteration and ore deposition in the Oraviţa-Ciclova area, South-western Banat. *D.S. Inst. Geol. Geofiz.*, **72-73**, 13-26.
- Constantinescu, E., Ilinca, G., Ilinca, A., 1988a. Contributions to the study of the Oravita Ciclova skarn occurrence, southwestern Banat. *D.S. Inst. Geol. Geofiz.*, **72-73/2**, 27-45.
- Fitzgerald, S., Leavens, P.B., Nelen, J.A., 1992. Chemical variation in vezuvianite. *Mineral and Petrol.* 46, 163-168.
- Gnos, E., Armbruster, T., 2006. Relationship among metamorphic grade, vesuvianite "rod polytypism", and vesuvianite composition. *American Mineralogist*, **91**, 862-870.
- Groat, L.A., Hawthornem F.C., Ercitt, T.S., 1992. The chemistry of vezuvianite. Can. Mineral., 30, 19-48.
- Istrate, G, Ştefan, A., Medeşan, A., 1978. Spurrite and tilleyite in the Cornet Hill, Apuseni Mountains, Romania. *Rev. Roum. Géol., Géogh., Géogr., sér. Géol.*, **22**, 143-153.
- Katona, I., Pascal, M.-L., Fonteilles, M., Verkaeren, J., 2003. The melilite (Gh₅₀) skarns at Oraviţa, Banat, Romania: transition to gehlenite (Gh₈₅) and to vezuvianite. *Can. Mineral.*, **41**, 1255 1270.
- Marincea, Ş., Bilal, E., Verkaeren, J., Pascal, M.-L., Fonteilles, M., 2001. Superposed parageneses in the high-temperature spurrite-, tilleyite-, and gehlenite-bearing skarns from Cornet Hill (Apuseni Mountains, Romania). *Can. Mineral.*, **39**, 1435 1453.
- Marincea, Ş., Dumitraş, D.-G., Ghineţ, C., Fransolet, A.M., Hatert, F., Rondeux, M., 2011. Gehlenite in three occurrences of high-temperature skarns from Romania: new mineralogical data. *Can. Mineral.*, **49**, 1001 1014.
- Marincea, Ş., Dumitraş, D.-G., Călin, N., Anason, A.M., Fransolet, A.M., Hatert, F., 2013. Spurrite, tilleyite and associated minerals in the exoskarn zone from Cornet Hill (Metaliferi Massif, Apuseni Mountains, Romania). *Can. Mineral.*, **51**, **3**, 359-375.
- Marincea, Ş., Dumitraş, D.-G., Ghinet, C., Bilal, E., 2015. The occurrence of hightemperature skarns from Oraviţa (Banat, Romania): A mineralogical overview. *Can. Mineral.*, **53**, **5**, 511-532.
- Oftedal, I., 1964. Vesuvianite as a host mineral for boron. In: Contributions to the mineralogy of Norway, **29**, *Nor. Geol. Tidsskr.*, **44**, 377-383.
- Ştefan, A., Istrate, G., Medesan, A., 1978. Gehlenite in calc-skarns from the Măgureaua Vaței Cerboaia (Apuseni Mountains Romania). *Rev. Roum. Géol., Géophys., Géogr., Sér. Géol.*, **22**, 155-160.
- Vanheyste, J., 2014. Cristallochimie et pétrographie de la vésuvianite et des minéraux associés provenant de skarns haute température de Roumanie. Mémoire de fin d'études (unpubl.), Université de Liège, 101 pp.
- Zepharovich, V. Von, 1859, 1857, 1893. Mineralogisches Lexicon für das Kaiserthum Oesterreich. I, II, III, Viena.

ASSESSMENT AND FORECASTING OF POLLUTION DUE TO ACCIDENTAL LEAKS ON SOIL AND GROUND WATER IN OIL EXTRACTIVE INDUSTRY

Daniel SCRĂDEANU, Mihaela SCRĂDEANU

Faculty of Geology and Geophysics, University of Bucharest, 6 Traian Vuia St, 020956 Bucharest e-mail: daniel.scradeanu@gg.unibuc.ro

Introduction

Mathematical models allow the assessment of the state of pollution of the polluted land remaining after a fuel storage objectives were removed by demolition from unsaturated zone of aquifers (underground tanks, pipelines, pumps and fuel distribution ramp)

Unsaturated zone is the seat of the most active and complex processes of pollution. By modeling the processes of the migration of the pollutants in the unsaturated zone was identified a ongoing process affecting strong the phreatique aquifer and the probability that the deeper aquifers to be affected by the pollution with petroleum products.

1. Geology and hydrogeology of the industrial area sudied

The hydrogeology of the studied area (site Electromontaj S.A. Bucuresti; *Fig.1*) are the subject of the three important natural factors that determine supply and groundwater regime: climatic factors, geomorphological factors and geological factors.

Climatic factors. The climate is moderate continental. The average annual temperature is 10-11°C. Lowest monthly average temperature is recorded in January, with an average of 3°C. Summer is very hot, average temperature in July is 23°C, sometimes even reach 35-40°C. With regard to freezing, the mean date of occurrence of the first frost is situated on 1 November, and the last frost April 3, the average is 90-100 days. Summer, each year, there are about 46 tropical days with maximum temperatures above 30°C.

Rainfall is low, averaging 585 mm per year, but higher in the summer: the highest average monthly rainfall amounts in June (about 85 mm) and the lowest in February (15 mm). In Bucharest there are 117 raining days/year. Under these conditions the average effective infiltration in Bucharest is:

$$I_e = P_m - E_{ra} = 585 - 413 = 172 \, \text{mm/year}$$

where E_m is evaluated with Turc formula (Scrădeanu, 2007).

Geomorphological factors. Site area associated fuel household SC Electromontaj SA is located in Bucharest Plain, between: plain Snagov (north), Câlnăului plain (south), meadow Arges-Sabar (west) and plain Mostiștea (east). Relief from Bucharest is monotonous, with altitudes ranging from quotas 95-55 m. Rivers Dâmbovița and Colentina separate Bucharest Plain in three relatively equal fields extending (Otopeni field, Colentina field and Cotroceni field) but distinct age and lithological constitution. Each of the three fields have two components: a high field located at 13-17 m relative altitude and three or two terraces (t₃, t₂, t₁) at 12-10 m, 7.8 m and 5.3 m relative altitude.

Colentina field is in the space between the rivers Colentina and Dâmboviţa. In its composition were separated one field (senso strictum), two terraces and two pieces of meadow, on the right of Colentina and to the left of Dâmboviţa (Enciu et al., 2008).

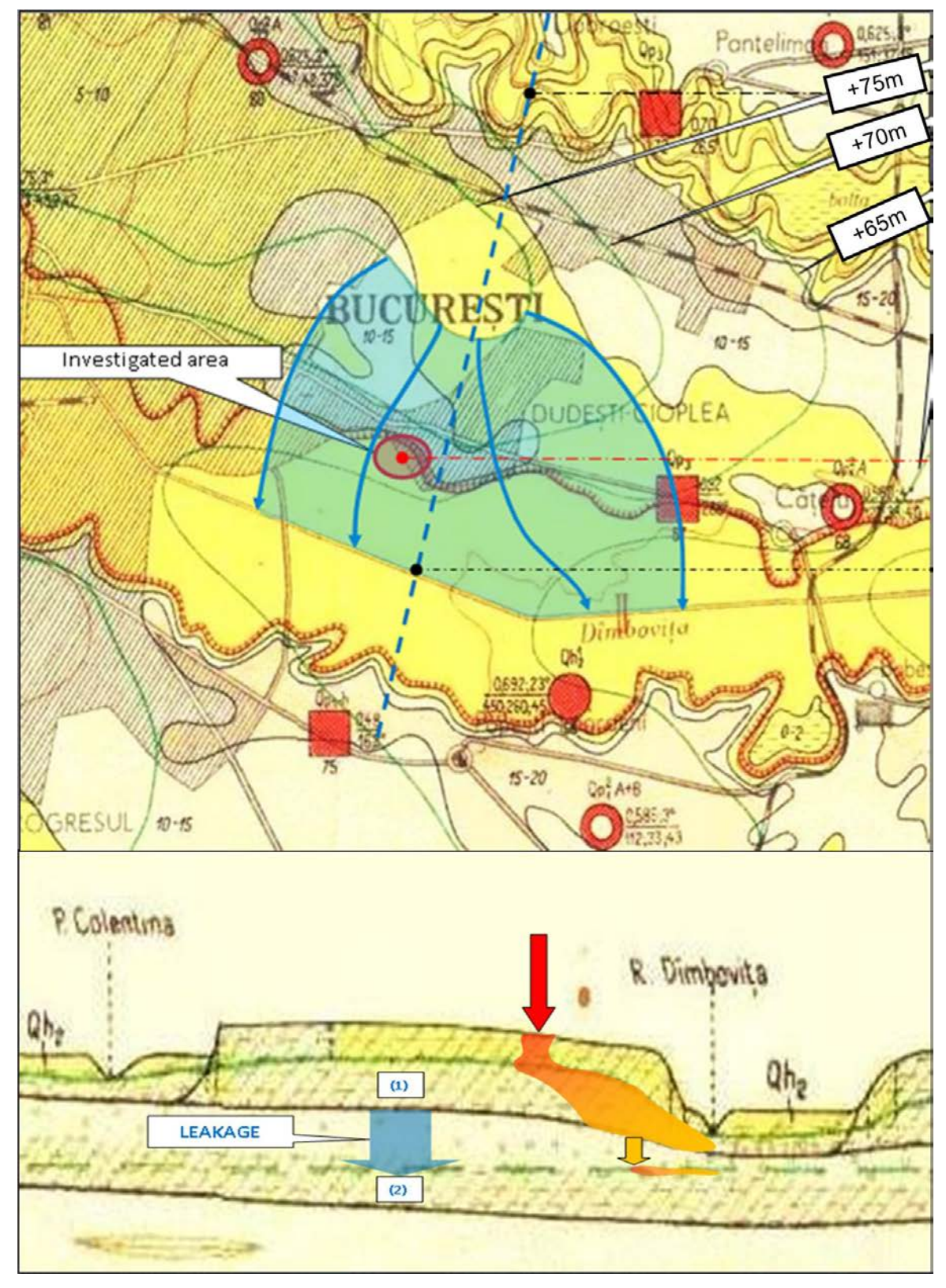


Fig. 1. General hydrogeological condition in the site of the former household fuels SC Electromontaj Bucharest (after Bandrabur et al., 1982).

Geological and hydrogeological factors. In the studied area develops a phreatic hydrostructure located in the Colentina and Mostistea formations from the interfluve Dâmboviţa-Ialomiţa. The site studied is located in the upper part of the phreatic hydrostructure, to depths up to 3 m, south-west of the

watershed of the first aquifer. The aquifer is fed by seepage and has high vulnerability to pollution, being unprotected by impermeable rocks to the top (Tevi and Călin, 2011). Groundwater flow directions are NE-SW, so that groundwater is drained by the river Dâmboviţa. Elevation of water level in thea area varies between +65 and +75m. Depth of water level is between 4 and 10 m. Hydraulic gradient at the site is less than 0.01.

Under the first aquifer is another phreatic aquifer, located in the sands of Mostistea with piezometric level 10 m below. The two aquifers comunicate by downward draining. Drain downward increases vulnerability to pollution of the second aquifer, from the sands of Mostistea.

Groundwater from all phreatic hydrostructure are bicarbonates with total mineralization around 0.80 grams / kilogram and 28.5 degrees German hardness.

2. Hydrogeological investigation of unsaturated zone

The objective of hydrogeological investigation was to evaluate the hydrogeological conditions of migration of petroleum products in the vadose/ unsaturated zone of the first aquifer. To investigate the unsaturated zone were seven sampling points for soil suction, soil moisture, conductivity, temperature, Total Petroleum Hidrocarbons (TPH) (Muszkat et.al., 1993).

For the investigation of unsaturated zone were used: logger Decagon EM50 with USB connectivity, simple humidity sensor Decagon 10HS with analog transmission, triparametru sensors: humidity, conductivity, temperature Decagon 5TE with digital transmission, sensor capillary suction Decagon MPS-1 with analog transmission.

Remote sensing and GIS techniques enable increased efficiency for assessment of the soil water content for unsaturated zone (Tevi and Tevi, 2012). The results of the measurements shows an area affected by the works made for greening area of fuel tank where the potential for suction decreases with depth, which promotes migration in depth of petroleum products.

3. Conceptual model of the hydrostructure

Migration of pollutants in the phreatic hydrostructyure of the investigated site has two main components:

- Vertical migration of contaminants:
 - \circ In the vadose zone of the first phreatic aquifer, with the piezometric level placed at the depth of 3.6 to 4 m in the investigated area
 - o Through the bottom of the first phreatic aquifer, by downward leakage
- Horizontally migration of contaminants, parallel to the direction of flow:
 - o In the first phreatic aquifer parallel to the direction NNE-SSW
 - o In the second phreatic aquifer, the aquifer from the Mostistea sands, parallel to the direction NV-SE

The model of pollutant migration in the vadose zone was based on TPH determined for the soil samples collected from the investigated area. THP values determined in the labs of ECOIND.

4. The model of pollutants migration through the vadose zone

Assessment of one dimensional groundwater flow and contaminant migration in the vadose zone was realized with WHI UnSat Suite Plus (VS2DT). VS2DT is a finite difference numerical model for simulating steady-state or transient unsaturated flow and transport. Typical applications of the VS2DT model include determining the fate of agricultural chemicals, landfill leachate, UST leaks, and accidental chemical spills as they migrate through the unsaturated zone towards the water table.

For the model of unsaturated zone was used: lithologic information for building a representative soil for the investigated site, humidity, capillary suction contents of THP determined on soil samples. Lithological column used for modeling has five lithological sequences: clay soil, sandy clay, sand and loamy sand

Humidity measured vertically varies between 15% and 30%. It was considered constant throughout the simulation period. The potential suction has been schematized by a continuous curve for all five lithological sequences based on measurements made during the investigation.

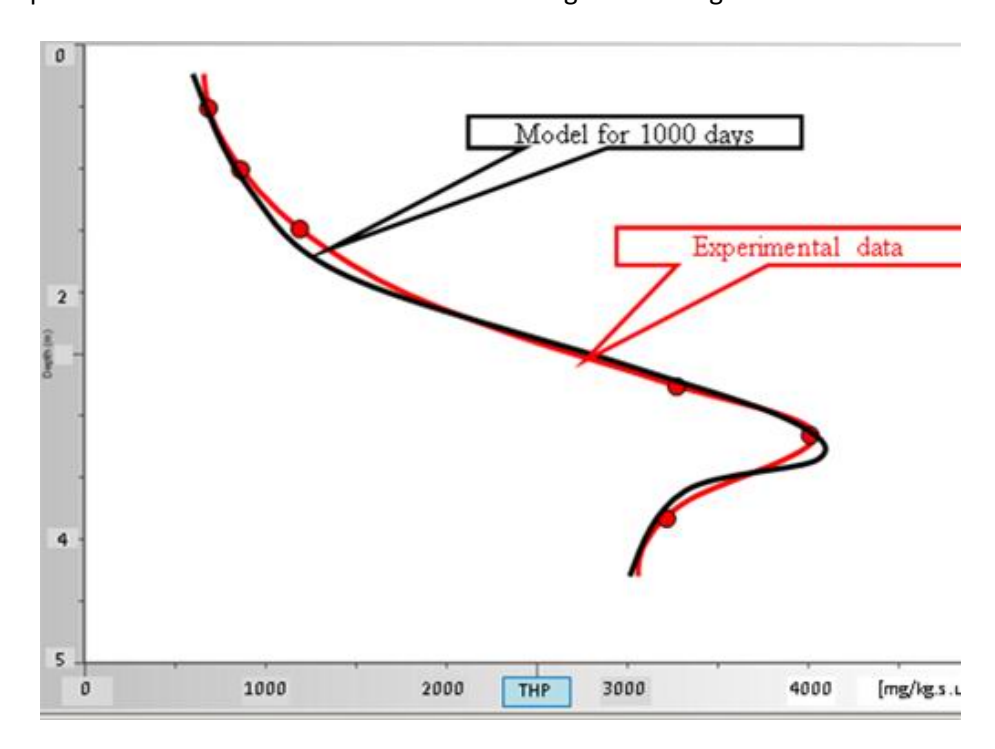


Fig. 2. TPH distribution with depth in the unsaturated zone of the site investigation (t = 1000 days).

The model of vadose zone was used to simulate a distribution of TPH after 1000 days migration time. Simulation result deviates by 10% compared to values determined at 1000 days after the start of pollution (Fig.2).

The model developed for the migration of petroleum products in vadose zone allow the following conclusions:

- vertical migration is very slow;
- pollution source is exhausted, the a maximum concentration of THP is at a depth of 3.0 m after a period of 1000 days;
- some soluble part of the petroleum products migrated in the vadose zone have reached the first phreatic aguifer and are driven by advection in NNE-SSW direction.

Full assessment of the hydrostructure pollution involves building of a coupled model including migration of petroleum product in vadose zone and the migration of soluble petroleum products in the first and the second phreatic aquifers. A coupled model involve a comprehensive program of monitoring the contaminated area for an extended period.

References

Bandrabur, T, Mihailă, N., Ghenea, A., 1982. Hydrogeological map of Bucharest scale. 1: 100,000. Geological Institute of Romania, Bucharest.

Fetter, C, W, 1993. Contaminant hydrogeology, Maxwell Macmillan International, New York, Oxford, Singapore, Sydney.

Muszkat, L., et. al., 1993. Unsaturated Zone and Ground-Water Contamination by Organic Pollutants in a Sewage-Effluent-Irigated Site, *No.4-GROUND WATER-July-August* 1993, **31**, 556-565.

Scrădeanu, D., Gheorghe A., 2007. *General hydrogeology*. Bucharest University Press, Bucharest, 350pp (in Romanian). Tevi, G., Tevi A., 2012. Remote sensing and GIS techniques for assessment of the soil water content in order to improve the agricultural practice and reduce the negative impact on groundwater Case study, Agricultural area Ştefan cel Mare, Călărași County. Water Science & Technology 66, 3, 580-586.

| Geosciences in the 21 st century |
|---|
|---|

Tevi, G., Călin A., 2011, Groundwater vulnerability assessment by DRASTIC method, case study - shallow aquifer from Pantelimon industrial area, RomAqua Journal 56, 2, ISSN 1453-6986.

STUDIES OF GEOLOGICAL HERITAGE IN GEOECOMAR: FROM GEODIVERSITY TO GEOCONSERVATION

Antoneta SEGHEDI, Titus BRUSTUR, Mihaela Carmen MELINTE-DOBRINESCU

National Institute of Marine Geology and Geoecology – GeoEcoMar 23-25 Dimitrie Onciul St., 024053 Bucharest, e-mail: seghedi@geoecomar.ro

Introduction

For the last 12 years, the study of geodiversity and geological heritage was a major research direction in GeoEcoMar. In time, it followed several steps, from inventorying and describing geological reserves and geosites to geological audit and quantitative assessment, with the ultimate goal to elaborate a coherent strategy for geoconservation. Areas investigated include both large protected areas like national or natural parks (II and V IUCN categories), but also nature reserves and nature monuments of paleontological and geological type (III and IV IUCN categories) in Romania. Moreover, GeoEcoMar was directly involved in the management of three marine protected areas for almost 10 years, until a recent change in legislation made this no longer possible. Lately, a project initiated by Ibn Zohr University in Agadir enabled GeoEcoMar experts, together with other Romanian partners (the University of Bucharest and the Geological Institute of Romania) to participate in field missions in Morocco, in order to assess the geoheritage of Anti-Atlas Mountains, the mining history and culture of the region, thus contributing to the sustainable development in the area.

Studies in natural and national parks and in geoparks

The first studies on geodiversity began in project PROMED (*Protected areas: asessment of environment quality in order to valorize local natural resourses and a sustainable local development*), funded by he Ministry of National Education. The project consortium included the Geological Institute of Romania as lead partner, along with GeoEcoMar, the University of Bucharest and the National Institute of Hydrology and Water Management. For 3 years starting with 2007, the joint project team investigated the geological and ecological diversity in eight protected areas (Măcin Mountains and Buila-Vânturariţa National Parks, Little Island of Brăila, Comana and Iron Gates Natural Parks, Mehedinţi Mountains and Buzău Geoparks and the Cheia geological reserve from Central Dobrogea). The project aimed at sustainable use and capitalization of local and regional resources of the protected areas (mineral deposits and rocks, fossil sites, aquifers, mineral or thermal springs, mining works, abandoned quarries or tailing dumps, etc.) (Seghedi et al., 2008). Along with an inventory of the geological heritage of the 8 protected areas, geoecological studies were conducted in order to assess the quality of the environment (Fig. 1) and identify solutions for mitigating the environmental pressure factors, identify the potential of natural and anthropic hazard. Various types of maps represented the project outputs, meant to be used by local authorities in the benefit of communities.

Promotional activities were also undertaken in order to increase awareness of local communities and tourists about the values and importance of local geoheritage and the ways it can be used to ensure a sustainable use of resources.

Inventorying and assessing paleontological reserves in the East Carpathians

From 2007 through 2015, GeoEcoMar also conducted geological and paleontological investigations in protected areas from the East Carpathians, for conservation and sustainable exploitation, in core projects

funded by the Ministry of Education and Research. Investigations started with an inventory of fossil sites from the Mesozoic deposits from the northern side of the Crystalline-Mesozoic zone of the East Carpathians (Rarău Massif), along with the assessment of the anthropogenic impact on fossil fish sites in Piatra Neamţ area. The ichnofossil sites previously described in the Upper Eocene of the Tarcău Nappe and in the lower Miocene of the Marginal Folds Nappe (Alexandrescu et al., 1986; Brustur, 1991, 1995, 2005; Brustur, Alexandrescu, 1993), as well as on the Limestone blocks at Bădila reserve (Buzău county), were also investigated.





Fig. 1. Members of the GeoEcoMar team during field work in project PROMED in the Iron Gates Natural Park, collecting samples for heavy metals analysis from the tailing dumps of former uranium mines located on the Danube tributaries.

In the meantime, technical support was granted to the city Hall of Piatra Neamţ municipality, related to the paleontological reserves with Oligocene fossil fishes at Cozla, Pietricica and Cernegura, as many samples with fossil fishes are hosted at the Natural Sciences Museum of the city (Fig. 2). Assessment of fossil sites indicated that both Pietricica and Cernegura fossil sites are relatively little affected by anthropic intervention, but Cozla reserve is in real danger due to the construction of the telegondola in Piatra Neamţ. With its foundations dug in the Oligocene formations hosting the fossil fishes, the artificial exposures created in the brown bituminous marls and lower disodilles are the favorite pray object of unscrupulous fossil collectors. Thus, human intervention seriously endangers one of the most important reserves of fossil fish in Romania and the world.

A next stage in GeoEcoMar studies was dedicated to protection and integrated management of the national geological and archaeological heritage. Based on integrated analysis and multidisciplinary studies of the natural and cultural heritage, new areas were proposed for protection as geological and paleontological reserves (the Racoş pyroclastic volcano, the Ormeniş Sfinx). A geological audit of the Pârâul Bozului paleontological reserve, rich in tool marks preserved on the bedding planes, revealed only a mild anthropic threat posed by waste dumping along the main access road.



Fig. 2. Oligocene ichtiofauna at Piatra Neamţ: *Capros caprossoides* (Cosmovici, 1887), from the collection of the Natural Science Museum.



Fig. 3. *Paleodictyon miocenicum* and *Helminthopsis* isp., deep marine ichnofauna from the Tarcău sandstone, Buzău valley.

Paleoichnological investigation in order to establish new paleontological reserves in the East Carpathians, conducted on the middle-upper Eocene deposits in Siriu-Nehoiu area, concluded that a rich ichnofauna is present in the Giurgiu-Ghelinţa flysch from the Tarcău Sandstone and Podu Secu Formation,

many ichnogenuses being graphoglyptidae, typical for the *Nereites* ichnofacies (Fig. 3). Along with sedimentological features, this ichnofauna, indicative of deep marine sedimentation, was proposed for protection as the paleoichnological reserve Pârâul Pascului. The accesibility of this reserve makes it an "in situ" educational material, useful not only to geologists, but also to pupils, students, as well as various categories of tourists and nature lovers. Paleoichnological research on the lower Miocene deposits in the Zăbala şi Putna valleys resulted in three new proposals for protection based on the high scientific value of the Năruja and Poiana paleontological sites, and on the educational value of the Bârseşti site for the schools of the neighboring villages (Brustur, 2009, 2010). Further paleoichnological research in Tazlău-Piatra Neamţ area, in order to propose new paleontological sites to the Vânători-Neamţ Natural Park, confirmed the good conservation status of the Gârcina ichnofossil site, while the high value of its vertebrate ichnofauna necessitates its protection by law. Easy access and high educational value make this site useful both for school visits and field trips during geological meetings.





Fig. 4. The Colţi amber shows about 160 colors and hues, dominantly dark, from red to black.

Fig. 5. The Living Fire at Terca, geological reserve and natural monument in Buzău Land Geopark.

Research in the Buzău Land UNESCO Aspiring Geopark

The EEA funded project GeoSust, a large consortium of Romanian and Norwegian partners, represented an opportunity for the GeoEcoMar team to study the geological sites in the Buzău Land UNESCO Aspiring Geopark by applying new methods and technology, including UAV system (Unmanned Aerial Vehicle). The main sites in the aspiring geopark are represented by forms of erosion and precipitation in salt (Meledic Plateau, Mânzăleşti salt bank), salt springs, sulphurous and feruginous springs, mud volcanoes and other phenomena resulted through degradation of oil fields (Pâclele Mari, Pâclele Mici, Focul Viu, Oil springs at Păcuri), amber sites, various sandstone concretions and spectacular erosional forms. The conservation status and vulnerabilities and threats to geological reserves and nature monuments (III IUCN category) were investigated: Colţi amber (Fig. 4), Pâclele Mici, Buzău salt, Bădila limestone blocks, the White Stone La Grunj, the Living Fire at Terca (Fig. 5), etc., along with other geological sites, like mineral springs at Fişici, the Old Ladies from Ulmet, or stratotypes of the Romanian and of the Dacian and other sites with paleontological and biostratigraphic value (Melinte-Dobrinescu et al., 2016; Popa et al., 2016). It is worth noting that none of the paleontological sites in the Buzău Land Geopark is protected by law, despite the fact that they host many unique fossils, like the endemic forms for the eastern Paratethys (starting with the Upper Miocene, the Sarmatian).

Qualitative and quantitative assessment of geodiversity in Dobrogea

In Dobrogea there are 31 reserves and nature monuments of geological, paleontological and mixed type, included in the Natura 2000 network of SCIs and SPAs. An assessment of geodiversity values, as well

as of vulnerabilities and threats to geodiversity, done previously for several paleontological reserves in Dobrogea, identified as main threats quarrying, installation of wind turbines, illegal fossil hunting and ignorance and lack of appreciation caused by lack of awareness (Aniţăi, 2013). Recently, a qualitative and quantitative assessment of geological and paleontological sites in Dobrogea and their preservation state was conducted in a project of GeoEcoMar (Seghedi, 2018). Studies revealed that, despite their high scientific, educational, landscape and tourist values, for most of the relevant geological or nature reserves, geoconservation measures are completely missing or inadequate. This is due to lack of knowledge and appreciation of geological heritage from the local communities and authorities, and even from the Natura 2000 site managers, due to legislation flaws.



Fig. 6. Piatra geosite, a new proposal for geological reserve, shows various tool marks and possibly biogenic traces superimposed on a bed surface modeled by ripples in Ediacaran turbidites, basement of Central Dobrogea.

One of the project's outputs was a local geodiversity action plans (GAPs) after the British model (Burek, 2012), proposing specific geoconservation measures: auditing of geodiversity, disseminating information on geodiversity, awareness increasing on geodiversity, publicity related to the value of the geological and geomorphological sites, establishing relationships with educational institutions in order to promote sites with great educational value, managing, conserving and supporting geodiversity, showing the social, economic and environmental benefits of geodiversity. The last objective of the strategy involves influencing local, regional and governmental policies. However, integration of GAPs into the local development plans and strategies is not an easy task and is intensive time-consuming.

Ten new geological reserves or geosites were proposed as the end of this study (Seghedi et al., 2018): Igliţa, Chior Tepe, Crapcea and Suluk for the Variscan deformation and volcanism, and Poşta for the Lower Jurassic ichnofauna of North Dobrogea Cimmerian orogen; Tariverde and Piatra (Fig. 6), representing exceptional preservation of ripple marks and enigmatic, biogenic traces and tool marks on bed surfaces in Ediacaran basement of Central Dobrogea; Ovidiu geosite, an artificial site in the Poarta Albă-Navodari canal, which exposes the Capidava-Ovidiu crustal fault separating the two tectonic blocks of the Moesian Platform, Central and South Dobrogea; Cuza Vodă, Agi Cabul and Peştera geosites, representing abandoned

quarries in Aptian, Lower Cenomanian and respectively Upper Cretaceous deposits of the South Dobrogea cover.

Investigating the paleontological and geological sites in Romania

In 2019, GeoEcoMar started a new project, which aims at analysing the geodiversity values of the most important geological and paleontological sites in each of the main geotectonic units in the country, in order to elaborate geodiversty action plans on local level and eventually a unitary strategy for geoconservation. Based on documentation and preliminary field work, it was possible to obtain a general picture of the distribution of nature reserves in the country (Table 1).

A total of 368 nature reserves of paleontological, geological and mixed type exist currently in Romania and the most numerous are those of mixed type. The largest number of paleontological reserves were designated in the Moesian Platform, followed by those in the Pannonian basin and its ramifications in the Carpathians. The majority of the paleontological sites in the western part of the Moesian Platform represent fossil sites in Romanian deposits. Because of sandy or shaly lithologies of the Romanian, a large part of these sites are ovegrown by vegetation, or destroyed either by natural causes (like landslides), or by human intervention (extracting rocks for domestic needs) (Pătruţoiu, 2010).

| Geotectonic unit | Paleontological | Geological | Mixed or | Destroyed | Total |
|---------------------|-----------------|------------|----------------|-----------|-------|
| | reserves | reserves | other reserves | | |
| Moldavian Platform | 6 | 3 | | 2 | 9 |
| Scythian Platform | 4 | | 2 | | 6 |
| Moesian Platform | 21 | 8 | 3 | 6 | 32 |
| Transylvanian basin | 6 | 17 | 5 | | 28 |
| Pannonian Basin | 17 | 1 | 2 | | 20 |
| South Carpathians | 11 | 24 | 44 | | 79 |
| East Carpathians | 16 | 44 | 28 | | 88 |
| Apuseni Mountains | 6 | 37 | 31 | | 74 |
| North Dobrogea | 1 | 2 | 29 | | 32 |
| Total | 88 | 136 | 144 | 8 | 368 |

Table 1. Paleontological and geological reserves in the main geotectonic units of Romanian territory.

The largest number of nature reserves are recorded in the East Carpathians, followed by the South Carpathians and Apuseni Mountains. Apparently, despite the dominance of gorges and tectonic klippen, the Apuseni Mountains show a rather equilibrated distribution of the reserves, covering the most relevant lithological assemblages and age ranges. Despite the rather large number of reserves, some rock assemblages, extremely important for the Variscan and Alpine geological history of South Carpathians, like the Devonian Tisovita-Iuţi ophiolite, or remnants of the Severin Nappe oceanic crust rocks, etc., are not protected yet. Instead, there is an abundance of reserves established on Tithonian-Neocomian limestones, due to their spectacular geomorphological and landscape features.

As Romanian legislation is not favourable to protection of geodiversity, the geological community should work together with national and local authorities and managers of larger protected areas, in order to increase the number of nature reserves or monuments of geological and paleontological relevance. They also need to collaborate for awareness increasing on our geological heritage and on the necessity to protect geological reserves with great scientific and educational value, threatened by natural hazards or human activities, as they can bring benefits for local and scientific communities.

Aknowledgements. Research for this paper was financed by the project PN 19 20 05 02, within the Core Program supported by the Ministry of Research and Innovation in Romania.

References

- Alexandrescu, G., Dumitrică, P., Brustur, T., 1986. A new ichnospecies of *Oniscoidichnus Brady* in the Lower Miocene molasse from Vrancea (Carpathian Foredeep). Dări de Seamă ale ședințelor Institutului de geologie și geofizică 70–71, 9–18.
- Aniţăi, N., 2013. Paleontological heritage în Dobrogea: protection, geoconservation, education and promotion. Geo-Eco-Marina 19, 145–178.
- Baucon, A., Bordy, E., Brustur, T., Buatois, L., Cunningham, T., De, C., Duffin, C., Gaillard, C., Felletti, F., Hu, B., Hu, L., Jensen, S., Knaust, D., Lockley, M., Lowe, P., Mayor, A., Mayoral, E., Muttoni, G., Neto de Carvalho, C., Pollard, J., Rindsberg, A., Seike, K., Song, H., Turner, S., Uchman, U., Wang, Y., Yi-ming, G., Zhang, W., Zhang, L., 2012. A history of ideas in ichnology. In: Bromley R.G. & Knaust D. (eds.) Trace fossils as indicators of sedimentary environments. Development of sedimentology 64, pp. 3-43, Elsevier, Amsterdam. ISBN 978-0-444-53813-0
- Brustur, T. 1991. Ascophyllum grigorasi n.sp. (Phaeophyta, Fucales) din Oligocen-Miocenul inferior de la Năruja (Vrancea, Carpaţii Orientali). Lucrările Seminarului geologic "Gr. Cobălcescu", III, 72-81, Univ. "Al. I. Cuza", Iaşi.
- Brustur, T., 1995. *Studiul paleoichnologic al formatiunilor cretacic-miocene din Moldavidele externe*. Universitatea Bucureşti, Rezumatul tezei de doctorat, 24 p.
- Brustur, T., 2005. An insect trace fossil (Ord. Coleoptera) in the Red Formation from theBozului Brook Paleontological Reservation (Vrancea County). Geo-Eco-Marina 9–10, Bucuresti
- Brustur, T., 2009. Lower Miocene jellyfish imprints in the Poiana (Vrancea county, Romania) a rare case of fossilization. Stud. Univ. Babeş-Bolyai, Geologia, Spec. issue, MAEGS-1, 183-185, Cluj-Napoca. ISSN 1221-0803
- Brustur, T., 2010. Oportunitatea ocrotirii punctului fosilifer cu hidromeduze de la Poiana (Vrancea, România). Ocrotirea Naturii, serie nouă, 46, 95-104. Ed. Acad. Rom., București.
- Brustur, T., Briceag, A., 2018. The age of the Gura Şoimului Formation from the Pleşu Anticline (Moldavian Sucarpathians, Romania) based on paleoichnology. Geo-Eco-Marina, 24: 119-126.
- Brustur, T., Alexandrescu, G., 1993. Paleoichnological potential of the Lower Miocene molasse from Vrancea (East Carpathians). Revue Roumaine de Géologie 37, 77–94.
- Burek, C.V., 2012. The role of LGAPs (Local Geodiversity Action Plans) and Welsh RIGS as local drivers for geoconservation within geotourism in Wales. Geoheritage, 4, 1-2, 45-63.
- Melinte-Dobrinescu, M.C., Brustur, T., Jipa, D., Macaleţ, R., Ion, G., Ion, E., Popa, A., Stănescu, I., Briceag, A., 2017. The Geological and Palaeontological Heritage of the Buzău Land Geopark (Carpathians, Romania). Geoheritage 9, 225–236.
- Pătruțoiu, T., 2010. Rezervatii paleontologice Plio-Pleistocene din Romania. Rezumatul tezei de doctorat, UBB Cluj, 1-50.
- Popa, A. Jipa, D., Rădan, S., Melinte, M., Brustur, T., 2016. Salt diapir exotic blocks from Bădila Nature Reserve (Buzău Land Geopark, Romania). A drone-based textural evaluation. Geo-Eco-Marina 22, 119-134.
- Seghedi, A., 2018. Geological heritage of Dobrogea: geodiversity, values and proposals for geoconservation. In: A. Seghedi, A. Mârza, I. Pojar, (eds.), Natural Heritage, Geodiversity, Geoconservation. National Conference, Bucharest, 7th of December 2018, Abstracts, 58-63. GeoEcoMar, ISBN 978-606-94742-4-2.
- Seghedi, A., Oaie, G., Anițăi, N., 2018. Dobrogea Patrimoniu geologic. GeoEcoMar, 65 pp, ISBN 978-606-94742-2-8.
- Seghedi, A., Iancu, V., Gheuca, I., Melinte, M., Brustur, T., Szobotka, S., Andrăşanu, A., Popa, M., Macaleţ, R., 2008. Geodiversitatea ca instrument în dezvoltarea durabilă a ariilor protejate. Geo-Eco-Marina 14, suppl. 1, 175-180.

WHO'S WHO – 500 ROMANIAN GEOLOGISTS – SCIENTIFIC WORKS

Lucian STANCIU, Eugen MOCANU

Geological Institute of Romania, 1 Caransebeş St., Bucharest, e-mail: luxluc9@yahoo.com

In the beginning there was the word... Then, in the Middle Ages, there were "a lot of words"

For 17 years, an electronic Geosciences data base in Excel format exists in Romania, and it is labeled Stanciu. This database shows three important qualities: it's corpulent, it's colorful, it's analytical. In 2008, the file contained 31,000 titles, in 2014 it had 92,000 titles, in 2018 (the Centenary year of Romania), 142,000 titles and in 2019, 147,000 titles.

| 4 | Α. | В | С | D | E | F | G | Н | - 1 | 1 | K | l | M | N | 0 |
|----|-----|----------------|---------|------|---------|--------|-----------------------------------|-----|------------|--|------|--|--|--|------------|
| 1 | 1 | Bibliotecă | Depozit | Raft | Nr.inv. | Marcaj | Autori | Nr. | aționalita | Sex | An | Titlu | Vol. | Colecția | Seria |
| 2 | 677 | Lucian Stanciu | | | | | BALTRES Albert | 1 | romana | masculi | 1976 | Carbonate Rocks and Evaporites - T | 15 | Carbonate Rocks | and Eva |
| 3 | 678 | BNR | | | | | BALTRES Albert | 1 | română | masculii | 1993 | Formaţiunea de Somova (Dobrogea | de Nord). | teze de doctorat | |
| 4 | 679 | Lucian Stanciu | | | 14734 | | BALTRES Albert | 1 | română | masculii | 1993 | Formațiunea de Somova (Dobrogea | de Nord). | rezumate de teze | de docto |
| 5 | 680 | Lucian Stanciu | | | 21589 | | BALTRES Albert | 1 | romana | masculii | 2003 | Unitățile litostratigrafice mezozoice p | 48 | Studii și Cercetări | geologie |
| 6 | 681 | Lucian Stanciu | | | 24782 | | BALTRES Albert | 1 | romānā | masculii | 2005 | Unitățile litostratigrafice mezozoice p | 49-50 | Studii și Cercetări | geologie |
| 1 | 682 | Lucian Stanciu | | | | | BALTRES Albert | 1 | română | masculii | 2002 | Fossil Diagenesis - Subtle Diagenetio | | Limnological Repo | |
| 8 | 683 | Lucian Stanciu | | | 29924 | | BALTRES Albert | 1 | romana | masculii | 2011 | Iulia (North Dobrogea, Romania): Lo | 85-1-2 | Romanian Journal | of Earth |
| 9 | 684 | Lucian Stanciu | | | | | BALTRES Albert, Avram Emil | 2 | romānā | masculii | 2003 | Păcuiul Lui Soare - Building Stones a | | DACIA - Revue d' | 002-200 |
| 10 | 685 | Lucian Stanciu | | | 21867 | | BALTRES Albert, Mirăuţă Elena | 2 | română | masculii | 1996 | Studii litostratigrafice și biostratigrafi | | Anuarul Institutului | ~ |
| 11 | 686 | Lucian Stanciu | | | | | BALTRES Albert, Mirăuță Elena, Gh | 3 | română | masculii | 1981 | The Triassic limestones from Popina | LXVI - 4 | Dări de Seamă al | e 1979 |
| 12 | 687 | Lucian Stanciu | | | 29802 | | BALTRES Albert, Stanciu Lucian | 2 | romānā | masculii | 2011 | Cercetări privind rocile utilizate la cor | IX | Peuce | ie-arhed |
| 13 | 688 | Lucian Stanciu | | | 23587 | | BAN Cristina, Tomozei Bogdan | 2 | română | feminin | 2006 | New data on the apoid hymenoptera | XLIX | Travaux du Museu | um d'Histo |
| 14 | 689 | Lucian Stanciu | | | 25943 | | BANARU Daniela, Crețeanu Mihaela | 3 | romānā | feminin | 2006 | Use of some stable isotopes (13C ar | | Acta Ichtiologica F | |
| 15 | 690 | Lucian Stanciu | | | 25943 | | BANARU Daniela, Gomoiu Marian, H | 3 | română | feminin | 2006 | Space-time variations of stable isoto | | Acta Ichtiologica F | Romanica |
| 16 | 691 | Lucian Stanciu | | | 25943 | | BANARU Daniela, Harmelin-Vivien M | 3 | romānā | feminin | 2006 | Stable isotope signature (13C and 15 | | Acta Ichtiologica f | Romanica |
| 17 | 692 | Lucian Stanciu | | | 4714 | | BANCILĂ Ioan | 1 | română | masculii | 1973 | Asupra prezenței unei formațiuni gips | | Studii și Cercetări | geologie |
| 18 | 693 | Lucian Stanciu | | | d | | BANCOS Dorel | 1 | română | masculi | 1998 | Mişcări de populație la granița româr | XVII-2 | Cercetări Istorice | |
| 19 | 694 | Lucian Stanciu | | | | | BANDOC G. | 1 | română | masculii | 2011 | Analiza statistică a variabilității sezon | iere și int | Protecția și Mana | gementul |
| 20 | 695 | Lucian Stanciu | | | 21087 | | BANDOC Georgeta | 1 | română | feminin | 2000 | Ultimele furtuni de pe litoralul române | IV | Comunicări de Ge | ografie |
| 21 | 696 | Lucian Stanciu | | | 22191 | | BANDOC Georgeta | 2 | română | | 2005 | Regimul temperaturilor și al precipita | | Comunicări de Ge | - |
| 22 | 697 | Lucian Stanciu | | | 24801 | | BANDOC Georgeta | 1 | romană | | 2003 | Tipuri de furtuni din Mord-Vestul bazi | nului Mări | Lucrările Stațiunii | de Cerce |
| 23 | 698 | BCU-București | | | | | BANDOC Georgeta | 1 | română | masculii | 2004 | Potentjalul eolian al litoralului române | CALL CONTRACTOR | and the second s | |
| 24 | 699 | Lucian Stanciu | | | 32246 | | BANDOC Georgeta | 1 | română | feminin | 2009 | Analiza factorilor hidrotermici din are | 13 | Environment & Pro | ogress |
| 25 | 700 | BNR | | | | | BANDOC Georgeta | 1 | romānā | masculii | 2005 | Potențialul eolioan al litoralului român | esc al Mà | Control of the Control | |
| 26 | 701 | Lucian Stanciu | | | | | BANDOC Georgeta, Degeratu Mirce | | română | PORT OF THE PERSON NAMED IN | 2001 | Frecvențele de apariție a valurilor du | | Comunicări de Ge | |
| 27 | 702 | Lucian Stanciu | | | 21088 | | BANDOC Georgeta, Degeratu Mirce | | română | N. Secondario | 2002 | Carelațiile medii locale și generatoar | The second second | Comunicări de Ge | |
| 28 | 703 | Lucian Stanciu | | | 21089 | | BANDOC Georgeta, Degeratu Mirce | | romana | 20,220,000,000 | 2003 | Relațiile dintre viteza vintului și carac | | Comunicări de Ge | |
| 29 | 704 | Lucian Stanciu | | | 24801 | | BANDOC Georgeta, Degeratu Mirce | | română | | 2003 | Frecvențele de apariție a valurilor du | | | |
| 30 | 705 | Lucian Stanciu | | | 24801 | | BANDOC Georgeta, Degeratu Mirce | | română | Name and Address of the Owner, where the Owner, which is the Own | 2003 | Relațiile între viteza vîntului și caracti | | | |
| 31 | 706 | Lucian Stanciu | | | 24801 | | BANDOC Georgeta, Degeratu Mirce | | română | feminin | 2003 | Corelațiile medii locale și generale în | ACCESS OF THE PARTY OF THE PART | | |
| 32 | 707 | Lucian Stanciu | | | | | BANDOC Georgeta, Dragomir Elena | 4 | română | And the second | 2013 | Evolving Characteristics and Potentia | A STATE OF THE PARTY OF T | | |
| 33 | 708 | Lucian Stanciu | | | | | BANDOC Georgeta, Strat Daniela, | 2 | română | feminin | 2007 | Analyses of some climatic indicators | III-1 | Analele Universită | tgeografi |
| 1 | H S | eet1 💯 | 31 | | | | | | | 14 | 1 | | | | - |

Fig. 1. Sample of the Earth Sciences bibliographic excel table, Stanciu – 2019.

The corpulency of the Geosciences file – Stanciu – 2019 is given by the 117 columns of the bibliographic Excel table. The most important sorting criteria (items) are its extreme columns (1 and 117). Sorting by column 1 – named the big-bang column – brings the viewer in the initial phase of the data base creation, being able to make collective corrections of terms or individual linguistic corrections in any other column. Column 117 is important because it indicates the initial provenance of information from the 19 subfiles "welded" into a mega excel file with over 500,000 titles. The other columns of the Excel table are

structured in three modules: 1 – the organizational module, 2 – the classical bibliographic module and the multilaterally developed scientific module (88 columns).

I also imagined a sociological sub-module for the Authors item, which allows to select authors by nationality, the sex of the first author and the number of authors. The "nationality" criterion facilitates the access to the foreign authors who have written about Romania or in Romania. Using the item "nationality", we can deliver to partner foreign libraries useful information related to dissemination of information created by foreign authors in publications printed in Romania. We suspect that not many analytical databases created abroad can electronically deliver us documentary listings with Romanian authors who have published in foreign series.

Another important item the data base is accessorized with is the "document type" column, which allows selecting the information according to several criteria: articles, books, reviews, information, theses, guidebooks, dictionaries, maps, encyclopedias.

In the Excel file *Who's Who 500 Romanian Geologists – Scientific Papers*, we began to introduce as many lists as possible of contributions published by members of the Romanian Academy, University staff and researchers. In just 3 months we processed 150 lists of works (15,000 titles). Over the next two years we intend to process 500 author lists in the field of geology.

The final size of "Stanciu's list" is expected to exceed 50,000 titles. The fulfilment of this hope is directly proportional to your vanity of preserving the record of your scientific creation in the most important Geoesciences database in Romania, which, like it or not, will bear the name of its creator.

ATMOSPHERIC PRESSURE IN PALEOCLIMATE. INTRODUCTION AND IMPORTANCE

Lia STELEA

Independent researcher, e-mail: lia.stelea@gmail.com

Given the current climatic crisis we're currently facing, we need more accurate representations of past climates and their interaction with fossil life. Three main components are necessary to define and model the state of the atmosphere: composition, temperature and pressure. Despite relatively well-studied temperature and composition estimates, which allow us to reconstruct global climatic models with some degree of certainty, aspects like global atmospheric pressure and air density were mostly overlooked. It is largely taken for granted that the global atmosphere had about the same mass as today, which would lead to a constant global atmospheric pressure throughout the ages.

If Earth's atmosphere had constant mass, changes in composition (e.g. the estimated increase of oxygen levels from 15vol% in Early Triassic up to over 30vol% during the Cretaceous (Holz, 2015)) would lead to the significant decrease of the proportion of other gases, such as argon and nitrogen. By current standards, this would be unlikely, because argon is inert and atmospheric nitrogen would have been very poorly retaken from the atmosphere (Berner, 2006). However, the proportion of argon could have been higher than today, as seen in analysis of air inclusions from amber, which can go over 2% moles Ar in dry air (Bellis and Wolberg, 1991), and is probably not radiogenic (Landis and Snee, 1991). The decrease in nitrogen levels, if it happened, would be due to a global nitrogen cycle quite different from that of today. If the proportion of oxygen increased, and nitrogen levels stayed approximately the same, the increased quantity of gas would lead to a higher air pressure at sea level (Berner, 2006). This is most probably the case.

The importance of knowing the paleoatmospheric pressure, first of all, is for better modelling of current climate and taking into account other processes that are overlooked by mainstream climate science. These which may prove crucial later on, as global atmospheric changes are complex and not limited to greenhouse gas emmisions and their immediate effects. Secondly, knowing about different atmospheric pressure/air density levels, present in the geological past, would help us in reconstructing ancient life, not only in appearance, but in function – from understanding different global biogeochemical cycles, to biomass productivity for given ecosystems, to size and physiology of certain animals. They can provide explanations for giant Paleozoic insects (Berner, 2006), evolution of vertebrate flight (Berner, 2006) and rapid dinosaur growth. Thirdly, atmospheric pressure at a given geological time would serve as a reference level for paleoaltimetry (Som et al., 2016). The latter is important because it would deepen our understanding of the tectonic history of the structures containing the analyzed rocks. Such studies may take for granted an atmospheric pressure of ~1 atm at sea level (e.g. Xia et al., 2012), but recent results show that, at least 2.7 billion years ago, atmospheric pressure was less than half that of today (Som et al., 2012; Som et al., 2016), and was probably higher than today's during late Paleozoic (Berner, 2006).

Therefore, the reconstruction of past atmospheric pressure levels is desirable and necessary.

Selective references

Bellis, D., Wolberg, D. L., 1991. Analysis of gaseous inclusions in fossil resin from a late cretaceous stratigraphic sequence. Global and Planetary Change 5, 1, 69-82.

Berner, R. A., 2006. Geological nitrogen cycle and atmospheric N2 over Phanerozoic time, Geology, 34, 5, 413-415.

Holz, M., 2015. Mesozoic paleogeography and paleoclimates – A discussion of the diverse greenhouse and hothouse conditions of an alien world. Journal of South American Earth Sciences 61.

Landis, G. P., Snee, L. W., 1991. ⁴⁰Ar/³⁹Ar systematics and argon diffusion in amber: implications for ancient earth atmospheres. Palaeogeography, Palaeoclimatology, Palaeoecology 97, 1, 63-67.

- Som, S. M., Buick, R., Hagadorn, J. W., Blake, T. S., Perreault, J. M., Harnmeijer, Jelte P., Catling, D. C., 2016. Earth's air pressure 2.7 billion years ago constrained to less than half of modern levels. Nature Geoscience 9, 448.
- Som, S. M., Catling, D. C., Harnmeijer, J. P., Polivka, P. M., Buick, R., 2012. Air density 2.7 billion years ago limited to less than twice modern levels by fossil raindrop imprints. Nature 484, 359.
- Xia, G., Yi, H., Zhao, X., Gong, D., Ji, C., 2012. A late Mesozoic high plateau in eastern China: Evidence from basalt vesicular paleoaltimetry. Chinese Science Bulletin 57, 21, 2767-2777.

NEW MINERAL OCCURRENCES ON THE NORTH SIDE OF VÂLCAN MOUNTAINS

Robert SZABO^{1, 2}, Gheorghe C. POPESCU², Delia-Georgeta DUMITRAȘ¹, Ciprian CONSTANTINA¹

¹Geological Institute of Romania, Caransebeș Str. 1, Sector 1, 012271 Bucharest, e-mail: robert.szabo@yahoo.com

²University of Bucharest, Faculty of Geology and Geophisics, Department of Mineralogy, Nicolae Bălcescu Blvd. 1, 020956 Bucharest, Romania

Researches carried out from 2014 untill present covered the area on the north side of the Vâlcan Mountains, between Tusu Valley in east and all the way to the Osliţa – Oslea ridge, in the west. These 37 km of wild beautiness have underlined three areas apart from the rest, regarding the presence of some new minerals not mentioned in this part of Romania untill now. The entire area was divided into several perimeters, this abstract presenting three of the most important: the Tusu river perimeter at the edge of Lupeni city, the Şiglăul Mare mountain perimeter near Câmpu lui Neag village, and the Scocul Jiului de Vest – Gârbovul brook a right tributary of the Jiul de Vest River.

From geological point of view, the northern flank of the Vâlcan Mountains belongs to the Danubian domain. Also the Getic – Supragetic nappe system is encountered along with the presence of some formations of the ophiolite – bearing Severin Nappe placed structurally between the Getic and the Danubian nappes.

The Danubian was first named by Codarcea, in 1940 and considered as autochthonous. New studies shown that the Danubian constitute a nappe system, representing the lowest part of the nappe pile in the South Carpathians. The Danubian nappe system has been divided in two parts: the Upper Danubian and the Lower Danubian. (Berza and Seghedi, 1983; Berza et al., 1983). The two subdivisions are separated by a major thrust planes and differ in their Mesozoic covers (Stănoiu, 1973; Kräutner et.al., 1981; Berza et al., 1983). In the Lower Danubian, two nappes have been separated: The Lainici and the Schela – Petreanu nappes (Kräutner et al., 1981, 1988; Berza et al., 1983, 1994). The pre-Alpine thrusts of the Lower Danubian nappes are of Variscan age and consists of Retezat-Parâng unit resting always structuraly upon the Vâlcan – Pilugu unit (Berza et al., 1988a, 1988b) .

The lithologies of the Danubian basement are represented by rock formations grouped as follows: the Lainici – Păiuș metasedimentary group and its intrusives in the Vâlcan-Pilugu Variscan unit and the Drăgșan metavolcanic group with its intrusives in the Retezat-Parâng Variscan unit, both beeing of late Precambrian age as shown by geochronological data (Liégeois et al., 1996).

The Lainici - Păiuș Group was described by Manolescu (1937) and updated subsequently by detailed mapping for several geological maps at scale 1:50.000. It is composed mainly of quartzite, biotite gneiss, marble and graphitic gneiss with minor amphibolite present. Rocks show a high temperature – low pressure type metamorphism, with pervasive migmatization (Savu, 1970). A major characteristic feature is the abundance of leucogranite leucosomes, as veins and lenses in the metasediments.

The Drăgșan Group is encountered on the northern side of the Vâlcan Mountains, following the line from west to east as follwos: Oslea – Osliţa – Şiglăul Mare – Negrele alignment, situated on the right bank of the Jiul de Vest River. It is composed of banded amphibolites and ultramafic bodies, augen gneisses, biotite gneisses and seldom marbles (Berza et al., 1988b). This group was intruded by the Retezat-Parâng and Culmea Cernei plutons. The Retezat pluton is composed of granodiorite and tonalite with some quartz diorite at its periphery (Liégeois et al., 1996).

In the Getic Nappe, The high-pressure rocks are restricted to the Sebeş, Lotru and Cumpăna terranes. For the studied area mainly important are the Sebeş and the Lotru units. The Sebeş unit has been divided lithologicaly in three subunitsas follows: Sebes 3 is composed of a monotonous sequence of aluminous schist and paragneiss, with some distinctive manganese-rich horizons marked by tephroite and spessartine—bearing paragneiss while Sebes 2 consists of a bimodal suite of quartzofeldspathic gneiss and amphibolite; Sebes 1 is composed mainly of terrigenous metasedimentary rocks, including mica gneiss, quartzofeldspathic gneiss and subordinate quartzite, marble and amphibolite. The Lotru unit is described as a volcano-sedimentary terrane with oceanic affinities, consisting largely of amphibolite and biotite—plagioclase gneiss. Scattered through the Lotru unit are dismembered layered metabasic-ultrabasic complexes, derived from lherzolite, dunite, plagioclase wehrlite and gabbro (Medaris et al., 2003).

As for the methods of laboratory investigations and analizes, the minerals were studied according to their structure, dimensions and number of specimens found. We used X-ray powder diffraction (XRD), infrared absorption spectrometry, micro-raman spectrometry, scanning electron microscopy (SEM), combined with energy dispersion spectroscopy (SEM–EDS). To complete the studies, optical analyzes were made.

The new mineral occurrences are from these three areas and consists mainly of oxides, sulphates and silicates. These minerals have never been mentioned on the northern slopes of the Vâlcan Mountains.

The Şigleul Mare perimeter stands out with the secondary copper minerals identified and the quartz crystals colored in green, related to the copper minerals. Chalcopyrite, $CuFeS_2$ is the most common of the copper minerals that have been identified in the Şigleul Mare perimeter. It occurs on cracks and in nests, being constantly transformed into secondary minerals.

Cuprite – Cu₂O (Fig. 1), the main secondary copper mineral observed in the samples from the studied perimeter. It was formed by the oxidation of chalcopyrite from the quartz vein and it is constantly accompanied by goethite.

Malachite, Cu₂²⁺(CO₃)(OH)₂, constantly occurs in relationship with chalcopyrite and some secondary iron minerals, such as lepidocrocite and goethite. SEM-EDS analysis indicated a chemical composition closed to the standard values for this mineral. Individual malachite crystals are very rare. In the studied samples, both individual crystals and scattered malachite on quartz were observed.

Dioptase, $Cu_6Si_6O_{18}\cdot 6H_2O$ was found in the oxidation zones of the primary copper minerals (*i.e.* chalcopyrite). It can be seen with the naked eye in the form of individual crystals on quartz, as well as under the microscope. The chemical analysis also indicated a composition closed to the standard values. Manganese is the new element that occurs in the chemical composition in a significant percentage. Considering that the other elements are according to the standards, it is possible that there is a particular Mn-dioptase. (Szabo and Popescu, 2017).

The other two perimeters are known for the new sulphate minerals encountered in this region and consists mainly of the pickeringite - halotrichite isomorphic series, along with alunogene.

Pickeringite MgAl₂(SO₄)₄* 22 H_2O, the aluminum and magnesium hydrated sulphate is the last term of the halotrichite-pickeringite isomorphic series. The macroscopic observation both in the field and with the binocular magnifying glass have highlighted the presence of this mineral in the form of fibrous aggregates up to 2 mm in size. The color ranges from white to yellowish in Scocul Jiului -Gârbovu to yellow in Tusu Valley. A silky luster has been observed. It is fractured in an uneven pattern, the flat surfaces presents no cleavage. The crystals observed in the two perimeters are monoclinic beeing elongated after the c axis. X-Ray powder diffractometry analyzes made possible to identify pickeringite wich appears intimately associated with halotrichite. The analyses were completed with micro-Raman, Infrared Spectrometry and Scanning Electron Microscopy.

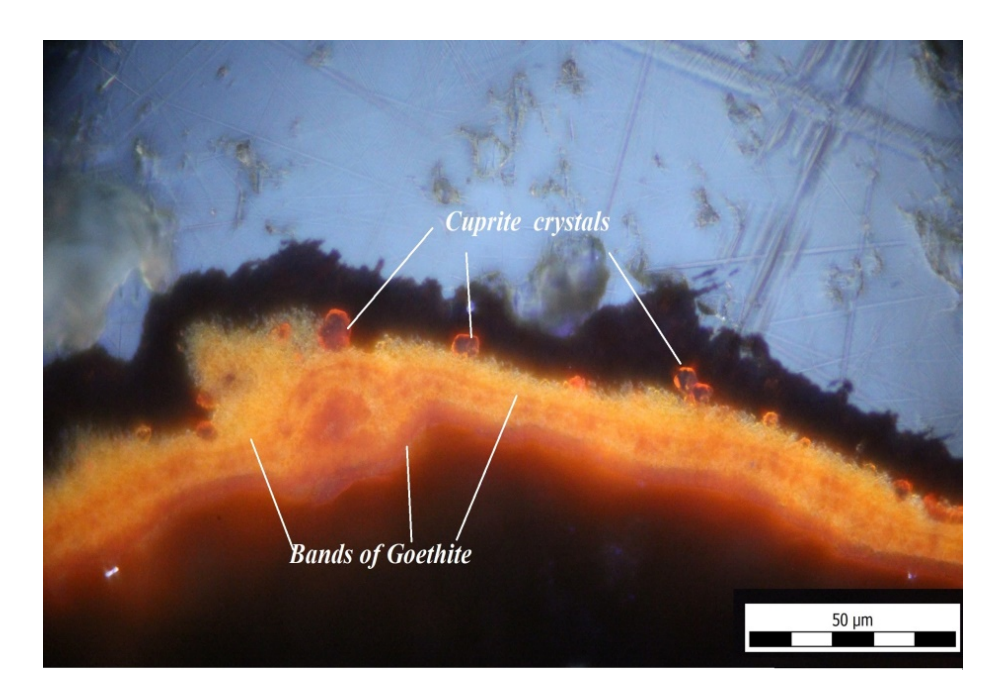


Fig. 1. Cuprite crystals with bands of goethite on a polished section.

Halotrichite FeAl₂(SO₄)₄ *22H₂O, the aluminum and iron hydrated sulphate, is the first term of the halotrichite-pickeringite isomorphic series. It has been observed with fibrous masses, having a green to pale green color. The luster is silky. It forms needle-like crystals up to 1 mm often beeing placed on the pickeringite wich he accompanies. X-ray powder diffractometry analyzes made possible to identify halotrichite in samples from Scocul Jiului de Vest – Gârbovul and Tusu Valley. In each of the samples the halotrichite appears intimately associated with pickeringite as mentioned before. After indexing the resulting diffractograms and applying the calculation methods used by Benoit since 1987, the values of the reticular parameters of halotrichite could be determined. The medium values for the four samples are: a = 6.182(7), b = 24.225(8), c = 21.056(6), Beta = 100.62(3) and V = 3102.15(3). The values obtained by our research are very close to the ones published by other scientists. The analyses were completed with micro-Raman, Infrared Spectrometry and Scanning Electron Microscopy.

Alunogen Al₂ (SO₄) $_2$ * **17** H₂O occurs in the form of small tabular crystals united in fibrous masses or crusts, sometimes presents small, semi-transparent crystals. In Scocul Jiului de Vest it is also encountered in massive forms. It is triclinic and has white to yellowish-yellow colors in Tusu, while in Scocul Jiului the color is yellow or it sometimes appears with a pronounced orange hue. It is optically positive. It belongs to the triclinic class. X-ray powder diffractometry analyzes made possible to identify alunogene wich appears intimately associated with pickeringite. After indexing the resulting diffractograms and applying the calculation methods, the values for the lattice parameters of alunogene determined are: a = 7.4205 (9), b = 26.9166 (7), c = 6.0534 (8), Beta = 97.0 (6), and V = 1197.894 (4). These values obtained for the alunogen identified in the Western Jiu Valley formations are very close to the data from the literature, presented in the table bellow. Reporting parameters between intensity (I) and spacing (d) are as follows: at I = 100, d = 4.48, I = 81, d = 4.39, I = 81, d = 4.32. The values of the reticular parameters in the literature are very close to those determined in the analyses.

In what concerns the pickeringite, this is intimately associated with halotrichite. The two minerals form an isomorphic series Halotrichite beeing the first term and pickeringite the last one. Halotrichite is the product resulting from the action of aluminum-rich sulfate solutions and iron ions, catalysed by a small amount of oxygen (Mastacan, Mastacan, 1976). Iron comes from pyrite while the magnesium comes from the dolomites that are found in the geological structures of the studied area. Substitution of Mg²⁺ with Fe²⁺ is permanent, therefore the two minerals do not appear separately for their identification and study, several methods beeing used in order to study them, the most significant in this case beiing Raman spectroscopy wich has proven to bee a powerful tool that highlights the bands specific to the two minerals.

Alunogen is formed as a product of alteration of rocks containing pyrite and aluminum. The Raman spectrum produced a v1 valence vibration at 992 cm⁻¹, which clearly shows the presence of this mineral in the perimeter studied.



Fig 2. Green color generated by the diffusion in the mass of white quartz, of a supergene malachite.

New studies have also made posible to identify minerals such as apatite - $Ca_5(PO_4)_3(CI/F/OH)$, zircon – ZrSiO₄ and *iron and titanium oxides* along with ilmenite, $Fe^{2^+}TiO_3$ some particular carbonates such as brownish calcite due to small amounts of iron impurities, aragonite (CaCO₃), possibly a nickel carbonate Gaspeite Ni(CO₃) (?) zeolite known as gismondine $Ca_2AI_4Si_4O_{16}$ *9H₂O. All of these are part of studies conducted in the present. Some of these minerals have been mentioned and others are new for the northern slopes of Vâlcan Mountains. Such is the case of a zeolite known as **gismondine** $Ca_2AI_4Si_4O_{16}$ *9H₂O.

The secondary **c**opper minerals identified in the Şiglău-Uricani perimeter are unknown since our research, representing a novelty for the northern flank of the Vîlcan Mountains. Some of these minerals are rare in the Carpathian Mountains, for example dioptase, wich has been mentioned only in Băiţa-Bihor (Udubaşa *et. al.*, 2002). It can be presumed that these secondary copper minerals could be the cause of the particular green color of quartz from the Şiglău-Uricani perimeter. For the moment, this is the only known occurrence of a green quartz in Romania. The green shade of the quartz (Fig. 2), named *Şiglău Green* (*Verde de Şiglău* in Romanian) (Szabo and Popescu, 2017), may be a diffusion in the mass of white quartz of a supergene malachite *who has enormous capacity to color it, as stated by Ramdhor*.

References

Berza, T., Seghedi, A., 1983. The crystalline basement of the Danubian Units in the central South Carpathians. An. Inst. Geol. Geof. LXI, 15-22.

Berza, T., Kräutner, H. & Dimitrescu, R., 1983. Nappe structure in the Danubian window of the Central South Carpathians. Anuarul Institutului de Geologie si Geofizica LX, 31-39.

Berza, T., Seghedi, A. & Drăgănescu, A., 1988a. The Danubian Units from the northern slope of the Vîlcan Mountains (South Carpathians). Dări de Seamă ale Institutului de Geologie și Geofi zică, 72-73/5: 23-41

Berza, T., Seghedi, A., Stănoiu, I., 1988b. The Danubian Units from the eastern part of the Retezat Mountains (South Carpathians). Dări de Seamă ale Institutului de Geologie și Geofi zică, 72-73/5: 5-22.

Berza, T., Balintoni, I., Iancu, V., Seghedi, A., Hann, H.P., 1994b. South Carpathians, ALCAPA II Field Guidebook, Romanian Journal of Tectonics & Regional Geology, 75, Supplement no. 2: 37-49, Bucureşti.

Codarcea, A., 1940. Voues nouvelles sur la tectonique du Banat et du Plateau de Mehedinti. An. Inst. Geol. Geof., XX, 1-74.

- Kräutner, H.G., Năstăseanu, S., Berza, T., Stănoiu, I., Iancu V., 1981. Metamorphosed Paleozoic in the South Carpathians and its relation with the pre-Paleozoic basement. Guide to excursion A, Carp. Balk. Geol. Assoc. Congr. XII, București, 116 pp.
- Kräutner, H.G., Berza, T., Dimitrescu, R., 1988. South Carpathians. In: V. Zoubek (Editor), Precambrian in Younger Fold Belts. J Wiley, London, 633-664.
- Liégeois, J.P., Berza, T., Tatu, M., Duchesne, J.C., 1996. The Neoproterozoic Pan-African basement from the Alpine Lower Danubian nappe system (South Carpathians, Romania). Elsevier, Precambrian Research 80, 281-301.
- Medaris, G. Jr., Ducea, M., Ghent, Ed., Iancu, V., 2003. Conditions and timing of high-pressure Variscan metamorphism in the South Carpathians, Romania. Lithos 70, 141-161.
- Manolescu, G., 1937. Étude géologique et pétrographique dans les Munții Vulcan (Carpates Méridionales). An. Inst. Geol. Rom., Vol. XVIII.
- Mastacan, Gh., Mastacan, I., 1976. Mineralogie, Vol II, Editura Tehnică, București.
- Mutihac, V., Mutihac, G., 1990. Structura geologică a teritoriului României. Editura Tehnică, București, 424 pp.
- Pavelescu, L., Pavelescu, M., 1964. Geologia și petrografia văii Jiului Românesc între Oslea și Petroșeni. An. Inst. Geol. Rom., Volumul XXXIII, București.
- Ramdohr, P., 1969. The ore minerals and their intergrowths. Pergamon Press, Oxford, London.
- Savu, H., 1970. Structura plutonului granitoid de Şuşiţa si relaţiile sale cu formaţiunile autohtonului danubian (Carpaţii Meridionali). Dări de Seamă ale Institutului Geologic, LVI/5, 132-153, Bucureşti.
- Szabo, R., Popescu, Gh., 2017. Preliminary data on secondary copper minerals from the Şiglău-Uricani perimeter, Vîlcan Mountains, Romania, Romanian Journal of Mineral Deposits 90, 1-2.
- Stănoiu, I., 1973. Zona Mehedinți Retezat, o unitate paleogeografică și tectonică distinctă a Carpaților Meridionali. D.S. Inst. Geol., LIX, 5, 127-171.
- Udubaşa, Gh., Ďuďa, R., Szakáll, S., Kvasnytsya, V., Koszowska, E., Novák, M., 2002. Minerals of the Carpathians. Sándor Szakáll (ed.), Granit Prague, 479 pp.

NEW APPROACHES ON CRYSTALLIZATION PRESSURE OF SOME LATE CRETACEOUS GRANITOIDS FROM ROMANIA

Mihai TATU^{a,b} & Elena – Luisa IATAN^a

^a Institute of Geodynamics "Sabba S. Stefanescu", Romanian Academy, 19–21, Jean-Louis Calderon Str., Bucharest 020032, Romania

^b Geological Institute of Romania, Caransebes Str. 1, RO-012271. Bucharest, Romania

During Late Cretaceous and also at the beginning of Paleogene period an important intrusive and effusive igneous activity was occurred along the territory between the Western Carpathians and Iran. This magmatism evolved in a geodynamic context marked apart from the appearance of sedimentary basins with complex evolution, molasses in general, but also of a very deep Gosau type (Schuller, 2004; Schuller et al., 2009), whose configuration and distribution within the alpine chain was controlled by an extensional tectonics that post-dated the meso-cretaceous alpine collisions, and on the other hand by the occurrence and evolution of a complex magmatism from a compositional point of view and as manifestation (intrusive and extrusive), most of it calco-alkaline, known in the geological literature as "banatitic" (von Cotta, 1864). With this type of rocks are linked a whole series of metalliferous accumulations that, by their variety of composition and content, have attracted the attention of specialists. Excepting the ages obtained by the K-Ar method on total rock or on ferromagnesian minerals (Bleahu et al. 1984), all other data are grouped strictly in the Campanian interval (Gallhofer, 2015), suggesting a magmatism that evolved in a narrow time window ("short-lived magmatism") typical for events managed by transpressive-transtensive tectonics with adiabatic detention up to the crust-mantle interface. This aspect, of narrow time interval, is confirmed by several investigative methods with a high degree of reliability (Gallhofer, 2015; Ciobanu et al., 2002). Genetically, this magmatic province was initially geodynamically linked to the Jurassic and Meso-Cretaceous subductions, models that in the second half of the last century and at the beginning of this century were considered due to the level of understanding of the igneous processes, the only formational and rational reasoning (Giuscă et al., 1966; Rădulescu, 1974; Ștefan et al., 1988; Vlad, 1997; Jankovic, 1997; Karamata et al., 1997; Handy et al., 2014; Gallhofer, 2015). Occasionally, multiple subduction hypotheses are exposed to justify the presence of various petrogenetic associations of different ages in neighbouring areas although the geological realities do not support them (Handy et al., 2014). The first paper that argues the postcollisional character of the banatites, in the particular case of those from Banat is that of Nicolescu et al. (1999). In this work, the author presents the situation in the Moravita valley basin, where the Ocna de Fier intrusion crosses the Ezeris-Coltan reverse fault, which separates the metamorphic series from Bocsita-Dâmoxa and Buchin from the Bocșa nappe. In a similar situation, along the Dognecea valley, the banatitic intrusions crossed the Dognecea thrust line that separates the supragetic nappes as Bocşa and Moniom. Both tectonic units were previously considered meso-cretaceous; Ezeriş-Colţan reverse fault is intra-Turonian (90 Ma), while the Dognecea thrust is Austrian (~ 100 Ma) (lancu 1986; Dallmeyer et al., 1996). Similar situations we meet in the Apuseni Mountains: the intrusion from Valea Cepelor (Arieşul Mare basin) seals the tectonic contacts between the Biharea / Poiana / Arieșeni units; all contacts between the mesocretaceous units within the Biharea massif are crossed by banatitic intrusions different in sizes: the Budureasa and Pietroasa massifs seal or cross meso-cretaceous units. To the ones presented above it is added that all the intrusions are non-deformed, and when this happens the deformation is broken, wide spaced, post intrusion.

This igneous province consists of granitoidic rocks and mafic rocks that proof various information about of the associated mineral deposits, the granite intrusions furnishing critical industrial materials and metals. For instance, porphyry copper (±Au) deposits are related to intrusions emplaced at relatively shallow depth (Chiaradia et al., 2012), while skarn copper (±Au) deposits are completely connected with comparatively deep intrusions (Burt, 1998; Meinert, 1998), as also the intrusions related gold deposits

(Yang et al., 2008). For that reason, estimation of the crystallization pressure (or depth) of granite intrusions can facilitate the elaboration of exploration models. Moreover, the depth of granite intrusions provides important data about the erosion depth and rate, and can thus supply solution for geodynamic reconstruction.

Several methods have been employed to assess the crystallisation pressures (or depths) of granite intrusions: geological mapping to recreate stratigraphic columns containing the intrusions; petrologic studies of the contact of associated rocks, fluid inclusion investigations, in experimental domain, in order to reproduce the environment of T-P-X-H2O for granite crystallization (Scaillet et al., 2016; Tuttle & Bowen, 1958), geophysical investigation in order to obtain 3D architecture of intrusions, and automatic phase-equilibrium modelling (Gualda and Ghiorso, 2013, 2014; Ghiorso and Gualda, 2015).

In 2017, Xue-Ming Yang from Manitoba Geological Survey (Canada) proposed a new numerical method in order to estimate the crystallization pressure of granite intrusions. This method is based on two polynomial equations obtained by an investigation of the existing haplogranite ternary phase diagram. The results of this study indicate that the crystallization pressure of the haplogranite system is directly correlated with normative quartz (Qtz) content and with the sum between the normative albite (Ab) and normative orthoclase (Or) contents of some granitic rocks.

$$P = -0.2426*(Qtz)^{3} + 26.392*(Qtz)^{2} - 980.74*(Qtz) + 12563$$
 (1)

$$P = 0.2426*(Ab+Or)^{3}-46.397*(Ab+Or)^{2}+2981.3*(Ab+Or)-64224$$
 (2)

 $R^2 = 0.9943$

where P is pressure in MPa, and R represents the correlation coefficient.

The selected samples are recalculated to dry and the obtained results are used in the calculation of the CIPW norm. The Qtz, Ab, Or components are brought to 100% to be used in equations. The difference between the two equations must be ≤16 MPa, but not less than 9 Mpa. The range of normative quartz contents must range from 15 to 40 wt%. When the sum between Ab and Or is greater than 70%, the quartz is in equilibrium at eutectic with two feldspars, and when the sum is below 70%, only one feldspar is in equilibrium with quartz. We tried in our study to apply this methodology to estimate crystallization pressures in case of some Upper Cretaceous intrusive and effusive rocks that outcrop in Banat, Apuseni Mountains and Poiana Rusca. Our selection of samples that were to be used in polynomial equations in order to estimate the crystallization pressure was taken account by the recommendations expressed by Yang (2017), namely the granites, rhyolites and granodiorites must be evolved.

Our results are present in Table 1 and in Figures 1 and 2. It can be observed that most of the values representing the crystallization pressures fall in the range 150 - 330 MPa, corresponding for 6-8 Km in depths at which the intrusions were placed. Only samples 98R23 and 98R16 representing granodiorites from Tincova and Bocsa respectively indicate values in the range 540 - 638 MPa which would correspond to depths of 16 - 17 Km. In any case, the data projected in the two diagrams have a nicely square correlation coefficient R^2 of 0.94 and the Spearman rank correlation coefficient is 0.999. Plotting our data in the ternary diagram Ab-Or-Q (Fig. 2, Anderson, 1996) we have been obtained the similar configuration that confirms the results.

As Yang says (2017), the values of crystallisation pressure estimated from equations 1 and 2 generally confirm the crystallization pressure of quartz with a single feldspar (alongside cotectic curves, or at relatively lower emplacement pressure of hypersolvus granites), and with two feldspars (at eutectic points, or at higher emplacement pressure of subsolvus granites). However, these pressures are generally

| Geosciences in the 21 st century |
|---|
| |

lower than those estimated by the Al-inhornblende barometry (Hammarstrom & Zen, 1986; Johnson & Rutherford, 1989; Schmidt, 1992), considering the importance of different fluids involved in crystallisation.

| | | | | | | | | | | | | | | | | | | | | | | | | | | | 1 |
|--|------------------|--------|--------|--------|--------|--------|--------|--------|--------|--------|--------|--------|--------|--------|--------|--------|--------|--------|--------|--------|--------|--------|--------|--------|--------|--------|---|
| | T sat ap | 924 | 880 | 895 | 878 | 868 | 899 | 886 | 888 | 890 | 896 | 883 | | | | | | | | | | | | | | | |
| | T sat Zr | 783 | 760 | 719 | 748 | 780 | 787 | 770 | 780 | 277 | 745 | 753 | | | | | | | | | | | | | | | |
| | P(2) | 158 | 304 | 202 | 291 | 151 | 161 | 250 | 193 | 303 | 540 | 627 | 260 | 239 | 245 | 260 | 166 | 191 | 210 | 217 | 213 | 329 | 180 | 151 | 209 | 331 | |
| | P(1) | 166 | 314 | 211 | 301 | 160 | 169 | 259 | 202 | 313 | 551 | 638 | 269 | 248 | 255 | 270 | 175 | 200 | 219 | 226 | 222 | 338 | 189 | 160 | 218 | 341 | |
| peratures | Total | 100.00 | 100.00 | 100.00 | 100.00 | 100.00 | 100.00 | 100.00 | 100.00 | 100.00 | 100.00 | 100.00 | 100.00 | 100.00 | 100.00 | 100.00 | 100.00 | 100.00 | 100.00 | 100.00 | 100.00 | 100.00 | 100.00 | 100.00 | 100.00 | 100.00 | |
| uration ten | ab (%) | 36.42 | 38.33 | 42.76 | 49.30 | 34.26 | 35.73 | 46.30 | 40.63 | 45.88 | 50.80 | 47.66 | 39.95 | 39.30 | 44.82 | 40.85 | 37.48 | 38.39 | 40.34 | 40.42 | 44.98 | 44.96 | 39.08 | 31.73 | 42.17 | 44.95 | |
| zircon sat | or (%) | 28.60 | 31.07 | 23.91 | 19.82 | 30.50 | 29.41 | 21.80 | 25.73 | 23.50 | 22.23 | 26.31 | 28.42 | 28.49 | 23.16 | 27.54 | 27.88 | 27.90 | 26.59 | 26.73 | 22.05 | 24.95 | 26.83 | 33.03 | 24.74 | 25.01 | |
| ia and their | 6%) 0 | 34.98 | 30.60 | 33.34 | 30.88 | 35.24 | 34.85 | 31.90 | 33.64 | 30.62 | 26.96 | 26.03 | 31.63 | 32.20 | 32.01 | 31.62 | 34.64 | 33.71 | 33.07 | 32.85 | 32.98 | 30.10 | 34.10 | 35.24 | 33.09 | 30.04 | |
| of Roman | Total | 88.16 | 85.15 | 77.74 | 81.81 | 82.78 | 81.12 | 76.56 | 80.93 | 80.30 | 77.86 | 77.47 | 82.91 | 82.20 | 78.51 | 74.97 | 90.75 | 87.61 | 83.05 | 86.08 | 81.62 | 83.64 | 90.74 | 86.60 | 82.66 | 83.66 | |
| atitic rocks | ab | 32.11 | 32.63 | 33.24 | 40.33 | 28.36 | 28.99 | 35.45 | 32.88 | 36.84 | 39.56 | 36.92 | 33.12 | 32.31 | 35.19 | 30.62 | 34.01 | 33.63 | 33.50 | 32.73 | 36.71 | 37.60 | 35.46 | 27.48 | 34.86 | 37.60 | |
| r some bar | Of. | 25.21 | 26.46 | 18.58 | 16.22 | 25.25 | 23.86 | 16.69 | 20.82 | 18.87 | 17.31 | 20.38 | 23.56 | 23.42 | 18.19 | 20.64 | 25.30 | 24.45 | 22.08 | 21.65 | 17.99 | 20.87 | 24.34 | 28.61 | 20.45 | 20.93 | |
| pressure fo | ò | 30.84 | 26.06 | 25.92 | 25.27 | 29.17 | 28.28 | 24.42 | 27.23 | 24.59 | 20.99 | 20.16 | 26.22 | 26.47 | 25.13 | 23.70 | 31.44 | 29.53 | 27.47 | 26.60 | 26.91 | 25.17 | 30.94 | 30.52 | 27.35 | 25.13 | |
| stallisation | SiO ₂ | 71.25 | 70.02 | 19.79 | 88.99 | 68.74 | 67.95 | 66.74 | 67.79 | 96.79 | 16.99 | 66.50 | 68.37 | 67.93 | 67.25 | 65.73 | 71.98 | 70.74 | 00.69 | 00.89 | 96.79 | 70.24 | 72.05 | 69.31 | 67.34 | 70.21 | |
| mation cry | Lithology | Rh | G | Cd | PD | G | PS | PD | PS | PD | PS | PS | Ð | PS | PD | PS | Rh | Rh | Rh | Ð | PD | Rh | G | Ð | Ð | Ð | |
| able 1. Estimation crystallisation pressure for some banatitic rocks of Romania and their zircon saturation temperatures | Sample I | R39 | DG019 | DG026 | DG047 | DG084 | DG085 | DG104 | DG108 | DG110 | 98R23 | 98R16 | 9335 | 9339 | 9321 | 9345 | 12 | 16 | 61 | 20 | 21 | 24 | 4 | 5 | 7 | 24 | |

Source of samples: R39 (Vander Auwera J. et al, 2015); DG019 – DG110 (Gallhofer D. 2015): 98R23, 98R16 (Dupont A. et al 2002); 9335 – 9345 (Stefan A. et al 1992); 12 – 21 (Stefan A. 1980); 24 (Istrate Gh. 1978); 4 – 24 (Istrate Gh., Bratosin I. 1976); lithology: Rh = rhyolite; G = granite; Gd = granodirite. Pressures P(1) and P(2) are in MPa and temperatures are in °C.

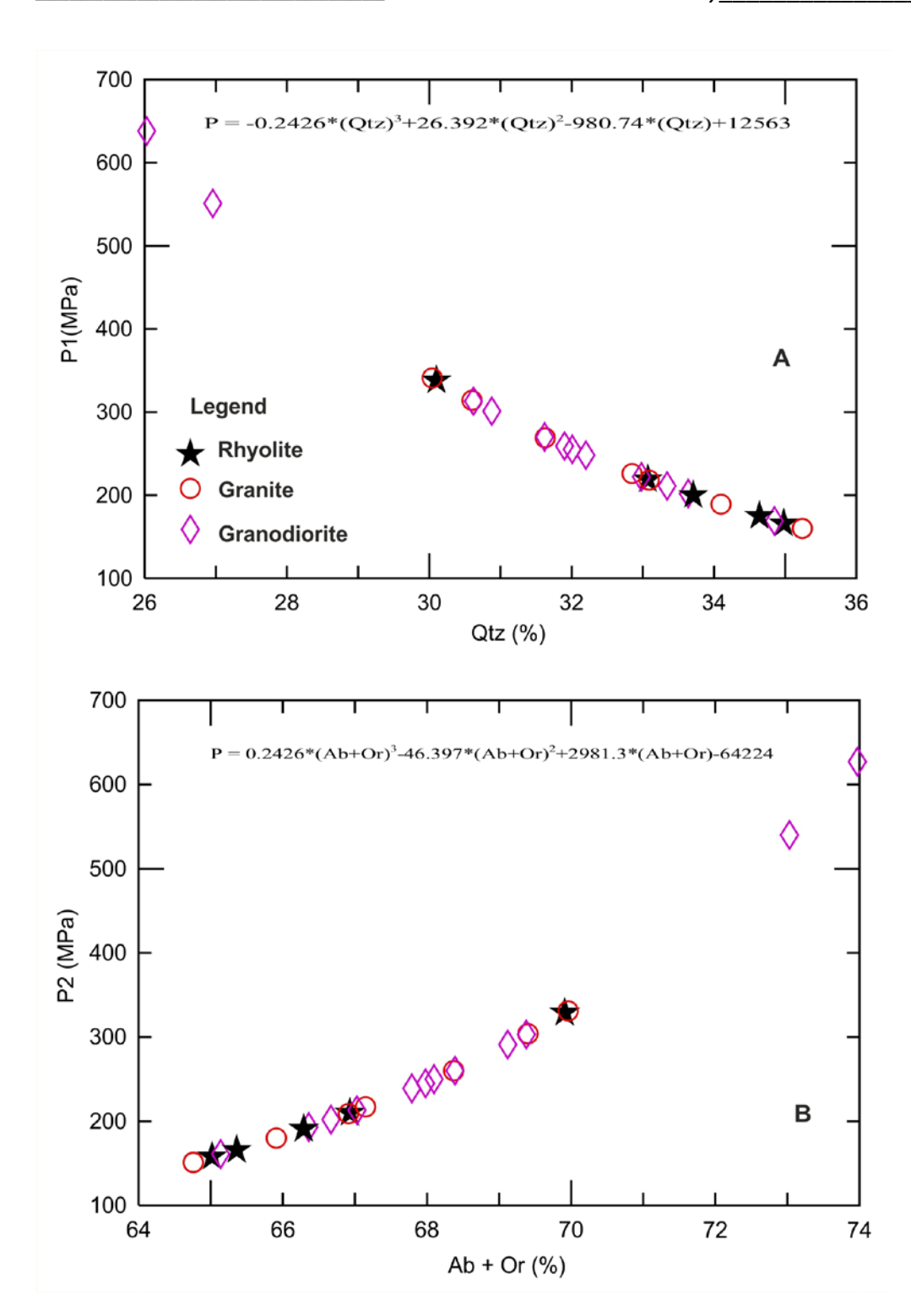


Fig. 1. Crystallization pressure (MPa) versus (a) normative Qtz content (wt.%) and (b) (Ab + Or) of some banatitic rocks.

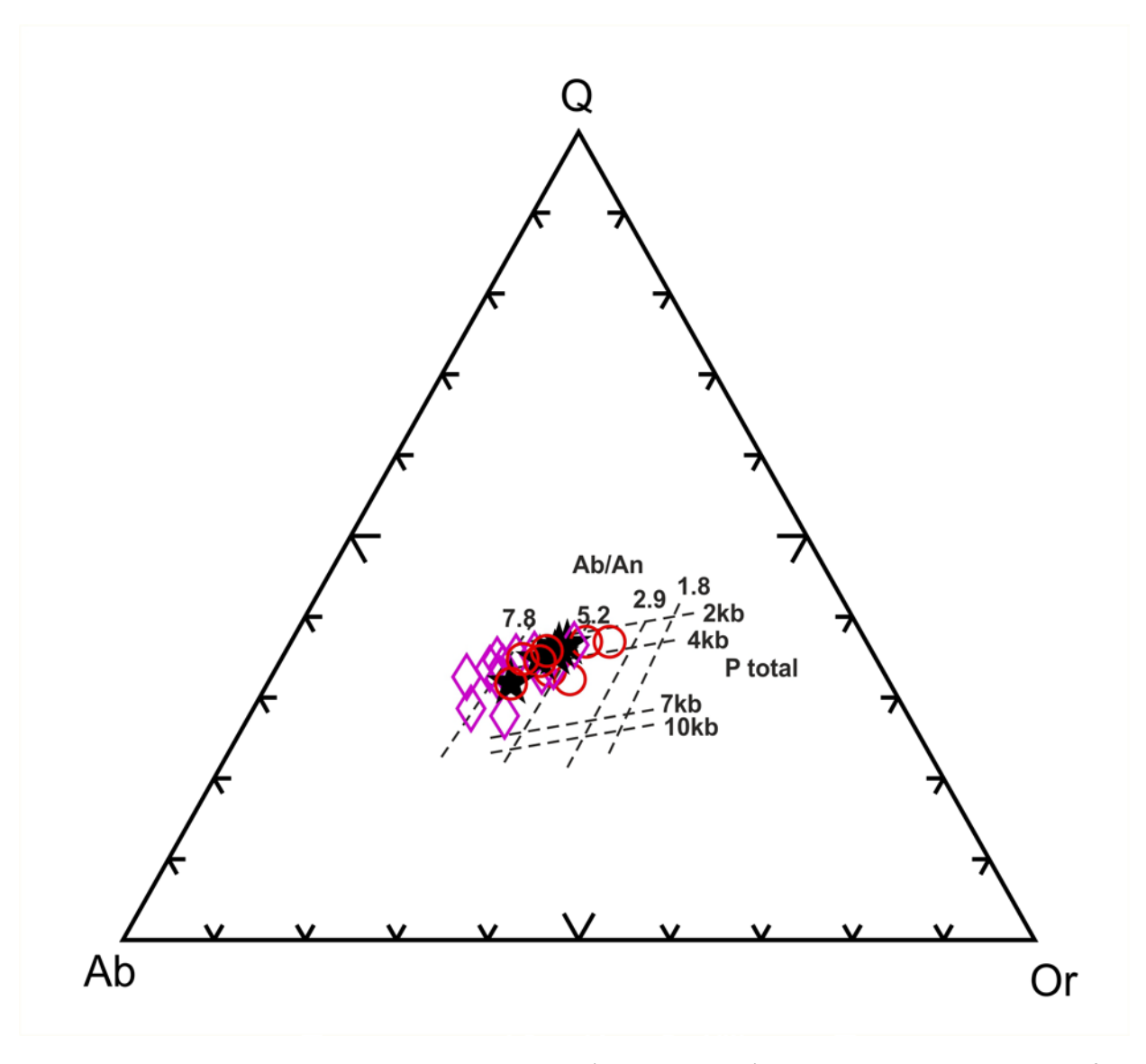


Fig. 2. Banatitic rocks plotted in ternary diagram Ab-Or-Q (Anderson, 1996). The legend is similar to the one from the figure 1.

Acknowledgments

This work was supported by grant of the Romanian Ministry of Research and Innovation, CCCDI – UEFISCDI, project number PN-III-P4-ID-PCCF-2016-4-0014, within PNCDI III and by a grant of the Romanian Ministry of Research and Innovation, CCCDI – UEFISCDI, project number PN-III-P1-1.2-PCCDI-2017-0346/29, within PNCDI III

39.53 MODEL OF THE SOLAR SYSTEM (BASED ON CYCLICITY OF GEOLOGICAL PHENOMENA)

Mircea ȚICLEANU¹, Alexandru ȚICLEANU², Radu NICOLESCU¹

¹Geological Institute of Romania, 1 Caransebeş St, Bucharest, Romania e-mail: mircea.ticleanu@yahoo.com ²Independent Researcher, Bucharest, Romania

This new model of the Solar System was first imagined by us (Ticleanu et al., 2016) and based on the premise that the phenomenon of capturing was widely present in the past of this planetary system. The Moon captured by Earth, Triton captured by Neptune, Charon captured by Pluto, represent the best examples in this sense. In all these cases, the captured planets transformed into satellites do not originate outside of the Solar System but within it, having as source either the internal telluric planetary subsystem (the Moon), or the subsystem of trans-Neptunian telluric dwarf planets (Triton and Charon).

Likewise, this model holds in regard the fact that within the Solar System, giant planets like Jupiter and Saturn in particular, can sometimes, circumstantially, become a secondary gravity center, able to draw out of their orbits telluric planets and transform them into their satellites. Thus, the Moon, Triton and Charon may represent former planets of the Solar System that were captured on different moments by larger or much larger planets (Earth, Neptune, Pluto), while they were drawn towards the secondary mass center of the Solar System, namely to the giant planets. These phenomena suppose an alignment of all planets on the same side of the Sun at those moments, and also the fact that other small planets have already become satellites of giant planets without being captured along their way. We could say that all large satellites of giant planets were initially telluric planets captured along time. Such a novel point of view raises the issue of initial positioning for these ex-planets within the Solar System.

A reanalysis of our planetary system and especially of the internal telluric subsystem led us to the idea that beyond a zero orbit (the Moon's former orbit at about 30.32 ml. km from the Sun), the internal telluric planets found themselves on orbits 39.53 ml. km of each other, regardless of their size. This value has been reached, step by step, by trying to determine the initial position as first planet of the Solar System, for the Moon. The almost circular orbit of the planet Venus was taken as a reference orbit for the internal telluric subsystem, and the average distances between the telluric planets led to this standard value (39.53 ml. km) through calibrations and recalibrations between the orbits of Mars and Mercury.

Such a perspective revealed that a planet could have orbited between Earth and Mars, one missing today, but also the fact that between Mars and the asteroid belt there were two other planets in the past. A brief view of the large satellites of giant planets, Jupiter and Saturn, lets us assume the missing planet between Earth and Mars is Ganymede and that between Mars and the asteroid belt were the former planets Titan and Callisto. Beyond the asteroid belt there could have been orbits of two smaller planets, now satellites of Jupiter, Io and Europa respectively. Thus, the internal telluric planet subsystem initially included the following planets that orbited on circular orbits of about 40 ml. km from one another, beyond the zero orbit of the Solar System: (the Moon), Mercury, Venus, Earth, (Ganymede), Mars, (Titan) and (Callisto). Thus, the orbits of the small ex-planets Io and Europa, were to be found between the asteroid belt and Jupiter.

So, the subsystem of internal telluric planets is presently strongly perturbed, especially by the powerful influence of the circumstantial secondary mass center, which acted over time. The first captured planets were probably lo and Europa, which became satellites of Jupiter. The next planets captured by the gas giants were Callisto (Jupiter) and Titan (captured by Saturn). After a significant impact (about 80,000 years ago) the planet that orbited between Earth and Mars was projected on a very wide, new ellipsoidal orbit. At an interval of about 3,600 - 3,500 years, this planet (for us, the Nebra or Nibiru planet) was periodically very close to Earth, fact recorded at a planetary level by the Heinrich series, respectively by the extended Heinrich series (Ticleanu et al., 2010). Finally, it was captured by Jupiter in a moment of great

proximity, after the last moment of the extended Heinrich series (at about 1,525 BC, marked by the explosion of the Terra – Santorini caldera) and became the present satellite of Jupiter, Ganymede. The Moon's capture occurred about 40,000 years ago and this cosmic phenomenon led to the increase of the duration of the precessional cycle/year (from 14,000 to the actual value of about 25,920 years), due to the position change of our planet's rotational axis (Ticleanu M. et al., 2008, 2009). As a consequence, the shift of the Moon towards the secondary mass center modified the rotational axis position of Mercury and Venus.

Also, the deeply deformed orbit of Mercury is due to the Moon's presence on the initial (zero) orbit and the reciprocal influence of these two planets. In this dynamic context it is important to establish the cosmic cause connected with the first change (of about 12 degrees) from the initial (vertical) position of the rotational axis of Earth, since very old times, because the annual cycles, tied to the existence of terrestrial seasons and to the sedimentary summer-winter sequences, are reflected by sediments from very old ages.

Regarding the satellites Triton (Neptune) and Charon (Pluto), the origin of these small ex-planets can be assumed to be from the subsystem of the trans-Neptunian dwarf planets (that Pluto also belongs to), but the moments of capture are very difficult to pinpoint in time. Still, these moments may correspond with the aligning of the giant planets on the same side of the Sun and with the periodic presence of different trans-Neptunian dwarf planets on these alignments.

It is interesting to note the fact that the average distances between the Sun and the large planets match with multiples of the standard value of 39.53 ml. km as follows: Jupiter ($18 \times 39,53$), Saturn – ($36 \times$), Uranus ($73 \times$) and Neptune ($114 \times$). Pluto is also at an average distance of 151×39.53 ml. km from the Sun. However, these lengths hold to account the Sun's centre, not the "zero orbit" (30.32×10^{-2}), the spatial reference for the subsystem of the internal telluric planets. Also, we have here a purely formal numeric coincidence: the average Sun – Pluto distance is 39.53×10^{-2} UA (UA is the average distance between Sun and Earth).

However the standard value (39.53 ml. km), that ideally stretched the orbits of the internal telluric planets initially, can be a relative value because the possible pulsations of our planetary system, indicated by the clear existence of the Valach climatic cycle with a period of 4.1 ma (Ticleanu M. et al., 1998 – Prague and 2005 – Belgrade), could extend or shrink the distance between the planetary orbits. Presently, in connection with the dynamic phases of this cycle, the planets of the Solar System are very slowly drawn towards the Sun and this contraction trend should continue another 820,000 years. The previous phase of this cycle led to the Quaternary Ice Age on Earth, following this trend of planets to drift away from the Sun (Ticleanu, 2012), with an inversion of direction flow in the Pasadenian tectonic phase (1.23 ma ago).

It is very interesting to compare this new model of the Solar System with the model of Lee (2008, 2010, 2012). This author has a completely different vision because he believes that all planets of the Solar System, including current large planetary moons, have originated from a hypothetical Proto-Jupiter in different moments, as a result of a natural dynamic evolution. This "Proto-Jupiter" is the successor of a so-called "brown body" which appeared at the beginning together with the Proto-Sun from a primary gas body of the Solar System, named by this author the "gas cloud".

It is also very important to note that in the memory of mankind an image was preserved of an old period without the Moon on the sky, today named "the Pre-Selenary Arcadian World", and data attesting the periodic closeness of the lost planet to the Earth (that evolved initially between Earth and Mars) are also preserved, including the name of this cosmic body (called "Nibiru" by the Sumerians, and "Nebra" by the old Europeans), today as the Ganymede satellite of Jupiter.

References

Lee, T. F., 2012. The use of basic physics theories to determine the step-by-step development of our Solar System. 34th International Geological Congress, Brisbane, paper based on the previous paper from 2008 (T. Frank Lee (2008) – The single body breakup origin of the Solar System) and from 2010 (T. Frank Lee (2010) – Origin of the Solar System).

Ţicleanu, M., Ţicleanu, N., Diaconiţă, D., Pauliuc, S., 1998. The temporal content of the Neogene coal generating cycles in Romania. 8th Coal Geology Conference, Abstracts, p. 64-65, Prague.

- Ticleanu, M., Ticleanu, N., Pauliuc, S., Constantin, P., Marinescu, Fl., Diaconiţă, D., 2005. The Valach climatic cycle (4.1 M.y.) the outlining of a pulsatory movement within Solar System by using sequential analysis of Senonian and Cenozoic coal facies located in Romania. Book of proceedings, 6th European Coal Conference, p. 177 184, Belgrade.
- Ticleanu, M., Constantin, P., Ticleanu, N., Nicolescu, R., Borcan, Gh., 2008. The sudden increase of the precessional cycle duration at the beginning of the Hengelo interstade (~ 39 ka BP). 33rd International Geological Congress, abstract and poster, Oslo.
- Ticleanu, M., Ticleanu, N., Nicolescu, R., Ion, A., Borcan, Gh., 2009. The capture of the Moon by the Earth around 40 ka BP from the geological perspective. 9th International Multidisciplinary Scientific GeoConference SGEM 2009, v. 1, p. 137-146, Albena, Bulgaria.
- Ticleanu, M., Nicolescu, R., Damian, R., Gridan, T., Grigoriu, S., Ion, A., Gheuca, I., 2010. "Global warming" the last warm phase of the climatic cycle of "mini-glaciations" (with about 1,000 years period). 10th International Multidisciplinary Scientific GeoConference SGEM 2010, Conference proceedings, v. 1, p. 45-53, Albena, Bulgaria.
- Ticleanu, M., 2012. Quaternary Ice Age the last cold phase of the Valach climatic cycle (with about 4.1 ma period), caused by the possible pulsations of the Solar System, 34th International Geological Congress, abstract, Brisbane, Australia.
- Ticleanu, M., Nicolescu, R., Ticleanu, A., 2016. The possible future of internal telluric planets and of trans-Neptunian dwarf planets: satellites of gas giants. 16th International Multidisciplinary Scientific GeoConference, SGEM 2016, Conference proceedings, v. III, p. 679 686, Albena, Bulgaria.
- Ticleanu, M., Nicolescu, R., 2017. Main cause of the planetary seismicity the radial (pulsatory) movements of the Earth 17th International Multidisciplinary Scientific GeoConference SGEM, v. 17, p. 229-236, Albena, Bulgaria.

CYCLOSTRATIGRAPHIC CHART OF THE MESO – NEOZOIC (CENOZOIC) TIME

Mircea ȚICLEANU¹, Alexandru ȚICLEANU², Radu NICOLESCU¹, Octavian COLȚOI¹, Flori CULESCU¹

¹Geological Institute of Romania, 1 Caransebes St., Bucharest, Romania ²Independent Researcher, Bucharest, Romania

This scheme is based on the idea that the stratigraphic limits of this time interval correspond to the temporal positions of a large number of distinct dynamic moments linked with two cycles: Valach climatic cycle (4.1 ma, pulsations of the Solar System) and Raup-Sepkoski cycle (26.78 ma, pulsations of our galaxy). Many of these moments, often perceived as tectonic phases or as important extinctions, led to various global changes which allowed the separation of the chronostratigraphic units of the current geologic time scale (GTS). So, this chart aims to calibrate the stratigraphic limits of the Meso-Neozoic time relative to temporal positions of some dynamic moments of these two cycles. But the dynamic moments associated to the Valach cycle (VhCy) are very common (at every 2.05 ma), while those due to the R-S cycle are rarer (at 13.39 ma). The dynamic series connected with the VhCy has, as a temporal reference, the Rhodanian phase (5.33 ma, occurred at Miocene-Pliocene limit), and the R-S series has, for temporal reference, the Wallachian phase, occurred 2.58 ma ago, at the Pliocene-Quaternary limit. We linked the previous term of R-S series to the Burdigalian-Langhian limit (15.97 ma), and this way it was possible to correct the R-S cycle duration (from 26 to 26.78 ma). The calibration of the stratigraphic limits of the Meso-Neozoic time was practically done by moving, with minimal values of corrections, the reference value of these limits to the nearest temporal positions belonging to both dynamic series. Because the dynamic moments of the R-S series are rare, we get in fact a characterization of these temporal units, from the view of the VhCy. It can be seen that some units have a temporal extension of 2.05 ma and others have 4.1 ma, 6.15 ma, 8.2 ma, 10.25 ma and 12.3 ma. But these latter units also have subunits with the duration equal to the period of the VhCy, sometimes with distinct names, with the Aptian as a great example. In addition, the limits of these units are placed either inside a cold phase of the VhCy (for the Miocene-Pliocene limit and for the limits corresponding to the temporal values 5.33 + 4.1 ma x n), or inside a warm phase of this cycle (for Tortonian-Messinian limit and for the limits corresponding to the temporal values of the series 7.38 + 4.1 ma x n). Among the limits that can be calibrated in relation to the dynamic moments of the RS cycle, we mention the Thanetian-Ypresian, Valanginian-Hauterivian and Norian-Rethian. These calibrations enable to presume that the Cretaceous-Paleogene limit is not related to our two series, thus corresponding with a dynamic moment of higher order (probably Vail-Payton megacycle) or to an unusual astronomical moment.

Our concerns regarding a complex cyclostratigraphic chart of the Neogene (for the Central Paratethys) (Ticleanu et al., 2018), also based on the previous perspective on dynamic causes of the tectonic phases (Ticleanu, 2013), helped to sketch a cyclostratigraphic chart of the Meso-Neozoic time. This chart is built first on the temporal position of the moments of the dynamic series associated with the Valach climatic cycle (Ticleanu et al., 2002), namely on the temporal position of the tectonic phases associated with this cycle. In this regard, we are also able to confirm the viability of the R–S cycles thus we rely on the correction of the dynamic series associated with this important cyclicity. This correction is based on the possible existence of two different tectonic phases between the Old Styrian phase and the Moldavian phase. The first can be linked to the Burdigalian–Langhian limit (at 15.97 ma) and was assimilated with the New-Styrian phase and the second, placed at 15.58 ma, connected with the VhCy, can be named Late New-Styrian phase. But our attempt envisages a particular elaboration of a GTS which kept all virtual moments of two forementioned dynamic series, figured as fine lines. Such a structure (texture) of cyclical nature of the GTS can provide the best picture of the chronostratigraphic subdivisions because it is a complex image simultaneously including temporal, dynamic and climatic aspects. This texture evidently

includes only the calibrated values of the chronostratigraphic limits of the GTS moved, with minimal corrections, on the temporal position of moments of the dynamic series of our two cycles (VhCy and RS cycles). It's important to specify that our approach here is mainly based on the GTS of Gradstein et al., 2004 respectively of Ogg G.(2004) because this chart seems to be the best approach regarding the geological time, and because the newest charts (including the last one, from 2018) have some important changes to be confirmed in the future, especially at the Triassic period level, changes already occurring in the International Cronostratigraphic Charts since 2009, respectively in the GTS of Walker & Geissman – 2009 and accepted by Cohen et al. – 2013 and 2018 after the publishing of the Furin team's study (2006).

Since 1982/1984 a new cycle, with a long time period (26 ma), was proposed by the American geologists D. Raup and J. Sepkoski jr. They advanced the idea that in the last 250 ma the biosphere was affected by 12 important extinctions periodically repeated at intervals of 26 ma. The authors did not indicate the possible cause of these extinctions, but they assumed that this cause has a cosmic nature. Among these extinctions a special place is occupied by the extinction placed at the K-P limit, connected with the extinction of the Dinosaurs. But the most severe extinction of this time is connected with the Permian-Triassic limit, which marks the beginning of the Mesozoic. Between these two important extinctions (P-T and K-P limit), now we consider a period of time of 185.5 ma. So, between these two extinctions it can be included 7 complete R-S cycles with a period of 26 ma (26 ma x 7 = 182 ma). Even more exactly, this period is of about 26.5 ma (185.5: 7 = 26,5 ma). But for Neozoic this period (26 or 26.5 ma) seems to be incorrect, especially with an extinction placed at 5 ma ago. However, this cycle seems to be viable if we consider the dynamic realities of the Neozoic, namely the temporal position of the Neogene tectonic phases. Among these phases, the Wallachian tectonic moment (at 2.58 ma) has a different temporal position and may be linked with our R-S cycle. Other Neogene phases (repeated at each 2.05 ma) correspond to the dynamic series due to the VhCy. The Rhodanian phase (at 5.33 ma) is the reference phase of this dynamic series that reflects the pulsatory movement of the Solar System. With a period of 26 ma (or of 26.5 ma) we set the previous term of the R-S cycle at about 28.58 ma (or at 29.05 ma), corresponding to the temporal position of the Helvetian phase, placed at the upper part of the Paleogene. But if we have a real R-S cycle reflecting the pulsations of our galaxy, with a 26 ma (or 26.5 ma) period, it is possible having also a dynamic moment of this cycle each 13 ma (or at 13.25 ma). In this case the real previous term of this series is placed at about 15.58 ma or at 15.83 ma. The first temporal position corresponds with a moment (New-Styrian phase) of the Valach dynamic series, but the second moment is placed near the Burdigalian/Langhian limit, at 15.97 ma. We presume that this last moment is, in fact, the real previous term of the R-S cycle and, in this case, the temporal distance before the Wallachian phase has a different value: 15.97 - 2.58 = 13.39 ma. With this data, it's possible to correct the R-S cycle period with the additional 13.39 + 13.39 = 26.78 ma. As a consequence, we have two different tectonic phases in place of the classical New-Styrian phase: the first at 15.97 ma and the second at 15.58 ma. In this case, it's necessary to keep the name New-Styrian phase for the first moment (linked with the Burdigalian-Langhian limit). For the second tectonic moment we suggest the name 'Late New-Styrian' phase.

Cyclostratigraphic calibration of the Meso-Neozoic limits can rely on the temporal position of the moments of two distinct dynamic series. The first is connected with the VhCy, having more frequent moments, and the second is due to the R–S cycles. For the Valach dynamic series we have, as temporal reference, the Rhodanian phase (at 5.33 ma) corresponding to the Miocene–Pliocene limit. The temporal position of the earliest moments of this series can be obtained by the addition of the value 2.05 ma to the 5.33 ma (5.33 + 2.05 + 2.05 + ...). The latest moments are evidently calculated by subtracting this value of 2.05 ma (5.33 – 2.05 – 2.05). If we consider the chronostratigraphic chart based on the absolute ages of the limits, it is obviously easy to calibrate in relation to them. For this reason, a very suggestive cyclostratigraphic scheme can be built by drawing (with lines) all the moments of this series, by reference to the temporal position of Rhodanian phase (5.33 ma). For a simplified scheme, this temporal texture can preserve only the moments which mark entire VhCys (of 4.1 ma period) (5.33 + 4.1 + 4.1 ...). Other moments of this series can be marked only if they are associated with some stratigraphic limits, obtained by calibration. Such a temporal basis highlights the relationship between the duration of the chronostratigraphic sub-divisions and the period of the VhCy. If we rely on the chronostratigraphic chart of Ogg (produced after GTS 2004 – Gradstein et al., 2004) it's possible to retain that some stages have a

duration equal to half a period of the VhCy (2.05 ma), others correspond to the duration of one VhCy (4.1 ma), others include two VhCy or three cycles of this period. Only the Miocene, as a super-stage, has the duration equal to 4.5 periodes of 4.1 ma. Also, the duration of some stages is equals to 1.5 periods of VhCy (namely of 6.15 ma). Some great stages, as the Aptian (with the duration equal to three VhCys) have in their structure three sub-stages, each with the duration equal to the period of the VhCy: Bedoulian, Gargasian & Clansayesian. Thus, it is possible to argue that a cyclostratigraphic chart of the last 251 ma reflects, first of all, the effects induced on Earth by the pulsations of the Solar System, whose radial movement determines the existence of the VhCy, respectively of the Valach dynamic series. It is no doubt that we have a similar situation in the pre-Mesozoic times – an easy to prove reality. A second dynamic series, very useful in relation to our cyclostratigraphic scheme, is due to the R–S cycles with a corrected period of 26.78 ma. The dynamic moments of this series are rarer (at each 13.39 ma) and, as a result, fewer limits can be calibrated in relation to the temporal values of this cycle in the last 251 ma. We can consider, in this regard, the following limits: Thanetian–Ypresian (with the calibration at 56.14 ma), Valanginian–Hauterivian (at 136.42 ma) and Norian–Rhetian (at 203.37 ma).

As conclusions, our attempt to imagine a cyclostratigraphic chart of the Meso-Cenozoic time led to the idea of a clear cyclic texture (fabric) of the geological time. This is due to the dynamic moments of a cycle that reflects the pulsatory-type movements of the Solar System and secondly to the dynamic moments of the R-S cycles that reflect the pulsations of our galaxy. These moments correspond to the chronostratigraphic limits of the GTS, based on absolute age data. This cyclostratigraphic texture of the geologic time allows the calibration of all chronostratigraphic limits of the Phanerozoic and allows the removal of intervals that approximates the temporal positions of these limits. This calibration is based on the reference values that mark these limits and emphasize the great quality of the methods used to determine the numerical ages of the sedimentary deposits. The cyclostratigraphic texture of the geological time has important temporal references: Rhodanian phase (due to the VhCy) and Wallachian phase (R-S cycles), and are based on the periods of these two dynamic cycles involving dynamic series with frequencies of 2.05 ma and 13.39 ma. This temporal texture can highlight some limits, which can be related to dynamic moments of other causes, distinct from causes determining the VhCy and the R-S cycles. The K-P limit can be an example in this regard. In addition, aspects of climatic nature are self-included in this cyclostratigraphic texture, based fundamentally on the key elements of the VhCy (its cold and warm phases).

References

Cohen, K. M., Finney, S. C., Gibbard, P. L., Fan J.–X., 2013. The ICS International Chronostratigraphic Chart. Episodes 36, 199 – 204.

Cohen, K. M., Harper, D. A. T., Gibbard, P. L., Fan J.–X., 2018. International Chronostratigraphic Chart of ICS.

Furin, S., Preto, N., Rigo, M., Roghi, G., Gianolla, P., Crowley, J. L., Browring, S. A., 2006. High-precision U-Pb zircon age from the Triassic of Italy: Implications for the Triassic time scale and the Carnian origin of calcareous nannoplankton and dinosaurs. Geology 34, 1009 – 1012.

Gradstein, F., Ogg, J., Smith, A., 2004. Geologic Time Scale. Cambridge Univ. Press.

Ogg, G., 2003. International Stratigraphic Chart, International Commission on Stratigrapy, (with numerical ages by GTS of Gradstein et al., 2004).

Raup, D. M., Sepkoski, J. J., 1982. Mass extinction in the marine fossils record, Science, 215, 1501-1503.

Raup, D. M., Sepkoski J., John, Jr., 1984. Periodicity of extinctions in the geologic past. Proceedings of the National Academy of Sciences of the USA, 81 (3), 801 – 805.

Ticleanu, M., 2013. Tectonic phases – dynamic effects of the moments of change of meaning of the radial motions involving Earth. SGEM 2013, v. I, 187 – 193, Albena.

Ticleanu, M., Ticleanu, Al., 2019. Cyclostratigraphic chart of the Meso-Neozoic (Cenozoic) time. Proceedings of SGEM 2019, v. 19, 133 – 139, Albena.

Ticleanu, M., Nicolescu, R., Culescu, F., 2018. Neogene cyclostratigraphical chart of the Central Paratethys. SGEM 2018, v. 18, 339 – 346, Albena.

Ticleanu, M., Ticleanu, N., Constantin, P., Pauliuc, S., Marinescu, F., 2002. The identification of the Valach climatic cycle – important achievement of Romanian geological research school. St. Univ. Babeş-Bolyai, Geol., XLVII, 2, 85–92, Cluj-Napoca.

| Geosciences in the 21 ^s | ^t century |
|------------------------------------|----------------------|
| | |

Ticleanu, M., Ticleanu, N., Pauliuc, S., Constantin, P., Marinescu, Fl., Diaconiţă, D., 2005. The Valach climatic cycle (4.1 m.y.) – the outlining of a pulsatory movement within the Solar System by using sequential analysis of Senonian and Cenozoic coal facies located in Romania. 6th ECoal Conference, Proceedings, 177 – 184, Belgrade. Walker, J. D., Geissman, J. W., 2009. Geologic Time Scale, Geological Society of America.



Research of excellence in river-delta-sea systems, to highlight regional and global climate changes



Acest proiect este finanțat de Ministerul Cercetării și Inovării prin Programul 1 – Dezvoltarea sistemului național de cercetare-dezvoltare, Subprogram 1.2 – Performanță instituțională -Proiecte de finanțare a excelenței în CDI, Contract nr.8PFE/16.10.2018

www.fluvimar.ro